Major ions, Stable isotopes, $^{87}Sr/^{86}Sr$ and Re in the headwaters of the Yamuna: Implications to chemical weathering in the Himalaya

Tarun Kumar Dalai

Ph. D. Thesis

December, 2001

Oceanography and Climate Studies Area
Physical Research Laboratory
Navrangpura, Ahmedabad - 380 009, India

Major ions, Stable isotopes, $^{87}Sr/^{86}Sr$ and Re in the headwaters of the Yamuna: Implications to chemical weathering in the Himalaya

Submitted to

The Maharaja Sayajirao University of Baroda, Vadodara, India

By

Tarun Kumar Dalai

For the degree of

Doctor of Philosophy in Geology

December, 2001

Oceanography and Climate Studies Area
Physical Research Laboratory
Navrangpura, Ahmedabad - 380 009, India

Certificate

I hereby declare that the work presented in this thesis is original and has not formed the basis for the award of any degree or diploma by any university or institution.

Tarun Kumar Dalai (Author**)**

Certified by

Prof. S. Krishnaswami (Guide**)**

Oceanography and Climates Studies Area
Physical Research Laboratory
Ahmedabad - 380 009, India

Prof. P. P. Patel (Co-guide**)**

Department of Geology
M. S. University of Baroda
Vadodara - 390 002, India

Prof. P. P. Patel

Head, Department of Geology
M. S. University of Baroda
Vadodara - 390 002, India

To my parents

Abstract

The major emphasis of this thesis is to understand and quantify chemical weathering and transport in the southern slopes of the Himalaya. This goal has been achieved through a detailed geochemical and isotopic investigation of river waters and sediments of the Yamuna River System (YRS) in the Himalaya, one of the major rivers in this region. Based on these measurements, this study aims at assessing the role of major lithologies such as silicates and carbonates, and minor lithologies such as evaporites and phosphates, in regulating the major ion chemistry, dissolved Sr and Ba budgets, $^{87}Sr/^{86}Sr$ of the rivers and CO_2 consumption by silicate weathering. The study also determines the impact of weathering of a trace lithology, organic rich sediments, on the riverine trace metal budgets of Re, Os and U, and CO_2 in the atmosphere.

River waters and sediments have been sampled from the YRS in the Himalaya for three different seasons and analyzed for major ion chemistry, Sr, Ba, stable isotopes ($\delta^{18}O$ and δD) and $^{87}Sr/^{86}Sr$. For the first time, a comprehensive geochemical study on Re geochemistry in a river system in the Himalaya has been undertaken through extensive measurements of dissolved Re in the YRS waters and Re in various source rocks.

The spatial and temporal variations in the stable isotopic composition of the YRS waters are regulated by source composition, i.e. monsoon precipitation which in turn is dictated by 'amount effect', recycling of moisture in the region and evaporation of rain during fall. Further, mixing of snow/glacial melt with rainwater and mixing of rivers during their flow all contribute to the isotopic composition of these rivers. The 'altitude effect' in the Himalaya, derived from the YRS water isotopic compositions, is 0.11 ‰ per 100m. This varies among the river basins in the Himalaya and seems to be dictated by the 'amount effect'.

Catchment lithology exerts strong control on the abundances of major ions, Sr and Ba, and $^{87}Sr/^{86}Sr$ of the YRS waters. Rivers in the upper reaches, draining predominantly silicates, have low TDS, Sr, Ba and high $^{87}Sr/^{86}Sr$. Downstream, they drain easily weatherable lithologies such as carbonates, evaporites and phosphates with a consequent increase in the concentrations of major ions, Sr and Ba, and a decrease in $^{87}Sr/^{86}Sr$.

Carbonate weathering contributes dominantly to the major ion chemistry of the YRS, the estimated upper and lower limits of their contributions to the cations average ~70% and ~50% respectively. Silicates contribute, on average, ~25% to the YRS cation budgets.

Sulphuric acid, generated via oxidation of pyrites, acts as an important agent of chemical weathering in the catchment.

Silicate contributions to the YRS Sr budget is in proportion to the silicate cations (~25%). $^{87}Sr/^{86}Sr$ show wide range, 0.7142 to 0.7932, with lower values typical of rivers in the lower reaches draining sedimentaries dominated by Precambrian carbonates and minor amounts of evaporites. The observation, that there is a strong correlation between silicate derived cations and $^{87}Sr/^{86}Sr$ and that rivers draining predominantly silicates have high $^{87}Sr/^{86}Sr$, suggest that silicate weathering regulates the high radiogenic Sr isotopic composition in these rivers. Precambrian carbonates, with lower Sr/Ca and $^{87}Sr/^{86}Sr$ than the YRS waters, is not a major component of Sr budget and high $^{87}Sr/^{86}Sr$ on a basin wide scale. On average, they can account for ~15% to the Sr of the YRS. Minor lithologies such as evaporites and phosphates, with relatively higher Sr concentrations and Sr/Ca also seem significant contributors to the YRS Sr budget. The high $^{87}Sr/^{86}Sr$ of the rivers, inherent from silicate weathering, is diluted by the Sr contributions from these lithologies, especially in the lower reaches. Vein-calcites occurring in granites can be an important source of Sr to the YRS, however, critical evaluation of their significance in influencing river water $^{87}Sr/^{86}Sr$ needs further detailed work on their Sr abundance and $^{87}Sr/^{86}Sr$.

Silicates and carbonates in the YRS basin contribute, on average, ~30% each, to the dissolved Ba in the YRS waters. They can be dominant contributors to the streams with low Ba concentrations. In the lower reaches, for tributaries with higher Ba, sources such as phosphorites have to be invoked.

The average dissolved Re concentrations in the YRS, 9.4 pM, is much higher than the reported global average, 2.1 pM. Estimations based on Re and major ion abundances in the crystallines and Precambrian carbonates show that, on average, they contribute insignificantly to the YRS dissolved Re budget. A very likely source for high Re in these waters is organic rich sediments such as black shales. Based on available data on Re in the black shales of the Lesser Himalaya, it has been estimated that Re from ~60 mg of black shales has to be released per liter of water to account for the measured average Re in the YRS. Currently no data is available on the distribution of organic rich sediments in the Yamuna catchment to determine if such requirement can be met. Using Re in rivers as an index of weathering of organic rich sediments, it has been shown that their weathering can

account for the measured concentrations of dissolved Os and U in the rivers draining the Himalaya. The dissolved Re flux from the Ganga and the Yamuna in the Himalaya is disproportionately higher compared to their contributions to the global water discharge.

Silicates though contribute ~25% of cations and Sr to the YRS waters, and major source for radiogenic $^{87}Sr/^{86}Sr$, their weathering in the Yamuna basin in the Himalaya is not intense, as evident from the water and sediment chemistry. The chemical index of alteration in the YRS sediments is ~60. This is most likely caused by higher rate of physical weathering, about an order of magnitude more than chemical weathering rate. The rate of chemical weathering of carbonates in the Yamuna and Ganga basins in the Himalaya is about four times higher than the rate of silicate weathering.

The contemporary CO_2 consumption rates via silicate weathering in the Ganga and Yamuna basins in the Himalaya, $(2\text{-}7)\times10^5$ moles km^{-2} y^{-1}, are significantly higher than those reported for other major river basins in the world. Together, they account for ~0.1% of the global CO_2 consumption via silicate weathering compared to ~0.1% and ~0.03% of their contribution to the global water budget and drainage area. The CO_2 consumption via silicate weathering in the Ganga and the Yamuna basins in the Himalaya, is roughly balanced by the release of CO_2 by oxidation of organic rich sediments, estimated using dissolved Re as an index of their weathering.

This study brings out possible dependence of silicate weathering on temperature, supportive of the hypothesis that silicate weathering is dependent on climate. Using the major ion data (silicate Na and Si) in the river waters, activation energy for overall silicate weathering in the catchment has been estimated to be 50-75 kJ mol^{-1}.

The present work, based on a very comprehensive measurements of several chemical and isotopic species in the YRS waters and solid phases from drainage basins, has quantified contributions from various lithologies to riverine budgets of these elements and isotopes and has addressed to some of the issues of recent debate. Further, influence of lithology and temperature on chemical weathering of silicates has been demonstrated.

Acknowledgements

This thesis has benefited from help and contributions of a number of individuals. I take immense pleasure in writing this acknowledgment.

I express deep sense of gratitude to Prof. S. Krishnaswami, my thesis supervisor, who has been instrumental to guide me through acquisition, interpretation and presentation of geochemical data that this work is all about. More importantly, he gave me freedom to fight with him during discussions, taught me how to adopt a quantitative approach and made me enjoy geochemistry so much.

Prof. P. P. Patel and Prof. M. P. Patel of M. S. University have provided valuable advice and criticism during the course of this study. I thank them for their interest in this work.

I am grateful to Dr. J. R. Trivedi for teaching me the nuances of mass spectrometry. I learned from him how to work in a clean laboratory. He allowed me to use his mass spec, clean lab and the computer, which has gone a long way to finish this work.Dr. M. M. Sarin has been patient enough to teach me analytical techniques. I have learned a lot from his knowledge and understanding on instruments, which helped circumvent the problems during data acquisition. His critical comments helped improve one of the chapters of this thesis. I am thankful to Sunil for his help during establishment of Re chemistry in waters in this laboratory. He also helped me with mass spectrometry. I thank Prof. B. L. K. Somayajulu for his concern, encouragement and advice. He has kindly provided inputs to a part of this thesis.

I am thankful to Prof. S. K. Bhattacharya for taking interest in my work and for his inputs to one of the chapters of this thesis. Dr. Kanchan Pande has been enthusiastic to provide help and advice whenever I needed. Discussions with Dr. R. Ramesh have been fruitful and rewarding. I thank all the members of PRL Academic Committee who spent their time to critically review my work from time to time. My heartfelt thanks to R. Bhushan and R. Rengarajan for proofreading this thesis. Thanks are due to N. Juyal, A. D. Shukla and M. G. Yadava for their help and encouragement.

Dr. L. S. Chamyal and S. Bhandari have been very helpful throughout and saved me a lot of time and efforts by making things work for me in M. S. University. I thankfully

acknowledge the help provided by Dr. Anil Kumar during analysis of Sr isotopes at NGRI, Hyderabad. Prof. K. Gopalan provided helpful suggestions on ion exchange chemistry of Sr. Prof. V. Subramanian kindly provided monthly discharge data for the Yamuna. R. A. Jani and P. Ghosh helped me during stable isotope analysis of waters. I thankfully acknowledge help of M. Dixit in some of the analysis. This thesis has improved by constructive comments of Profs. K. K.Turekian and A.E. Kump and Dr. B. Peucker-Ehrenbrink. I thank authorities of Wadia Institute of Himalayan Geology, Dehradun for providing logistics during field campaigns.

It has been sheer joy to be in company of the Chemistry Gang: Ravi, Renga, Bhavsar, Pauline, Rajesh, Koushik, Anirban, Neeraj, Sudheer, who have been very supportive of this work through their help, criticism and encouragement. Folks! You all have been great.

I will always carry ineffable memories of moments I shared with a number of friends and individuals in PRL. The list includes, but is not limited to; Shikha, Shajesh, Sai, Duli, Rishi, Santosh, Sankar, Supriyoda, Vinai, Kaushar, Sudeshna, Subrata, Aninda, Arun, Lokesh, Tarak, Manoj, Ravindra, Neerja, Sanjaybhai and Jayendra. I thank all who have helped me at various stages of this work.

I sincerely thank staffs of the library, the computer center, the workshop, liquid nitrogen plant and glass blowing facility of PRL for their help.

I am highly indebted to my parents for their moral support, goodwill and encouragement, without which this work would not have been possible.

CONTENTS

List of Tables

List of Figures

Chapter 1

Introduction

1.1 INTRODUCTION

Weathering and erosion of rocks on continents are important processes in the geochemical cycles of elements. These processes regulate the composition of the atmosphere, the oceans and the sedimentary rocks. Rivers serve as the major pathways through which the continental rain and weathering products reach the oceans. The nature and extent of physical and chemical weathering, which together constitute continental denudation, are reflected in the sediment (suspended and bed) load and dissolved constituents of the rivers respectively. Chemical weathering of bedrocks depends on a number of variables, two of the important ones being lithology and availability of protons for chemical reactions. Protons are provided by carbonic acid, produced from solution of CO_2 and sulphuric acid, released from oxidative weathering of pyrites. This makes chemical weathering a major process in controlling the atmospheric CO_2 budget. Among the chemical weathering processes, silicate weathering is unique as it is responsible for CO_2 drawdown from the atmosphere and hence serves as a negative feedback in stabilizing the global temperature on a million-year time scale (Berner and Berner, 1997). Thus, geochemical and isotopic investigation of rivers provide valuable information on biogeochemical cycles, fluxes of elements and isotopes to the ocean, weathering and erosion rates of continents and contemporary CO_2 consumption via chemical weathering. Further, understanding the geochemistry of elements and isotopes, which serve as potential tracers to study various Earth System Processes at present and in the past, requires knowledge on their release via rock-water interaction in the natural aqueous environments and their behavior during transport in the rivers.

The origin and uplift of high mountains in a region, bring about climate change, influences the general hydrology and fluvial dynamics; and modifies the regional landscape (Ruddiman and Prell, 1997). One example of this is the Himalayan uplift and associated climate change. The Himalaya, 2400 km long and 250 to 300 km wide mountain barrier, rising to 500-8000 m above sea level, critically influences the atmospheric circulation of the Asian continent and exercises a dominant control on its climate. The mountain range is responsible for the unique monsoon climate that prevails in the subcontinent. There are about 1500 glaciers in the Himalaya, spreading over nearly 33,200 km^2 in the higher altitudes, which have an important role in the water budgets of the Himalayan rivers (Valdiya, 1998).

The rivers draining the Himalaya, a relatively young active mountain chain, contribute significantly to the global water and sediment discharge (Milliman and Meade, 1983; Berner and Berner, 1996) and influence the oceanic elemental and isotopic geochemistry. It is suggested that the uplift of the Himalaya and associated monsoonal rainfall, rapid physical erosion, all contribute to enhanced chemical weathering of silicates which in turn results in increased consumption of atmospheric CO_2. The drawdown of atmospheric CO_2 via silicate weathering in the Himalaya has been invoked as a driver of the Global Cenozoic cooling (Raymo and Ruddiman, 1992). This hypothesis is in line with the knowledge that chemical weathering of silicate minerals in the continents serves as the primary sink for atmospheric CO_2 on a multi-million year time scale. The enhanced chemical weathering in the Himalaya has also been thought to influence the major ion and various trace metal and isotopic budgets of the oceans. For instance, the steady rise in $^{87}Sr/^{86}Sr$ and $^{187}Os/^{186}Os$ of the seawater through late Cenozoic has been ascribed to weathering of silicates and organic rich sediments in the Himalaya (Raymo and Ruddiman, 1992; Richter et al., 1992; Pegram et al., 1992; Turekian and Pegram, 1997). Similarly, weathering in the Himalaya has also been proposed to be controlling the marine uranium budget (Sarin et al., 1990). Indeed, the Sr isotope evolution of the oceans through the Cenozoic has been used as supporting evidence in favour of enhanced silicate weathering in the Himalaya (Raymo and Ruddiman, 1992; Richter et al., 1992). This suggestion has become a controversy and the use of high radiogenic Sr isotopic composition in rivers as a proxy for silicate weathering has become a matter of debate. Such a controversy has sparked interests among a number of researchers to take up geochemical studies in the river basins of the Himalaya.

The results of Palmer and Edmond (1989) and Krishnaswami et al. (1992) showed that rivers draining the Himalaya, especially the head waters of the Ganga-Brahmaputra (G-B) system, have very high radiogenic Sr isotopic composition (high $^{87}Sr/^{86}Sr$) and high Sr abundance compared to other major rivers in the world. This lent support to the hypothesis of Raymo and Ruddiman (1992). Richter et al. (1992), based on the then available data on Sr fluxes from the Himalayan rivers, their $^{87}Sr/^{86}Sr$ and timing of the uplift of the Himalaya, concluded that chemical weathering associated with Himalayan Orogeny could have accounted for the observed increase in $^{87}Sr/^{86}Sr$ of the oceans during the Cenozoic.

Though there is a general consensus that rivers draining the Himalaya have contributed significantly to the Sr isotopic evolution of the oceans, the issues concerning the source(s) of high radiogenic Sr (^{87}Sr) in these rivers, its mass balance in them and the use of $^{87}Sr/^{86}Sr$ in the rivers as a proxy of silicate weathering have been a matter of intense debate and remain contentious. Krishnaswami et al. (1992) proposed that granites/gneisses in the Himalaya, with very high $^{87}Sr/^{86}Sr$ as possible source for high ^{87}Sr in the rivers of the Ganga-Brahmaputra (G-B) system. Harris (1995) suggested metasediments from the Higher Himalaya as candidates for the high $^{87}Sr/^{86}Sr$ in these river waters. Palmer and Edmond (1992), Quade et al. (1997), Blum et al. (1998) and English et al. (2000) proposed that the metamorphosed carbonates and calc-silicates in the Himalaya, which acquired high ^{87}Sr from the coexisting silicates during fluid exchange via widespread metamorphism, could be sources for high $^{87}Sr/^{86}Sr$ in the rivers draining the Himalaya. Galy et al. (1999) concluded that silicates in the Lesser Himalaya and in the Siwaliks are sources of the high $^{87}Sr/^{86}Sr$ in the Ganga-Brahmaputra rivers. Blum et al. (1998) and Jacobson and Blum (2000), based on studies of the Raikhot watershed in the Nanga Parbat region, proposed that disseminated calcite occurring in trace amounts in the silicate rocks is the predominant source of dissolved Ca and Sr to the streams draining the silicate bedrock. If carbonates or disseminated calcites truly control the Sr and its isotopic composition in rivers draining the Himalaya, the idea of using $^{87}Sr/^{86}Sr$ in the river waters as a proxy of silicate weathering in the Himalaya does not stand valid and needs to be re-evaluated.

Singh et al. (1998) carried out a detailed elemental and Sr isotopic study on the Precambrian carbonates, sampled extensively across the Lesser Himalaya and concluded that these carbonates can not account for the Sr load and its highly radiogenic isotopic composition of river waters in this region on a basin wide scale though they could be important for particular streams. Krishnaswami et al. (1999), in an attempt to characterize the sources of cations and Sr in the Ganga-Ghaghra-Indus (G-G-I) source waters, brought out the difficulty in making Sr mass balance in these rivers and underlined the importance of sources in addition to silicates and Precambrian carbonates in contributing to the Sr budget.

Estimation of contemporary weathering rate and CO_2 consumption via silicate weathering in the Himalaya requires understanding of proton sources that release solutes to rivers from rocks via chemical weathering. Considering that the lithological set up in the

Himalaya is diverse and complex, such exercises have proved to be difficult (Krishnaswami et al., 1999; Galy and France-Lanord, 1999). Further, the validity and accuracy of mass balance calculations in achieving these goals depend on the end member compositions used. One way of having better constraints on end member compositions is careful sampling of the streams draining predominantly single lithology. This is also not quite straightforward, as it is very difficult to find rivers draining monolithologic units. Inspite of this, estimates are available on the silicate weathering rates and associated CO_2 consumption for a few river basins in the Himalaya. These include the G-B system (McCauley and DePaolo, 1997; Galy et al., 1999), Ganga-Ghaghara-Indus system (Krishnaswami et al., 1999) and Chinese rivers (Gaillardet et al., 1999).

The river Yamuna, draining the western part of the Ganga catchment in the southern slopes of the Himalaya, is the largest tributary of the Ganga (Negi, 1991). The river, at its confluence at Allahabad, carries water one and half times that of the Ganga (Rao, 1975). In its course the Yamuna drains a variety of lithologies in the Lesser Himalaya giving ample opportunity to examine the influence of lithology on water chemistry. A part of this thesis is devoted to quantification of contributions of various sources to major cations in the Yamuna River System (YRS) in the Himalaya, estimation of weathering rate and CO_2 consumption flux via silicate weathering and mass balance of riverine Sr using data on chemistry and $^{87}Sr/^{86}Sr$ of water, bed load and various source rocks in the Yamuna basin and better constraints on the source composition. The contentious issues on source(s) of Sr in the rivers draining the Himalaya, as discussed earlier, would be addressed in some detail in this study. The importance of silicate weathering in the southern slopes of the Himalaya in consuming CO_2 from the atmosphere and in contributing to the ^{87}Sr budget of the rivers would also be discussed.

The origin and evolution of the Himalaya, as mentioned earlier, have influenced the onset of the Indian monsoon and affected the climate, vegetation (relative abundance of C4 and C3 grasses), erosion and weathering in the region (Cerling, 1997; Prell and Kutzbach, 1997). It is established that at present the Himalayan ranges control the monsoonal precipitation in the Indian subcontinent. The rivers in the Himalaya draw their water from the orographic precipitation as well as from melting of glaciers in the region. Understanding the influence of altitude, distance from the cloud source and hydrological processes operating in

these catchments such as mixing, evaporation and evapotranspiration is important for the purpose of modeling water budget in the region. As a part of this thesis, stable isotopes (oxygen and hydrogen) have been measured in the waters of the YRS to characterize aources of river waters and processes controlling the stable isotopic composition of river waters in the region. Processes such as the "amount effect" and the "altitude effect" have been addressed in detail with the problems associated in deciphering them in a catchment, particularly in a Himalayan watershed, where the physiographic set up is diverse and complex. These data also provide inputs to the estimation of paleoaltitudes based on $\delta^{18}O$ in carbonates and for comparing the intensity of paleo-monsoon in the Himalaya with that of the present (Garzione et al. 2000a, b).

Analogous to Sr isotopes, marine records show that the Os isotopic composition ($^{187}Os/^{186}Os$ and $^{187}Os/^{188}Os$) of seawater has been steadily increasing through the Late Cenozoic (Pegram et al., 1992; Turekian and Pegram, 1997). The osmium isotopic composition in seawater is dictated by contributions from continental weathering (radiogenic component) and mantle material and cosmic dust (non-radiogenic component). The continental crust has an average $^{187}Os/^{186}Os$ of ~11 (Esser and Turekian, 1993) whereas the $^{187}Os/^{186}Os$ for the mantle material and cosmic dust is ~1 (Luck and Allegre, 1983; 1991). That of seawater value of 8.8 for $^{187}Os/^{186}Os$ (Levasseur et al., 1998) requires that continental weathering dominantly controls the seawater Os isotopic composition, consistent with the measured $^{187}Os/^{186}Os$ of river waters (Sharma et al., 1999; Levasseur et al., 1999). An increased flux of continental osmium or an increased supply of radiogenic osmium from continents can bring about an increase in the seawater $^{187}Os/^{186}Os$. The Cenozoic increase in $^{187}Os/^{186}Os$ has been ascribed to the uplift of the Himalaya and consequent enhanced chemical weathering, especially of the ancient organic rich sediments such as black shales in this region (Pegram et al., 1992; Turekian and Pegram, 1997). Since Re and Os have a tendency to get associated with organic matter, black shales and other organic rich sediments during their formation scavenge Re and Os from the aqueous environment (Ravizza and Turekian, 1989; Crusius et al., 1996; Morford and Emerson, 1999) with a preference for Re. Hence black shales, to start with, have elevated Re/Os compared to other rock types. The decay of ^{187}Re to ^{187}Os results in high $^{187}Os/^{186}Os$ in black shales. Hence rivers draining catchments containing black shales will have elevated $^{187}Os/^{186}Os$. Although the role of

weathering of black shales in the Himalaya in influencing the $^{187}Os/^{186}Os$ of seawater has not been fully assessed, it has been found that rivers in the Himalaya have more radiogenic osmium isotopic composition compared to other major rivers in the world (Levasseur et al., 1999; Sharma et al., 1999). Black shale occurrences have been reported in the Himalaya, which are usually associated with pyrites. Pyrites, in oxic environment, undergo oxidation to produce sulphuric acid, a strong weathering agent. Considering that black shales are easily weatherable and during weathering they release a suite of cations along with Re and Os to the weathering solutions, rivers draining black shales in the Himalaya are expected to have elevated Re in their waters. Indeed, one sample from the Ganga measured and reported by Colodner et al. (1993b) does show Re concentrations of 8.2 pM compared to the global average value, 2.1 pM. There has been, however, no systematic attempt till date, to assess the impact of various lithologies including organic rich sediments in regulating the dissolved Re in river systems. Therefore, river waters of the YRS and various source rocks have been analyzed for Re to characterize its sources to these rivers. In addition to the source characterization, these data allow inferences on the comparative geochemistry of Re and Os during weathering and transport, as well as on the role of black shales in contributing to the riverine budget of various trace metals such as Re, Os and U. This study, for the first time, attempts to use dissolved Re in the waters as a proxy to study organic matter oxidation in the Himalaya and associated CO_2 flux to the atmosphere. Furthermore, the extent of mobility of Re and Os assessed in this study has implications to geochronometry of rocks/sediments using Re-Os systematics.

1.2 OBJECTIVES OF THE THESIS

This thesis focuses on chemical weathering in the Yamuna River Basin in the Himalaya and addresses to the following objectives based on a comprehensive study of major ion composition, $\delta^{18}O$, δD, Sr, Ba and Re abundances and $^{87}Sr/^{86}Sr$ in the Yamuna River and many of its tributaries in the Himalaya and in selected solid phases of their catchment.

1. To characterize nature and extent of chemical weathering in the Yamuna drainage basin.
2. To assess the relative contributions of various lithologies controlling the solute budgets in the YRS.

3. To constrain the role of silicate vs. carbonate weathering in controlling Sr, Ba abundances and $^{87}Sr/^{86}Sr$ in these rivers and the contemporary CO_2 consumption due to silicate weathering.
4. To evaluate the role of various hydrological and meteorological processes in the catchment in governing the stable isotopic composition of the rivers.
5. To determine the significance of black shale weathering in contributing dissolved Re to the Yamuna River System and its impact on the budgets of Os, U in rivers and CO_2 release to the atmosphere.
6. To assess the overall significance of rivers draining the southern slopes of the Himalaya (the Ganga, the Yamuna and the Indus) in influencing the global budgets of selected elements and isotopes and CO_2 consumption via silicate weathering through synthesis of the present results with those available in literature.

1.3 STRUCTURE OF THE THESIS

This thesis is divided into six chapters.

Chapter 1 introduces the thesis topic and the problems to be addressed in the present study. The chapter also gives a detailed background on the extent of studies carried out on this topic and the nature of controversies and debates existing on the issues discussed in this thesis.

Chapter 2 details the study catchment, sampling and analysis carried out for this study. Part I of this chapter focuses on general geology and climate of the catchment and describes some of the rivers sampled. Part II discusses sampling of river waters, sediments and source rocks, analytical methods employed to carry out various measurements as well as precision and accuracy of measurements.

Chapter 3 presents and discusses the stable isotope systematics in the YRS waters. In conjunction with available data on the local precipitation, influence of various processes such as evaporation, rainout from the clouds and local topography in regulating the isotopic composition of river waters is assessed. Further, this study has been integrated with available results on the Ganga and the Indus systems.

In ***Chapter 4***, abundances of major ions, Sr, Ba and $^{87}Sr/^{86}Sr$ in river waters, bed sediments and source rocks are presented. These data have been used to assess the nature and

extent of contemporary chemical weathering in the catchment and to characterize sources of major ions, Sr and Ba in river waters. The role of various lithologies in contributing to the Sr isotopic budget of the YRS is also assessed. Finally, the present day weathering rates and CO_2 consumption fluxes via silicate weathering in the Yamuna basin in the Himalaya are estimated. The major ion data have also been used to derive "apparent activation energy" for overall silicate weathering in the Himalaya.

Chapter 5 presents Re abundances in the YRS streams/rivers, mine waters and various source rocks. Using these data, the contributions of Re to the YRS waters, from major and minor lithologies in the Yamuna basin in the Himalaya, has been estimated. Using dissolved Re in the YRS as a proxy, the role of weathering of organic rich sediments in contributing to various trace metals such as U and Os and CO_2 release to rivers/atmosphere via oxidation is assessed.

Synthesis of the results obtained in this study and broad conclusions drawn from them are presented in ***Chapter 6***. Future work that to address some of the issues that have borne out from this work are also outlined.

Chapter 2

Materials and Methods

I. MATERIALS

2.1 GENERAL INFORMATION ON THE STUDY CATCHMENT

The objective of this thesis, as mentioned earlier, is to assess the role of various lithological units in contributing to the major ions, Sr and Re budgets and Sr isotope systematics of the Yamuna River System (YRS) in the Himalaya and to evaluate the role of silicate vs. carbonate weathering on the Sr isotopic composition of the river waters. This study also focuses on CO_2 consumption rates associated with silicate weathering in the YRS and the Ganga basins in the southern slopes of the Himalaya. To achieve these goals, it is necessary to have information and knowledge on weathering of silicates, sources of protons contributing to it and factors controlling chemical weathering such as general geology, climate and vegetation of the catchment. This chapter provides details on broad lithology and geohydrology of the Yamuna basin, sampling methods and analytical techniques employed for measurements of various parameters.

The Yamuna though rises in the Higher Himalaya, a significant part of its drainage is contained in the Lesser Himalaya. The Main Central Thrust (MCT) demarcates the boundary between the Lesser and the Higher Himalaya in the north whereas the Main Boundary Thrust (MBT) defines the boundary between the Lesser Himalaya and the Siwaliks in the south (Gansser, 1964). The Higher Himalaya is characterized by tectonically active topography, comprising of very thick piles of Precambrian high-grade metamorphics and granitic gneisses, the oldest rocks of the Himalaya (Valdiya, 1980; 1998) known as Higher Himalyan Crystallines (HHC).

The Lesser Himalaya, covering a zone of 60 to 100 km wide in between the Siwaliks and the Higher Himalaya, represents a relatively gentle and mature topography with gentle slopes and deeply dissected valleys which bear the evidences of recent rejuvenation (Valdiya, 1980). On an average the elevation ranges from 1500 m in the valley beds to 2700 m along the crest of the ridges (Devi, 1992). The Lesser Himalaya comprises of Precambrian-Paleozoic sedimentary strata with minor occurrences of displaced crystallines (Valdiya, 1980). The sedimentaries are divided in to two NW-SE elongated sequences by the crystalline klippe lying in between. The northern sequence of Precambrian sedimentaries is known as the *inner belt* whereas the southern part, known as the *outer belt*, contains sediments of possible Paleozoic age (Valdiya, 1980). The folded autocthonous sedimentaries

of the inner belt are divided into the Damtha and Tejam Groups. The Damtha Group, consisting of the Chakrata and Rautgara Formations is conformably overlain by the Tejam Group comprising the Deoban (≈Shali) and Mandhali (Sor) Formations. The sedimentary successions of the outer belt is divided into the Blaini, Infra-Krol, Krol and the Tal Formations, together known as the Krol Belt.

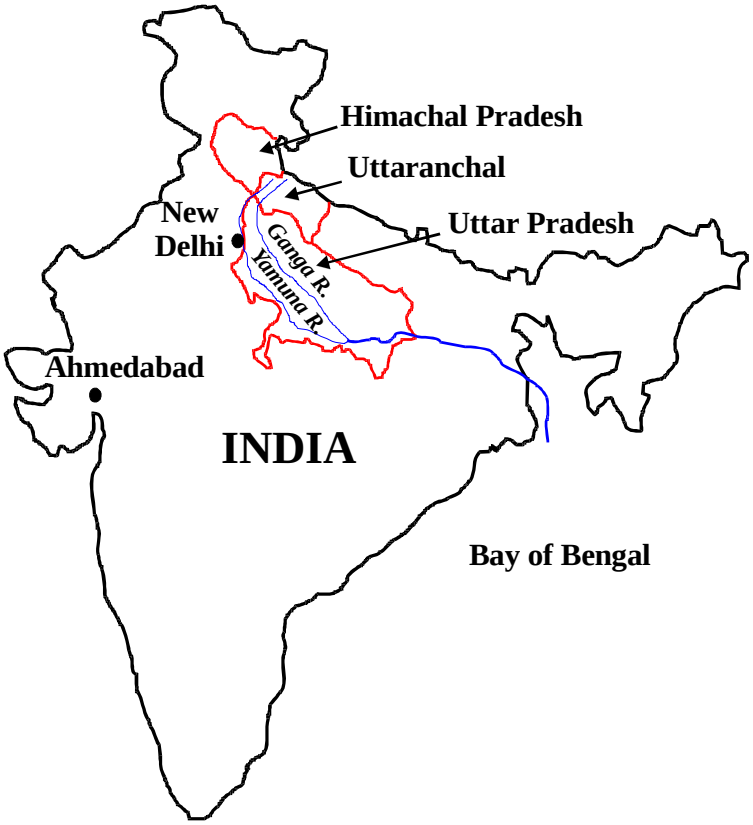

Fig. 2.1 Map of India The Ganga and the Yamuna from their origin in the Higher Himalaya to their confluence.

Siwaliks form the southern front of the Himalaya. These are made up of sediments deposited by the ancient Himalayan rivers in their channels and floodplains. There are flat stretches within the otherwise rugged Siwalik terrane called the "duns" consisting of gravelly deposits in depressions of now vanished lakes that were formed in the synclinal valleys (Valdiya, 1998).

The drainage basins of the Yamuna and its tributaries in their upper reaches in Himalaya cover the northwestern part of the Uttaranchal State (Figs. 2.1, 2.2). They flow through various formations in the Lesser Himalaya comprising diverse lithology set in complex stratigraphic position due to the faulting and thrusting activities. The following

section provides a compilation of the available information on the lithology drained by the Yamuna and its tributaries. Much of the information given below is drawn from Valdiya (1980).

2.1.1 Major rivers of the Yamuna River System in the Himalaya

The Yamuna

The Yamuna originates in the Yamunotri Glacier at the base of the Bandarpunch peak in the Higher Himalaya (Negi, 1991). The glacial lake of Saptarishi Kund, near the Kalind Mountain, at an altitude of 4421 m, is the source of the river. The Yamuna runs almost parallel to the Ganga till it joins the latter at Allahabad. Among all the tributaries of the Ganga, the Yamuna has the largest drainage area and stands second in terms of water discharge. It receives waters from glacier/snow melt in the source region, from monsoon rains and from springs and various tributaries along its course downstream. The Yamuna has a number of tributaries in the Himalaya, prominent among them are the Tons, Giri, Aglar, Asan and Bata. Near its source in the Higher Himalaya, the Yamuna drains mainly the crystallines of Ramgarh and Almora Groups (Fig. 2.3). The Almora granites, at their northern

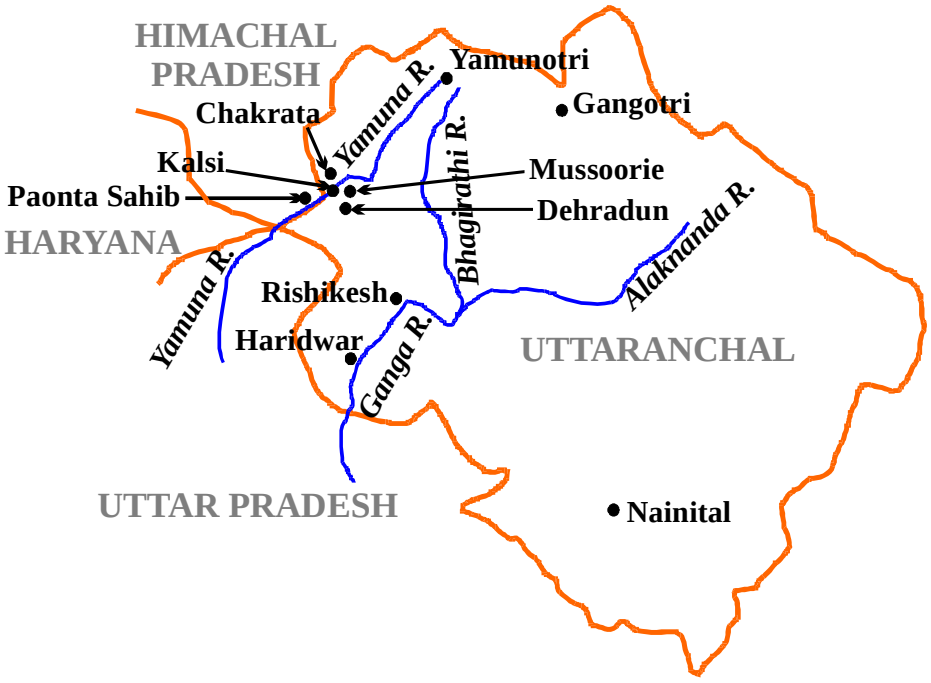

Fig. 2.2 Yamuna River in its upper reaches. Also shown are the Bhagirathi and the Alaknanda and the major towns in the Yamuna River Basin.

border, are reported to have graphitic horizons of schistose graphitoid quartzites (Gansser, 1964). The metamorphics in the Almora and Ramgarh Groups have occurrences of graphitic/carbonaceous schists and carbonaceous schist-marble alternations (Valdiya, 1980). Occurrences of calc-schists and marble with sulphide mineralization have been reported in the areas upstream of Hanuman Chatti (Jaireth et al, 1982). From the Higher Himalaya the Yamuna flows in the southwest direction and enters the Lesser Himalaya where it drains a variety of lithologies. These will be described in their order as the Yamuna flows downstream. Past the Higher Himalaya, it flows through a large stretch of massive sericitic quartzite of Berinag Formation surmounted by patches of muddy quartzites, conglomerates and purple slates of Rautgara Formation. The river then drains the Barkot units comprising carbonaceous schistose phyllites intruded by dolerite sills near Barkot and chloritic phyllite with subordinate metasiltstone and quartzite near Naugaon (Valdiya, 1980). Downstream, it passes through the massive dolomitic limestone and marble of Mandhali and Deoban Formations associated at places with carbonaceous and grey slate. The Yamuna then enters a large stretch of the sedimentaries of the Chakrata Formation which constitute purple and green micaceous greywacke interbedded with slate and siltstone. Further downstream, it drains Chandpur Formation comprising of phyllites and phyllitic slates alternating with metagreywacke and metasiltstones; Nagthat Formation comprising purple and green sercitic quartzites with subordinate slates and siltstones and Bani-Subathu Formations which constitute oolitic and shelly limestones and flysch-like sediments. Barites occur in the silisiclastic sediments of Nagthat Formations in the Tons river section (Sachan and Sharma, 1993) and in the lower horizons of Krol limestones at Maldeota and Shahashradhara, where they occur as pockets and veins (Anantharaman and Bahukhandi, 1984). Southwest of Kalsi, the Yamuna enters the Siwaliks comprising the channel and floodplain deposits by the Himalayan rivers in the past.

In the Lesser Himalaya, occurrences of grayish black, black and bleached shales are reported in the Infra Krol the Lower Tal, the Deoban and the Mandhali Formations (Gansser, 1964; Valdiya; 1980). These are exposed at a number of locations in the Yamuna and the Tons catchment, the largest being at Maldeota and Durmala, around Dehradun, where phosphorite is mined economically.

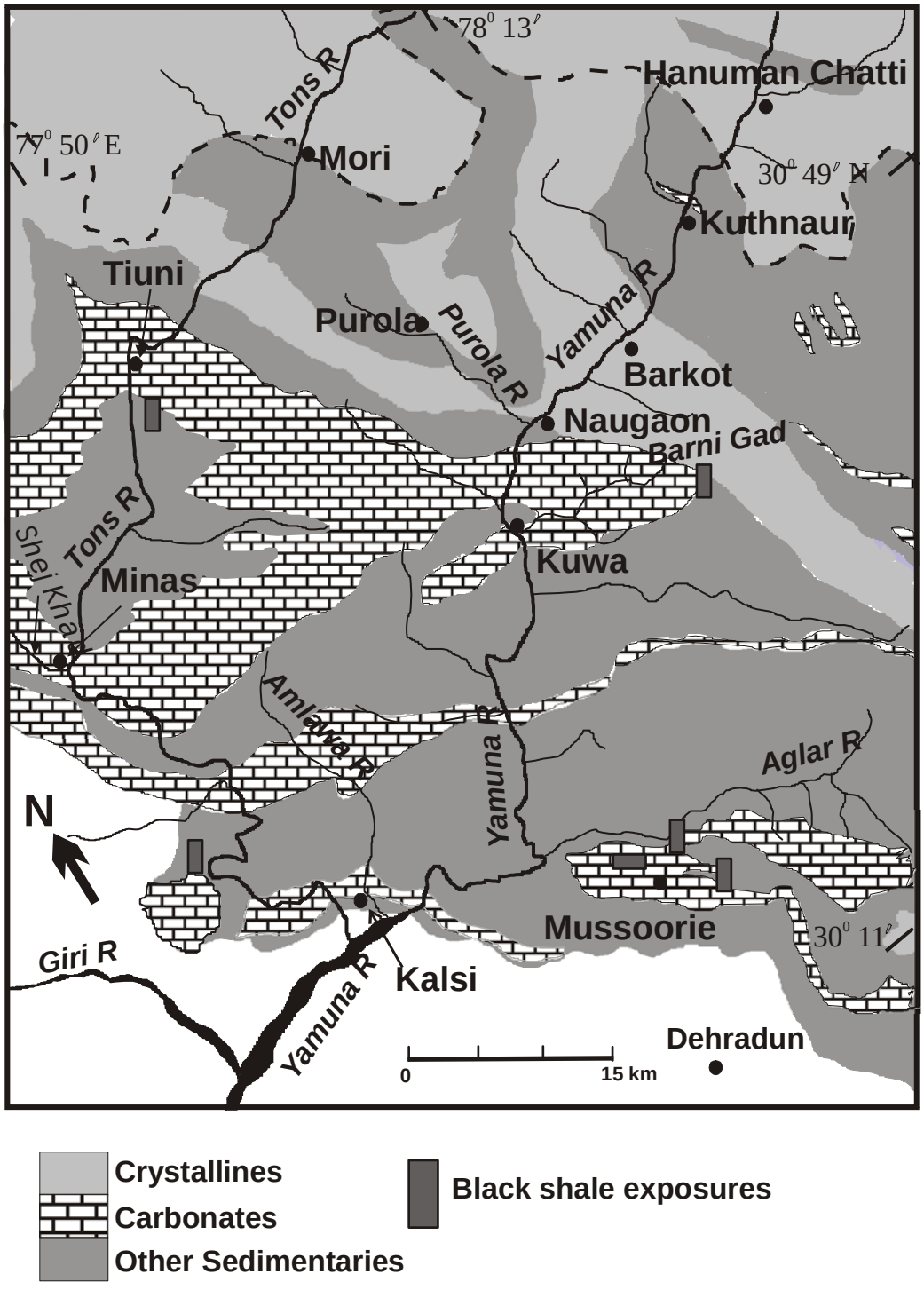

Fig. 2.3 Lithology map of the Yamuna catchment in the Himalaya

Gypsum occurs in Krol Formation in the form of pockets and bands (Anantharaman and Bahukhandi, 1984; Valdiya, 1980). Near Shahashradhara, gypsum is found as replacement deposits in the upper Krol dolomitic limestones and is economically workable. Geothermal springs occur mainly in and around the source region, in Yamunotri and Janaki Chatti.

Fig. 2.4. River Yamuna at Rampur Mandi. The site is ~200 m upstream of the point where the Giri merges with the Yamuna.

The Yamuna has been dammed at Dakpathar, 6 km downstream of Kalsi. Alpine, sub-alpine, temperate and sub-tropical vegetation covers the Yamuna catchment. The main human settlements along the river are Yamunotri, Hanuman Chatti, Barkot, Naugaon, Kalsi, Vikasnagar and Paonta.

The Tons

The Tons River is the major tributary of the Yamuna. It takes its name at Naitwar, where the two rivers, the Supin and the Rupin originating in the Higher Himalaya and draining predominantly the Almora Crystallines merge together (Negi, 1991). Hereafter, the Tons flows a large distance along the border of Himachal Pradesh and Uttaranchal before merging with the Yamuna at Kalsi. The Tons, along its course, drains similar types of lithology as described for the Yamuna. In its catchment, black shales occur in areas around Tiuni and Lokhandi area on the Chakrata-Tiuni road. It joins the Yamuna at Kalsi, where it carries twice the water that is carried by theYamuna (Rao, 1975).

Its catchment bears some of the densest forests in the western Himalaya. These are primarily birch, fir, spruce, blue pine, chir pine and moru oak forests. The settlements along the river are Naitwar, Tiuni and Minas.

The Aglar

The river Aglar originates as a number of small streams fed by groundwater on the western slope of the ridge separating the drainage of the Yamuna and the Bhagirathi (Negi, 1991). Thereafter it flows in western direction to join the Yamuna at a place called Yamuna Bridge. The streams draining the limestones and slates of the Krol Formation in the northern slopes of the Mussorie Ridge and conglomerates, grey phyllitic slates and carbonaceous pyritous slate of Blaini Formation contribute water to the Aglar. The slates of the Krol Formation in the Aglar valley are iron-stained and black carbonaceous (Valdiya, 1980). The Krol dolomitic limestones in this area have pockets of gypsum and intercalations of green and grey pyritic slates (Valdiya, 1980). In its course, it also drains dirty quartzites with intercalations of siltstones and slates of Nagthat Formation and green and grey carbonaceous phyllites of Chandpur Formation alternating with greywacke. Pebbles of black shales were found in the riverbed of the Aglar during the water and bedrock sampling.

The Giri

The Giri River originates near Shimla as a spring fed by ground water and flows along the northern base of the Nahan ridge in its lower course and joins the Yamuna near Paonta Sahib (Negi, 1991). It drains conglomerates, sandstones, siltstones, quartzites, phyllites, carbonaceous and pyritiferous shales and slates with interbeded of limestones of Simla and Jaunsar Group, lithology of the Tal, Krol and Blaini Formations (Srikantia and Bhargava, 1998).

The Asan

Two spring-fed streams emanating from the limestone caves of the Mussoorie ridge merge to form the Asan River which flows south-west to join the Yamuna near Herbettpur (Negi, 1991). In its lower reaches it drains predominantly the Siwaliks. Broad river terraces developed along the middle and lower courses of the river are under cultivation. Sub tropical forests occur in the upper catchment of the river.

The Bata

The river Bata originates in the boulder below the Nahan ridge in Himachal Pradesh as the Jalmusa-ka-khala fed by rainwater and joins the Yamuna downstream of Paonta Sahib (Negi, 1991). It drains predominantly the sandstones of the Siwaliks with minor conglomerates and claystones.

Didar Gad

This stream originates in the Higher Himalaya and drains the Almora Crystallines before joining the Yamuna.

Barni Gad

It drains the chloritic phyllites and blue limestones of Mandhali Formation and dolomitic limestones of Deoban Formation before joining the Yamuna near Kuwa. It draws water from a number of tributaries in its upper reaches.

The Pabar

The Pabar (Fig. 2.5) is a large tributary of the Tons. It rises from the Dhauladhar Range in the Shimla district and is fed by the Chandra Nahan glacier and springs emanating from underground water (Negi, 1991).

Fig. 2.5 River Pabar, about 500 m upstream of its confluence with Tons. Heavy rains in its upper reaches during sampling period has made its water muddy.

It joins the Tons near Tiuni. In its upper reaches it drains the lithology of the Almora Crystallines, the Ramgarh Group. Downstream it flows through the Nagthat quartzites and greenish gray phyllites and slates alternating with gray-black carbonaceous and pyritous limestones.

Godu Gad

It originates in the Higher Himalaya where it drains the Almora Crystallines (Valdiya, 1980) comprising biotite-rich felspathic schist and bitotite-sericite phyllonite. It flows through massive coarse-grained sercitic quartzite of Berinag Formation before it joins the Tons near Mori.

Shej Khad

It is a tributary of the Tons. Shej Khad drains predominantly the dolomites and dolomitic limestones of Deoban Formation before it joins the Yamuna near Minas.

2.1.2 Climate of the Yamuna catchment

The drainage basins of the Yamuna and its tributaries, covering the northwestern part of the Uttaranchal State (Fig. 2.1, 2.2), experience tropical monsoon climate with much variability introduced by the altitude, mountain barriers, air masses and their movement (Devi, 1992). Altitude and mountain barriers are major factors that regulate much of the variations in the rainfall and temperature in the region. January is the coldest month while the maximum temperature is in the month of June. After June, the temperature decreases with the onset of southwest monsoon with a secondary maximum of temperature in September when there is a sharp drop in the cloudiness in the region. Both diurnal and annual ranges of temperatures decrease from the plains up to the elevations ranging from 2100 to 2400 m, beyond which they again increase. The amount of insolation received along the mountain slopes differs according to the gradient and direction of slopes. South and southwest facing slopes are expected to receive maximum insolation than those facing north and northeast as the sun remains south of the area throughout the year. Fig 2.6 shows the monthly temperature variations in some of the places in the Yamuna catchment. The driest month of April and May have the largest diurnal range and the most humid months July and August have the least. The annual relative humidity in the catchment is about 65 %. Higher relative humidity is observed along the southern slopes of the Himalaya as the monsoon winds are forced to

ascend leading to their adiabatic cooling and condensation of moisture. Therefore, high humidity is observed at Mussoorie, Nainital and Chakrata varying from 85 to 95 % during the monsoon months. The amount of rainfall varies with elevation as well as with the location. Heavy orographic rainfall occurs on the windward side of the ranges with a rapid decrease of rainfall on the leeward side.

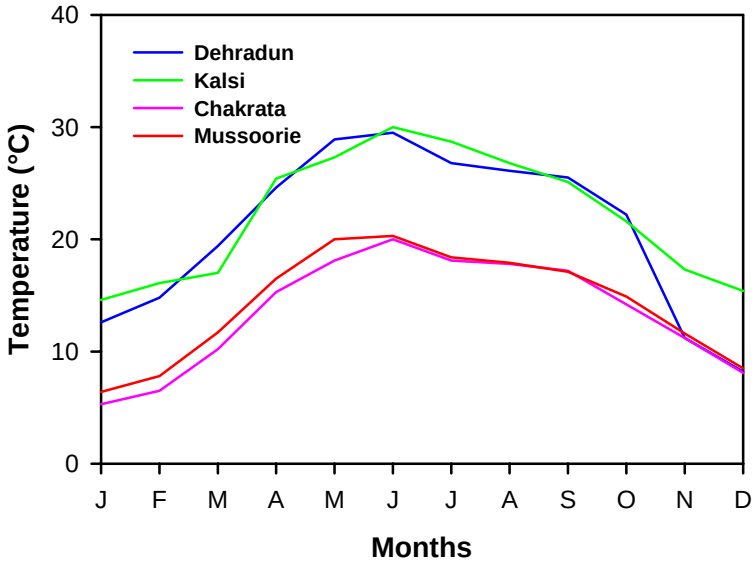

Fig. 2.6 Mean monthly temperature variations in the Yamuna catchment in the Himalaya (Devi, 1992).

The summer rain gradually decreases in amount as one moves along the Himalayan range from east to west. In general, the amount of rainfall increases with elevation except over the northern snowclad areas. The tropical storms and depressions largely influence the local rainfall. Such storms form over the Bay of Bengal and the Arabian Sea and enter the region from southeast and southwest. Heavy rains are associated with slowly moving tropical cyclones due to an increase in the duration of rainfall. The southwest monsoon hits the region around the last week of June and withdraws around the last week of September. The annual rainfall at Dehradun and Kalsi, situated at the foothills of the Himalaya, is ~210 cm whereas in Mussoorie, lying on the windward side of the mountain slope, receives an annual rainfall of ~270 cm. About 80 % of this is contributed by southwest monsoon during July-September (Fig. 2.7). Short duration high intensity rains are common. During monsoon, heavy flood in the Yamuna causes serious damage in the region. Study on peak floods shows that many of them are recorded during late September and early October (Agarwal and Chak, 1991). Occasional heavy rains during these periods, when the catchment is nearly saturated with

water and the river is full, results in floods during this month. Floods in July, August and early September are generally milder. Potential evapotranspiration (P.E.), which represents the water loss in the hydrological cycle, shows large monthly variations in the Yamuna catchment (Fig. 2.7).

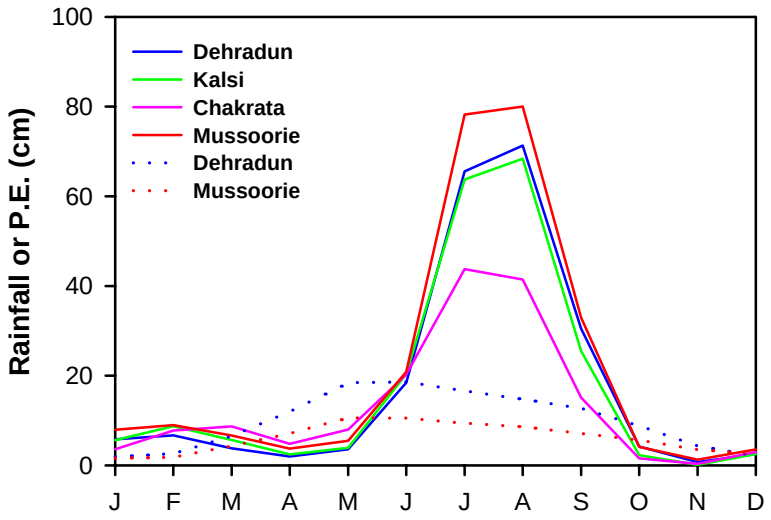

Fig. 2.7 Mean monthly rainfall (solid lines) and potential evapotranspiration (dotted lines) variation at some stations in the Yamuna catchment in the Himalaya (Devi, 1992).

The factors controlling P. E. are temperature, distances from the sea, altitude, characteristics of the rainfall, cloudiness of the sky etc. All these factors form a complex combination influencing the distribution of temperature and consequently the distribution of P.E. over the region. The mean values of P.E. during the summer are five to six folds higher than those during the winter. In the mountain and the foothill regions, during monsoon period, due to higher precipitation and low potential evapotranspiration, the water yield is higher with a large annual variation (Devi, 1992).

Soil formation is governed by the climate (precipitation and temperature), parent lithology, vegetation and gradient in the catchment. The soils in these regions have been grouped as brown-hill soils (Devi, 1992) which form from weathering of granite, gneiss and garnetiferrous and biotitic schist. Based on the pedogenic soil forming processes under the climatic and topographic conditions, four types of soils are found: (i) red loam (in dry places), (ii) brown forest (in surfaces with moderate organic content), (iii) podsol (in humid condition) and (iv) meadow soils (near *nallas* and cool, shady and perennially moist places). Soils on the slopes (15 to 40 percent) are shallow due to erosion and mass wasting processes

(Ghildyal, 1990) and usually have very thin surface horizons. Soil loss in the region varies with the extent of vegetation. Variability in temperature, precipitation and soil thickness also influences the distribution of vegetation in the catchment. Intensive cultivation is observed on terraced hillslopes.

The Yamuna emerges from the hills near Tajewala where the water is taken off by the western and eastern Yamuna canals. The YRS drains an area of about 9600 km^2 in the Himalaya with an annual water flow 10.8×10^{12} liters at Tajewala (Jha et al., 1988, Rao, 1975). About 80% of the water discharge occurs in the month of July, August and September. Monthly variation of water flow in the Yamuna at New Delhi Bridge is given in Fig. 2.8. The total length of the Yamuna from its origin till its confluence with Ganga at Allahabad is 1376 km.

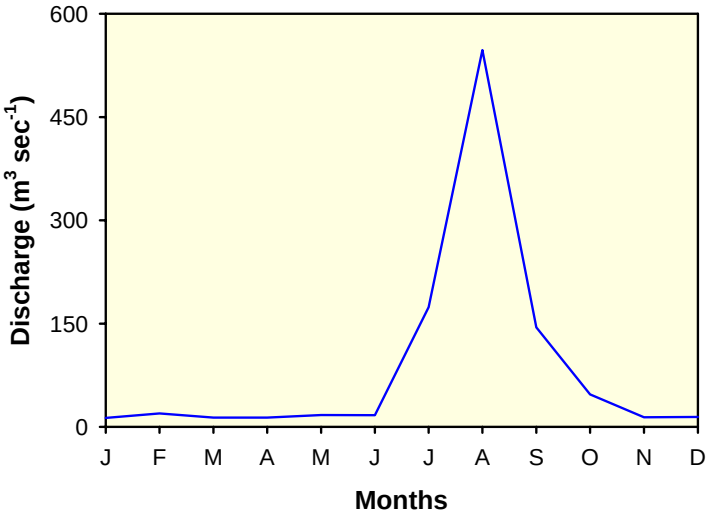

Fig. 2.8 Mean monthly variation of the water discharge in the Yamuna at New Delhi Bridge. More than 80% of the discharge occurs during July, August and September. Data from V. Subramanian (personal communication, 2001)

II. METHODS

To achieve the objectives as outlined earlier, samples of river water, riverbed sediments and various source rocks (granites, carbonates and phosphates) were collected and analyzed for suite of chemical constituents and properties. Details of sampling, sample preparation and analytical techniques are discussed below.

2.2 SAMPLING

(a) River water

Three field campaigns were carried out during October 1998, June and September 1999 corresponding to post-monsoon, summer and monsoon periods respectively (Appendix 2.1). Samples of river water and bed sediments were collected along the entire stretch of the Yamuna and its tributaries in the Himalaya, from near its source at Hanuman Chatti to its outflow at the foothills at Saharanpur (Fig 2.9). In addition, few granite samples were collected from outcrops in and around Hanuman Chatti. Water samples were collected by and large from midstream to avoid local inhomogeneity. Samples were collected in pre-cleaned plastic carboys, which were profusely rinsed with the ambient river water before sampling. About 150 ml of the water was kept in pre-cleaned polyethylene bottles for alkalinity measurements. The remaining water was filtered through 0.4μ Nulceopore® polycarbonate filters within 3-6 hours of their collection. An aliquot of the filtered water of each sample was acidified to pH <2 with ultrapure HNO_3 (Seastar baseline). Acidified samples were stored in acid cleaned HDPE bottles and the unacidified samples in HDPE bottles that were kept in distilled water for several days. Before sample storage, bottles were thoroughly rinsed with filtered river waters. All the sample splits were carried to the laboratory for measurements of various parameters.

For preparation of blanks, double distilled or Milli Q water was passed through Nulceopore® filter papers at sampling site. Acidified and unacidified aliquots of this water were carried to the laboratory to assess the blank contribution resulting from sample processing.

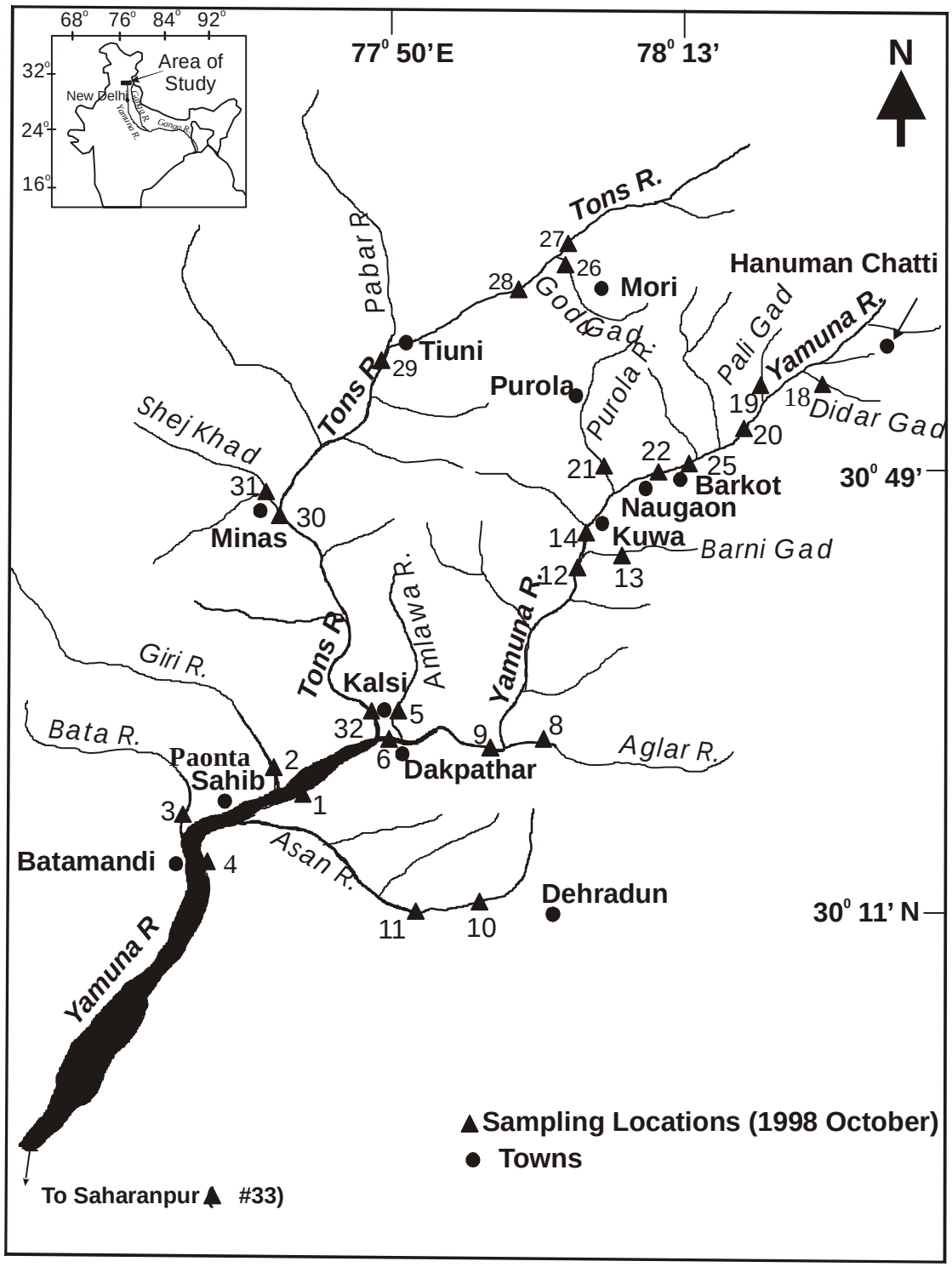

Fig. 2.9 Sampling location map. Locations are only given for October 1998 collection.

(b) Riverbed sediments

Bed sediments were collected from the midstream as well as from the riverbanks with a plastic scoop and stored in zip-lock polythene bags. In the lab, sample aliquots were dried at ~90°C in an oven and sieved using nylon sieves to less than 1 mm size. The <1 mm size fraction of the sediments were powdered either in a Spex ball mill with acrylic container and methylacrate balls or in an agate mortar, sieved to -100 mesh with nylon sieves. Samples larger than 100 mesh were repeatedly powdered to bring all the materials to -100 mesh size. During powdering care was taken to ensure that the samples did not come in contact with any metal surfaces. After thorough homogenization, powdered samples were stored in clean plastic bottles for elemental and isotopic analyses.

(c) Bed rocks

Granite samples were collected from the outcrops in the Yamuna catchment. Rock masses were broken with a hammer, fresh rocks were chipped and stored in plastic bags. In the laboratory, chunks of fresh rocks were hand picked, pulverized and powdered in agate mortars and sieved to -100 mesh through nylon sieves. Sample powders, after thorough homogenization, were stored in clean plastic bottles for analysis.

Phosphorite samples collected by Singh (1999) from Maldeota and Durmala phosphorite mines were powdered and stored following the procedures outlined above for the bedrocks and granites.

2.3 ANALYTICAL TECHNIQUES

2.3.1 River water

(i) Altitude measurement of sampling locations

Altitudes of the sampling locations were measured using an altimeter (Pretel, Model: ALTIplus K2) only for the summer collection (June 1999). The altitude measurements were made w.r.t. the altitude of RW99-2 site. These measured values were calibrated with the altitude of Hanuman Chatti which was known from maps provided by the U.P. State Department of Tourism. For the monsoon (September 1999) and post-monsoon (October 1998) seasons, the altitude was assigned to those locations from where sampling has been done also during summer.

(ii) pH and temperature

pH of the water samples were measured at site using microprocessor based pocket size pH meter (Eutech Cybernetics Model: pH Scan2) with a precision of ±0.1 pH unit. Prior to the measurement, the meter was calibrated w.r.t. buffer solutions of pH 4, 7 and 9.2, freshly prepared from the buffer capsules (Merck®). It was observed during the field campaigns that the pH measured by dipping the electrode of the meter in the river flow and that measured in the river waters collected in a plastic jug were same within the precision of the instrument.

Temperature was measured in the river waters of summer and monsoon collections using a pocket temperature meter (MA Line) with a precision of ±0.1 °C. The measurements were made by dipping the probe into the river flow. The readings attained steady values within 2-3 minutes.

(iii) Major ions

Alkalinity was measured in unfiltered water samples. In the samples from first campaign (October 1998), alkalinity was measured at site by acid titration using a mixed indicator (Merck®). The samples collected during the next two campaigns were analyzed for alkalinity by both manual titration at the sampling site as well as using an Auto Titrator (Metrohm 702 SM Titrino) using a combined glass electrode and fixed pH end point method. The alkalinity values obtained by auto titrator were found to be about 4% higher (Fig. 2.10). The auto

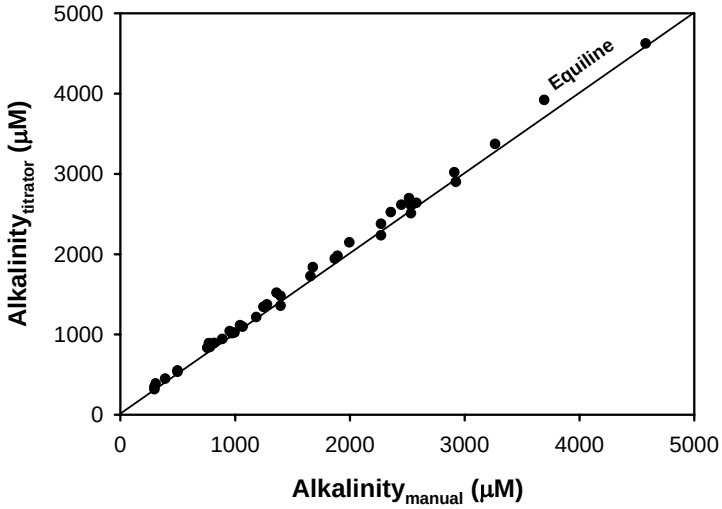

Fig. 2.10 Comparison of alkalinity measurements by manual titration and auto titrator. The values by auto titrator are on average, ~4% higher.

ANALYTICAL SCHEME FOR SAMPLING AND MEASUREMENTS

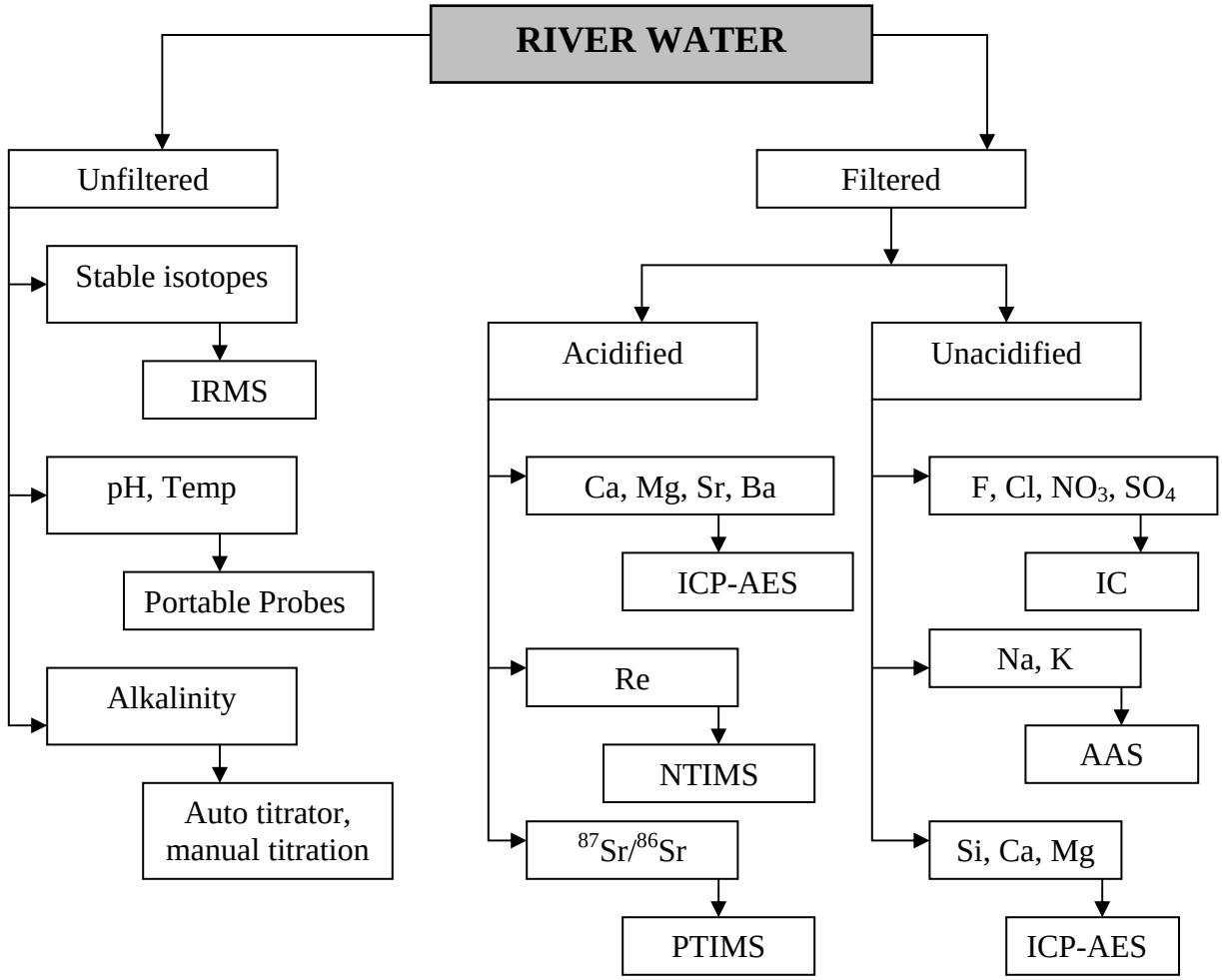

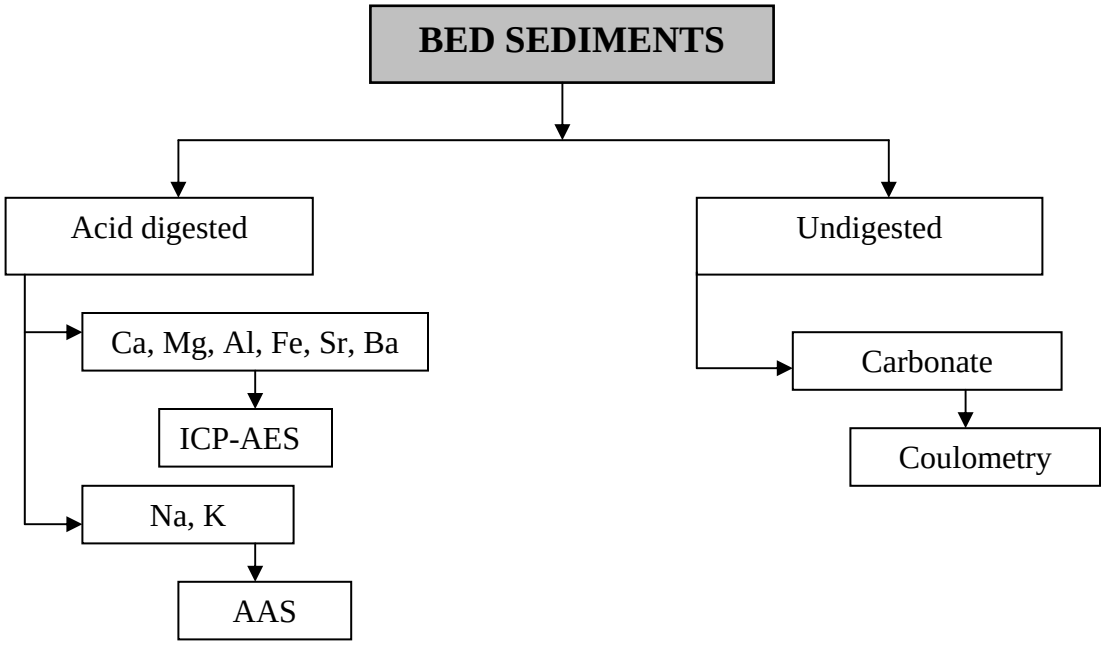

titrator data, for the later two collections, have been accepted and used for all calculations and interpretations. Based on repeat analysis of a number of samples, the reproducibility of alkalinity measurements by auto titrator is ~1% (Appendix 2.2).

Na and K concentrations in the waters were measured by flame-AAS (Perkin Elmer, Model 4000). Calibration was achieved using standard solutions prepared in the laboratory by dissolving analytical grade NaCl and KCl. The concentrated stock solutions were suitably diluted to bring the concentration in the linear analytical range. Based on replicate analysis of the samples, the precision of the measurements are 2.2% and 3.1% for Na and K respectively (Appendix 2.2).

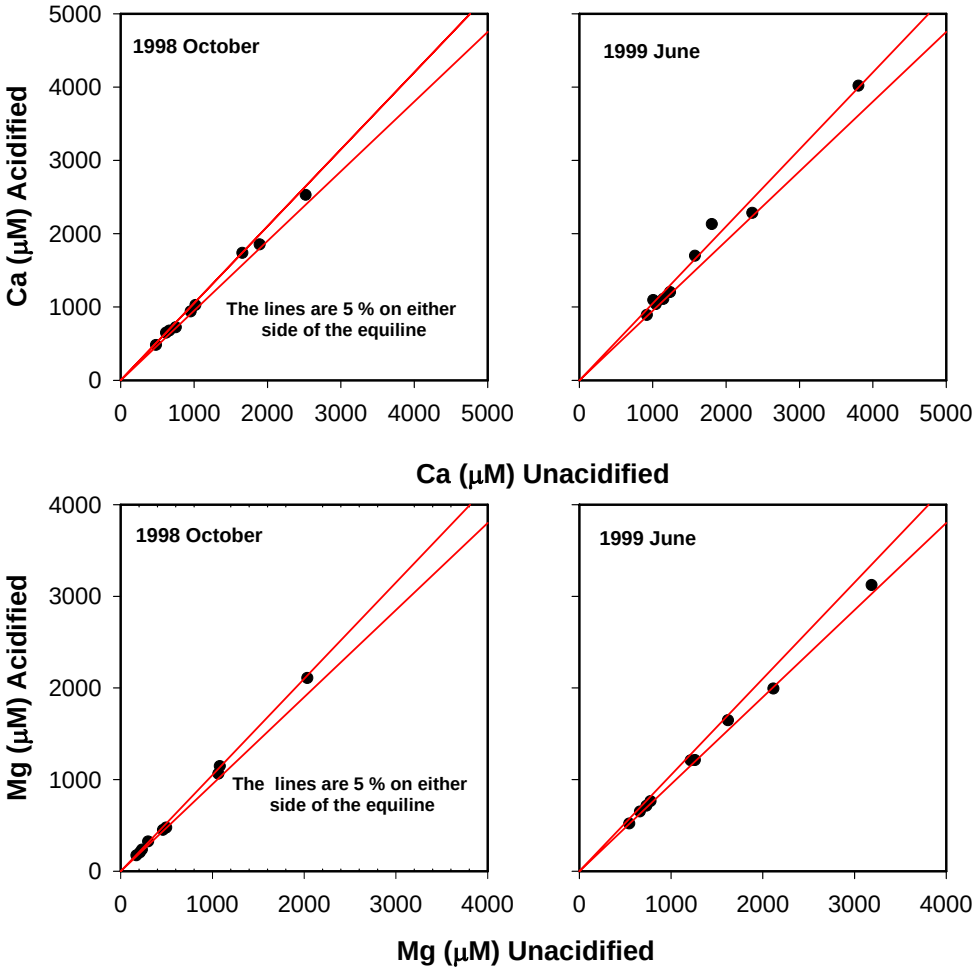

Fig. 2.11 Ca and Mg measurements in unacidified and acidified aliquots of water samples. The concentrations agree within the analytical precision. The analysis was carried out about 10 weeks after sampling.

Si, Ca and Mg were measured by ICP-AES (Jobin Yvon, Model 38S) in unacidified filtered water samples, by sequential scanning of emission lines at wavelengths 251.611, 279.806 and 422.673 nm respectively. The ICP Spectrometer has a Czerny-Turner monochromator of 1 m focal length and 3600 grooves/mm holographic grating with a typical resolution of 0.006 nm, measured w.r.t Cobalt emission line at 228.616 nm. The laboratory standards for Ca, Mg and Si were prepared by dissolving analytical grade $CaCO_3$, pure Mg metal and Na_2SiF_6 respectively. The working calibration curves were generated from these standards. Commercial standards (Merck®) were analyzed on the same calibration lines to check the accuracy of the measurements. At times, the instrument was calibrated w.r.t. commercial standards and elemental concentrations in the laboratory standards were ascertained using these calibration lines. The results of standard analysis for accuracy check are given in the Table 2.1. In a number of water samples, Ca and Mg were analyzed both in the unacidified and acidified filtered aliquots to check on the calcite precipitation, if any, during the period from sampling to analysis. The analysis shows that Ca concentrations in both acidified and unacidified samples were same within the analytical uncertainties (Fig. 2.11) suggesting that over the storage period of 10 weeks, there is no measurable loss of Ca via calcite precipitation in laboratory from these water samples. In addition to analysis of Si by ICP-AES, a number of samples were also analyzed by spectrophotometer using the molybdenum blue method. These data were in good agreement, except in a few samples for which the ICP values were marginally higher. (Fig. 2.12).

F, Cl, NO_3 and SO_4 in the water samples were measured by Ion Chromatography (Dionex series 2000i/SP). The instrument was calibrated w.r.t. standard solutions prepared in the lab from the respective salts (NaF, NaCl, KNO_3 and Na_2SO_4). Cl, NO_3 and SO_4 were separated on a AS4A column using a mixture of 1.8 mM Na_2CO_3 and 1.7 mM $NaHCO_3$ as an eluent, while F was separated on a AS14A column using an eluent of 3.5 mM Na_2CO_3 and 1.00 mM $NaHCO_3$. River waters were analyzed at 10 μS and 30 μS scale whereas rainwater samples were analyzed at 3 μS scale. Check standards of various concentrations were run to check the accuracy and precision of the measurements (Table 2.1). The reproducibility of SO_4 measurements, based on repeat runs of samples is about ±5.4% (Appendix 2.2). The precisions of F, Cl and NO_3 measurements assessed by repeat analysis of standard solutions of varying concentrations (Table 2.1) are better than ±5%. At concentrations less than 0.5 mg

ℓ^{-1}, it is ±10%. The procedural blanks processed at the sampling sites, always produced signals below the detection limits of the instrument (50 μg ℓ^{-1} for F, Cl and NO_3 and 500 μg ℓ^{-1} for SO_4 at 10 μS).

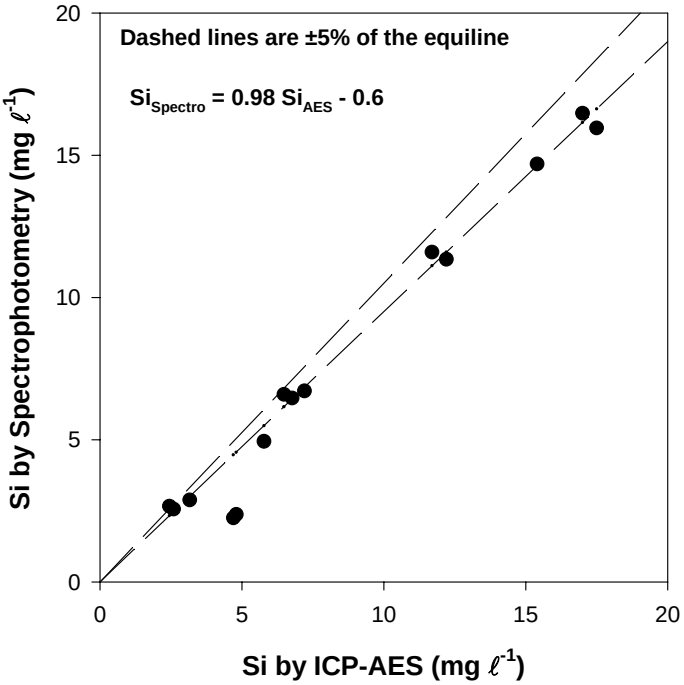

Fig.2.12. Comparison of Si measurement by ICP-AES and spectrophotometry

Table 2.1 Analysis major ions in standards for accuracy check

Parameter	n	Concentration (mg ℓ^{-1})	
		Expected	Measured
Ca	15	10	10.3±0.3
	4	20	20.2±0.7
Mg	15	2	2.05±0.11
	4	4	4.03±0.16
Si	8	2	2.06±0.06
	12	5	5.01±0.18
F	8	0.25	0.24±0.02
	5	0.5	0.48±0.02
	16	1	0.96±0.05
	4	2	2.08±0.06
Cl	7	0.25	0.24±0.03
	5	0.5	0.48±0.04
	17	1	1.03±0.02
	4	2	2.05±0.04
NO_3	14	1	1.02±0.02
	4	2	2.12±0.04
SO_4	4	8	8.44±0.09
	13	20	20.7±0.8

(iv) Strontium and Barium

Sr and Ba concentrations in river water were analyzed in the filtered acidified samples by ICP-AES coupled with a ultrasonic nebulizer (USN). The USN assembly consists of a piezoelectric transducer operating at very high frequency, 1.4 MHz. The water samples are fed by a peristaltic pump onto the face of a quartz plate attached to the transducer. The high frequency oscillations produce fine uniform size aerosols of samples of the size ~10 times smaller than those produced by pneumatic nebulizers. A stream of argon gas then sweeps these aerosols into a heating chamber maintained at 140 °C. The USN is coupled with a desolvation system which consists of a condensation cooler (at ~5 °C) to remove the majority of the solvent (water) aerosols thereby allowing only "dry" aerosols to enter the plasma. This prevents the excessive cooling effect and hence results in improvement of detection limits significantly (Galli and Oddo, 1992; Brenner et al., 1992, Nham, 1992).

Table 2.2 Analysis of Sr and Ba in standards for accuracy check.

Sr ($\mu g\ \ell^{-1}$)				Ba ($\mu g\ \ell^{-1}$)			
n	**Expected**	**Measured**		**n**	**Expected**	**Measured**	
		Mean	**Range**			**Mean**	**Range**
4	5	5.1±0.2	4.9-5.3	5	5	4.8±0.1	4.8-4.9
3	10	9.8±0.2	9.7-10.0	8	10	9.9±0.6	9.0-10.8
13	20	19.8±0.7	18.5-21.3	5	20	19.7±0.5	19.0-20.2

The instrument was calibrated w.r.t. standard solutions prepared from analytical grade salts [$Sr(NO_3)_2$ and $Ba(NO_3)_2$] in the laboratory and the commercial standards (Merck®) were read on these calibration lines. The measured concentrations in the standards agreed with expected values (Table 2.2). The standards were spiked with NaCl solutions to closely match their TDS concentrations with those in river waters. Addition of NaCl in the standards also helps to keep high ionic strength thereby avoiding any possible adsorption of elements onto the walls of the peak tubing of USN. Based on repeat analysis of the samples, the precisions of the measurements are ~3% for Sr and ~5% Ba (Appendix 2.2). Solutions of reference standards G-2 (~6000 times diluted) and W-1 (~3500 times diluted) were analyzed to check the accuracy of the measurements, the results are given in Table 2.3.

Table 2.3 Results of Sr and Ba analysis in reference standards G-2 and W-1.

	G-2 - Measured (μg ℓ^{-1})		W-1 - Measured (μg ℓ^{-1})	
	Sr	**Ba**	**Sr**	**Ba**
	87.8	307	65.7	45.3
	85.2	316	63.5	47.0
	87.9	302	64.7	47.7
	89.4	368	61.2	48.1
Mean measured	***87.6±1.7***	***323±30***	***63.8±1.9***	***47.0±1.2***
Expected[a)]	***80.0***	***315***	***54.3***	***47.1***

[a)]Expected values based on Potts et al. (1992) and dilution of G-2 and W-1 solutions.

(v) Rhenium

Re was measured in waters, granite and carbonate samples. The analytical and measurements scheme of Re measurements in river waters is given in Fig. 4.13. Typically about 100 g of filtered, acidified sample was weighed, spiked with ^{185}Re and stored as such, for at least 24 hours, for sample-spike equilibration. The samples were then dried, digested with ultra pure HNO_3 (Seastar baseline) and taken in 7 ml of 0.8N HNO_3. This solution was loaded onto ion exchange column packed with anion exchange resin (AG1×8, 100-200 mesh). Re was purified through ion exchange in two steps, the first column with a resin volume of 1 ml and the second with 100 μl resin (Trivedi et al., 1999). The resin was loaded onto quartz columns packed with Teflon wool. In the 1ml columns, resin was cleaned with 6N HCl (2 ml twice) and 8N HNO_3 (2 ml thrice), conditioned with 0.8N HNO_3 (3 ml thrice) before loading the sample solution. The columns were washed with 0.8N HNO_3 (3 ml four times) and pure Re was eluted with 8N HNO_3 (4 ml thrice). The eluate was dried, oxidized in conc. HNO_3 and taken in 1ml 0.8N HNO_3. This solution was loaded onto a 100 μl resin column cleaned with 6N HCl (1 ml twice) and 8N HNO_3 (1 ml thrice), conditioned with 0.8N HNO_3 (1 ml thrice). The columns were washed with 0.4N HNO_3 (1 ml thrice) and pure Re eluted in 8N HNO_3 (1 ml thrice).

Pure Re fractions were dried, oxidized with conc. HNO_3 and dissolved in 0.2N HNO_3 during initial phase of analysis and taken in pre-cleaned Teflon tubes attached to a micro syringe. They were loaded and evaporated on high purity degassed Pt filaments (H. Cross

Company, USA). About 10 μg of specpure $Ba(NO_3)_2$ solution was loaded on top of the sample on the Pt filament and put in the mass spectrometer.

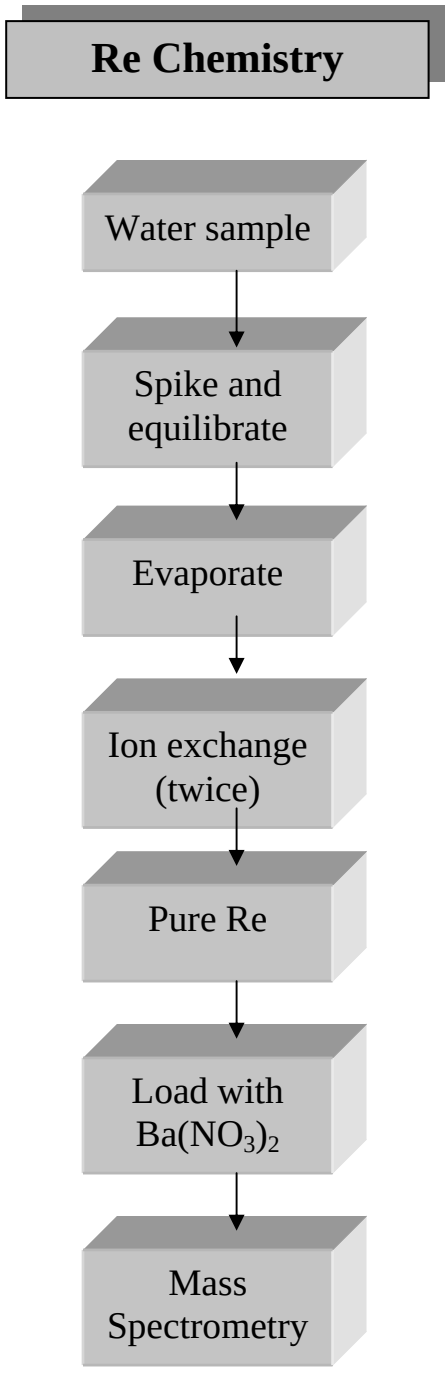

Fig. 2.13 Flow diagram of Re chemistry

It was found that by loading the sample in HNO_3 medium, emission of Re signal was delayed perhaps due to the presence of organic matter. Afterwards, the samples were taken in quartz

distilled water for loading which facilitated the easy emission of the Re signal allowing the samples to be run at a lower temperature than previously done. Re was analyzed in the samples by Negative Thermal Ionization Mass Spectrometry (N-TIMS) following the procedures of Trivedi et al. (1999). Re signal as ReO_4^- was scanned at masses 249 and 251. Corrections for oxide interference were made ($^{185}Re\ ^{16}O_3\ ^{18}O^-$ on $^{187}Re\ ^{16}O_4^-$) to calculate Re concentrations (Trivedi et al., 1999). The ^{185}Re spike used in this study is diluted from the concentrated spike described in Trivedi et al. (1999) and has a strength of 1.193 ng g^{-1}. This spike was calibrated w.r.t. the standard from time to time during the course of the analysis (Table 2.4).

Table 2.4 Re Standard Calibration *(w.r.t. spike 1D : 1.193 ng g^{-1})*

Date	**N**	**X±2σ (ng g^{-1})**	**X±2σ_μ (ng g^{-1})**
03/05/99	141	38.22±0.56	38.22±0.05
22/06/99	93	38.49±0.36	38.49±0.04
01/08/99	79	38.48±0.79	38.48±0.09
02/08/99	105	38.30±0.56	38.30±0.05
Weighted mean		***38.40±0.25***	***38.37±0.03***

This value compares with the values of 37.6 ng g^{-1} based on dilution and the 37.22±0.03 ng g^{-1} as measured by Singh (1999). The above results of calibration exclude one run of the standard with a value of 40.53±0.35 ng g^{-1}.

For the chemistry and mass spectrometry followed for Re analysis, all the acids and water used were of ultrapure quality. HNO_3 was procured from Seastar Chemicals Inc., Canada. Commercially available HCl (analytical grade) was purified in the lab first by distilling it at sub-boiling temperatures using a quartz still and then redistilled in a Teflon distillation set-up under an infra red lamp. Commercially available distilled water was first quartz distilled once in the lab to produce double distilled water (DD H_2O) which was redistilled twice in another quartz distillation set-up. This water (QD H_2O) was used for wet chemistry and mass spectrometry. The Teflon wares (vials and beakers) were procured from Savillex Corporation, USA. The vials, beakers and the quartz columns were initially cleaned thoroughly with DD H_2O, boiled in conc. HNO_3 for several hours, rinsed profusely with DD

H_2O and finally with QD H_2O. The Savillex vials were then filled with a cleaning solution of HF, HNO_3 and H_2O in 2:2:1 ratio, sealed, wrapped with cling films in a plastic petri-dish and kept under infra red lamp for several hours to days. The vials were emptied, rinsed several times with DD H_2O and finally with QD H_2O before use.

The blank contribution of Re to the measured signals was ascertained mainly through incremental analysis. In this approach, 3 or 4 aliquots of the same sample, ranging in size between 10-200g were analyzed for Re. The results, when plotted between the weight of sample analyzed vs. the amount of Re measured, yield an intercept which equals the total procedural blank (Fig. 2.14). In addition, independent determination of the Re blank was made by measuring its contribution from the chemical procedure carried out with all the reagents in quantities similar to those used for the samples. The total Re blank in the present study is determined to be 3.7 pg based on 6 sets of incremental analyses and 6 reagent blank measurements (Table 2.5). This value has been used for blank correction. A part of this total Re blank results from the contribution of Re from Pt filaments. This contribution, measured by running Re-spike loaded on Pt filaments with Ba $(NO_3)_2$, was in the range of 0.2 to 1.9 pg at currents same as or marginally higher than those applied during the sample runs. The blank correction in bulk of the samples is less than 5 % of the measured Re signals, only in four of them (out of 60) the correction exceeded 10 %. The precision of Re measurements, based on the several repeat analyses, is better than 5 % ($\pm 2\sigma$, Table 2.6). The range in the Re concentrations in the samples analyzed in this study is much larger than the blank correction and the precision of the measurements. Out of 75 analyses made (river and mine waters), only in 7 the blank correction would exceed 10 % even if an upper limit of 6.5 pg (mean + 1σ) Re blank is used for the correction. This amount of blank correction is much lower compared to magnitude of two orders of variations observed in the dissolved Re concentrations in the Yamuna and its tributaries. Hence the interpretations and conclusions drawn based on these data (Chapter 5) are not affected blank corrections.

Table 2.5 Re blank contribution (pg)

	Procedural	Incremental
	9.25	5.58
	6.50	3.13
	1.69	0.77
	2.48	4.76
	5.96	3.51
	0.88	0.00
Mean (n = 12)	***3.71±2.77***	

Table 2.6 Results of repeat Re analysis (ng ℓ^{-1})

Sample Code	1	2	3
RW98-4	2.71±0.05	2.78±0.05	2.75±0.05
RW98-6	1.10±0.04	1.08±0.02	
RW98-8	3.52±0.17	3.49±0.15	
RW98-13	0.89±0.04	0.81±0.05	0.85±0.05
RW98-16	0.99±0.04	1.02±0.05	1.02±0.02
RW98-21	0.31±0.04	0.31±0.04	
RW98-31	3.49±0.15	3.48±0.05	
RW99-6	1.47±0.01	1.47±0.06	1.40±0.06
RW99-29	1.93±0.08	1.76±0.06	
RW99-53	0.65±0.02	0.62±0.03	0.66±0.03
RW99-59	0.98±0.04	1.01±0.03	1.02±0.06

Errors are ±2σ

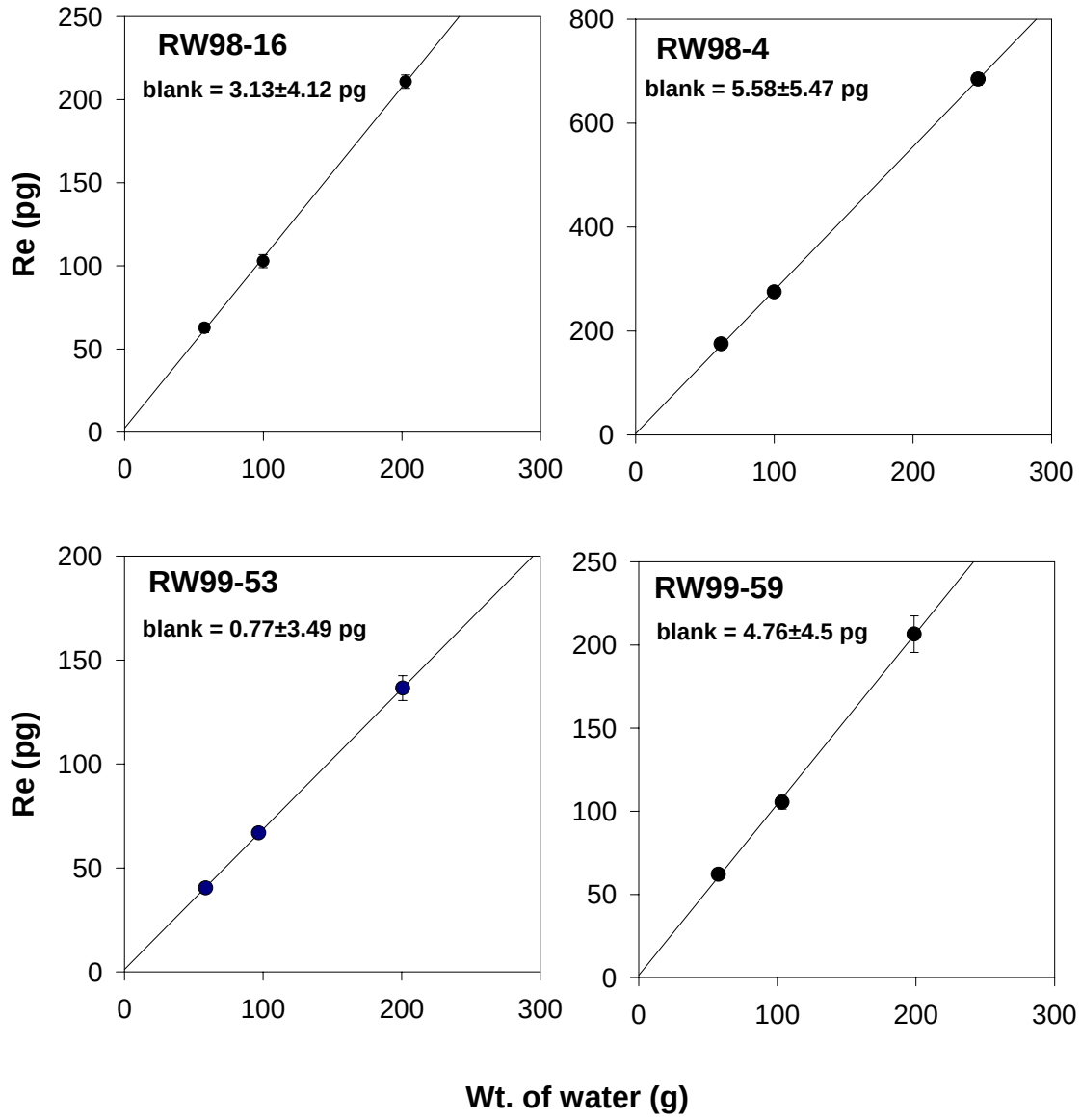

Fig. 2.14 Weight of water analyzed vs. total amount of Re in the sample. The intercept of the regression line gives a measure of the total rhenium blank. The error bars are ±2σ in the Re concentrations.

(vi) Sr isotopes

Sr isotopic abundance were measured in the water and rock samples by a triple collector TIMS (VG 354) at National Geophysical Research Institute, Hyderabad. Sr was separated from Rb and other matrix elements through ion exchange chromatography. The ion exchange columns were made of quartz tubes (ID = 6 mm, OD = 8 mm). The columns were packed with cation exchange resin (Dowex 50X8, 200-400 mesh) to a height of 16 cm. About 50-150 mℓ of water samples were taken in FEP beakers and were kept on a hot plate for drying (these volumes were decided, based on Sr concentration, to yield at least 1 μg Sr load). At incipient dryness, few drops of conc. ultrapure HNO_3 was added and the samples were then dried completely. To this dilute quartz distilled (QD) HCl was added and the samples were dried. This procedure was repeated to ensure complete chloride conversion of Sr in the samples. The dried samples were taken in 1.5 mℓ 2N QD HCl and centrifuged for about 5 minutes in 3 mℓ quartz centrifuge tubes. During centrifugation, the tubes with the samples were covered with parafilms. The supernatant solution was loaded on to the resin column (pre-cleaned with 6N HCl and conditioned with 2N HCl) using a quartz pipette. The walls of the column of reservoirs were washed with 0.5 mℓ 2N HCl twice after the sample solutions passed through completely. The columns were washed with 2N HCl (about 7 times the column volume) before the pure Sr fractions were eluted (with 2N HCl). The pure Sr fractions were collected in 15 mℓ round bottom Savillex vials, evaporated to dryness and stored for analysis. After every sample, the columns were cleaned with about 40 mℓ 6N HCl and 20 mℓ QD water and conditioned with about 25 mℓ 2N HCl. The columns were calibrated from time to time especially when a new batch of acid was used.

The pure Sr fractions were dissolved in 0.5N HNO_3, taken in pre-cleaned Teflon tubes and loaded and evaporated directly on degassed high purity Ta filaments already loaded with H_3PO_4. Sr isotopic measurements were carried out both in single as well as triple collector mode. During the period of analysis SRM 987 standard was run a number of times which yielded an error weighted $^{87}Sr/^{86}Sr$: 0.710184±0.000006 (2σ, n = 9). Some samples were processed in replicate and analyzed for their isotopic abundance. The results of the repeat analyses are given in Table 2.7. Few samples were run twice to check the instrument performance and a few were run both in single as well as triple collector mode (Table 2.7).

Procedural blanks were assessed by processing the distilled water filtered at sampling site and the reagents used for the sample processing. Based on six runs, the blanks for the present study centered at 3.6±0.8 ng. $^{87}Sr/^{86}Sr$ in the blanks were not measured and hence $^{87}Sr/^{86}Sr$ in the samples were not corrected for blank contributions. Using the amount of sample Sr load and assuming $^{87}Sr/^{86}Sr$ to be 0.7 in the blank, it can be calculated that measured $^{87}Sr/^{86}Sr$ will be altered at 10^{-4} only in four of 55 samples analyzed.

Table 2.7 Repeat measurements of Sr isotopes

Sample	Run-I	Run-II
RW98-2[a)]	0.71920 (3)	0.71929 (1)
RW98-11[a)]	0.71491 (3)	0.71491 (5)
RW99-29[a)]	0.72292 (1)	0.72304 (1)
RW99-58[a)]	0.73446 (1)	0.73445 (2)
RW99-63	0.72835 (5)[b)]	0.72840 (1)[c)]
RW99-64	0.73317 (4)[b)]	0.73316 (4)[c)]
RW99-13	0.75548 (2)[d)]	0.75543 (2)[e)]
RW99-29R	0.72307 (1)[d)]	0.72304 (1)[e)]

[a)]processed and run in duplicates, [b)]run in single collector, [c)]run in triple collector, [d)]first run in triple collector, [e)]second run in triple collector. The numbers in the parentheses indicate error on the last decimal places (±1σ).

(vii) Stable isotopes:

The oxygen and hydrogen isotope measurements were carried out on unfiltered water samples using a water equilibration system and GEO 20-20 mass spectrometer (PDZ Europa, U.K.). 1 ml of water sample was pipetted into a glass bottle with airtight stopcock, equilibrated with tank CO_2 (35^oC, 12 hours) for oxygen and tank H_2 (35 ^oC, 12 hours in presence of platinum catalyst) for hydrogen. Aliquots of equilibrated CO_2 and H_2 were cryogenically separated (Epstein and Mayeda, 1953; Brand et al., 1996). The flushing, filling and sampling of gases were done using a Gilson auto sampler controlled by the mass spectrometer software. The isotopic compositions of CO_2 and H_2 were analyzed following standard IRMS procedures (Allison et al., 1995). Along with each batch of samples, a laboratory water standard (NARM, Narmada River Water, $\delta^{18}O$ = -4.52‰, δD = -35.2‰) was also measured using which the final sample δ-values (w.r.t. V-SMOW) were calculated. The overall precision, based on repeat measurements of about 16 samples, is ±0.1‰ for $\delta^{18}O$

and ±1.2‰ for δD (Fig. 2.15). For δD, two sets of repeat analysis showed significant difference, ~4‰ each. Excluding these runs, the precision of δD becomes ~0.8‰.

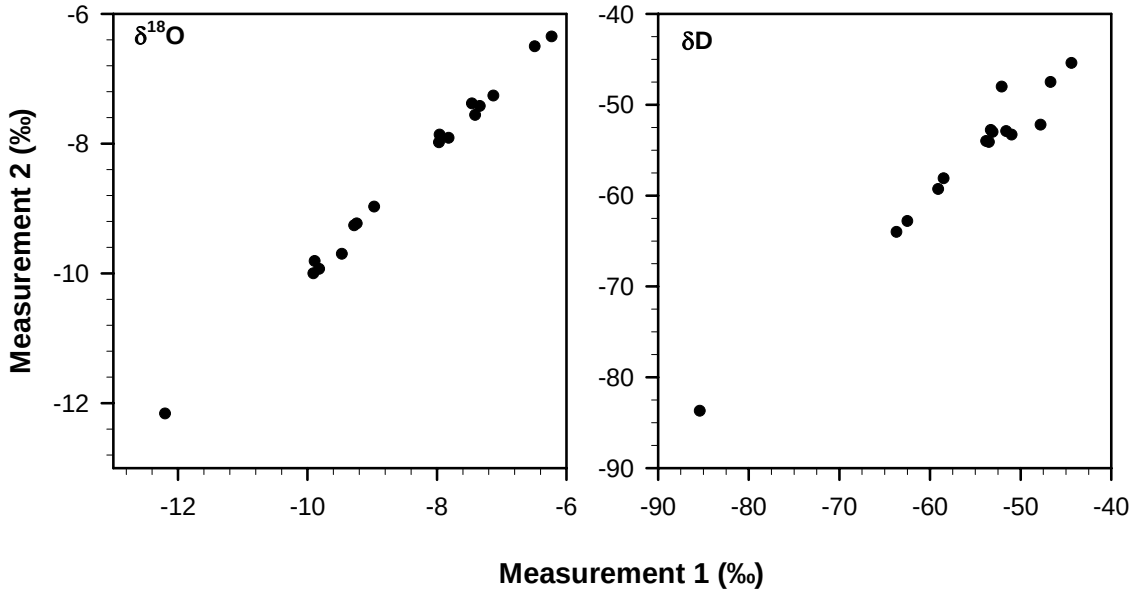

Fig. 2.15 Repeat measurements of $\delta^{18}O$ and δD in river water samples

2.3.2 Rocks and bed sediments

(i) Dissolution

~500 mg of powdered sample (bed rock/granite) was weighed and dissolved in PTFE dish with HF-HCl-HNO_3-$HClO_4$ mixture. For some samples, it was necessary to centrifuge the sample-reagent mixture and attack the residue afresh with the acids. The final solution was taken in 1N HCl and made up to a known volume. These were used for elemental analysis after suitable dilution wherever necessary. USGS rock standards (G-2 and W-1) were also dissolved along with the samples. Reagents used in the sample dissolution procedure were taken to assess the blank concentration from reagents.

(ii) Major ions

Ca, Mg, Al, Fe in bedrock samples were measured by ICP-AES. The instrument was calibrated with laboratory standards prepared as: Ca from $CaCO_3$, and Mg, Al and Fe from pure metals. The USGS standard G-2 and commercial standard solution (Merck®) were run on the same calibration curves. Na and K in the acid digested samples were measured by flame AAS. Standards for calibration were prepared in the laboratory by dissolving analytical

grade NaCl and KCl salts. Mixed or single working standards were prepared in the range of 2 to 10 mg ℓ^{-1} for Na and 1 to 10 mg ℓ^{-1} for K to generate linear calibration curves. Accuracy of the measurements was checked by analyzing the concentrations of major ions of reference standard G-2 on the same calibration curve. Measured concentrations agreed well with the reported values (Table 2.8, Fig. 2.16). Reagent blanks always produced signal negligibly small compared to the sample signals. Few samples, dissolved in replicates, were run to check the reproducibility of the major ion measurements in the bed sediments (Fig. 2.17).

Table 2.8 Results of major ion analysis in reference standard G-2

Element (%)	Reported[a)] (%)	Measured (%)
Na	3.02	3.02
K	3.73	3.66
Ca	1.41	1.39
Mg	0.46	0.46
Al	8.01	8.02
Fe	1.85	1.82

[a)]Reported values from Potts et al. (1992)

(iii) Strontium and Barium

Sr and Ba in the bed sediments were measured by ICP-AES coupled with the pneumatic nebulizer. W-1 dissolved along with the samples were run in the calibration line made from the solution of G-2. Sr and Ba concentrations measured in W-1 were in good agreement with the reported values (Table 2.9)

Table 2.9 Sr and Ba analysis in reference standard W-1 (pneumatic nebulizer)

Run#	Sr (ppm)	Ba (ppm)
1	190	151
2	205	163
3	181	154
4	187	156
4	202	169
6	189	154
Mean	***192±8***	***158±6***
Reported[a)]	***187***	***162***

[a)]Reported values from Potts et al. (1992)

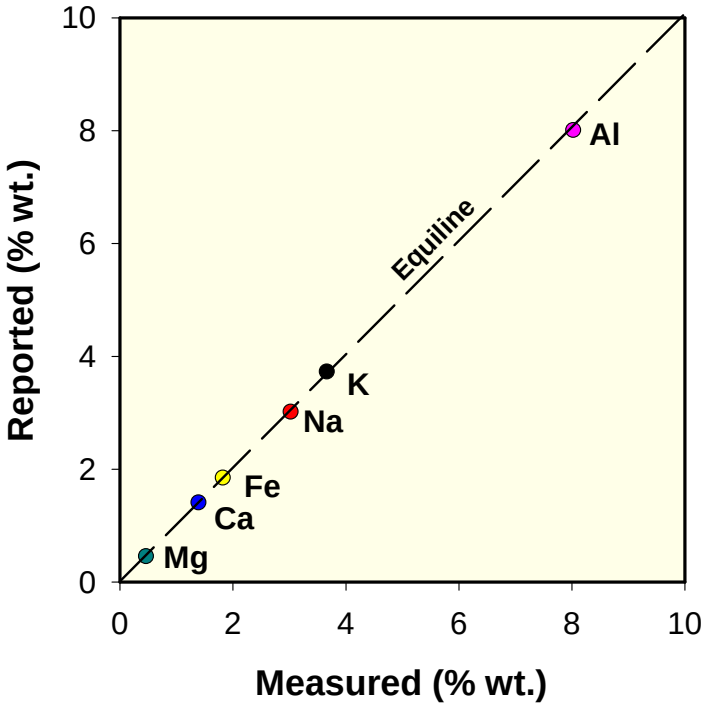

Fig. 2.16 Comparison of measured and reported (Potts et al., 1992) elemental concentrations in the reference standard G-2.

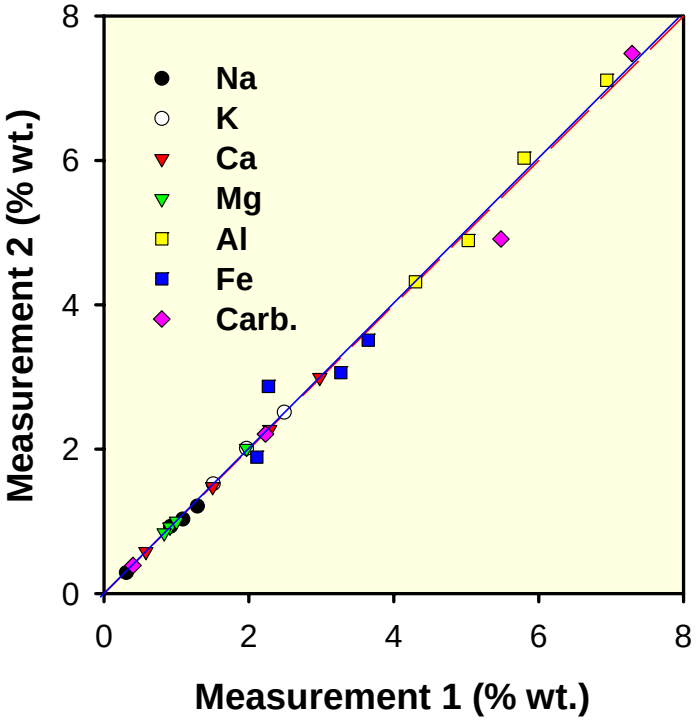

Fig. 2.17 Replicate analysis of bed sediments. Replicate analyses of the samples agree well within the analytical precision. Equiline (dashed red) and the regression line (solid blue) overlap on each other.

(iv) Carbonate contents

Carbonate contents in the bedrocks and granites were measured by Coulometric method (UIC Coulometer, Model: 5012). The analytical calibration was carried with standard solutions made from pure Na_2CO_3 salts dried in oven for 8-10 hours. CO_2 was evolved from ~10-100 mg of powdered sediment/granite samples by treating them with 40% orthophosphoric acid for 10 minutes at 70 °C in an extraction unit in the Coulometer. Compressed air stripped of CO_2 (by passing the air through a 50 % KOH solution) was used as a carrier gas. The liberated CO_2 from the samples was swept by the carrier gas and dried by passing through a column of activated silica gel and anhydrous $MgClO_4$. The dried CO_2 was then passed through the coulometer titration cell. Carbonate contents in the bed sediments were calculated assuming that all CO_2 is from $CaCO_3$. Considering the abundance of dolomites in the catchment (Valdiya, 1980) and high Mg measured in some of the bedrock samples it is likely that part of the carbonates is dolomites. Some samples were run in replicates based on which the reproducibility of the measurement was ascertained to be better than 4 % (Appendix 2.2, Fig. 2.17).

Appendix 2.1

Rivers, locations and seasons of sampling, pH and temperature of the water samples.

Code	River	Location	Drainage Basin[a)]	Season[b)]	pH	Temp. (°C)
Yamuna mainstream						
RW98-16	Yamuna	Hanuman Chatti	HH	PM	8.3	
RW99-13	Yamuna	Hanuman Chatti	HH	S	8.7	10.2
RW98-20	Yamuna	D. of Pali Gad Bridge	LH	PM	8.4	
RW98-25	Yamuna	Barkot	LH	PM	8.7	
RW99-19	Yamuna	Barkot	LH	S	8.9	19.4
RW99-17	Yamuna	Kuthnaur village	LH	S	8.5	15.7
RW98-22	Yamuna	U. of Naugaon	LH	PM	8.7	
RW99-18	Yamuna	Near Lakhmandal	LH	S	9.2	20.2
RW98-15	Yamuna	U. of Barni Gad's confluence	LH	PM	8.7	
RW98-14	Yamuna	D.of Barni Gad's confluence	LH	PM	8.9	
RW99-11	Yamuna	D.of Barni Gad's confluence	LH	S	9.1	21.1
RW98-12	Yamuna	D. of Nainbag	LH	PM	8.6	
RW98-9	Yamuna	D. of Aglar's confluence	LH	PM	8.7	
RW99-51	Yamuna	D. of Aglar's confluence	LH	M	8.6	18.1
RW98-6	Yamuna	U. of Ton's confluence	LH	PM	8.7	
RW99-30	Yamuna	U. of Ton's confluence	LH	S		
RW99-64	Yamuna	U. of Ton's confluence	LH	M	8.4	22.1
RW99-31	Yamuna	D. of Ton's confluence	LH	S	8.4	26.9
RW99-53	Yamuna	D. of Ton's confluence	LH	M	8.5	20.6
RW98-1	Yamuna	Rampur Mandi, Paonta sahib	LH	PM	8.6	
RW99-2	Yamuna	Rampur Mandi, Paonta sahib	LH	S	8.6	21.9
RW99-58	Yamuna	Rampur Mandi, Paonta sahib	LH	M	8.4	20.6
RW98-4	Yamuna	D. of Bata's confluence	LH	PM	8.4	
RW99-5	Yamuna	D. of Bata's confluence	LH	S	8.9	25.9
RW99-55	Yamuna	D. of Bata's confluence	LH	M	7.7	27.5
RW98-33	Yamuna	Yamuna Nagar, Saharanpur	LH	PM	8.4	
RW99-7	Yamuna	Yamuna Nagar, Saharanpur	LH	S	8.7	30.5
RW99-54	Yamuna	Yamuna Nagar, Saharanpur	LH	M	8.2	24.1
Tributaries						
RW98-17	Jharjhar Gad	Hanuman Chatti-Barkot Road	HH	PM	8.2	
RW98-18	Didar Gad	Hanuman Chatti-Barkot Road	HH	PM	8.0	
RW99-14	Didar Gad	Hanuman Chatti-Barkot Road	HH	S	8.3	12.7
RW98-19	Pali Gad	Pali Gad Bridge	HH, LH	PM	8.4	
RW99-16	Pali Gad	Pali Gad Bridge	HH, LH	S	8.1	18.3
RW99-15	Bajri Gad	U. of the bridge over it	LH	S	8.4	13.7

RW98-13	Barni Gad	Kuwa	LH	PM	9.2	
RW99-12	Barni Gad	Kuwa	LH	S	9.1	29.7
RW98-23	Oli Gad	Kuwa-Kapnol Road	LH	PM	8.7	
RW98-21	Purola	Between Naugaon and Purola	LH	PM	8.7	
RW99-20	Purola	Purola-Naugaon Road	LH	S	9.1	21.1
RW98-24	Gamra Gad	Near the bridge over it	LH	PM	8.7	
RW98-26	Godu Gad	Purola-Mori Road	HH, LH	PM	8.3	
RW99-21	Godu Gad	Purola-Mori Road	HH, LH	S	8.8	22.9
RW99-27	Pabar	U. of confluence with Tons	HH, LH	S	7.9	19.9
RW98-27	Tons	Mori	HH	PM	8.1	
RW99-22	Tons	Mori	HH	S	8.4	14.4
RW98-28	Tons	D. of Mori	LH	PM	7.9	
RW99-26	Tons	Before Pabar joins	LH	S	8.0	16.7
RW98-29	Tons	Tiuni	LH	PM	8.0	
RW99-28	Tons	Tiuni	LH	S	7.8	17.7
RW98-31	Shej Khad	Minas	LH	PM	8.6	
RW99-23	Shej Khad	Minas	LH	S	8.7	24.2
RW99-25	Tons	Before Shej Khad joins	LH	S		
RW98-30	Tons	Minas, after confluence	LH	PM	8.4	
RW99-24	Tons	Minas, after confluence	LH	S	8.7	23.4
RW98-5	Amlawa	Kalsi-Chakrata Road	LH	PM	8.6	
RW99-62	Amlawa	Kalsi-Chakrata Road	LH	M	8.4	23.8
RW98-32	Tons	Kalsi, U. of confluence	LH	PM	8.7	
RW99-29	Tons	Kalsi, U. of confluence	LH	S	9.0	27.8
RW99-63	Tons	Kalsi, U. of confluence	LH	M	8.5	21.3
RW98-8	Aglar	U. of Yamuna Bridge	LH	PM	8.8	
RW99-10	Aglar	U. of Yamuna Bridge	LH	S		
RW99-52	Aglar	U. of Yamuna Bridge	LH	M	8.5	22.4
RW98-2	Giri	Rampur Mandi	LH, SW	PM	8.4	
RW99-3	Giri	Rampur Mandi	LH, SW	S	8.5	27.8
RW99-57	Giri	Rampur Mandi	LH, SW	M	8.3	26.6
RW98-3	Bata	Bata Mandi	LH, SW	PM	8.5	
RW99-4	Bata	Bata Mandi	LH, SW	S	8.9	27.4
RW99-56	Bata	Bata Mandi	LH, SW	M	7.9	27.8
RW98-10	*Tons*	*Tons Pol*, Dehradun	LH	PM	8.6	
RW99-65	*Tons*	*Tons Pol*, Dehradun	LH	M	8.4	25.3
RW98-11	Asan	Simla Road Bridge	LH, SW	PM	8.3	
RW99-1	Asan	Simla Road Bridge	LH, SW	S	8.3	26.6
RW99-61	Asan	Simla Road Bridge	LH, SW	M	7.9	27.4
Ganga						
RW98-34	Ganga	Rishikesh	LH	PM	8.6	
RW99-6	Ganga	Rishikesh	LH	S	8.4	15.7

RW99-59	Ganga	Rishikesh	LH	M	8.4	18.6
RW99-8	Bandal	Near Maldeota	LH	S		
Springs						
RW98-7	Kemti Fall	Dehradun-Mussourie Road	LH	PM	8.2	8.2
RW99-9	Kemti Fall	Dehradun-Mussourie Road	LH	S		
RW99-60	Spring	Shahashradhara	LH	M	7.1	7.1

[a] LH: Lesser Himalaya, HH: Higher Himalaya. [b]PM: post-monsoon, S: summer, M: monsoon..

Appendix 2.2 Coefficients of variation for properties measured

Based on duplicate analysis of a number of samples, the coefficients of variation for various measurements were calculated using the formula:

$$CV(\%) = \left[\frac{1}{2n} \Sigma \left(\frac{d_i}{x_i} \right)^2 \right]^{\frac{1}{2}} \times 100$$

where d_i is the difference between the duplicates with mean x_i and n is the total sets of duplicates analyzed.

ELEMENT	N	COEFF. VAR (%)
Na	15	2.21
K	14	3.09
Ca	33	4.39
Mg	33	4.85
Alk.	8	1.04
SO_4	15	5.36
Carb.	5	3.67
Sr	15	2.71
Ba	11	4.64

N = number of repeat measurements. The results of major ions, Sr and Ba are in water samples and carbonates in bed sediments.

Chapter 3

Stable Isotopes in the Yamuna River System

3.1 INTRODUCTION

Stable isotopes of oxygen and hydrogen being the constituents of water molecules serve as "ideal conservative" tracers to study hydrological processes. Variations in the isotopic ratios ($^{2}H/^{1}H$ and $^{18}O/^{16}O$) in water are brought about in response to processes such as mixing of water from different sources, condensation of water vapour and evaporation of water. The variations in stable isotope ratios in waters are used to characterize these hydrological processes operating in surface and groundwater systems and to trace their sources.

Rivers receive waters from various sources: precipitation, snow/glacial melt and groundwater influx. The relative contributions of these sources vary with time of the year depending on the locations of the river catchment. The water budget of a river is controlled by processes such as mixing of its tributaries, evaporation during its transit and its interaction with the groundwater regime. Rivers which receive waters mainly from precipitation at a certain period of the year (e.g. monsoon period in India), respond to changes in the isotopic composition of the precipitation, the time of response being dependent on factors such as the size of the river, gradient of the river bed and vegetation in the catchment. Measurement of stable isotopic composition in the rivers can have many applications. These include identification of the sources of water, assessment of the mixing proportions among them and the estimation of evaporation losses (Ingraham, 1998). In addition, comparison of stable isotope data of river waters with those of precipitation and ground waters from the same region can be used to evaluate infiltration of river water to subsurface aquifers and the role of evapotranspiration in water budget of precipitation (Payne, 1983; Gat and Matsui, 1991; Krishnamurthy and Bhattacharya, 1991; Ingraham, 1998). More recently, Lambs (2000), using $\delta^{18}O$ and conductivity and their mixing relation in stream waters of the Bhagirathi river near Gangotri in the Himalaya, quantified the relative contributions of glacier and snow melt to its water budget.

This chapter presents δD-$\delta^{18}O$ systematics of the Yamuna River System (YRS). The comprehensive stable isotope data acquired in this study in conjunction with those available for New Delhi precipitation (IAEA, 1998), help to infer the sources of water to the YRS and assess the role of processes such as recycling of moisture via evaporation of rainwater and river water, mixing of rain and snow melt, rainout from the cloud mass and the catchment

topography in controlling the isotopic composition of the YRS. The altitudinal variations in the river water isotopic composition, an aspect discussed in some detail in this study, has important implications to (i) tracking the source of water recharging at different elevations and (ii) reconstruction of paleoelevation in the Himalayan region (Chamberlain and Poage, 2000; Garzione et al., 2000a, b).

Prior to this work, $\delta^{18}O$ and δD measurements in the headwaters of the Ganga and the Indus draining the Himalaya have been used to derive information on source(s) of water to these rivers and 'altitude effect' of precipitation in the catchment area as imprinted in the rivers (Ramesh and Sarin, 1992; Bartarya et al., 1995; Pande et al., 2000). Garzione et al. (2000a,b) studied the variation of $\delta^{18}O$ with altitude in the tributaries of the Seti River and the Kali Gandaki in the Nepal Himalaya and used these data in conjunction with $\delta^{18}O$ of carbonates to estimate paleoelevation of Tibet.

The results of the present study have been integrated and compared with those from the Ganga and the Indus headwaters (Ramesh and Sarin, 1992; Pande et al., 2000) and the Gaula catchment (Bartarya et al., 1995) to better understand the variability in the stable isotope composition of the rivers draining the southern slopes of the Himalaya and their implications to paleoaltitude estimation.

3.2 RESULTS AND DISCUSSION

The $\delta^{18}O$ and δD values of the Yamuna mainstream and its tributaries for the three sampling periods are presented in the Table 3.1. They range from -6.2 to -10.3‰ and -41.7 to

$\delta^{18}O$ and δD respectively, corresponding to the altitude range of ~500 to ~2400 m. In general, the isotopic composition of the streams are more depleted during monsoon and in samples from higher altitude. The isotopic composition of the Yamuna waters are slightly enriched in ^{18}O and D compared to the Ganga headwaters ($\delta^{18}O$: -7.8 to -14.4‰ and δD: -51 to -103‰, Ramesh and Sarin, 1992) and depleted relative to streams of the Gaula river catchment in the Lesser Himalaya (-5.2 to -9.0‰ and -37 to -63‰; altitude ~550-1700 m, Bartarya et al., 1995). These differences most likely result from altitude and seasonal effects. Among the Ganga headwater samples, those from the Bhagirathi (at Gangotri) and Kedarganga collected at ~3000 m altitude, close to their glacial melt source have the most depleted isotopic composition (Ramesh and Sarin, 1992). The ranges in isotopic composition for the remaining Ganga headwaters are within those observed for the (Table 3.1). In addition

to altitude, some variability in the isotopic composition of these two river systems can arise from seasonal effects (see following section) as the Ganga samples were collected during April whereas those from Yamuna were sampled in June, September and October.

Table 3.1 δD, $\delta^{18}O$, deuterium excess and ΣCat* data of the Yamuna and its tributaries in the Himalaya.

Code	River	Altitude (m)	Season[a)]	$\delta^{18}O$ (‰)	δD (‰)	d[b)] (‰)	ΣCat*[c)] (µEq)
Yamuna mainstream							
RW98-16	Yamuna	2350	PM	-10.3	-67.1	15.3	1069
RW99-13	Yamuna	2350	S	-9.4	-62.1	13.1	1056
RW98-20	Yamuna		PM	-9.9	-63.7	15.5	1101
RW98-25	Yamuna	1465	PM	-9.2	-58.1	15.5	1188
RW99-19	Yamuna	1465	S	-8.6	-56.2	12.6	1269
RW98-22	Yamuna		PM	-9.0	-57.9	14.1	1226
RW99-17	Yamuna	1737	S	-9.0	-59.3	12.7	1196
RW99-18	Yamuna	1234	S	-8.6	-55.5	13.3	1454
RW98-15	Yamuna		PM	-9.0	-58.5	13.5	1480
RW98-14	Yamuna		PM	-8.7	-57.9	11.7	1581
RW98-12	Yamuna		PM	-8.7	-57.0	12.6	1467
RW99-11	Yamuna	1219	S	-8.1	-55.9	8.9	1686
RW98-9	Yamuna		PM	-8.7	-57.5	12.1	1959
RW99-51	Yamuna		M	-9.9	-72.0	7.2	903
RW98-6	Yamuna	768	PM	-8.5	-57.2	10.8	2060
RW99-30	Yamuna	768	S	-8.0	-53.1	10.9	2536
RW99-64	Yamuna	768	M	-8.7	-57.5	12.1	1675
RW99-31	Yamuna	500	S	-7.9	-52.7	10.5	2204
RW99-53	Yamuna	500	M	-9.9	-70.0	9.2	1007
RW98-1	Yamuna	628	PM	-9.1	-61.7	11.1	1432
RW99-2	Yamuna	628	S	-8.6	-59.2	9.6	2167
RW99-58	Yamuna	628	M	-9.9	-67.3	11.9	1274
RW98-4	Yamuna	601	PM	-7.9	-53.5	9.7	3279
RW99-5	Yamuna	601	S	-7.4	-51.0	8.2	3538
RW99-55	Yamuna	601	M	-7.8	-53.8	8.6	2785
RW98-33	Yamuna	484	PM	-10.3	-68.5	13.9	2973
RW99-7	Yamuna	484	S	-7.8	-54.4	8.0	3063
RW99-54	Yamuna	484	M	-9.5	-65.5	10.5	1495
Tributaries							
RW98-17	Jharjhar Gad		PM	-9.0	-57.6	14.4	544
RW98-18	Didar Gad		PM	-9.2	-60.6	13.0	290
RW99-14	Didar Gad		S	-8.6	-55.6	13.2	319
RW98-19	Pali Gad	1851	PM	-8.3	-52.7	13.7	1127
RW99-16	Pali Gad	1851	S	-7.6	-48.7	12.1	1621
RW98-13	Barni Gad		PM	-8.4	-55.8	11.4	2533
RW99-12	Barni Gad		S	-7.4	-53.0	6.2	3839
RW98-21	Purola	1443	PM	-8.1	-52.4	12.4	1746
RW99-20	Purola	1443	S	-7.5	-51.6	8.4	3161
RW99-15	Bajri Gad	2060	S	-7.3	-52.1	6.3	472
RW98-23	Oli Gad		PM	-8.3	-54.1	12.3	1912
RW98-24	Gamra Gad		PM	-8.6	-56.1	12.7	1835

RW98-26	Godu Gad		PM	-8.2	-51.8	13.8	498
RW99-21	Godu Gad		S	-7.8	-54.6	7.8	895
RW98-27	Tons	1419	PM	-10.2	-66.9	14.7	524
RW99-22	Tons	1419	S	-9.8	-61.1	17.3	472
RW98-28	Tons		PM	-10.2	-65.4	16.2	551
RW99-26	Tons	1217	S	-9.2	-59.4	14.2	409
RW99-27	Pabar	1224	S	-8.5	-58.6	9.4	697
RW98-29	Tons		PM	-10.1			642
RW99-28	Tons		S	-9.0	-58.3	13.7	536
RW99-25	Tons		S	-9.3	-61.7	12.7	701
RW98-31	Shej Khad	1004	PM	-9.3			2074
RW99-23	Shej Khad	1004	S	-8.3	-57.4	9.0	3073
RW98-30	Tons	1004	PM	-9.7	-62.5	15.1	1297
RW99-24	Tons	1004	S	-8.6	-58.7	10.1	2550
RW98-5	Amlawa		PM	-7.9	-53.3	9.9	2106
RW99-62	Amlawa		M	-8.1	-53.8	11.0	2174
RW98-32	Tons	770	PM	-9.0	-59.3	12.7	2614
RW99-29	Tons	770	S	-8.3	-55.6	10.8	2603
RW99-63	Tons	770	M	-9.8	-65.6	12.8	1856
RW98-8	Aglar	948	PM	-8.3	-54.8	11.6	4255
RW99-10	Aglar	948	S	-7.7	-53.7	7.9	9152
RW99-52	Aglar	948	M	-8.3	-61.1	5.3	4177
RW98-2	Giri		PM	-7.3	-50.7	7.7	5707
RW99-3	Giri		S	-6.8	-48.1	6.3	7156
RW99-57	Giri		M	-7.2	-50.7	6.9	4540
RW98-3	Bata	615	PM	-7.6	-47.8	13.0	3069
RW99-4	Bata	615	S	-6.4	-44.2	7.0	4047
RW99-56	Bata	615	M	-7.1	-48.2	8.6	3276
RW98-10	Tons		PM	-7.3	-46.7	11.7	5122
RW99-65	Tons		M	-6.5	-41.7	10.3	4291
RW98-11	Asan		PM	-6.8	-45.3	9.1	6098
RW99-1	Asan		S	-6.2	-44.4	5.2	5531
RW99-61	Asan		M	-6.6	-44.0	8.8	5872
Springs							
RW98-7	Kemti Fall		PM	-8.6	-57.4	11.4	9142
RW99-60	Shahashradhara		M	-6.9	-44.7	10.5	34950

a)S = summer, M = monsoon, PM = post-monsoon, **b)**d =$\delta D - 8\delta^{18}O$. **c)**ΣCat* = Na*+K+Ca+Mg, Na* is sodium corrected for cyclic contributions using Cl as an index (Data from table 4.1).

3.2.1 Seasonal variation

In regions, such as the YRS basin, experiencing monsoon precipitation, there is heavy downpour during three months, July, August and September of every year. The local rainfall in the YRS basin, is largely governed by tropical storms and depressions forming over the Bay of Bengal and Arabian Sea which enter into the region from southeast and southwest direction (Devi, 1992). Such intense rainfall during monsoon is characterized by lighter stable isotopic composition, compared to those during the non-monsoon months, as monsoon

rains are derived from cloud mass which become isotopically lighter by progressive rainouts during their movement (Rozanski et al., 1993; Araguas et al., 1998).

The $\delta^{18}O$ and δD values of the YRS samples, indeed, show clear seasonal variations (Table 3.1), samples from the monsoon season (September) being more depleted in ^{18}O and D compared to those collected during summer (June, Fig. 3.1, Table 3.1). This trend, as

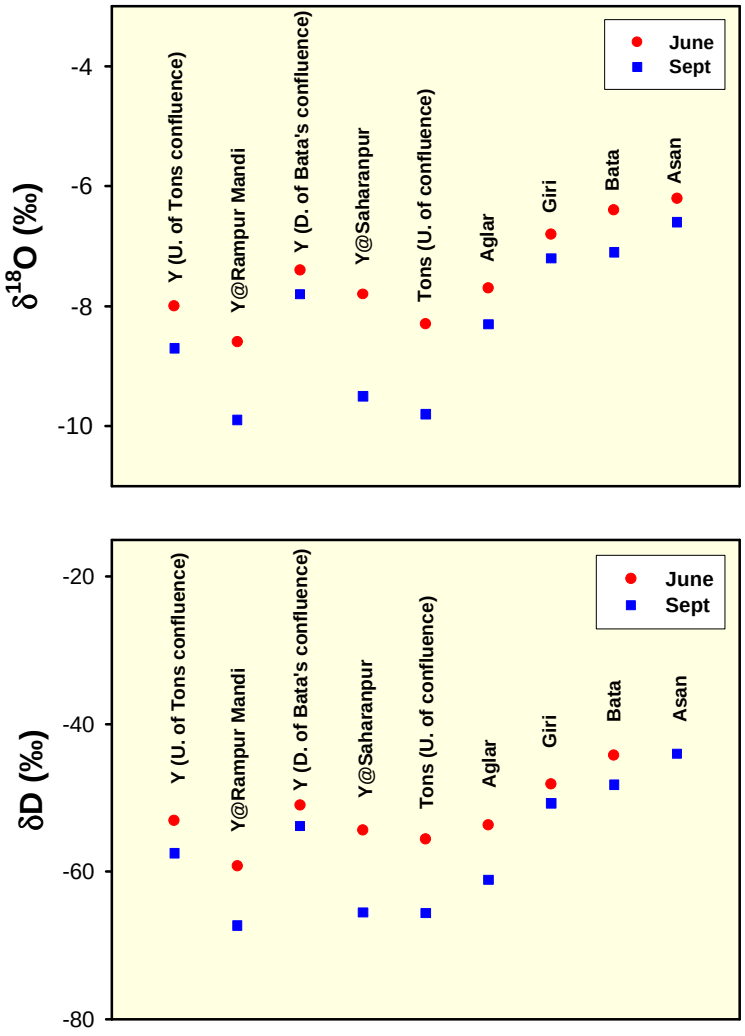

Fig. 3.1 Seasonal variation of $d^{18}O$ and dD in the YRS. June samples are enriched in ^{18}O and D compared to September samples. Y: Yamuna, D: downstream, U: upstream

already discussed, can be explained in terms of heavy rainfall during monsoon, commonly known as "amount effect". In north India, air-masses carrying large amount of moisture move from the source region during monsoon season and shed a significant fraction of their moisture during their transit in spells of heavy rainfall events. Such rainouts continuously

deplete the heavy isotopes from the onward moving clouds. As a result, vapor clouds farther away from source, such as those reaching the Himalayan region, are isotopically depleted and precipitation from such clouds are characterized by lower δ-values. The isotopic composition of precipitation at any given location, therefore, would depend, in addition to the the initial isotopic composition of the cloud vapour and temperature of condensation, on the fraction of moisture removed from the cloud by condensation prior to reaching the location. This fraction is likely to vary with season, with more rain out during the monsoon thus making its impact more pronounced in September as it is a month with more rainfall than June. Thus, the oxygen isotopic ratios in September samples are expected to be depleted relative to those in June. This is consistent with the results (Fig. 3.1) that $\delta^{18}O$ of September samples are 0.5-1.5‰ depleted compared to June samples. Rozanski et al. (1993) also observed a decrease in $\delta^{18}O$ of precipitation at New Delhi with an increase in the amount of precipitation during the period of May to September. Heavy monsoonal precipitation undergoes little post condensation exchange with the water vapor and evaporation compared to the light rainfall thus enhancing the amount effect (Hoffmann and Heimann, 1997). During monsoon season, lower temperature, higher humidity and rapid downpour does not allow evaporation of rains and their significant exchange with water vapour after their condensation, whereas rainfall during June, being less in amount, is likely to undergo appreciable exchange when the temperature is relatively higher. Hence heavier isotopic composition of the YRS waters during June can also be due to possible evaporation of the waters during their flow or as a result of partial evaporation of rain which contribute water to the YRS during this month (see later sections).

3.2.2 The $\delta^{18}O$-δD relationship

The isotopic composition of the river waters, usually, is related to that of local precipitation. In small drainage systems, $\delta^{18}O$ and δD of runoff is identical to that of local precipitation whereas in large river systems, the rivers carry an "average" signature of the precipitation in the drainage basin.

Regression line drawn in a $\delta^{18}O$-δD space for the global precipitation defines the Global Meteoric Water Line (GMWL) and that for the precipitation in a region is named the Local Meteoric Water Line (LMWL). The slope of the GMWL is ~8 (Craig, 1961; Rozanski et al., 1993). The regional precipitation, if not influenced by processes such as evaporation,

defines a LMWL with a slope close to 8. This slope becomes <8, if the raindrops undergo evaporation during their fall. Hence relation between $\delta^{18}O$ and δD in rain and surface waters helps to assess the role of evaporation in altering their isotopic composition. $\delta^{18}O$-δD relations in river waters when compared with those of GWML and LWML, provide information on the isotopic composition of the source. In addition, it also yields information on the preservation/alteration of stable isotopic composition of precipitation contributing to the streams and evaporation of stream waters during their transit.

(a) Monsoon:

Fig. 3.2 presents the $\delta^{18}O$-δD plot for the monsoon (September) samples. Regression analysis of the data (Williamson, 1968) gives the best fit line (BFL):

$$\delta D = (7.71\pm0.27)\delta^{18}O + (7.13\pm2.3), \quad (n = 14, r = 0.98, p< 0.005, \text{Table 3.2}) \qquad (1)$$

The slope of the BFL for the monsoon period (Fig. 3.2) is marginally lower than that of the global meteoric water line (GMWL; Rozanski et al. 1993):

$$\delta D = (8.17\pm0.06)\delta^{18}O + (10.35\pm0.65) \qquad (2)$$

but similar to that derived for precipitation at New Delhi for the monsoon period, July, August and September for the years 1961-95 (IAEA, 1998):

$$\delta D = (7.80\pm0.05)\delta^{18}O + (7.2\pm0.4) \quad (n = 79, r = 0.99) \qquad (3)$$

The eqn. 3 can be considered as the local meteoric water line (LMWL). The similarity in the slopes of rain waters at Delhi (eqn. 3) and the September river water samples, with values of 7.7±0.3 to 7.8±0.1, suggests that evaporation of raindrops during the interval between their condensation and fall, and that of the river water during its flow, if any, is only minor and that the isotopic composition of precipitation is well preserved in stream waters of monsoon season. Further, the observation that the value of the slope in the September samples (Fig. 3.2) is not significantly different from 8, suggests that the rainfall in this region during monsoon occurs essentially under equilibrium condition obeying Rayleigh condensation. These two sets of data taken together (equations 1 and 3) suggest that the monsoon meteoric water line (MMWL) in this part of the Himalaya can be characterized by a slope of ~7.8 and an intercept ~7.

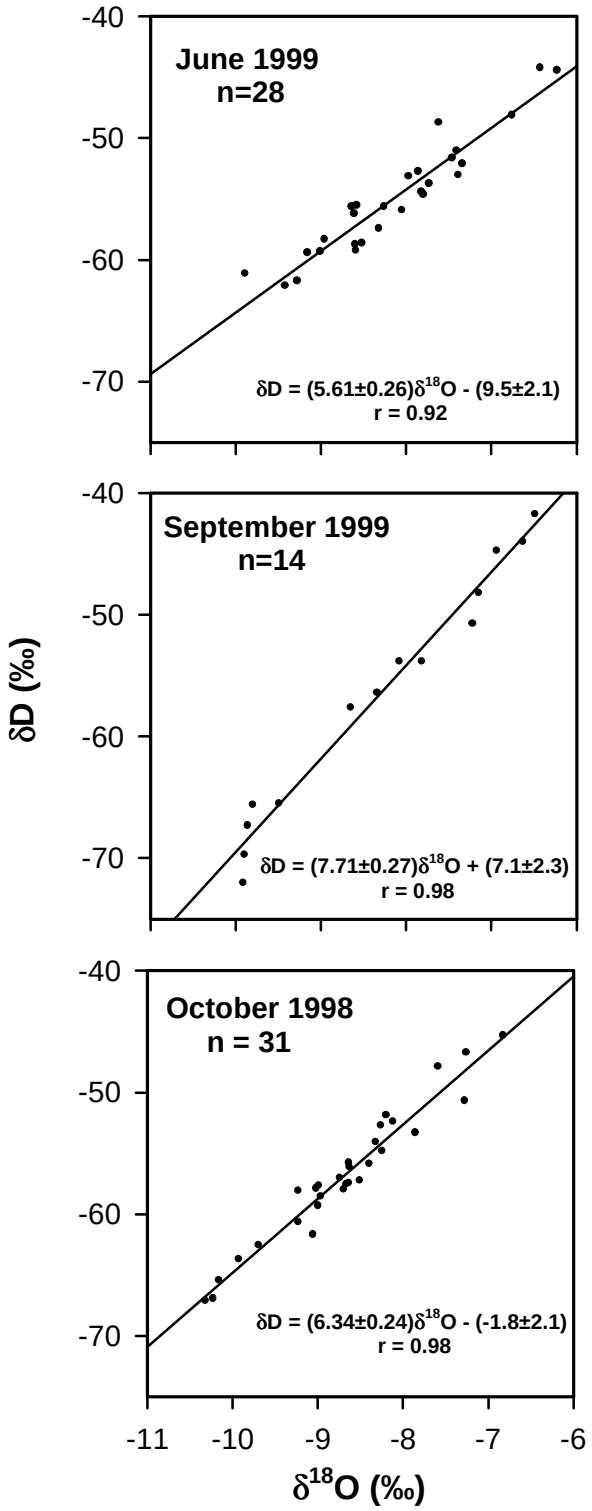

Fig. 3.2 d^{18}O-dD co-variation plots for samples from the Yamuna and its tributaries during three different sampling periods. The number of samples and the regression equations [calculated using Williamson (1968)] are also given. The errors are ±1s.

(b) Summer and post-monsoon:

The Yamuna waters collected during June (summer) and October (post-monsoon) show the following relations:

$$\delta D = (5.61\pm0.26)\delta^{18}O - (9.5\pm2.1) \quad (n = 28, r = 0.92, p < 0.005) \qquad (4)$$

and $$\delta D = (6.34\pm0.24)\delta^{18}O - (-1.8\pm2.1) \quad (n = 31, r = 0.98, p < 0.005) \qquad (5)$$

respectively. The slopes of the BFLs of these periods (Table 3.2) are less than those of the monsoon BFL and the GMWL (Table 3.2), indicating that evaporation of waters at some stage has taken place. This could be from the falling raindrops contributing to these streams and/or from the stream waters during their flow. Statistical analysis of available $\delta^{18}O$ and δD data in rainwaters from New Delhi (IAEA) during June yields the relation:

$$\delta D = (6.26\pm0.07)\delta^{18}O + (2.83\pm0.2) \quad (n = 29, r = 0.95, p < 0.005) \qquad (6)$$

The slope of this line (eqn. 6) is significantly lower than that of GMWL and is marginally higher than that for the June waters (eqn. 4) but similar to that for the October collection (eqn. 5). The lower value of rainwater slope than that of GMWL suggests that the isotopic composition of streams in this region during summer is controlled predominantly by the composition of rainwater which themselves have undergone evaporative enrichment. The marginally lower slope in rivers during June, if validated by more data, can be because of some amount of evaporation during their flow. The slightly higher value of the slope during October, compared to that during June, can be due to differences in the source and/or evaporation. It must, however, be mentioned that as waters of the YRS represent a composite of melt water from glaciers and several previous rains, the agreement in slope values among the various δD-$\delta^{18}O$ plots (eqns. 1-6) allows only to draw broad inferences. It is difficult, for example, to discern quantitatively from these slopes and associated errors, the relative significance of evaporation of rain drops during their fall vis-a-vis during their flow in the streams though the latter seems to be of minor importance in the samples analyzed.

***(c) Comparison with the Ganga headwaters and Gaula catchment*:**

As mentioned earlier, Ramesh and Sarin (1992) and Bartarya et al. (1995) have reported δD-$\delta^{18}O$ measurements in the streams of the Ganga headwaters and the Gaula catchment in the Himalaya. The slope and intercept of the BFL for the Ganga headwaters (Ramesh and Sarin, 1992) are same, within errors, as those for the Yamuna samples during monsoon (Table 3.2):

$$\delta D=(7.45\pm0.23)\delta^{18}O + (8.0\pm2.0) \quad (n = 23, r = 0.98, p<0.01) \qquad (7)$$

This is intriguing considering that the Ganga samples were collected in April when the dominant source of water to the rivers is snow and glacier melt. The results of Bartarya et al. (1995) on snow and rain water samples from the Gaula catchment area in the Lesser Himalaya, south-east of the amuna and the Ganga headwaters, show that they cover a wide range, 0.1 to -13.7‰ and -3 to -106‰ for $\delta^{18}O$ and δD respectively. The $\delta^{18}O$ - δD plot, for these snow and rain samples, shows significant scatter with a slope and intercept of 7.13 and 14.97 respectively. The lower value of slope relative to GMWL has been interpreted in terms of evaporation of rain drops during their fall (Bartarya et al., 1995). Interestingly, the springs and streams in the Gaula catchment have a higher slope of ~8.36 and intercept 10.7 but the line is less well defined as the data points have less spread.

Table 3.2 δD-$\delta^{18}O$ relation and deuterium excess in the Yamuna, Ganga and Indus headwaters in the Himalaya and New Delhi rainwater

Samples	Month	No. of samples	Slope[a)]	Intercept[a)]	r	d (‰)[b)] range	d (‰)[b)] mean
YRS	Sept.	14	7.71±0.27	7.1±2.3	0.98	5.3-12.8	9.6±2.2
N. Delhi Rain	July-Sept.	79	7.80±0.05	7.2±0.4	0.99	0.2-19.5	8.8±4.0
YRS	June	28	5.61±0.26	-9.5±2.1	0.92	5.2-17.3	9.9±3.1
YRS	Oct.	31	6.34±0.24	-1.8±2.1	0.98	7.7-16.2	12.7±2.0
N. Delhi Rain	June	29	6.26±0.07	2.8±0.2	0.95	-22.3-14.6	1.9±9.5
Ganga[c)]	April	23	7.45±0.23	8.0±2.0	0.98	6.2-21.0	13.7±3.1
Gaula[d)]	Feb.-Oct.	20	8.36±0.59	10.7±5.2	0.86	2.2-21.6	9.6±4.8
Indus[e)]	August	19	9.12±0.29	31.1±4.2	0.98	7.8-18.4	14.7±3.1

[a)]Slopes and intercepts are calculated based on Williamson (1968). Errors are ±1σ. r is correlation coefficient.
[b)]Deuterium excess values, range, mean and one standard deviation. [c)] Ramesh and Sarin (1992), [d)]Bartarya et al., (1995), [e)]Pande et al.(2000).

3.2.3 Deuterium excess:

The "deuterium excess" in a precipitation sample is defined as $d = \delta D - 8\delta^{18}O$ (Dansgaard, 1964). It results primarily due to non-equilibrium processes (Dansgaard, 1964) and is the difference between the measured δD value and the expected equilibrium value calculated based on the measured $\delta^{18}O$. The magnitude of d values is determined by conditions of the vapour source (e.g. relative humidity, temperature and wind speed over the evaporating surface) and moisture recycling in the area experiencing the precipitation

(Rozanski et al., 1993). The deuterium excess of the stream waters in the YRS, for the three periods of sampling, ranges from 5.2‰ to 17.3‰ with a mean of ~11‰ (Table 3.2), 2.5‰ higher than the long term annual average of 8.5‰ observed for precipitation at New Delhi (Araguas et al., 1998). The mean d values for the three seasons though overlap with each other within errors (Table 3.2); samples collected during June have relatively lower d values compared to those in September and October (Fig. 3.3). About half the number of June samples have d values less than 10‰ (Table 3.1), which is typical of continental precipitation events with moisture source from the oceans (Dansgaard, 1964). It is suggested (Araguas et al., 1998) that partial evaporation of raindrops below the cloud base, under conditions of low relative humidity and light rainfall, can substantially reduce the d values of rains collected at ground level. The relatively low d values in samples collected from the YRS during June are likely to be caused by contributions from partially evaporated rains. This is consistent, as already discussed, with the observed lower slopes of $\delta^{18}O$-δD regression lines for both the YRS waters and New Delhi precipitation during June (section 3.2.2). It can be seen in Table 3.2 that the New Delhi rains during June have mean d values lower than those for monsoon season. This attests to the idea that the rainwater undergoes evaporation during their fall during this month resulting in lower deuterium excess in them. Datta et al. (1991) attributed lower d values in rainfall at New Delhi during nonmonsoon periods to the partial evaporation of raindrops during their fall. Araguas et al. (1998) also observed that at New Delhi, during January to May, d values of rainfall gradually decrease with an increase in $\delta^{18}O$ which was explained in terms of enhanced evaporation of raindrops below the cloud base.

There is a significant inverse correlation between $\delta^{18}O$ and d values for the June and October samples (Fig. 3.4). In the upper reaches of the YRS, samples are depleted in ^{18}O and have higher d whereas the samples in the lower reaches have enriched ^{18}O and lower d values. This trend can result from different mixing proportions of water from two end members, i.e. snow/glacier melt water and precipitation. Snowmelt would give higher d and lower $\delta^{18}O$ values as kinetic fractionation involved during the formation of snow results in high d excess values (Cooper, 1998). This component would be more dominant at higher altitudes.

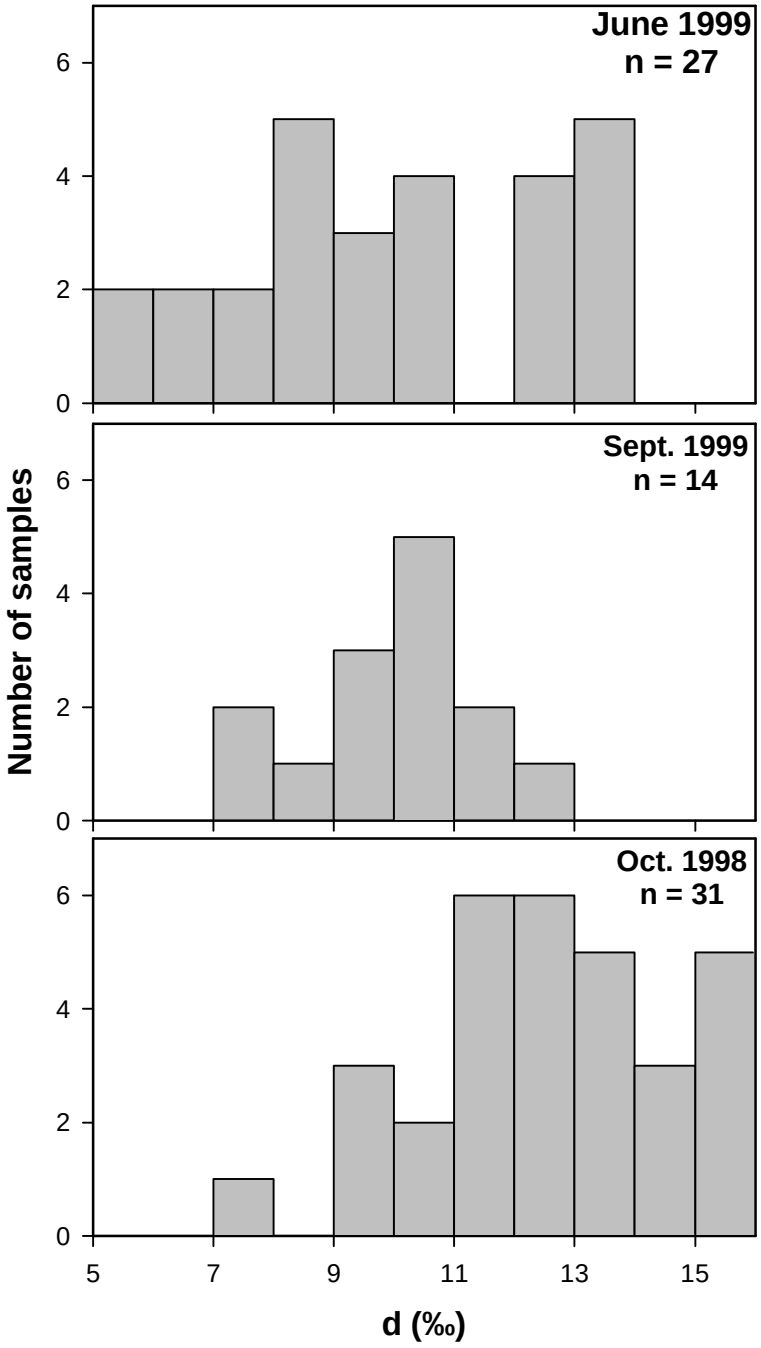

Fig. 3.3 Distribution of deuterium excess (d) in the YRS for three sampling periods. Samples collected in October have higher d values than those collected in June and September. RW99-22 not plotted

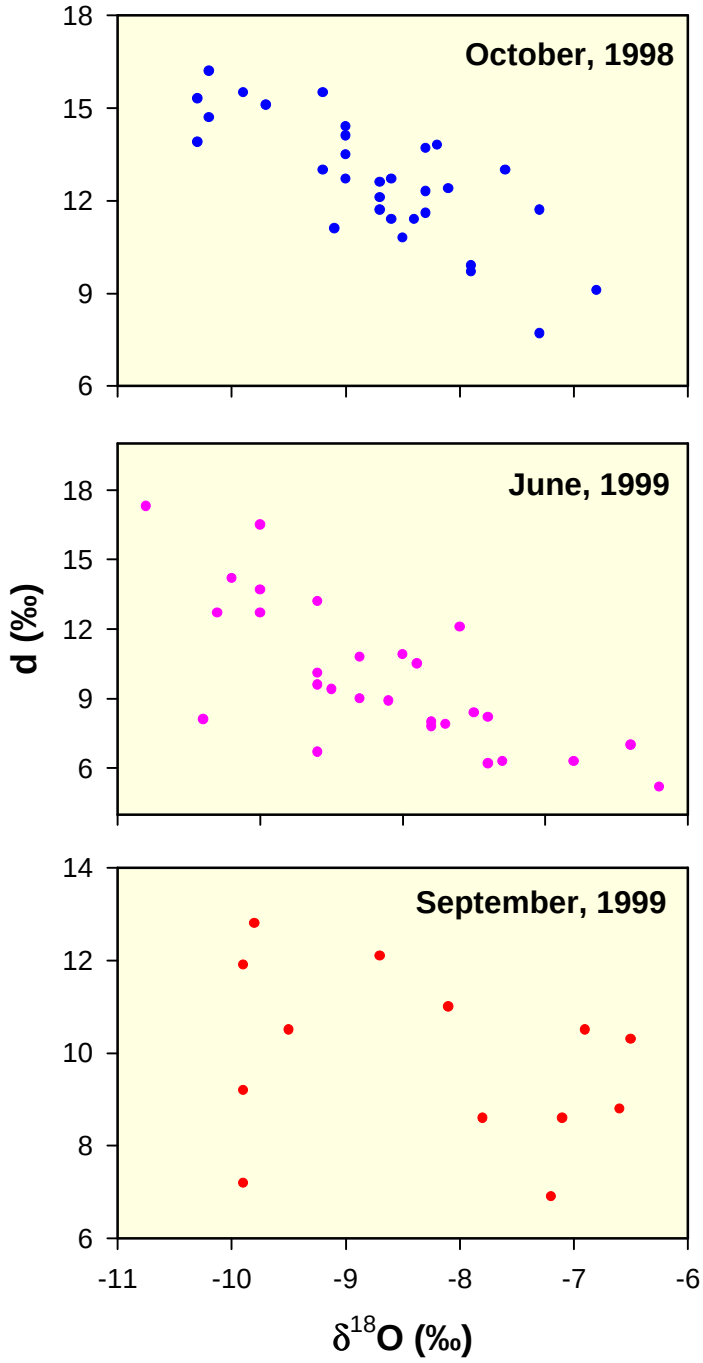

Fig. 3.4 Scatter plot of deuterium excess (d) vs. $d^{18}O$ in the YRS for three sampling periods. A negative correlation is evident for October and June whereas September data show more scatter.

It is also seen from the data (Fig. 3.3, Table 3.1) that in general, October d values are higher relative to those in June and September samples. October samples have an average d of 12.7 compared to 9.6 and 9.9 for September and June respectively [Considering that the numbers of samples analyzed were different during these periods, difference of mean test was performed to determine if the mean d values are indeed different. The results show that the mean d of October is different than that of June (t = 4.69) and September (t = 4.78) at 95 % confidence level]. About 90% of the samples collected during October have d values greater than 10 (Fig. 3.3). Deuterium excess in precipitation, as already mentioned, depends on the source vapour conditions as well as the moisture recycling in the area. The long term average d value for the New Delhi precipitation is about 8.5 (Araguas et al., 1998), however, it exhibits large scatter over the year. During October, many of the d values of New Delhi precipitation are >10. Hence it is likely that high d values observed in October samples of the YRS reflect the signature of the source, i.e. precipitation characterized by moisture recycling (cf. Krishnamurthy and Bhattacharya, 1991). Addition of re-evaporated moisture from continental basins as well as vegetation surface to the water vapour moving inland can also bring about high d values in the precipitation (Njitchoua et al., 1999). Hence higher d values for the October samples can result from enhanced contribution of recycled moisture to precipitation through evaporation and/or evapotranspiration during this period when there is a bloom in vegetation after the monsoon rainfall.

In September samples of the YRS, the d values are in between those of June and October (Fig. 3.3). Also, the plot of $\delta^{18}O$ vs. d shows considerable scatter during this period (Fig. 3.4). This can arise because the relative contribution of recycled moisture to rain during September is likely to be less. The rainfall in this region during September is generally much higher than that during October. For example at Dehradun located in the lower reaches of the YRS, the rainfall in September is about 8 to 10 times higher than that in October. Therefore, the relative contribution of the recycled moisture to the October rains (the retreating period of the monsoon) from post-monsoon vegetation bloom is likely to be more. This is supported by available data on rainfall and evapotranspiration at selected locations in the Yamuna catchment. During September, the rainfall far exceeds the evapotranspiration whereas in October, evapotranspiration is more than rainfall resulting in a net loss in the water budget of the region (Devi, 1992; Chapter 2, Fig. 2.7). Hence the influence of recycled moisture via

evapotranspiration is likely to be pronounced in the isotopic composition of the October rainfall. As a result, deuterium excess in October are higher than those during September. In addition, the fact that September samples were fewer in number and were collected primarily from lower altitudes may also contribute to lower d values.

Thus, in the waters of the Yamuna and its tributaries the variability in the deuterium excess seem to be controlled primarily by three processes, i.e. mixing of snowmelt and precipitation, partial evaporation of raindrops and recycling of moisture through evaporation of soil water and evapotranspiration from vegetation.

3.2.4 Altitude effect

It is well established (Yurtsever and Gat, 1981; Clark and Fritz, 1997) that the isotopic composition of precipitation varies with elevation of the sampling location. When air masses are orographically lifted, they cool and the ensuing precipitation is enriched preferentially in the heavier isotopes. As a result, the next phase of precipitation at still higher altitude is relatively depleted in heavy isotopes; this progressive depletion with height is known as "altitude effect". The altitude effect depends on factors such as the precipitation history, the topography and the precipitable moisture remaining in the cloud. The altitude effect on $\delta^{18}O$ in mid-latitude precipitation generally ranges between 0.15 to 0.30 ‰ for each 100 m of altitude gained (Schotterer et al., 1996). Both continental effect and altitude effect are manifestations of Rayleigh distillation: one operating on a large spatial scale due to cloud migration and the other operating in a given region due to continuous extraction of water from the rising cloud due to drop in temperature with height. Bhattacharya et al. (1985) and Krishnamurthy and Bhattacharya (1991) have observed continental effect in northern Indian precipitation and have modeled these data to determine the sources of water vapor to the cloud system. Since precipitation is the dominant source of water in streams, particularly during monsoon, their isotopic composition should also reflect the altitude effect associated with precipitation. However, as stream water at any given site represents a mixture of waters from various streamlets draining from higher altitudes up to the site, it is likely to be isotopically lighter relative to the local precipitation at that site. As a result, the altitude effect estimated in stream waters will be partially reduced from that of precipitation. The results for the Ganga head waters (Ramesh and Sarin, 1992) and streams from Gaula catchment area (Bartarya et al., 1995) showed that there is a decrease in $\delta^{18}O$ and δD values of waters with

increase in altitude of sampling locations. Studies of Garzione et al. (2000 a, b) in the Seti River and the Kali Gandaki watersheds in Nepal also show the altitude effect in $\delta^{18}O$ of the streams.

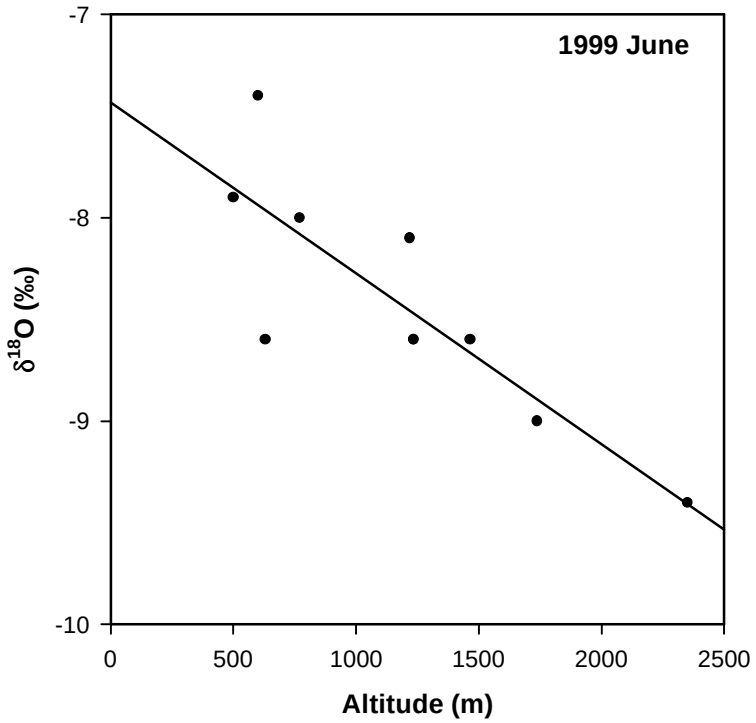

Fig. 3.5 $d^{18}O$-Altitude plot for the Yamuna samples collected in June. The slope of the regression line is a measure of the altitude effect (see Table 3.3 and text).

The altitude-$\delta^{18}O$ data for the Yamuna mainstream in the Himalaya (Fig. 3.5, Table 3.3) show that the altitude effect for the Yamuna during summer and post-monsoon are similar within errors with values of 0.09 and 0.11‰ per 100 m respectively. The calculation of altitude effect during monsoon was not done as only 6 samples of the Yamuna mainstream were collected covering an altitude range of only ~480 to 770 m. Considering that the range in isotopic composition together with the slope and intercept of the altitude-$\delta^{18}O$ plots are similar during summer and post-monsoon, these data were combined to derive an average altitude effect for the Yamuna (Table 3.3):

$$\delta^{18}O = (-0.107\pm0.005) \times 10^{-2}\,\text{Altitude(m)} \;\; -7.33\pm0.06 \;\; (r = -0.85,\ p < 0.01) \qquad (8)$$

The slope of the regression line gives an altitude effect of 0.11‰ per 100 m for $\delta^{18}O$. This compares with the values of 0.09-0.29 reported for various river systems in the Himalaya (Table 3.3). The altitude effect in the YRS is lower compared to 0.19‰ per 100 m for the

Ganga headwaters (Ramesh and Sarin, 1992) and 0.14‰ per 100 m for the streams in the Gaula catchment area (Bartarya et al., 1995), but very similar to 0.09‰ per 100 m for the Indus (Pande et al., 2000). Garzione et al. (2000 a, b) derived an altitude effect of 0.29‰ per 100 m for $\delta^{18}O$ in the tributaries of the Seti River and the Kali Gandaki in the western-central Nepal. Chamberlain and Poage (2000) estimated, from the available data set, a global average altitude effect of 0.21‰ per 100 m for $\delta^{18}O$ in the surface waters.

In order to compare the altitude effect estimated from springs and streams with that in precipitation, it is necessary to correct for the effect of integration of $\delta^{18}O$ signatures in rivers from higher altitudes to the sampling altitudes as was done by Ramesh and Sarin (1992). Their model, based on simplified assumptions, suggests that the altitude effect derived for river water data would be a factor of two lower than that in the precipitation. Application of Ramesh and Sarin (1992) model to the YRS data would yield a value of 0.22‰ per 100m for altitude effect for $\delta^{18}O$ in precipitation in the region. Simple modification of this model by including the effect of evaporation during stream flow does not change this value significantly. The integration effect in Seti River and Kali Gandaki data (Garzione et al., 2000a, b) is expected to be significantly less as they are based predominantly on $\delta^{18}O$ data on small tributaries. Therefore, in this case the measured altitude effect in rivers, 0.29‰ per 100m, is expected to be close to that in precipitation.

Table 3.3 Altitude-$\delta^{18}O$ relation in River Systems in the Himalaya

River	Month	No. of samples	Altitude effect[a)]	Intercept	r
Yamuna	June	10	-0.09±0.01	-7.4±0.1	-0.84
Yamuna	October	6	-0.11±0.01	-7.9±0.1	-0.86
Yamuna	June, Oct.	16	-0.11±0.01	-7.3±0.1	-0.85
Ganga[b)]	April	5	-0.19±0.01	-8.4±0.2	-0.98
Gaula[c)]	Feb, June, Oct	30	-0.14±0.01	-6.3±0.2	-0.69
Indus[d)]	August	6	-0.09±0.01	-12.1±0.4	-0.58
Seti[e)]	March, April	12	-0.29±0.03	-5.9±0.2	-0.96
Kali-Gandaki[e)]	Sept, Oct	38	-0.29±0.01	-6.8±0.3	-0.96

[a)] in ‰ $\delta^{18}O$ per 100m, calculated based on Williamson (1968). Errors are $\pm 1\sigma$.
[b)] Ramesh and Sarin (1992), [c)] Bartarya et al. (1995), [d)] Pande et al. (2000), [e)] Garzione et al. (2000a, b).

It is seen from the compilation in Table 3.3 that the measured altitude effects vary at least by a factor of two among various river systems draining the southern slopes of the Himalaya. The cause for such significant differences in the altitude effect in the major rivers needs to be better understood. A likely explanation for these differences is that they are caused by variable amount effect. The fraction of moisture being rained out in different catchment varies depending on local topography and temperature. Indeed, the role of amount effect has been invoked by Araguas et al. (1998) to explain the oxygen isotope composition of rainfall in the southern part of south-east Asia and by Rozanski et al. (1993) to account for the lack of correlation between $\delta^{18}O$-temperature in this region with surface temperature 20-30°C. Thus, if we accept the hypothesis that rainout is the dominant factor influencing the altitude effect, we can estimate the fraction of moisture removed in the Yamuna catchment as the cloud mass ascends in the Himalayan region. Based on $\delta^{18}O$ and δD values of the streams at the foothills of the Himalaya (Dehradun, RW98-10, Table 3.1) and at the highest sampling location (Hanuman Chatti, RW98-16, Table 3.1) and a simple Rayleigh distillation model we estimate that the cloud mass loses about 25% of its moisture by rainout during its ascent between these two locations (Appendix-3.1). Following a similar approach and using $\delta^{18}O$ and δD values of the Ganga at the foothills and at altitude ~2400 m, it is estimated that the cloud mass loses about 30% of its moisture in the Ganga catchment. Slightly higher estimated rainout in the Ganga cacthment is as expected and attests to the idea that amount effect predominantly governs the altitude effect in this region. It is to be noted that the amount of rainfall in the Himalaya shows a variation with the topographic set up (e.g. north vs. south facing slopes, Devi, 1992). Hence the amount effect, which influences the altitude effect in the region, is to some extent regulated by the local topography. Other factors which may also contribute to these variability are relative mixing proportions from various sources. The Yamuna samples were collected in June and October when summer monsoon is the major source of water, whereas the Ganga samples collected in April may have a dominant glacial melt component. In addition, there could be difference in the supply of moisture to the clouds through evaporation of soil water and evapotranspiration from vegetation.

Comparison of altitude effect in surface water of the Himalayan river systems shows that it varies by a factor of ~2 in catchments lying within a distance of a few hundred kilometers. Such variation may have implications to use of altitude effect in estimation of

paleoelevation in the region. Chamberlain and Poage (2000) compiled data on variations of $\delta^{18}O$ in surface waters with altitude all across the globe and derived an average lapse rate of $\delta^{18}O$ with altitude. They used this average lapse rate and $\delta^{18}O$ in authigenic minerals (kaolinite and smectite) to estimate the paleorelief of mountain ranges. Garzione et al. (2000a, b) estimated the paleoelevation of Tibet using the contemporary altitude effect in the Kali Gandaki and Seti River basins and $\delta^{18}O$ of Miocene-Pliocene carbonates from the southern Tibetan Plateau. Implicit in the above studies is the assumption that altitude effect in the past is the same as that of present day and that it is invariant over the spatial scale of paleoelevation reconstruction. Variations of altitude effects by a factor of ~2, as revealed in this study, in catchments only a few hundred kilometers apart points to the need to have careful scrutiny of the validity of the above assumptions.

3.2.5 Stable isotope-stream chemistry relationship

Stable isotope composition of river waters is determined by the source water isotope systematics, mixing and evaporation. Studies of river water properties such as temperature, chloride concentration and conductivity in conjunction with its stable isotope composition have provided useful information on their sources of water and their mixing proportions (Rodhe, 1998; Lambs, 2000). Lambs (2000) observed a negative correlation between conductivity and $\delta^{18}O$ in surface waters of the Bhagirathi which was attributed to a two component mixing between the isotopically depleted glacial melt with higher conductivity and isotopically enriched snowmelt with lower conductivity.

In this section, we examine the relation between ΣCat^* (the concentration of total cations, ΣCat, in river waters corrected for cyclic component estimated using chloride as an index, $\Sigma Cat^* = \Sigma Cat - Cl$ in equivalent units) and $\delta^{18}O$ in the Yamuna mainstream. The mainstream integrates the contributions of cations and water of various tributaries draining the catchment. At any point in the mainstream, its elemental and isotopic composition represent the "average" contribution of the whole catchment, from its source till that point. Hence downstream variation of cation contribution from the catchment lithology should be best reflected in the mainstream. The extent of chemical weathering (and hence ΣCat^*) in the river basins would depend upon factors such as lithology temperature and vegetation, among others. In the Yamuna basin in the Himalaya, the extent of chemical weathering near the

source is expected to be less intense due to lower temperature, sparse vegetation and dominance of crystalline rocks compared to that along its course downstream in the Lesser Himalaya characterized by warmer climate, more vegetation and more abundance of sedimentary rocks such as carbonates. Thus, as a result of all these, ΣCat* is expected to increase along the course of the Yamuna, consistent with the observation that it trebles from 1056 and 1069 μEq at Hanuman Chatti to 3063 and 2973 μEq at Saharanpur during June and October respectively (Table 3.1).

Fig. 3.6 is a plot of log(ΣCat*) vs. $\delta^{18}O$ for the Yamuna mainstream during the three seasons of sampling. The data shows a significant correlation that can be described by the relation:

$$\log(\Sigma Cat^*) = 0.19\delta^{18}O + 4.85 \quad (r = 0.89, n = 26) \qquad (9)$$

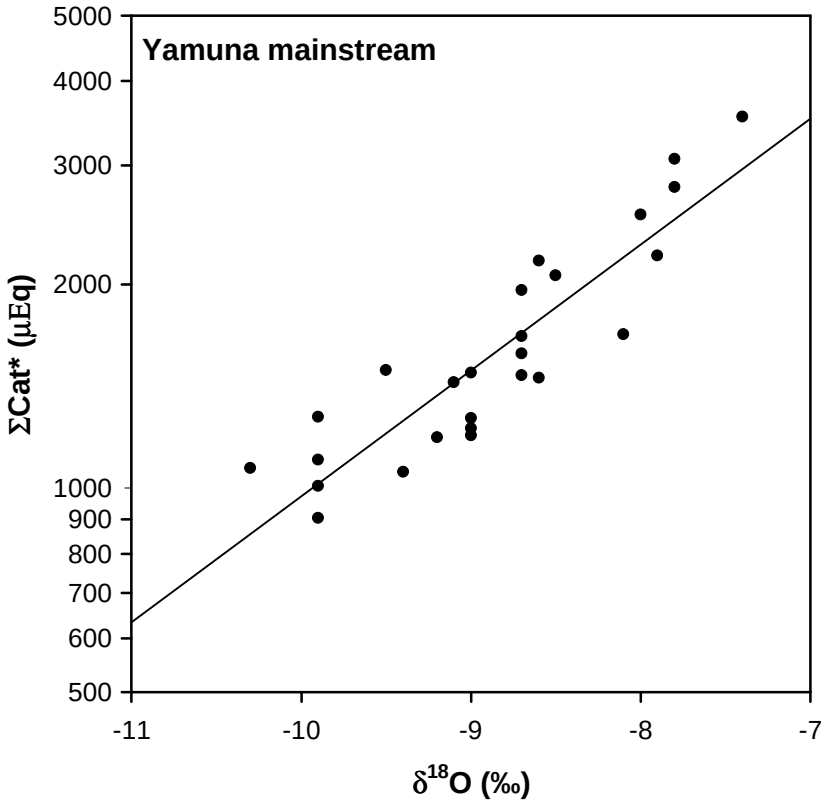

Fig. 3.6 Plot of log SCat vs. $d^{18}O$ (total cations corrected for cyclic contributions (see text) in the Yamuna mainstream waters. A tight correlation is evident (#RW98-33 not plotted).*

The above relation results because these properties, $\delta^{18}O$ and ΣCat* are both influenced by a common variable, altitude, and unlikely to be because of a causal link between them. The variations in $\delta^{18}O$ and ΣCat* along the course of the Yamuna are brought

about by independent processes, altitude effect and intensity of chemical weathering respectively. Chemical weathering of various rocks is influenced by factors such as lithology, temperature, vegetation and rainfall, whereas $\delta^{18}O$ of the river water is influenced by continentality, temperature and topography of the catchment. In the YRS basin, the temperature varies with altitude, at higher altitudes it is lower. At higher altitudes ΣCat* is lower because of lower temperature and less abundance of easily weatherable lithologies such as sedimentaries. $\delta^{18}O$ is more depleted because the source waters are derived from cloud which are expected to be depleted in ^{18}O because of rainout during its traverse. ΣCat* abundance, indeed, shows a negative correlation with altitude, but with larger scatter. However, considering that physical processes such as mixing and evaporation are likely to affect both ΣCat* and $\delta^{18}O$ similarly and that data on altitude are limited in this study we have used their interrelation to draw inferences on the altitude dependence of ΣCat*. Altitudinal variations in lithology and temperature contributes to ΣCat* variation in the YRS. If, however, weathering of "monolithologic" system (such as silicates) is considered, then it seems to depend mainly on temperature. This dependence is seen in the YRS silicate cations (Na* and Si) which has been used to deduce activation energy of silicate weathering in the catchment (Chpater 4, section 4.2.8).

Relation (9) suggests that ΣCat* would increase by a factor of ~1.5 for every 1‰ increase in $\delta^{18}O$. Considering that the $\delta^{18}O$ altitude effect is ~0.11 ‰/100m (Table 3.3), it can be inferred from the plot that ΣCat* would double as the Yamuna traverses downstream by ~1.4 km in altitude in the Himalaya. The Tons river results also show a correlation between ΣCat* and $\delta^{18}O$ for the two seasons, summer and postmonsoon for which data are available. However, pooling the data of the Yamuna and Tons exhibits a larger scatter ($r = 0.77$, $n = 37$). If the Tons and the Yamuna data are combined then the ΣCat* doubling would be per ~1.6 km decrease in altitude, a result similar to that obtained for the Yamuna mainstream but more representative of the Yamuna River System in the Himalaya.

3.3 CONCLUSIONS

The Yamuna and its tributaries in the Himalaya have been extensively sampled and analyzed for their oxygen and hydrogen stable isotope compositions. These measurements have led to the following observations and conclusions:

(i) δD values in the Yamuna and its tributaries range from -41.7 to -72.0‰ and $\delta^{18}O$ from -6.2 to -10.3‰, the most depleted values being in the monsoon and high altitude samples. The seasonal trends can be understood in terms of amount effect which is more pronounced during monsoon, a season characterized by heavy rainfall events, which deplete the heavy isotopes from the forward moving clouds.

(ii) The δD and $\delta^{18}O$ relation for the monsoon samples yield a slope of 7.71±0.27, quite similar to that for rainwater at New Delhi 7.80±0.05, suggesting that the isotopic signatures of rainfall are well preserved in the stream waters during this season. A similar conclusion is also borne out from samples collected in June, however, the slope of the δD-$\delta^{18}O$ plots for the YRS streams and the rain water at New Delhi during this season center around ~5.8, showing definite evidence of evaporative enrichment of rain during their fall. The deuterium excess in the YRS and New Delhi precipitation suggests that high d values in the YRS during October can be due to an inherent signature of a source with a significant component of recycled moisture.

(iii) The "altitude effect" in $\delta^{18}O$ in the YRS samples is derived to be 0.11‰ per 100m, about a factor of two less than that reported for the Ganga headwaters. This difference in the deduced altitude effects between the Yamuna and the Ganga headwaters is attributable primarily to the influence of amount effect on isotope fractionation. Such large variability in the altitude effect in the river catchments in the Himalaya suggests that reconstruction of paleoelevation in the Himalaya based on the present day altitude effect should be accompanied by proper assessment of altitude effect in the region.

(iv) The $\delta^{18}O$ and the major cation abundances (corrected for cyclic components) in the Yamuna mainstream show a strong positive correlation This relation may arise from a common variable influencing both of them, i.e. altitude. The correlation leads to the inference that the major cation abundance would double as the Yamuna flows about 1.4 km. downstream.

Appendix-3.1

The rainout process by which the raindrops are continuously removed from the cloud vapor by condensation occurs essentially under equilibrium condition. At any given time the isotopic composition in the rainfall is given by the Rayleigh condensation equation:

$$R_l = \alpha R_0 f^{\alpha-1} \quad \text{(A1)}$$

where R_l is the ratio of the isotopes ($^{18}O/^{16}O$ or D/H) in the evolved liquid (rain), R_0 is the initial ratio in the vapour, f is the fraction of the vapor remaining and α is the temperature dependent isotope fractionation factor during the vapor-liquid transition.

Using the isotopic composition of the stream at the foothills in the catchment as αR_0 and that of the stream at the highest sampling location as R_l, the residual fraction of the vapor and hence the amount of rainout can be calculated using equation (A1).

Rainout calculated from $d^{18}O$

From equation (A5):

$f = \exp[\ln(R_l / \alpha R_0)/(\alpha-1)]$

since $\alpha R_0 = R_{\ell_o}$, we have $f = \exp[\ln(R_l / R_{\ell_o})/(\alpha-1)]$

or $f= \exp[\{\ln((\delta_l+1000)/(\delta_o+1000))\}/(\alpha-1)]$ (A2)

Taking δ_o = -7.3‰ (Tons at Dehradun, RW98-10) and δ_l = -10.3‰ (Yamuna at Hanuman Chatti, RW98-16), f varies between 72 to 76% (using the values of α from 1.0093 to 1.0112 in temperature range 25 to 5 ^oC, Clarke and Fritz, 1997), hence the rainout from the cloud during its movement between these two locations is 28 to 24%.

Rainout calculated from dD

Taking δ_o = -46.7‰ (Tons at Dehradun, RW98-10) and δ_l = -67.1‰ (Yamuna at Hanuman Chatti, RW98-16), f varies between 76 to 81% (using the values of α from 1.079 to 1.105 in temperature range 25 to 5 ^oC, Clark and Fritz, 1997), hence the rainout from the cloud during its movement between these two locations is 24 to 19%.

Chapter 4

Major ions, Sr, Ba and $^{87}Sr/^{86}Sr$ in the Yamuna River System: Chemical weathering and CO_2 consumption in the Himalaya

4.1 INTRODUCTION

Chemical and isotopic investigation of rivers provide useful and important information on the source(s) of major ions, trace elements and isotopes to them, elemental and isotopic fluxes to the sea, chemical weathering rates in the catchment they drain and CO_2 drawdown in their basins. Knowledge on these aspects is essential in assessing the importance of chemical weathering of silicates as a negative feedback in stabilizing the global temperature on a multi-million year time scale (Berner and Berner, 1997). Further, characterization of sources of Sr and its isotopes in rivers draining the Himalaya have implications to interpretation of marine Sr isotope records.

The rivers draining the Himalaya assume global importance as they contribute significantly to the global budget of water and sediment discharge. Draining a young and active mountain chain, they regulate marine geochemistry of a number of elements and isotopes. In recent years, these rivers, especially those draining the southern slopes of the Himalaya, have caught attention of several workers because of possible connection between the uplift of the Himalaya and the Cenozoic climate change (Raymo and Ruddiman, 1992). In the "tectonics-weathering-climate" hypothesis, uplift of the Himalaya has been invoked as a possible driver for the Cenozoic cooling, through uplift induced intense silicate weathering and consequent enhanced CO_2 drawdown from the atmosphere. This hypothesis stems from observation that $^{87}Sr/^{86}Sr$ of seawater started rising steadily since the initiation of the uplift of the Himalaya and the idea that $^{87}Sr/^{86}Sr$ in rivers can be used as a proxy of silicate weathering. Testing such a hypothesis requires estimation of silicate weathering rates and CO_2 drawdown in the region and proper characterization of sources of Sr in these river systems in the Himalaya. If, for example, the $^{87}Sr/^{86}Sr$ in these rivers are regulated by lithologies other than silicates, then the above hypothesis would not stand valid.

Previous work on rivers draining the southern slopes of the Himalaya include those of Sarin et al. (1989, 1992a), Pande et al. (1994) and Krishnaswami et al. (1999) on the major ion chemistry of the headwaters of the Ganga, Indus and the Ghaghara. These studies brought out the dominance of carbonate weathering in contributing to the dissolved load of these rivers and provided estimates of CO_2 consumption rates via silicate weathering in their drainage basins. Galy and France-Lanord (1999), based on studies of major ions and $\delta^{13}C$ of dissolved inorganic carbon in the Kali Gandaki basin, assessed the role of carbonic and

sulphuric acids in contributing protons to the weathering reactions and derived the alkalinity fluxes and CO_2 consumption rates. More recently, Karim and Veizer (2000) carried out extensive studies on the headwaters of the Indus to determine the sources of cations to these rivers. On a global scale, Gaillardet et al. (1999), based on a compilation of data on major rivers, estimated the contemporary CO_2 consumption fluxes via silicate weathering in the drainage basins of the rivers draining the Himalaya. Handa (1972) and Jha et al. (1988) have also reported major ion composition of the Yamuna river. These measurements, however, are mainly in the lower reaches of the Yamuna and its tributaries in the plains.

The contribution of Sr from the rivers draining the Himalayan region and their $^{87}Sr/^{86}Sr$ has much significance in the mass balance of marine Sr and its isotopic composition (Richter et al., 1992). The issue of sources of Sr to these rivers, however, has been a matter of controversy among various workers. Studies on Sr isotopes in Himalayan river systems showed that the rivers draining the Himalaya, particularly its southern slopes, have both high Sr concentration and $^{87}Sr/^{86}Sr$ compared to other major rivers of the world (Krishnaswami et al., 1992; Palmer and Edmond, 1989, 1992; Trivedi et al., 1995). Available information on the sources of Sr isotopes, mass balance of Sr and $^{87}Sr/^{86}Sr$ in the river systems in the Himalaya have been diverse and at times controversial. Krishnaswami et al. (1992) and Edmond (1992) suggested silicates as the important source of high $^{87}Sr/^{86}Sr$, whereas Palmer and Edmond (1992) proposed metamorphosed carbonates to be responsible for the high radiogenic composition in these rivers. Singh et al. (1998) and Krishnaswami et al. (1999), based on studies of Precambrian carbonate outcrops in the Lesser Himalaya, concluded that on a basin wide scale silicate weathering exerts dominant control on high $^{87}Sr/^{86}Sr$ of many of the Ganga-Ghaghara-Indus source waters though carbonates might be important in particular streams. Their data synthesis also brought out the need for additional source(s) other than silicates and carbonates occurring in the catchment to balance the Sr budget of these rivers. Galy et al. (1999) concluded that silicates in the Lesser Himalaya and in the Siwaliks are sources of the high $^{87}Sr/^{86}Sr$ in the Ganga-Brahmaputra rivers. Quade et al. (1997) based on a study of soil and detrital carbonates in river basins in Nepal proposed that carbonates exert dominant control on high $^{87}Sr/^{86}Sr$ in the rivers in the Himalaya. Blum et al. (1998) and Harris et al. (1998), based on major ion chemistry and Sr isotopes in the Bhote Kosi and Raikhot rivers, underlined the importance of weathering of carbonates and

disseminated calcites in influencing the Sr budget and its radiogenic composition in the rivers draining the Himalaya.

This chapter presents and discusses major ion composition, Sr, Ba and $^{87}Sr/^{86}Sr$ in headwaters of the Yamuna River System in the Himalaya. The data have been used to assess the relative contributions of various lithologies to major ions of these rivers, to derive CO_2 consumption rates in the basin via silicate weathering and to estimate apparent activation energy for overall silicate weathering in the basin. Attempts are also made to establish a balance for dissolved Sr in the YRS and to assess relative control of various lithologies in regulating the Sr isotopic composition of these rivers. Some of the controversial issues such as the role of vein calcites in influencing the Sr isotopic compositions of rivers have also been addressed in relation to the Yamuna system. The results of CO_2 drawdown in the YRS basin has been compared with those of the headwaters of the Ganga-Ghaghara-Indus to obtain an estimate of contemporary CO_2 drawdown in the southern slopes of the Himalaya and its significance on a global context.

4.2 RESULTS AND DISCUSSION

4.2.1 Major ion chemistry

The data on major ions, silica and TDS in the rivers and springs are given in Table 4.1. These include samples from the YRS, the Ganga at Rishikesh (at the foothills of the Himalaya) and the Bandal, a stream flowing through the phosphorite-blackshale-carbonate formations near Maldeota. The spring samples analyzed are from the Kempti Fall (RW98-7, RW99-9) and Shahashradhara (RW99-60). The chemical composition of the bed sediments from rivers/streams of the YRS and granites collected around Hanuman Chatti are given in Table 4.2. The temperatures of the water samples were measured only during summer (June 1999) and monsoon (September 1999) expeditions. It ranged from 10-30 °C, the lower temperatures are typical of samples from the upper reaches (Appendix-2.1). The river waters are mildly alkaline in nature, covering a pH range of 7.7-9.2, with bulk of the samples having values in a narrow range of 8.5±0.2 (Appendix-2.1).

Table 4.1 Major ions, Sr, Ba and $^{87}Sr/^{86}Sr$ in the Yamuna River System, the Ganga and Spring waters.

Code[a)]	Season[b)]	Na μM	K μM	Ca μM	Mg μM	F μM	Cl μM	NO_3 μM	SO_4 μM	Alk. μM	Si μM	TDS mg ℓ^{-1}	Sr nM	Ba nM	$^{87}Sr/^{86}Sr$
Yamuna main stream															
RW98-16	PM	67	56	388	100	16	30	13.5	113	780	92	88	381	64	0.75158
RW99-13	S	81	45	397	89	18	43	b.d.	129	834	77	91	287	47	0.75543
RW98-20	PM	89	55	392	104	15	36	14.6	100	855	112	93	412	77	0.75725
RW98-25	PM	110	52	406	133	11	52	13.0	76	960	126	100	422	70	0.74985
RW99-19	S	185	46	450	122	n.m.	106	b.d.	116	1022	100	110	374	47	
RW99-17	S	133	47	438	97	n.m.	54	b.d.	126	944	91	102	314	49	
RW98-22	PM	117	52	422	133	10	53	13.3	76	990	127	103	468	77	0.74887
RW99-18	S	171	47	511	155	n.m.	97	b.d.	117	1215	100	125	343	53	
RW98-15	PM	108	50	500	186	10	50	12.5	72	1260	140	124	386	77	0.74598
RW98-14	PM	110	48	525	211	9.2	50	12.1	63	1445	144	136	402	81	0.74495
RW99-11	S	168	42	576	204	n.m.	84	b.d.	108	1480	114	144	486	69	
RW98-12	PM	136	35	504	167	6.5	46	19.0	66	1260	176	125	903	85	0.73757
RW98-9	PM	123	40	611	308	7.6	42	17.9	220	1440	158	157	1164	145	0.72595
RW99-51	M	60	50	332	76	6.7	23	6.6	40	894	109	85	309	37	0.73964
RW98-6	PM	136	39	664	299	7.7	41	18.2	216	1575	169	168	1347	159	0.72831
RW99-30	S	206	48	835	354	n.m.	96	7.5	417	1725	115	205	1494	138	
RW99-64	M	119	39	590	186	7.1	34	12.4	154	1344	155	140	993	84	0.73317
RW99-31	S	175	44	720	310	12	75	b.d.	405	1357	96	172	1461	134	0.72556
RW99-53	M	76	51	352	100	7.8	24	20.6	93	1041	112	102	646	63	0.73263
RW98-1	PM	112	46	481	171	8.0	29	28.4	101	1085	167	117	728	131	0.73518
RW99-2	S	221	46	706	272	n.m.	56	46	165	1943	221	194	921	180	
RW99-58	M	92	42	452	130	6.2	24	24.5	100	1039	137	109	522	76	0.73446
RW98-4	PM	255	52	1019	497	8.1	60	35	333	2369	211	254	1802	310	0.72356
RW99-5	S	306	49	967	661	n.m.	73	5.7	556	2508	193	285	2044	269	
RW99-55	M	262	61	920	344	9.8	67	44	288	2900	183	274	1484	349	0.72447
RW98-33	PM	213	61	928	451	10	58	33.5	268	2250	220	236	1513	315	0.72657

RW99-7	S	242	85	948	448	11	56	5.8	321	2608	204	262	1664	321	0.72657
RW99-54	M	122	58	500	173	9.5	32	15.7	192	1520	146	151	895	158	0.72624
Tributaries															
RW98-17	PM	38	68	182	41	3.2	7.7	26.9	27	473	98	51	197	77	0.77113
RW98-18	PM	33	32	91	24	2.2	5.7	15.8	11	293	87	32	126	25	0.79320
RW99-14	S	42	31	107	21	n.m.	9.8	b.d.	28	347	83	36	121	17	
RW98-19	PM	41	44	413	113	3.1	10.3	14.9	61	945	117	94	352	77	0.73992
RW99-16	S	49	46	617	155	n.m.	18.4	b.d.	137	1373	106	135	326	82	
RW99-15	S	50	31	174	28	n.m.	13.1	23.9	39	450	104	49	139	45	
RW98-13	PM	139	35	796	404	5.0	42	2.0	58	2205	201	200	649	137	0.73754
RW99-12	S	249	49	1075	732	n.m.	73	b.d.	111	3372	238	302	993	155	
RW98-23	PM	172	79	619	232	n.m.	42	b.d.	31	1740	220	161	889	871	
RW98-21	PM	107	33	538	284	4.3	37	4.5	32	1560	163	142	609	102	0.73679
RW99-20	S	172	41	967	545	n.m.	76	b.d.	79	2672	200	243	683	100	
RW98-24	PM	156	20	535	312	4.1	36	16.0	26	1650	232	153	689	38	0.73748
RW98-26	PM	89	49	133	53	6.9	12.2	8.3	19	450	200	53	259	39	0.77495
RW99-21	S	184	66	254	84	12	32	b.d.	44	843	253	91	379	50	0.76858
RW99-27	S	88	47	247	47	n.m.	26	10.5	102	533	110	65	324	62	
RW98-27	PM	64	45	182	35	11	19	14.4	62	383	116	49	200	47	0.76059
RW99-22	S	58	36	177	23	n.m.	22	b.d.	82	389	77	47	156	29	
RW98-28	PM	73	45	189	40	11	26	13.2	58	383	119	50	221	46	0.76145
RW99-26	S	58	35	148	22	n.m.	24	b.d.	72	317	67	40	168	29	
RW98-29	PM	78	46	221	50	10	23	15.0	62	495	138	60	256	57	0.74954
RW99-28	S	66	38	199	30	n.m.	25	b.d.	81	378	79	48	225	36	
RW98-31	PM	125	23	727	254	4.8	35	26	159	1575	206	166	1071	191	0.72927
RW99-23	S	152	28	998	470	n.m.	43	4.2	257	2377	176	238	1037	228	
RW99-25	S	82	44	251	52	n.m.	30	b.d.	99	550	92	65	274	44	
RW98-30	PM	98	37	436	160	8.3	31	17.9	100	990	163	107	594	119	0.73676
RW99-24	S	137	32	833	378	n.m.	41	5.0	217	1980	157	200	835	172	
RW98-5	PM	204	20	750	209	4.7	36	32	127	1820	239	181	1941	87	0.73684

RW99-62	M	217	19	772	214	4.6	33	26	150	1836	222	184	1438	68	0.73972
RW98-32	PM	152	52	808	411	11	29	20.6	581	1395	186	202	2196	177	0.72693
RW99-29	S	155	50	822	392	10	31	3.4	777	1097	105	197	2199	123	0.72292
RW99-63	M	108	42	621	243	8.5	22	18.9.	340	1113	138	146	1343	99	0.72835
RW98-8	PM	154	28	1099	957	9.7	39	28	1052	2115	217	318	4429	391	0.71502
RW99-10	S	227	30	2358	2116	n.m.	52	b.d.	3072	2640	196	622	13410	282	
RW99-52	M	162	28	1172	842	9.7	41	6.5	1139	2146	228	328	4772	296	0.71473
RW98-2	PM	259	50	1658	1065	9.8	48	58	1115	2834	231	399	4546	439	0.71920
RW99-3	S	298	53	1807	1621	8.3	51	22	2046	3524	186	547	4638	446	0.72050
RW99-57	M	258	44	1404	736	8.5	42	38	880	2697	217	348	3517	338	0.71954
RW98-3	PM	275	42	954	460	6.7	77	39	395	1867	241	229	1679	n.m.	0.72107
RW99-4	S	372	49	1064	776	n.m.	54	b.d.	923	2233	167	309	2915	231	
RW99-56	M	306	47	1084	424	6.8	94	54	386	2524	230	274	1809	274	0.72060
RW98-10	PM	204	33	1512	959	13	57	25	1226	2610	227	384	5758	538	0.71415
RW99-65	M	187	30	1429	623	10	30	b.d.	707	2614	234	320	4280	347	0.71591
RW98-11	PM	330	46	1893	1080	11	225	164	975	3840	351	479	2491	764	0.71491
RW99-1	S	349	33	1491	1213	n.m.	256	151	714	4257	378	468	1793	725	
RW99-61	M	324	55	1887	972	11	225	119	822	3920	303	461	2870	530	0.71421
Ganga and Bandal															
RW98-34	PM	102	45	452	195	11	27	18.2	165	1035	151	117	626	n.m.	0.73856
RW99-6	S	106	46	446	176	11	24	17.5	204	1014	81	115	712	78	0.73657
RW99-59	M	76	37	397	150	8.6	21	10.6	145	891	116	99	507	72	0.73849
RW99-8	S	116	45	1226	1260	7.1	35	9.0	909	3020	141	366	2108	257	0.72116
Springs															
RW98-7	PM	54	27	2520	2035	n.m.	49	19.0	2913	2340	142	587	12794	n.m.	0.70954
RW99-9	S	74	23	3805	3187	n.m.	34	12.8	5454	3406	145	975	25200	239	
RW99-60	M	281	53	13366	3942	n.m.	3.4	b.d.	15401	4623	175	2412	62086	83	0.70972

[a)]RW - river water, [b)]S = summer, M = monsoon, PM = post-monsoon. n.m.: not measured, b.d.; below detection limit

Table 4.2 Chemical composition of bed sediments and granites from the YRS basin.

Sample Code[a)]	Na (%)	K (%)	Ca (%)	Mg (%)	Al (%)	Fe (%)	Carb. (%)[b)]	Sr (ppm)	Ba (ppm)
Sediments									
RS98-1	0.98	1.46	1.57	0.82	4.51	2.36	3.27	69	319
RS98-2	0.86	1.99	2.18	1.47	5.90	3.17	7.29	63	471
RS98-3	0.57	1.30	0.80	0.73	4.05	2.15	1.48	51	278
RS98-4	1.04	1.56	1.55	0.93	4.44	0.47	3.43	77	367
RS98-5	1.29	2.49	0.58	0.91	7.11	3.27	1.16	52	447
RS98-5R	1.21	2.51	0.58	0.92	6.94	3.06	n.m.	54	484
RS98-6	1.21	1.43	1.88	1.09	4.10	1.91	3.77	75	297
RS98-8	0.37	1.60	10.1	5.79	3.02	1.37	43.5	156	535
RS98-9	1.06	1.32	1.79	0.98	3.89	1.89	2.96	78	286
RS98-11	0.47	1.92	0.39	0.82	5.24	2.35	0.11	56	497
RS98-12	1.14	1.40	1.45	0.88	3.82	1.61	1.71	74	286
RS98-13	1.09	1.97	2.29	1.97	5.80	2.27	3.93	71	427
RS98-13R	1.03	2.01	2.27	2.01	6.03	2.87	n.m.	74	433
RS98-14	1.19	1.37	1.50	0.78	3.71	1.91	1.44	62	245
RS98-18	1.64	3.01	0.81	0.97	5.86	2.04	0	64	507
RS98-19	0.92	1.14	2.98	1.00	5.05	3.65	5.48	85	265
RS98-19R	0.93	n.m.	2.99	1.00	4.89	3.51	n.m.	88	272
RS98-20	1.54	2.01	1.74	0.76	4.86	1.92	2.23	91	400
RS98-21	0.69	1.51	0.48	0.53	3.15	1.24	0.40	48	319
RS98-22	1.31	1.52	1.50	0.83	4.30	2.11	1.63	72	285
RS98-22R	1.29	1.55	1.48	0.84	4.32	1.89	n.m.	72	296
RS98-25	1.38	1.77	1.39	0.88	4.53	2.02	1.16	75	328
RS98-26	0.63	1.04	0.73	0.52	3.28	2.81	0	45	201
RS98-27	1.31	1.76	0.92	0.59	4.89	2.12	0	98	422
RS98-28	1.26	1.64	0.88	0.54	4.47	1.98	0	94	394
RS98-29	1.05	1.26	0.84	0.43	4.29	3.00	0	75	303
RS98-30	0.94	1.65	1.56	0.86	5.23	4.24	3.53	74	420
RS98-31	0.88	2.24	2.06	1.14	6.49	3.37	6.47	65	549
RS98-32	1.19	1.47	1.44	0.79	4.97	2.63	2.56	104	381
RS98-33	0.98	1.59	1.29	0.91	5.22	2.92	2.84	78	419
Granites									
GR98-1	3.67	1.58	1.13	0.23	n.m.	n.m.	0.71	90	122
GR98-2	4.11	3.80	0.80	0.54	n.m.	n.m.	0.16	130	377
GR99-1	3.51	3.64	1.21	0.50	n.m.	n.m.	0.76	153	396
GR99-2	3.63	3.99	0.71	0.35	n.m.	n.m.	0.92	110	333

[a)]RS: bed sediment, GR: granite, n.m.: not measured, R: replicate analysis. [b)]calculated assuming all carbonates to be $CaCO_3$.

The total cation charge (TZ^+) balances that of the total anions (TZ^-) in most of the samples. Regression analysis of TZ^+ and TZ^- in the YRS yield a line with a slope of 0.98±0.01 (indistinguishable from 1.0 within error) and $r^2 = 0.989$ (Fig. 4.1).

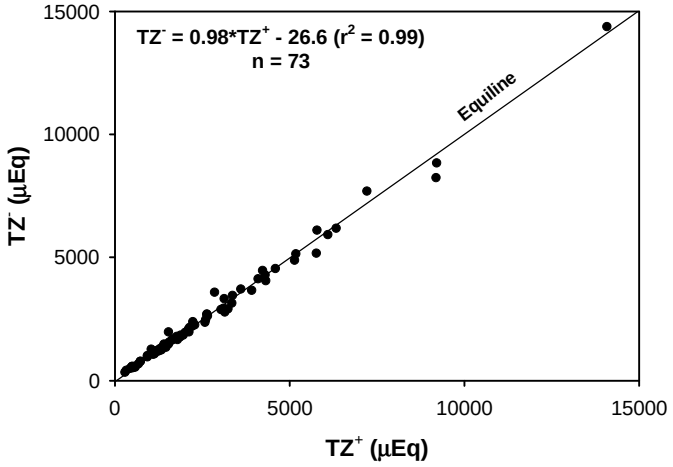

Fig. 4.1 Plot of TZ^+ vs. TZ^- for the YRS rivers. Most of the samples plot on the equiline.

Out of the 80 samples analyzed (Table 4.1), 68 samples exhibit normalized inorganic charge balance [NICB = $(TZ^+-TZ^-)/TZ^+$] less than 10%, indicating that the major ions measured in this study by and large account for the charge balance. Bulk of the remaining 12 samples had $TZ^->TZ^+$, the cause for which is unclear. The data, however, suggest that the contributions from organic acids and ligands to the charge balance in the YRS samples analyzed is not significant as reported for tropical rivers such as the Nyong (Viers et al., 2000) and those draining the Guayana Shield (Edmond et al., 1995).

The total cations (TZ^+) and total dissolved solids (TDS) in the YRS range from ~300 to ~9200 µEq and ~32 to ~620 mg ℓ^{-1} respectively. Both TZ^+ and TDS show spatial and temporal variations. Spatially, the samples collected from the upper reaches have lower TZ^+ and TDS, temporally the summer (June) samples have more TDS than those collected during post-monsoon (October) and monsoon (September) seasons. Previous studies from our group (Sarin et al., 1989; Singh 1999, unpublished results) have reported major ion composition of the Ganga at Rishikeshand the Yamuna at Saharanpur. The earlier data are compared with those measured in this study in Table 4.3. The results for the Ganga at Rishikesh, are remarkably similar for most of the major ions suggesting that over nearly two decades, its

major ion composition during monsoon has remained nearly the same. For the Yamuna, the data of Sarin et al. (1989) are for samples collected in March, during which no sampling was done in the present study. If, however, March data of Sarin et al. (1989) are compared with those of June samples collected in this study, it is seen that the former show lower concentrations of ions (by 30-40 %) than that measured in this work (Table 4.3). These differences could arise due to intra and/or interannual variations in water chemistry.

Table 4.3 Temporal variations in the Ganga and Yamuna major ion chemistry

Component	**Ganga at Rishikesh[a)]**			**Yamuna at Saharanpur[b)]**	
	Sarin et al., 1989	*Singh, 1999*	*This study*	*Sarin et al., 1989*	*This study*
Ca	353	355	397	590	948
Mg	153	122	150	329	448
Na	59	65	76	203	242
K	38	43	37	45	85
HCO_3	894	900	891	1677	2608
SO_4	121	82	145	251	321
Cl	23	23	21	52	56

[a)]sampled during monsoon (September). [b)]Sarin et al. (1989) sampled during March, this work during June.

The TDS in the YRS, as mentioned earlier, range from ~32 to ~620 mg ℓ^{-1}, with more than 80% of the samples having TDS >80 mg ℓ^{-1} (Table 4.1, Fig. 4.2). The lower TDS values (≤50 mg ℓ^{-1}) are in tributaries of the Yamuna and the Tons in their upper reaches where the lithology is predominantly Higher Himalayan Crystallines (Fig. 2.3). The TDS in the

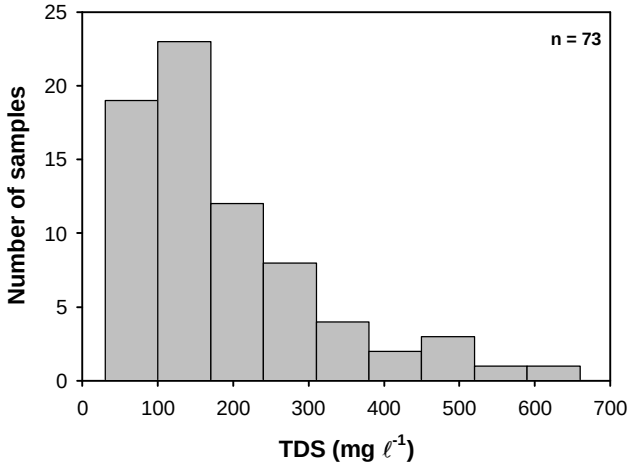

Fig. 4.2 Distribution of total dissolved solids (TDS) in the YRS. The TDS range from ~32 to ~620 mg ℓ^{-1}.

Yamuna even at Hanuman Chatti, however, is quite high, ~90 mg ℓ^{-1}, though the location is only about 10 km downstream of its glacier source. This underlines the significant role of glacier melt waters in contributing to the major ion budget of the Yamuna at this site. Many glacier melt waters from the Himalaya, e.g. Dokriani, Pindari all have high TDS, ~32 to 220 mg ℓ^{-1}, attributed to weathering of carbonates by CO_2 and H_2SO_4 (Hasnain and Thayyen, 1999; Pandey et al., 2001). The relatively high concentration of Ca in the sample at Hanuman Chatti (RW98-16, RW99-13, Table 4.1) supports such a contention. The TDS values of the YRS are higher than those in the headwaters of the Ganga (Sarin et al., 1992) and are either similar to or lower than those in the Indus (Karim and Veizer, 2000; Pande et al. 1994). These TDS values are lower than those in the Kali Gandaki and its tributaries, draining the Tethyan Sedimentary Series (TSS) and Lesser Himalaya (LH), but much higher than those in the Trisuli and its tributaries which drain mainly the Higher Himalayan Crystallines (HHC) in the Nepal Himalaya (Galy and France-Lanord, 1999). The YRS rivers in the lower reaches have TDS similar to those in the Changjiang, Mekong and Xijiang, rivers draining the northern slopes of the Himalaya (Gaillardet et al., 1999).

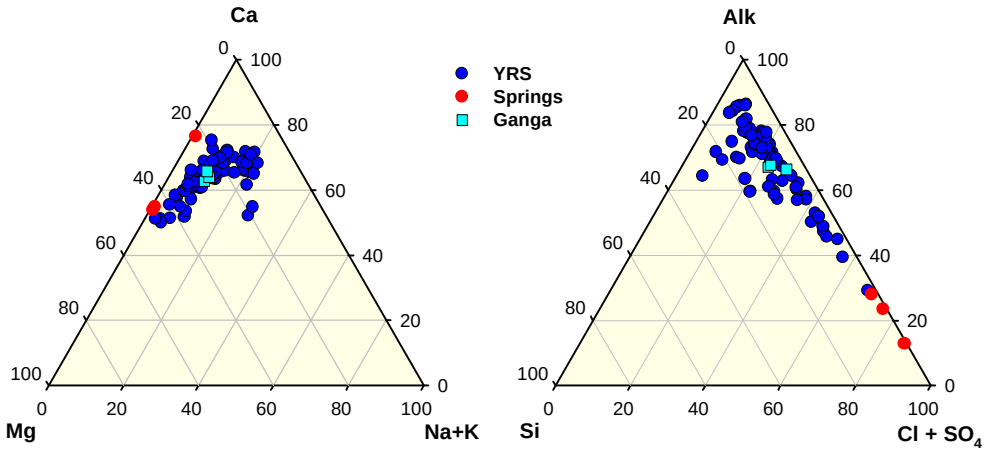

Fig. 4.3 Ternary plots for the YRS, Ganga and Spring waters. Cations for most of the samples plot close to the Ca apex suggestive of dominance of carbonate weathering in the catchment. Anions plot on the mixing line of alkalinity and SO_4+Cl, suggesting contributions from carbonate-evaporite-pyrite weathering (see text).

On a global scale, the TDS in the YRS are generally higher than those in the Amazon, Congo, Niger and in the streams draining the Guayana shield (Boeglin and Probst, 1998; Edmond et al., 1995; Edmond and Huh, 1997; Gaillardet et al., 1997; Negrel et al., 1993) but

are either similar to or lower than those in the rivers draining basaltic terrains such as the Reunion Island and the Deccan Traps (Louvat and Allegre, 1997; Dessert et al., 2001).

Among the cations, Ca is the most abundant followed by Mg, together they constitute ~90% of TZ^+. The major cations decrease as Ca>Mg>Na>K (Table 4.1), a trend similar to that observed in the Ganga headwaters (Sarin et al., 1992). This is clearly evident in the ternary cation plot (Fig. 4.3) in which most of the samples cluster around the Ca apex with a

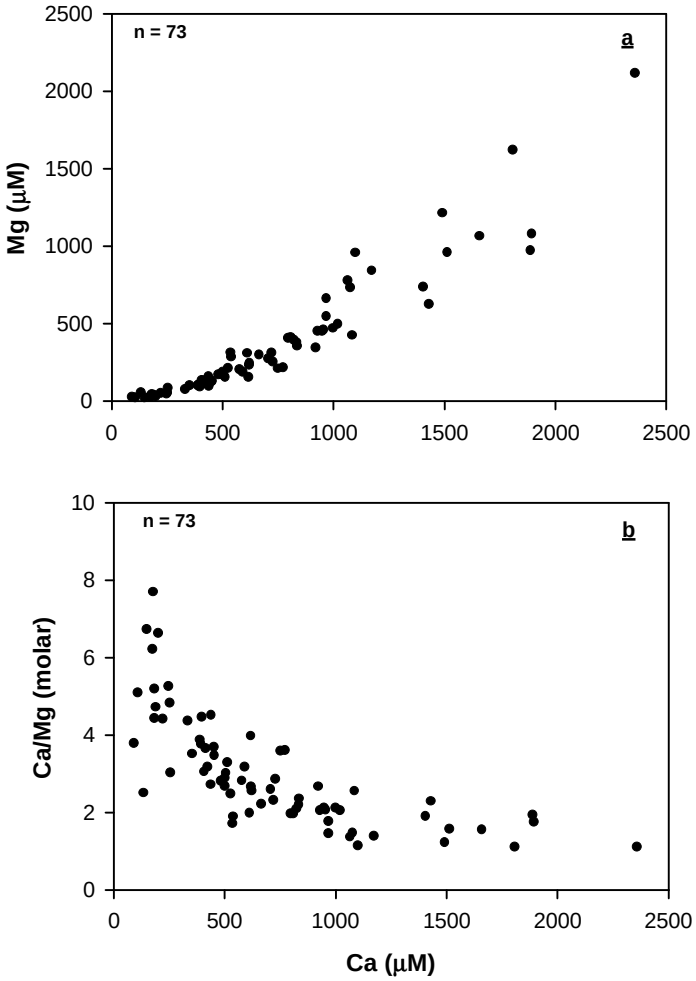

Fig. 4.4 Scatter plot Mg concentration (a) and Ca/Mg molar ratio (b) against Ca in the YRS waters. Mg abundances show a strong positive correlation with Ca suggestive of a common source. Ca/Mg ratios decrease with increasing Ca, dolomite weathering and/or preferential removal of Ca (as calcites) can contribute to the observed trend.

few of them tending towards the Mg apex. This is characteristic of limestone and dolomite weathering, consistent with the lithology of the drainage basin. Mg shows a significant positive correlation with Ca (Fig. 4.4a). The Ca/Mg molar ratios average about 3, with a range from 1.1 to 7.7. The range and mean of Ca/Mg in the YRS are similar to those in the

Ganga headwaters (range: 1.9 to 7.6, mean: 3.3, Sarin et al., 1992a). In the YRS, Ca/Mg decreases with increasing Ca concentration (Fig. 4.4b), low Ca/Mg (1-2) are mainly in streams such as the Aglar, Asan, Giri, Bata and the Yamuna and the *Tons* in the lower reaches (Table 4.1, Fig. 4.4b) all of which flow through terrains abundant in Precambrian

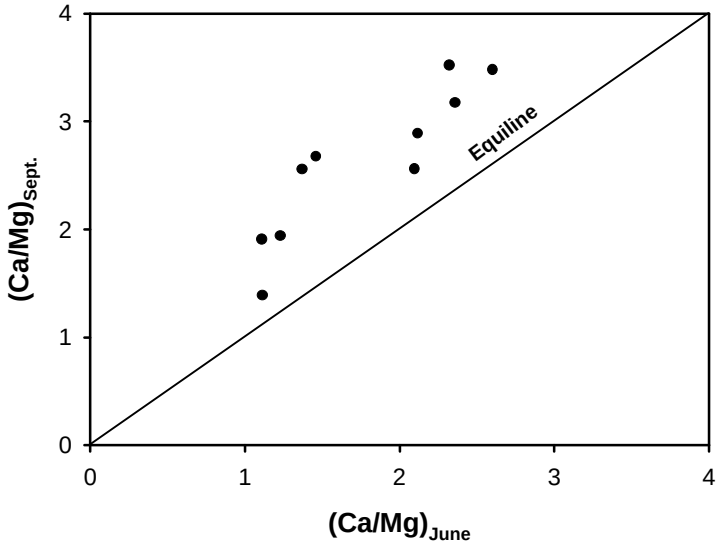

Fig. 4.5 Seasonal variation of Ca/Mg in the YRS waters. September (monsoon) samples have higher Ca/Mg ratios than the June (summer) samples.

carbonates. A likely cause for the low Ca/Mg in these waters is the supply of Ca and Mg via dissolution of dolomites that constitute a major portion of the Precambrian carbonates (Singh et al., 1998). A closer inspection of the data reveals that in samples collected from the lower reaches of the YRS during monsoon have higher Ca/Mg than those collected during the summer season (Fig 4.5). This could be due to relatively rapid dissolution of calcite during the monsoon period when the water flow is high. Alternatively, low Ca/Mg during summer can result if Ca is preferentially removed from the rivers by precipitation (e.g. calcite), a mechanism invoked by Sarin et al. (1989) to explain seasonal variations in Ca/Mg in the Ganga river system in the plains. Calcite precipitation, if any, is more likely to occur during summer than during the monsoon, considering that the cation and alkalinity concentrations are in general higher during summer. To assess whether calcite can precipitate from the waters of the YRS, calcite saturation index (CSI) was calculated using pH, HCO_3 and Ca data following the approach of Drever (1997). These calculations were made for two temperatures, 15 °C and 25 °C, for river waters with temperatures ranging between 10-20 °C

and 20-30 °C respectively. The results show wide range of calcite saturation with bulk of the river waters being supersaturated with calcite (Fig. 4.6).

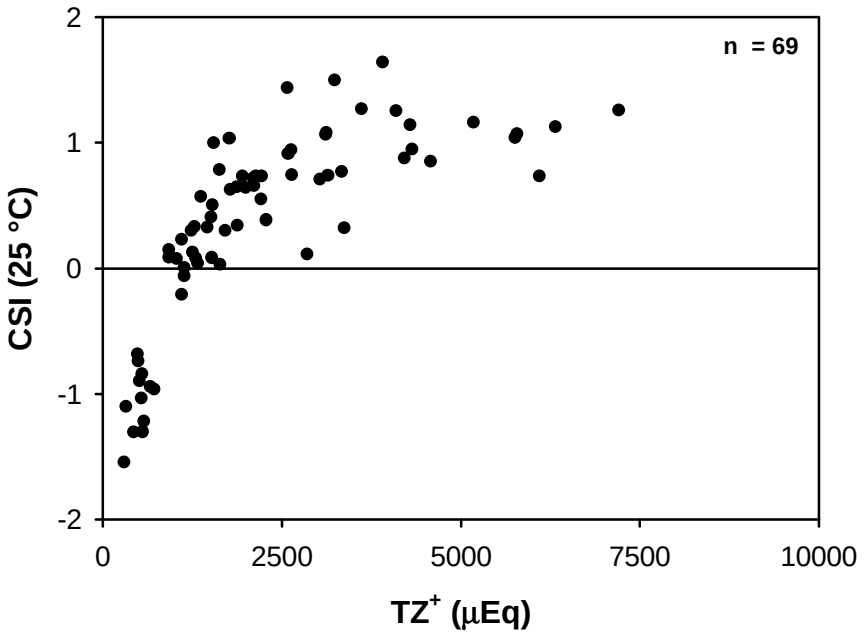

Fig. 4.6 Calcite saturation index (CSI) in the YRS rivers/streams. Bulk of the samples are supersaturated with calcite, the degree of saturation seems to show an increasing trend with total cation charge. Rivers in the upper reaches generally have CSI <0.

The impact of supersaturation on the precipitation of calcite is uncertain, though it is interesting to note that the rivers Aglar, Asan, Giri, Bata, *Tons* at Dehradun, Barni Gad which have low Ca/Mg ratios also have high degree of calcite supersaturation (CSI ≥1). The observation that Ca and Mg concentrations in unacidified river water samples measured several weeks after the collection, is nearly identical to those measured in the acidified samples (Fig. 2.11, Chapter 2), suggests that there is no measurable loss of Ca via precipitation in the laboratory. The lack of nucleation process may be responsible for preventing precipitation of calcite and thereby aid in maintaining its supersaturation. If this result can be extended to YRS rivers, it would indicate that calcite precipitation and preferential loss of Ca may not be a cause for altering Ca/Mg in samples analyzed. This inference, however, needs to be validated through more detailed laboratory and field studies. Use of carbonate content of bed sediments to determine if calcite precipitation occurs, also does not yield unambiguous conclusions. This is because these sediments contain detrital carbonates derived from the drainage basin. Indeed, Galy and France-Lanord (1999), based

on Sr, C and O- isotopic composition of the bed load in rivers of the Nepal Himalaya and Bangladesh and carbonate bedrocks, inferred that the bed carbonates are mainly of detrital origin. Thus, the origin of higher carbonate contents in the bed sediments of the Yamuna and its tributaries draining the lower reaches (Table 4.2) is uncertain, it can either be of detrital origin or of calcite precipitation or both.

The tributaries of the Yamuna and the Tons in their upper reaches, flowing mainly through crystallines, are undersaturated with calcite. These streams are low in TZ^+ and have much less carbonates in their bed sediments. It is seen that in general summer samples have higher CSI values. This is expected as both Ca and alkalinity show higher abundances during summer (Table 4.1). This trend is reflected in the general trend of CSI with TZ^+ (Fig. 4.6).

There is considerable excess of Na over Cl, the range in Na/Cl molar ratio being 1.4 to 7.3 (mean 3.6). This suggests that on an average, contribution of Na from recycled marine salt and evaporite dissolution is only about a third of its abundance and that bulk of Na has to be derived from silicate weathering. Inspite of this, on an average, Na^* and K together [Na^* = (Na-Cl), Na corrected for cyclic salt and evaporite dissolution] constitute only ~10 % of the TZ^+ suggesting that silicate weathering is not a major source of cations to these rivers on a basin wide scale (see later discussion). Godu Gad and Didar Gad, which flow mainly through silicate terrains have Na^*+K contribution to TZ^+ as high as ~25%. These streams also have high SiO_2 contribution to TDS (see discussion below) and highly radiogenic $^{87}Sr/^{86}Sr$ (Table 4.1). K/Na^* molar ratios in the YRS range from 0.1 to 2.2 with an average 0.6. In general, streams in the upper reaches have high K/Na^* (≥ 1). The K/Na^* decreases with increasing Na^* (Fig. 4.7). This decrease is mainly due to increase in Na^* in the lower reaches, the K concentrations in the waters by and large center around 30-50 μM (Table 4.1).

The dissolved silica concentrations of the YRS lie in the range of 67 to 378 μM (Table 4.1). This range is marginally higher than that in the Ganga headwaters (42 to 294 μM; Sarin et al., 1992). The Si concentrations in the YRS rivers are generally similar to those in the rivers draining the Nepal Himalaya (Galy and France-Lanord, 1999) but is lower than those in the rivers draining basaltic rocks (Louvat and Allegre, 1997; Dessert et al., 2001). The dissolved Si concentrations in the rivers draining the northern slopes of the Himalaya, the Changjiang, the Mekong and the Xijiang (Gaillardet et al., 1999) are, in general, lower than those in the YRS rivers. On an average, SiO_2 accounts for ~7 % of the TDS (wt. basis).

Its contribution to the TDS in the YRS streams, varies from ~2 to ~23%, the streams draining predominantly silicates, the Godu Gad and the Didar Gad have higher SiO_2 contribution to TDS whereas the Shahashradhara spring water has the lowest. $(Na^*+K)/(TZ^+)^*$ in the YRS show a significant positive correlation with SiO_2/TDS, the regression line having a slope of 0.68 (r^2 = 0.81, Fig. 4.8). This trend suggests that an increase in relative contribution of silicate (Na*+K) to TZ^+ is accompanied by an increase in silica contribution to the TDS. Further, the trend in Fig. 4.8 is an indication that weathering of silicate minerals is the dominant source of dissolved SiO_2 to the waters and that its supply via quartz dissolution does not seem to play an important role in regulating the dissolved silica budget, an inference attested by low value of the intercept (0.01) of the regression line (Fig. 4.8).

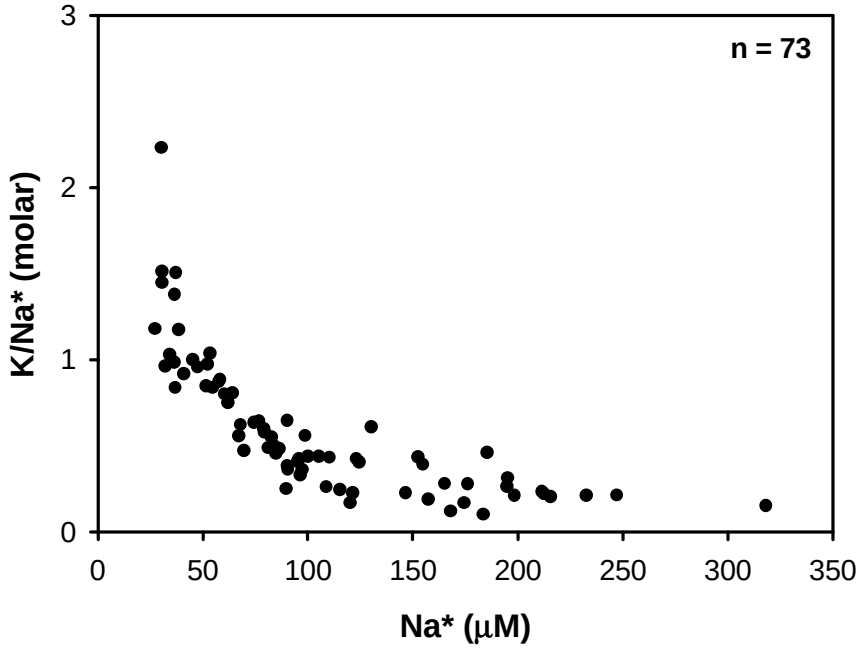

Fig. 4.7 Variation of K/Na vs. Na* in the YRS samples. The decrease in K/Na* with Na* is primarily due to increase in Na* concentration.*

It is also seen from the data (Fig. 4.9) that the Si abundance and TZ^+ are positively correlated, albeit with some scatter especially at higher TZ^+ values. This correlation seems to suggest that the weathering of silicates and other lithologies occur roughly in the same proportion in the drainage basins of the YRS. A possible reason for the scatter at high TZ^+ values could be weathering of carbonates and/or evaporite dissolution, which adds to the TZ^+, but with very little Si. The samples of the Giri (RW99-3) and Aglar (RW99-10), with very high TZ^+ (>7000 μEq), fall far away from the trend set by the other samples. These

rivers drain carbonates of Krol Formations, which have been known to have pockets of gypsum in them. Further, they have high SO_4 (>2000 μM), Ca and Mg, with SO_4>Ca and samples collected from these rivers during post-monsoon have high Re (Chapter 5). It can be

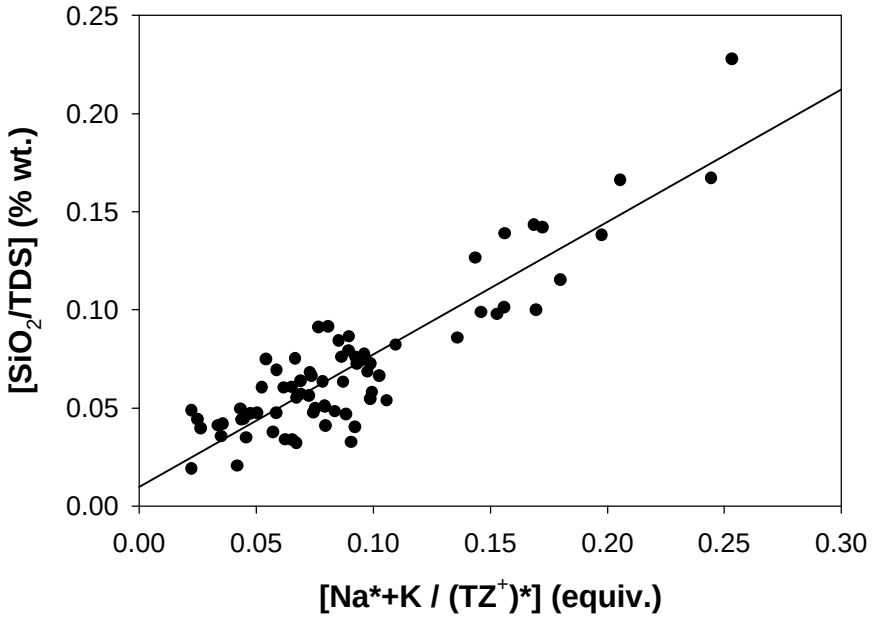

Fig. 4.8 Plot of SiO_2/TDS vs. (Na+K)/TZ^+ for the YRS waters. A strong positive correlation is evident (r^2 = 0.81) indicating that increase in contribution of (Na*+K) to total cations is accompanied by an increase in SiO_2 contribution to TDS. This covariation can be interpreted in terms of supply of SiO_2 and (Na*+K) to rivers via silicate weathering.*

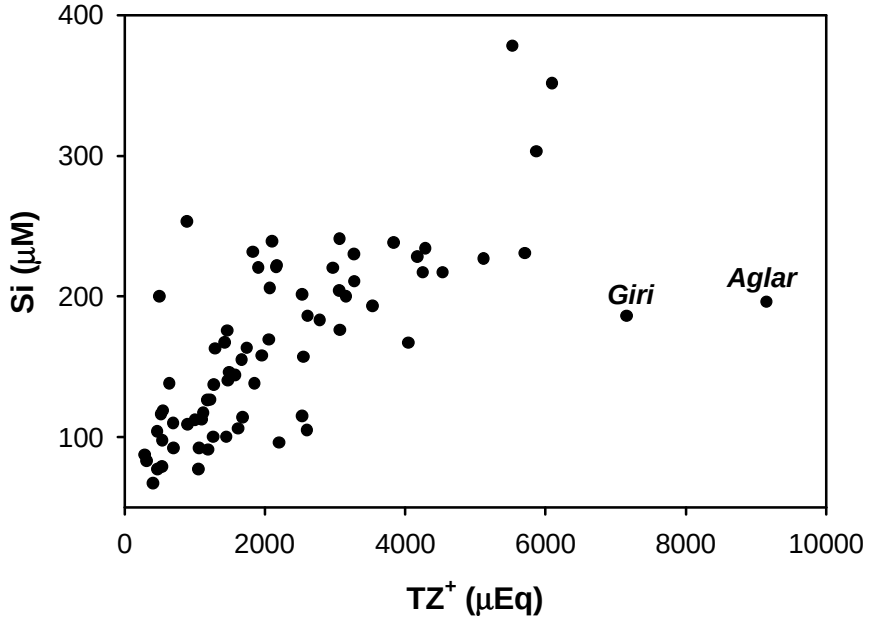

Fig. 4.9 Scatter plot of Si vs. TZ^+ in the YRS waters. A positive correlation is seen with larger scatter at higher TZ^+.

inferred from all these data that the waters in these rivers derive cations mainly from weathering of carbonates by carbonic and sulphuric acids and gypsum dissolution. Consequently they have high TZ^+ and less Si compared to the other rivers.

Carbonate alkalinity is the dominant anion in the river waters analyzed and in bulk of the samples it exceeds 70% of the TZ^-. The molar abundance of anions decrease as alkalinity>SO_4>Cl>NO_3>F except in the summer sample of the Aglar (RW99-10) and the spring waters (Kempti Fall and Shahashradhara) where SO_4>alkalinity. The SO_4 concentration exhibits a general increase from the upper to lower reaches. Rivers draining the crystallines in the upper reaches have SO_4 <100 μM whereas the Giri, Bata and Aglar, flowing through the Lesser Himalayan sediments which are reported to contain evaporites and black and gray shales (Valdiya, 1980) associated with pyrites, have >400 μM SO_4.

On a ternary anion diagram (Fig. 4.3), the data points fall along the alkalinity-(SO_4+Cl) line characteristic of carbonate-evaporite-sulphide weathering. The SO_4/Cl molar ratios in the YRS, though show a wide range, 0.7 to ~59 (average ~7), most of the values center around 3±2. Only 10 samples of 73 in the YRS, have SO_4/Cl>20. These samples are from the Aglar, *Tons* at Dehradun, the Giri and the Tons (after its confluence at Kalsi). The highest SO_4/Cl, 59 is in the June sample of Aglar which has also high values, 27 and 28 during October and September respectively. The significantly higher SO_4 relative to Cl is an indication that if evaporites are a major source of SO_4 to these waters, then their composition must be dominated by gypsum/anhydrite with only minor amounts of halite. Such a contention is supported by very high SO_4/Cl (4530) in the spring waters of Shahashradhara. In addition to evaporites, oxidative weathering of pyrites can also contribute SO_4 to the waters. Evaporite dissolution would supply Ca and SO_4 to the waters in the ratio 1:1. If SO_4 is also derived from H_2SO_4 generated via pyrite oxidation, it can result in SO_4/Ca>1. The observation that some of the rivers have SO_4≥Ca (Table 4.1) is an evidence for the supply of SO_4 to them by pyrite oxidation. Further, the evidence for oxidative weathering of pyrites throughout the YRS drainage basin is provided by significant positive correlation between Re and SO_4 in the YRS waters; which has been attributed to weathering of organic rich sediments containing high Re by sulphuric acid released from oxidation of pyrites which are generally associated with them (Chapter 5; Dalai et al. 2001a).

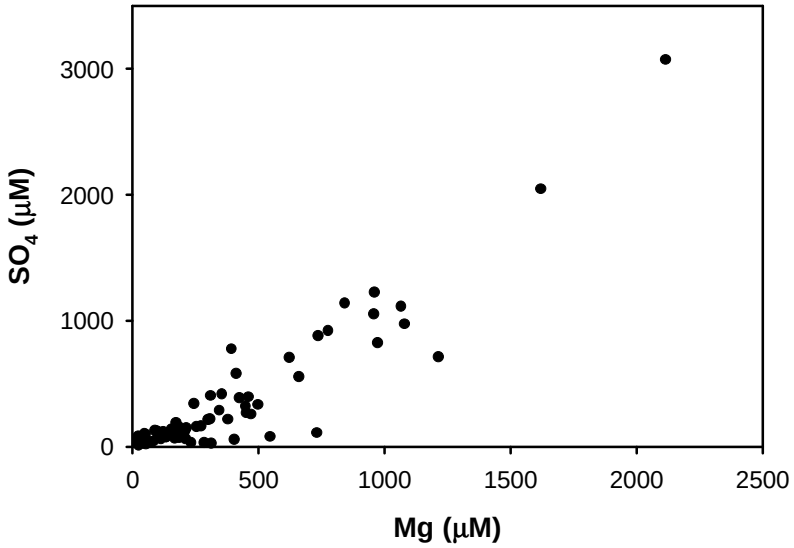

Fig. 4.10 Scatter plot of SO_4 vs. Mg in the YRS waters. A strong positive correlation is evident (r^2 = 0.85), a likely result of weathering of dolomites by sulphuric acid.

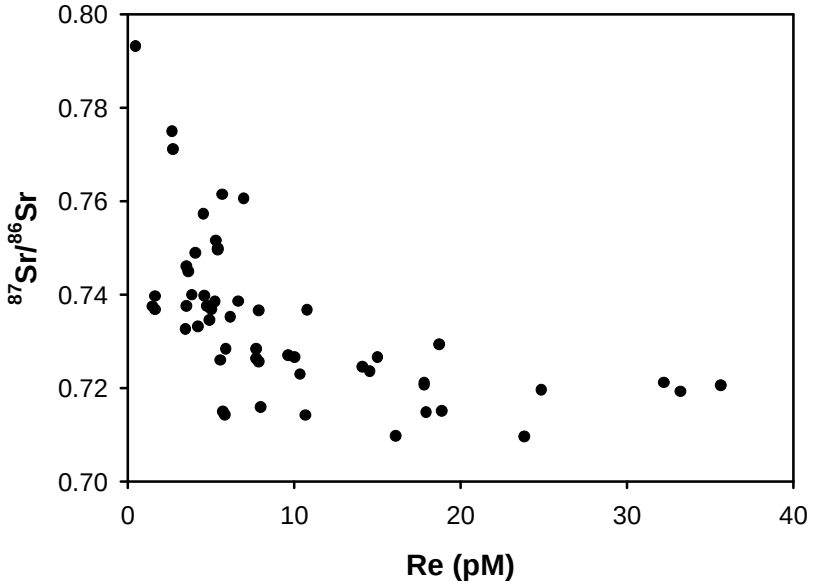

Fig. 4.11 Scatter plot of $^{87}Sr/^{86}Sr$ vs. dissolved Re in the YRS waters. An inverse trend suggests that weathering of lithologies associated with organic rich sediments contribute Sr with low $^{87}Sr/^{86}Sr$ to the YRS.

Other evidences in support of pyrite oxidation in the YRS drainage basin come from the positive correlation between Mg and SO_4 and the anticorrelation between $^{87}Sr/^{86}Sr$ and dissolved Re (Figs. 4.10 and 4.11). The correlation of Mg with SO_4 most likely results from weathering of dolomites by H_2SO_4. Similarly the inverse correlation between $^{87}Sr/^{86}Sr$ and Re can be understood in terms of weathering of organic rich sediments and associated pyrites

and carbonates/phosphates. The organic rich sediments contribute Re, and H_2SO_4 produced via pyrite oxidation release Sr from carbonates/phosphates with low $^{87}Sr/^{86}Sr$.

The NO_3 abundance generally centers around a few tens of μM, with lower values in the rivers draining the upper reaches (Table 4.1). The Yamuna samples from Saharanpur and its tributaries Asan, Giri, Bata all have higher NO_3 concentration, with values exceeding 30 μM (Table 4.1). One of the sources of the nitrate to rivers is fertilizers (Berner and Berner, 1996). The impact of agriculture on NO_3 abundances in the YRS is difficult to assess, as our knowledge on the agricultural practices and fertilizer uses in the drainage basins of these rivers is very limited. However, Asan river samples which have the highest NO_3 (>100 μM, Table 4.1) and high chloride (>200 μM) abundances among all the rivers, anthropogenic contribution could be a concern. Collins and Jenkins (1996) observed that terrace agriculture and use of nitrogenous mineral fertilizers elevated the concentrations of NO_3 and base cations in the streams draining the Middle Hills of the Nepal Himalaya.

Fluoride concentrations in the YRS are quite low, ~2 to 18 μM with a mean 9±3 μM, with no discernible trend along their course. They are in general lower than those in the Ganga headwaters (Sarin et al., 1992) and similar to those in the rivers draining the Nepal Himalaya and the Ganga-Brahmaputra in Bangladesh (Galy and France-Lanord, 1999).

4.2.2 Sources of major ions in the YRS

Major ions are supplied to rivers via atmospheric deposition, chemical weathering of various lithologies in the basin and anthropogenic sources. The dissolved concentrations of major elements and their ratios in the rains and streams/rivers of the YRS are examined, with suitable assumptions, to constrain the contributions from these sources. These results are used to derive silicate and carbonate weathering rates in the YRS basin and associated CO_2 consumption.

Considering that the YRS in the Himalaya is reasonably "pristine" and "remote" from thickly populated areas (particularly in its middle and upper reaches), anthropogenic contribution to its major ion budget is unlikely to be of importance. The impact of atmospheric deposition on the dissolved load can be gauged from the chemical composition of rain and snow in the region. Generally sea salt aerosols and atmospheric dust are the dominant sources of major ions to rain and snow in basins such as the YRS which are remote. In this study, three individual rainwater samples were collected from Dehradun and

analyzed for their major ions (Table 4.4). Of these, one sample (#3, Table 4.4) had a significant amount of particulate matter, this sample also has much higher concentrations of major ions compared to the other two samples. It seems likely that the particulate matter may have contributed to the high dissolved load in this sample and therefore it may not represent a "typical" rain sample of the region. Therefore, the data of this sample is not considered in the following discussions. Precipitation samples could not be collected from the upper reaches of the YRS, however, data are available for snow and ice samples from the Chhota Shigri (altitude: 4000-5600 m. latitude: 32°19'N, Nijampurkar et al., 1993) and Pindari glaciers (altitude: 3600-5720 m, latitude: 30°16' to 30°19'N, Pandey et al., 2001). These glaciers are located in the same range of altitude (~3300-6300 m) and latitude as the Yamunotri glacier.

Table 4.4 Chemical composition of rain, snow and glacier ice (μM)

Sample	Na	K	Ca	Mg	Cl	NO_3	SO_4	Ref.
Rain 1	0.2	0.8	0.7	0.4	3.2	—	4.5	1
Rain 2	0.2	0.8	1.3	0.7	3.8	—	4.8	1
Rain 3	1.7	7.3	65	6	13	61	47	1
Chhota Shigri (snow)	14	7	6	4	21	8	2	2
Chhota Shigri (ice)	8	3	2.6	1.4	11	7	1.8	2
Dokriani Bamak (snow)	10	3.4	4.2	2.4	19	3.4	6.8	3

1: This study, 2: Nijampurkar et al. (1993); 3: Sarin and Rao (2001)

It is seen from the data in Table 4.4 that among the major ions, atmospheric deposition can be important as a source only for chloride in the YRS. The chloride concentration in rain is ~5 μM and that in the snow/ice is ~20 μM compared to 5.7-256 μM in rivers and streams (Table 4.1). As bulk of the rivers in the YRS have >30 μM chloride, rainwater contribution of chloride to the YRS in general is <15 %. In a few streams, however, chloride is quite low <10 μM (Table 4.1), in these cases much of the Cl can be of atmospheric deposition. The inference that the atmospheric deposition of chloride is <15 % in bulk of the river samples, suggest that dissolution of halites is the major source of chloride to these rivers.

The contribution of Na to rivers/streams from atmospheric deposition can be estimated from Na/Cl ratios in rains/snow, which is ~0.5 (Table 4.4). Using this value, the Na contribution from atmospheric deposition is calculated to be, on average, <5% of its

concentration in rivers. K concentration in rains is <1 μM and that in the snow/glacier is ~3 μM (Table 4.4). This is less than ~15 % of its abundance even in the Amlawa river, which has the lowest K among all the rivers analyzed (Table 4.1). Ca and Mg in rainwater and snow/glacier samples are negligibly small (Table 4.4) to be of any significance to their river water budget.

(i) Silicate weathering

One of the main goals of this work, as mentioned earlier, is to constrain contemporary silicate and carbonate weathering rates in the Yamuna River Basin in the Himalaya. This goal can be achieved if the contributions of major cations to the rivers and streams of the YRS via silicate and carbonate weathering can be determined. Na in the waters is derived from cyclic salts, halite dissolution and silicate weathering, whereas the dominant source of K is silicates. Using Cl as an index of cyclic salts and halites, the silicate component of Na can be estimated as

$$Na_s = Na_r - Cl_r \text{ and } K_s \approx K_r$$

where the subscripts s and r refer to 'silicate' and 'river' respectively (Na_s is same as Na*). Bulk of the Na in the YRS, as mentioned earlier, is derived from silicate weathering. This, coupled with the observation that the YRS waters have measurable quantities of K and SiO_2, suggests that silicate weathering is an ongoing process in the basin. In estimating Na_s, it is assumed that the contribution of Na from carbonates is negligible. The Na/Ca molar ratio in Precambrian carbonates of the Krol Group is ~0.002 (Mazumdar, 1996). Given the Ca concentration in the YRS rivers range from ~90 to 2360 μM (Table 4.1), the Na contribution from these carbonates would be 0.2 to 4.7 μM. These values are much lower than the Na abundance in the rivers. Further, it is likely that Na in these carbonates is associated with silicates which are contained in them.

Rivers derive their Mg from carbonates and silicates whereas sources for Ca are carbonates, evaporites, silicates and minor phases such as phosphates. Apportionment of dissolved Ca and Mg (particularly Ca) among their various sources is more difficult because of uncertainties associated with the end member values and assumptions pertaining to their nature of release during weathering (Krishnaswami et al., 1999). Inspite of this, as discussed below, useful limits on silicate weathering contribution to the dissolved budgets of Ca and Mg in the YRS can be made.

The silicate component of Ca and Mg (Ca_s, Mg_s in moles ℓ^{-1}) can be derived as:

$$(Ca)_s = Na_s \times (Ca/Na)_{sol}$$

$$(Mg)_s = Na_s \times (Mg/Na)_{sol}$$

where $(Ca/Na)_{sol}$ and $(Mg/Na)_{sol}$ are the molar ratios released to river waters from the silicates in the drainage basins during their chemical weathering. The reliability on $(Ca/Na)_{sol}$ determines the uncertainties associated with Ca_s (and Mg_s) estimates. Krishnaswami and Singh (1998) and Krishnaswami et al. (1999) used values of 0.7±0.3 and 0.3±0.2 for $(Ca/Na)_{sol}$ and $(Mg/Na)_{sol}$ ratios. This compares with values of 0.5 and 0.2 respectively for $(Mg/K)_{sol}$ and $(Ca/Na)_{sol}$ used by Galy and France-Lanord (1999) for estimating the silicate contribution of Ca and Mg to the rivers in the Nepal Himalaya. (The $(Ca/Na)_{sol}$ ratio used by Galy and France-Lanord (1999) is based on (Ca/Na) in whole rock silicate composition of the Higher Himalaya (HH) and Lesser Himalaya (LH) and in plagioclase of the HHC, whereas the value of Krishnaswami et al. (1999) is based on (Ca/Na) in LH granites/gneisses, soil profiles and in rivers draining predominantly silicates. Among these, the Ca/Na in rivers is generally much higher than those in the granites/gneisses and those based on soil profiles resulting in a higher $(Ca/Na)_{sol}$). Bulk of the drainage basin of the YRS lies in the Lesser Himalaya. The average (Ca/Na) molar ratio in granites and gneisses of the LH is 0.46±0.28 (Krishnaswami et al., 1999). This is marginally higher than the value of 0.32±0.29 in HH crystallines (Krishnaswami et al., 1999). Granites from Hanuman Chatti (Table 4.2) and Sayana Chatti (Biyani, 1998) in the Higher Himalaya have Ca/Na, 0.15±0.13, which is within errors of those for the HH crystallines. (Ca/Na) in the bed sediments of the YRS (having no carbonate, Table 4.2) is 0.44±0.14. If river waters receive Ca and Na from these rocks in the same proportion as their abundance, then the $(Ca/Na)_{sol}$ would be in the range of 0.15-0.46. The Ca/Na* in Jola Gad (tributary of the Ganga), Didar Gad (tributary of the Yamuna) and Godu Gad (tributary of the Tons), flowing primarily through silicate terrains, are in the range of 1.15-1.6. These ratios are much higher than those in the silicate rocks, probably because of contribution of Ca to waters from carbonates and evaporites. Thus, based on data on the granites/gneisses of LH and HH, soil profiles in the LH and selected rivers Krishnaswami et al. (1999) used a value of 0.7±0.3 for $(Ca/Na)_{sol}$. In the present work, this value is used for estimation of Ca_s in the YRS. In addition, calculations are also made using $(Ca/Na)_{sol}$ = 0.35±0.15, similar to those observed in rocks. Similarly for $(Mg/Na)_{sol}$ a value of 0.3±0.2 has

been used. This value is based on the Mg/Na in LH crystallines (0.65±0.45), HH crystallines (0.31±0.28), granites from Hanuman Chatti and Sayana Chatti (0.15±0.08) and bed sediments with no carbonate (0.51±0.16).

From these values, the fraction of cation contributions from the silicates to the rivers, $(\Sigma Cat)_s$, can be calculated as:

$$(\Sigma Cat)_s = \frac{\Sigma(X_i)_s}{(\Sigma Cations)_r} = \frac{(Na_s + K_r + 0.7 \times Na_s + 0.3 \times Na_s)}{(Na_r + K_r + Mg_r + Ca_r)}$$

$(\Sigma Cat)_s$ in the YRS range from ~7 to 63% (molar) with an average of (25±11)%. It is important to observe that by decreasing the $(Ca/Na)_{sol}$, from 0.7 to 0.35, the range and average of $(\Sigma Cat)_s$ decreases marginally, 6 to 54% and (22±10)%. The distribution $(\Sigma Cat)_s$ estimated using 0.7 and 0.35 as $(Ca/Na)_{sol}$, is shown in the Fig. 4.12. As expected, the streams flowing mainly through silicate lithology, the Godu Gad and Didar Gad, have the highest silicate cation contributions, 54-63% and 42-47% respectively for summer and post monsoon periods using 0.7 and 0.35 as $(Ca/Na)_{sol}$. $(\Sigma Cat)_s$, in general, is higher in the tributaries of the Yamuna and Tons in the upper reaches where they drain predominantly crystallines. $(\Sigma Cat)_s$ are the lowest in the spring waters of Kempti Fall and Shahashradhara, ~0.5-3 %. Interestingly, $(\Sigma Cat)_s$ in the Yamuna at Batamandi and Saharanpur, where the river carries an integrated signature of weathering contributions from its entire basin in the Himalaya, is 20-28 %, suggesting that the calculated average of $(\Sigma Cat)_s$ in the YRS basin is reliable and not biased by sampling (or exclusion) of particular streams. The calculated $(\Sigma Cat)_s$, using two values of $(Ca/Na)_{sol}$, translates to 2.5 and 20.5 mg ℓ^{-1} of silicate cations in various rivers and ~1 to13 % wt. of TDS, during three seasons. The $(\Sigma Cat)_s$ in the Ganga waters at Rishikesh, based on the data in Table 4.1, is ~19-27 %. This compares well with the $(\Sigma Cat)_s$ estimate made earlier in the Ganga water at Rishikesh, 21-30 % (Krishnaswami et al., 1999).

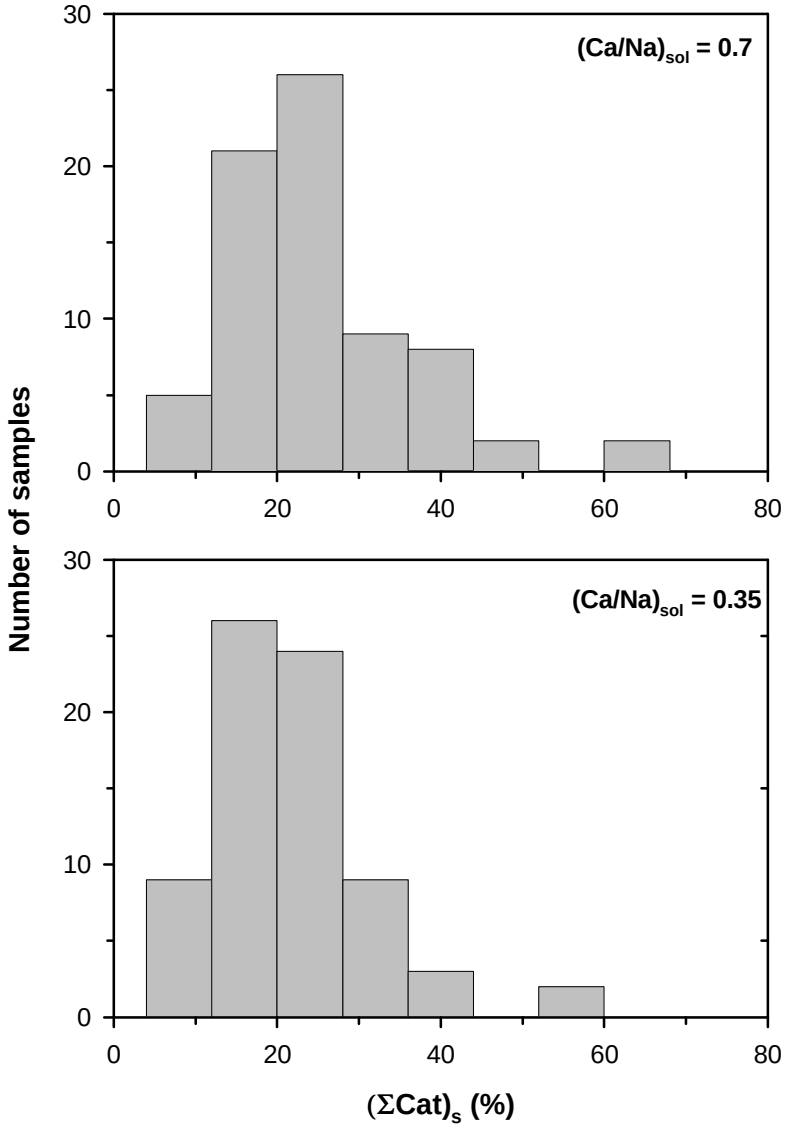

Fig. 4.12 Distribution of $(SCat)_s$ in the YRS waters estimated using two different values of $(Ca/Na)_{sol}$ (see text for details).

$(\Sigma Cat)_s$ estimates for the YRS rivers show that in monsoon samples, with a few exceptions, they are either equal to or higher than those in the summer and post-monsoon samples (Fig. 4.13) Exception to this trend are the samples from the Yamuna at Rampur Mandi and the river Bata. This observation can result due to exposure of fresh silicate minerals by physical erosion during high water flow and their consequent weathering. This contention is supported by the observation that in many of the streams $^{87}Sr/^{86}Sr$ is higher during the monsoon period (see section 4.2.3). This result, however, differs from that

reported by Krishnaswami et al. (1999). This may be because their inference was based on samples collected during different years.

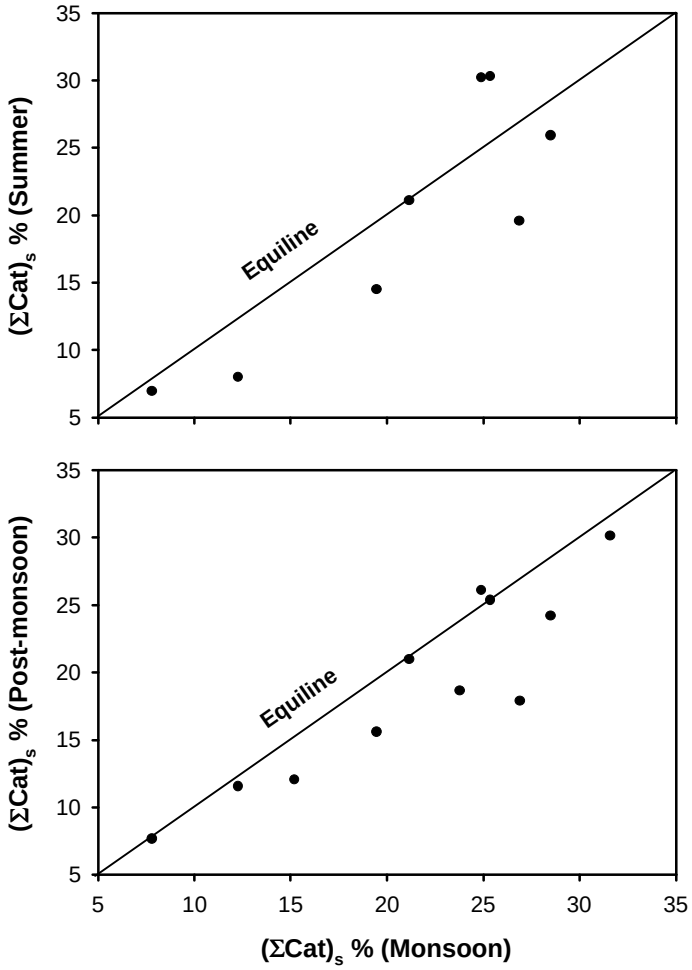

Fig. 4.13 Seasonal variation of $(SCat)_s$ in the YRS waters. In general, monsoon samples have higher $(SCat)_s$ than those collected during summer and post-monsoon.

Independent approach to gauge the intensity of aluminosilicate weathering in the catchment is from the Si/(Na*+K) ratios in river waters and values of chemical index of alteration of river sediments. The Si/(Na*+K) ratio is dependent on different silicate weathering reactions occurring in the basin. For example, Na-feldspar weathering to beidellite would yield a value of 1.7 for Si/(Na*+K) in the waters whereas K-feldspar weathering to kaolinite would give a ratio of 3 (Huh et al., 1998). The dissolved Si/(Na*+K) in the YRS varies from ~0.5 to 3.0 with an average ~1.2. The low average value of the ratio

in the YRS indicates that silicate weathering is not intense in the basin. Major ion data on the bed sediments (Table 4.2) support such an inference.

A measure of the degree of chemical weathering of these sediments can also be obtained from their Chemical Index of Alteration (CIA):

$$CIA = ([Al_2O_3]/[Al_2O_3+CaO^*+Na_2O+K_2O]) \times 100$$

where CaO^* represents Ca in the silicate fraction (Nesbitt and Young, 1982). During silicate weathering cations are released to solution depending on their solubility. For unweathered granites the CIA values would fall in the range of ~45-55, whereas in soil profiles generated by extensive weathering (as evident from their very low Na, Ca and K abundances) would yield a CIA of ~100. Similarly, unaltered albite, anorthite and K-feldspar have CIA ~50, 30 to 45 for fresh basalts and kaolinites close to 100 (Nesbitt and Young, 1982). In this study, bed sediments (sieved to <1 mm size and powdered to -100 mesh) from the YRS have been analyzed. CIA for the YRS sediments vary from ~51 to 69 with an average of ~60. (These values are uncorrected for any contribution of Ca from phosphates. Further, carbonates in the YRS catchment consist of both limestones and dolomites, with an average Ca/Mg wt. ratio 2.9 (Singh et al., 1998). Using this Ca/Mg ratio in the bed carbonates, the CIA for individual samples would be marginally lower, yielding an average ~59). In general, CIA for the YRS sediments in the lower reaches are higher suggesting relatively enhanced weathering in this region. This is expected as vegetation, soil CO_2 and temperature are relatively higher in the lower reaches. Furthermore, in these regions the contact time of water with the minerals is likely to be longer as they have shallower gradient than the upper reaches. The average CIA value in the YRS sediments is low and less than those in average shale (70-75) indicating that chemical weathering of silicates in the Yamuna basin in the Himalaya is not intense, consistent with the inference drawn earlier from Si/(Na*+K) in the waters. Ahmad et al. (1998) reported low values of CIA in the Indus bed (48-52) and suspended sediments (60-65) and concluded that mechanical erosion and weathering dominate their chemistry. In a region under active tectonic activity such as the YRS basin, with steep gradient and monsoon climate, physical erosion is likely to be more dominant than chemical weathering.

(ii) Carbonates and evaporite weathering

Carbonate is a major lithology in the drainage basin of the YRS, especially in the Lesser Himalaya (Fig. 2.3). The Precambrian carbonates which are widely exposed in the

drainage basins of the Yamuna, Tons and many of their tributaries such as Barni Gad, Shej Khad, Giri, Aglar are made of both calcites and dolomites (Singh et al., 1998; Valdiya, 1980). Evaporites are also reported to occur as pockets in the Krol carbonates in the drainage basins (Valdiya, 1980), however, their areal coverage and abundance are not well documented. Considering that both these lithologies can be weathered far more easily than silicates, they are expected to contribute significantly to the major ion budget of the YRS. The major ion abundances indeed support such a contention. Carbonate alkalinity and Ca are the major anion and cation in the YRS, with Ca, on an average, balancing ~70% of the alkalinity (Fig. 4.14a). This is a strong indication of dominance of carbonate weathering in the catchment. (Ca+Mg) exceed the alkalinity (Fig. 4.14b), but by and large balance (SO_4+alk) (Fig. 4.15), and together they account for 95% of the major ions (Table 4.1). This can be interpreted in terms of supply of these ions through weathering of Ca and Mg carbonates (and other phases such as phosphates) by H_2CO_3 and H_2SO_4 as well as supply of Ca and SO_4 via dissolution of gypsum/anhydrite. Evidence for pyrite oxidation in supplying H_2SO_4 for weathering of carbonates is seen in excess (or near equivalence) of SO_4 over Ca in a few samples and the significant correlation between Re-SO_4 (Chapter 5, Dalai et al., 2001a). Similarly, the strong linear correlation observed for Sr-SO_4 in these waters can result from the dissolution of evaporites (see later discussions on Sr). All these observations suggest that the cation and anion budgets of streams and rivers of the YRS is dominated by carbonate and evaporite weathering and pyrite oxidation, with the carbonates making larger contributions to the major ion balance. It is important to isolate the contribution of gypsum derived SO_4 from that via pyrite oxidation, as it has implications to the supply of protons for weathering and hence to CO_2 consumption. This is a difficult exercise to carry out in the YRS from the available major ion data and lithological information. It can, however, be inferred from the significant positive correlation between Mg and SO_4 in the YRS (Fig. 4.10) that carbonate weathering via H_2SO_4 exerts a dominant control on the SO_4 balance in these rivers. If all the SO_4 in the YRS is from oxidation of pyrites, then on average a fourth of the protons would be contributed by H_2SO_4 for weathering in the basin. Galy and France-Lanord (1999), in their studies of headwaters of the Narayani Basin in the Nepal Himalaya, observed that the primary source of sulphate in these waters is oxidation of sulphides.

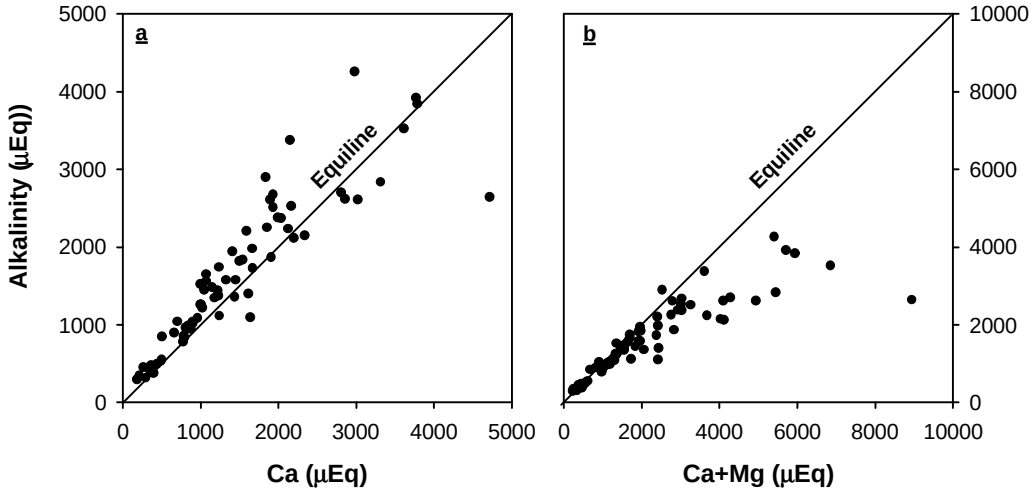

Fig. 4.14 Scatter plots of alkalinity vs. Ca (a) and Ca+Mg (b) in the YRS waters. Ca balances bulk of the alkalinity in the waters, Ca and Mg together exceed alkalinity requiring other anions to balance them.

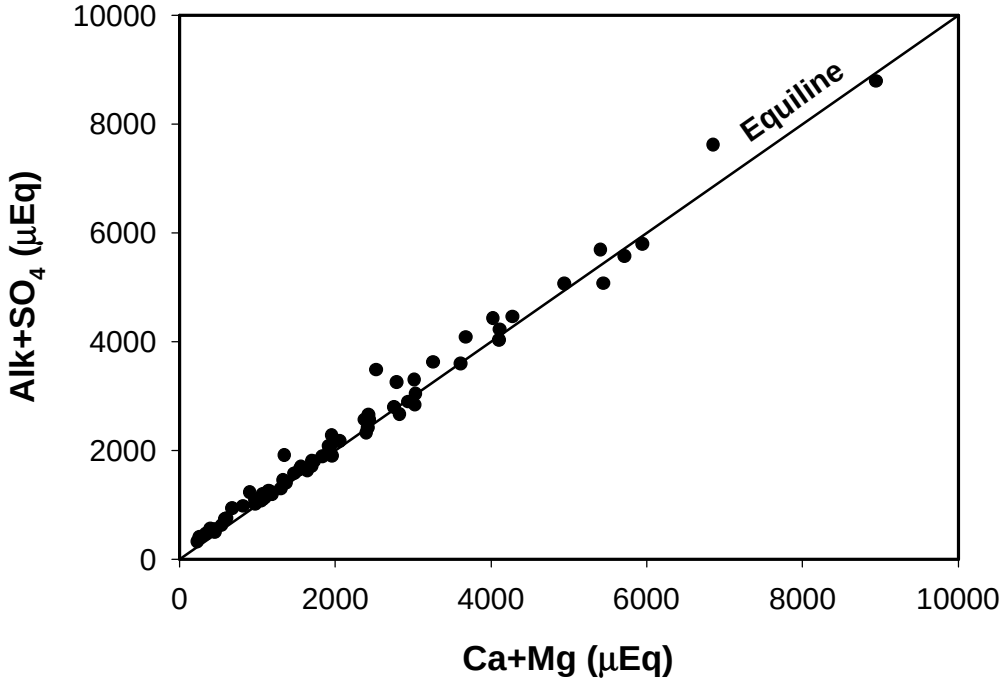

Fig. 4.15 Scatter plot of Ca+Mg vs. Alk+SO_4 in the YRS waters. The data by and large fall on the equiline, as the abundances of other cations and anions in the YRS rivers/streams are much lower.

An upper limit of carbonate contribution to the YRS cations can be derived as:

$$(\Sigma\mathrm{Cat})_{\mathrm{carb}} = \frac{(\mathrm{Ca_r} - \mathrm{Ca_s}) + (\mathrm{Mg_r} - \mathrm{Mg_s})}{(\mathrm{Na_r} + \mathrm{K_r} + \mathrm{Mg_r} + \mathrm{Ca_r})}$$

In this calculation, it is assumed that Ca and Mg are contributed only from silicates and carbonates. This assumption is valid for Mg, however, for Ca it can overestimate the carbonate contribution as Ca can also be supplied to rivers via dissolution of gypsum (and

weathering of other phases such as phosphates). The calculated $(\Sigma Cat)_{carb}$ in the YRS range from ~32 to 91% , with a mean of 70±12% (for $Ca_s = 0.7Na_s$). These correspond to ~3-140 mg ℓ^{-1} of Ca+Mg in the YRS from carbonate weathering. A *lower limit* on the (Ca+Mg) supply from carbonates can be derived as:

$$(\Sigma Cat)_{carb} = \frac{\left[Ca_r - (Ca_s + Ca_{ev}) + (Mg_r - Mg_s)\right]}{(Na_r + K_r + Mg_r + Ca_r)}$$

Ca_{ev} (contribution of Ca from evaporites) is estimated assuming that all SO_4 in the YRS waters is from evaporites. This would yield a *lower limit* of Ca supply from carbonates. The calculated $(\Sigma Cat)_{carb}$ range from ~24 to 78% (mean ~50%), corresponding to ~2-63 mg ℓ^{-1} of Ca+Mg in the YRS [In six samples with $SO_4 \geq Ca$, after correction for Ca from silicates, estimated $(\Sigma Cat)_{carb}$ becomes negative, these have been excluded for the calculation of range and mean of $(\Sigma Cat)_{carb}$]. The calculation provides an *upper limit* of Ca supply to the YRS cations from evaporites (Ca_{ev}), this varies from ~3 to 55%, with a mean of ~20%. The cation balance in a few selected rivers is given in Table 4.5. These calculations assume that *all* SO_4 to be of evaporite origin and $(Ca/Na)_{sol}$ from silicate weathering is 0.7. The calculated carbonate Ca, therefore, is *lower limit* and evaporite Ca would be *upper limit*. It is seen from the results in Table 4.5 that Na and K in waters is dominated by contributions from silicate and Mg from carbonates. For Ca, carbonates are the major sources in most of the samples, in a few of them, however, evaporite contributions can be significant.

Table 4.5 Cation balance in selected streams of the YRS[a)], percentage contributions.

Cations	Atmospheric/ Cyclic	Silicate	Carbonate	Evaporite
Yamuna@Hanuman Chatti (RW98-16)				
Na	6	55	1	32
K	4	96	0	0
Ca	0	7	64	29
Mg	0	11	89	0
(SCat)	*1*	*21*	*55*	*22*
Didar Gad (RW98-18)				
Na	13	83	1	0
K	6	94	0	0
Ca	0	21	67	12
Mg	0	34	66	0
(SCat)	*4*	*47*	*43*	*6*
Yamuna@Batamandi (RW98-4)				
Na	2	77	1	20

K	4	96	0	0
Ca	0	13	54	33
Mg	0	12	88	0
(SCat)	*0.4*	*24*	*54*	*21*
Yamuna@Saharanpur (RW98-33)				
Na	2	73	1	23
K	3	97	0	0
Ca	0	12	59	29
Mg	0	10	90	0
(SCat)	*0.4*	*22*	*58*	*19*
Tons@Mori (RW98-27)				
Na	7	70	1	16
K	4	96	0	0
Ca	0	17	49	34
Mg	0	39	61	0
(SCat)	*2*	*41*	*34*	*22*
Tons@confluence (RW98-32)				
Na	3	81	1	13
K	4	96	0	0
Ca	0	11	17	72
Mg	0	9	91	0
(SCat)	*0.5*	*21*	*36*	*42*

a) Ca_{ev} is estimated assuming *all* SO_4 is derived from evaporites, and hence an *upper limit*. Ca_{carb} is a *lower limit*, as part of SO_4 (and Ca) also result via weathering of carbonates by sulphuric acid.

4.2.3 Dissolved Sr and $^{87}Sr/^{86}Sr$ in the YRS

The results on Sr and Ba concentrations and $^{87}Sr/^{86}Sr$ in the water samples are given in Table 4.1. The Sr concentration and $^{87}Sr/^{86}Sr$ in the YRS range between 120-13,400 nM and 0.7142-0.7932 respectively (Table 4.1). The Sr abundances in the Yamuna and its tributaries in the upper reaches are similar to those in the Ganga source waters, but in the lower reaches the tributaries of the YRS have more Sr. The rivers draining the northern slopes of the Himalaya, the Changjiang and Xijiang have similar Sr concentrations as those in the Yamuna in the lower reaches, however, the Mekong has higher Sr concentration (Gaillardet et al., 1999) than those in the Yamuna but similar to or lower than those in its tributaries in the lower reaches.

In general, the YRS streams in the upper reaches are more radiogenic in Sr isotopic composition than the ones in the lower reaches. The stream, Didar Gad, draining predominantly silicates (Fig. 2.9, Table 4.1) has the highest $^{87}Sr/^{86}Sr$ (0.7932). The spring waters of Shahashradhara have the highest Ca (~13,400 μM) and Sr (~62,000 nM) and low $^{87}Sr/^{86}Sr$ (0.7097). The $^{87}Sr/^{86}Sr$ in the YRS are similar to those reported in the Ganga headwaters (Krishnaswami et al., 1992), however, the tributaries of the YRS in the lower

reaches are less radiogenic than the Ganga source waters. $^{87}Sr/^{86}Sr$ in the YRS are in general higher than those in the Indus waters (Pande et al., 1994; Karim and Veizer, 2000), in rivers draining the basaltic terrains (Louvat and Allegre, 1997, Dessert et al., 2001) and much higher than the global river water average, 0.7119 (Palmer and Edmond, 1989). The rivers draining the northern slopes of the Himalaya have lower $^{87}Sr/^{86}Sr$ than those in the YRS.

The results of this study on Sr concentration and $^{87}Sr/^{86}Sr$ in the Ganga at Rishikesh and in the Yamuna at Saharanpur are compared with those available in the literature for the same locations (Palmer and Edmond, 1989; Krishnaswami et al., 1992, Table 4.6). The comparison shows that for both the Ganga and the Yamuna, there are measurable differences in Sr concentrations (±20%) and $^{87}Sr/^{86}Sr$ (0.2-0.3%) between the samples collected during the same season. These differences reflect inter/intra annual variations in the water properties.

Table 4.6 Comparison of Sr concentration and $^{87}Sr/^{86}Sr$ in the Ganga and the Yamuna: Present work and earlier reported values.

	Period	***Sr (nM)***	***$^{87}Sr/^{86}Sr$***	***Reference***
Ganga (Rishikesh)	Sept. 1982	580	0.7365	Krishnaswami et al. 1999
	Sept. 1999	507	0.73849	This study
	Nov. 1983	760	0.7408	Krishnaswami et al. 1999
	Oct. 1998	626	0.73856	This study
	Mar. 1982	800	0.7399	Krishnaswami et al. 1999
	June 1999	712	0.73657	This study
Yamuna (Saharanpur)	Mar. 1982	1360	0.7270	Palmer and Edmond, 1989
	June 1999	1664	0.72657	This study

$^{87}Sr/^{86}Sr$ in the Yamuna main channel seem to be primarily governed by the contributions from its tributaries. $^{87}Sr/^{86}Sr$ rises from 0.75158 at Hanuman Chatti to 0.75725 near Pali Gad Bridge (Table 4.1, Fig. 4.16), after Didar Gad and Jharjhar Gad, the tributaries with high radiogenic Sr composition, merge with the Yamuna. Downstream of Paligad Bridge, $^{87}Sr/^{86}Sr$ in the main channel decreases as tributaries with higher Sr concentration and lower $^{87}Sr/^{86}Sr$ merge. Lithology exerts a significant control on $^{87}Sr/^{86}Sr$ of the Yamuna along its course, the decrease in $^{87}Sr/^{86}Sr$ in lower reaches results mainly from contributions

from easily weatherable sedimentaries such as carbonates, evaporites and phosphates. These sedimentaries generally have wide range of Sr/Ca in them, with $^{87}Sr/^{86}Sr$ which overlap with each other but lower than those in silicates (Table 4.7). Evaporites and phosphates have higher Sr abundances compared to silicates and carbonates. The Sr/Ca in the Pc carbonates (Singh et al., 1998; Mazumdar, 1996) are lower than those in evaporites and phosphates (Table 4.7). The tributaries, the Aglar, the Giri, the Bata and the Asan, which drain these sedimentaries in the lower reaches, have high Sr and relatively low $^{87}Sr/^{86}Sr$. As these rivers merge with the Yamuna, its Sr concentration in the main channel increases with a consequent drop in $^{87}Sr/^{86}Sr$ (Fig. 4.16).

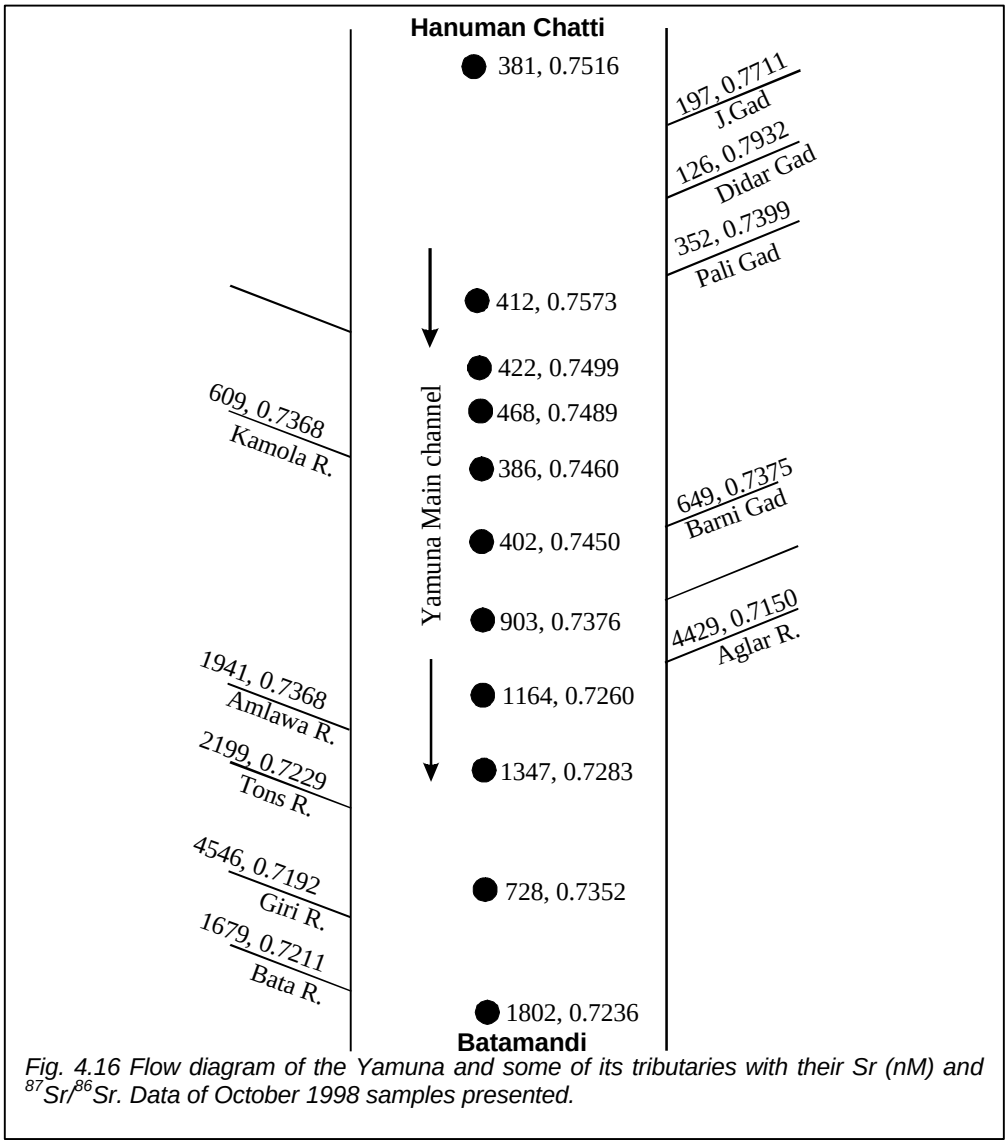

Fig. 4.16 Flow diagram of the Yamuna and some of its tributaries with their Sr (nM) and $^{87}Sr/^{86}Sr$. Data of October 1998 samples presented.

Table 4.7 Sr/Ca and $^{87}Sr/^{86}Sr$ in various lithologies

Lithology	Sr/Ca (nM/μM)	$^{87}Sr/^{86}Sr$
Crystallines	0.25	0.80[a)]
Carbonates	0.20	0.7081-0.7162[b)]
Evaporites	2.9[c)]	0.7097[c)]
Phosphorites	2.2[d)]	0.7095-0.7124[e)]

[a)]from Krishnaswami et al. (1999). [b)]for carbonates in the Yamuna catchment (Singh et al., 1998). [b)]Sr/Ca based on data from Wedepohl (1978) and $^{87}Sr/^{86}Sr$ based on the data of spring waters of Shahashradhara. [d)]data from Mazumdar (1996). [e)]based on analysis of four phosphorite samples from Maldeota and Durmala mines as a part of this work.

Sr/Ca (nM μM^{-1}) in the YRS varies from 0.5 to 5.7 and average 1.6±0.9. In general, Sr/Ca in the streams/rivers are lower in the upper reaches and increase in the lower reaches. Sr abundances in the YRS show positive correlation with the Ca, Mg among the cations and alkalinity and SO_4 among the anions whereas $^{87}Sr/^{86}Sr$ vary inversely with all these properties (Table 4.8, Figs. 4.17-4.20). Similar trends are also seen with respect to TDS, this is expected as Ca, Mg, SO_4 and alkalinity make up >90% of TDS. Statistical analysis of Sr with these parameters (Table 4.8) shows that there is significant scatter around the best-fit lines, possibly indicating contributions from multiple end members. This might also be contributing to the intercepts observed for these lines (Table 4.8). Regression lines on plots of $^{87}Sr/^{86}Sr$ vs. 1/Ca and $1/SO_4$ have intercepts of 0.718 and 0.726 respectively (Table 4.8), higher than the $^{87}Sr/^{86}Sr$ for Pc carbonates in the YRS basin, evaporites and phosphorites (Table 4.7). Implications of these values would be discussed in latter sections.

Table 4.8 Interrelation of Sr, Ba and $^{87}Sr/^{86}Sr$ with major ions in the YRS.

Pair	*n*	*Slope*[a)]	*Int.*	r^2
Sr-Ca	73	3.25	-903	0.66
Sr-Mg	73	4.29	-126	0.76
Sr-SO_4	73	3.67	192	0.90
Sr-TDS	73	12.12	-829	0.66
Ba-Sr	69	0.08	44	0.76
Ba-Ca	70	0.32	-59	0.81
$^{87}Sr/^{86}Sr$-1/Ca	50	8.15	0.718	0.80
$^{87}Sr/^{86}Sr$-1/SO_4	50	0.89	0.726	0.63

[a)]nM μM^{-1} for regression of Sr and Ba with major ions, nM $(mg\ \ell^{-1})^{-1}$ for Sr-TDS, nM nM^{-1} for Sr-Ba. Int.: intercept.

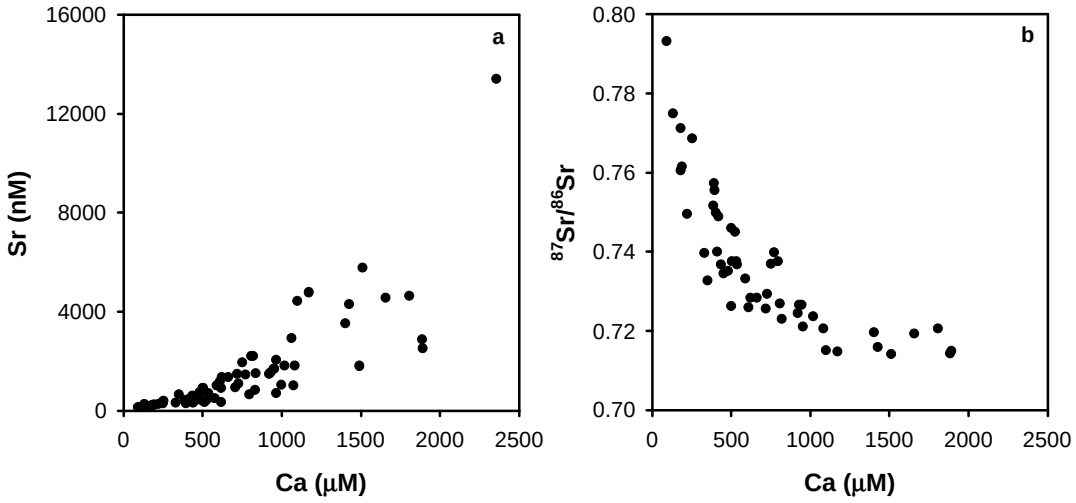

Fig. 4.17 Scatter plots of Sr (a) and $^{87}Sr/^{86}Sr$ (b) with Ca in the YRS waters. Sr derived from Ca rich lithologies such as carbonates, evaporites and phosphates dilute the radiogenic Sr isotopic composition of these waters.

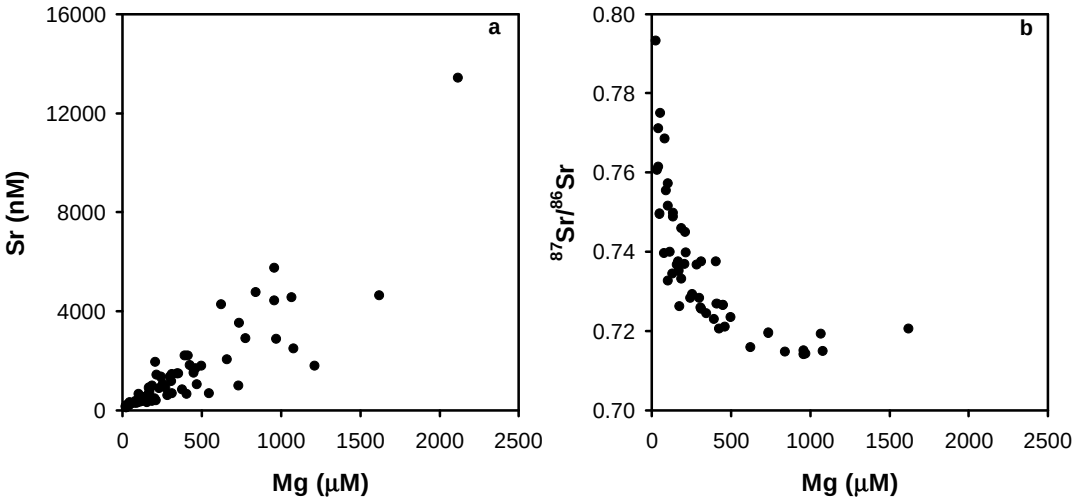

Fig. 4.18 Scatter plots of Sr (a) and $^{87}Sr/^{86}Sr$ (b) with Mg in the YRS waters. There exists a significant positive correlation between Sr and Mg (r^2=0.76). $^{87}Sr/^{86}Sr$ decreases with increasing Mg. Dolomite weathering contributes Mg whereas associated lithologies such as evaporites and phosphates seem to be contributing to Sr with low $^{87}Sr/^{86}Sr$.

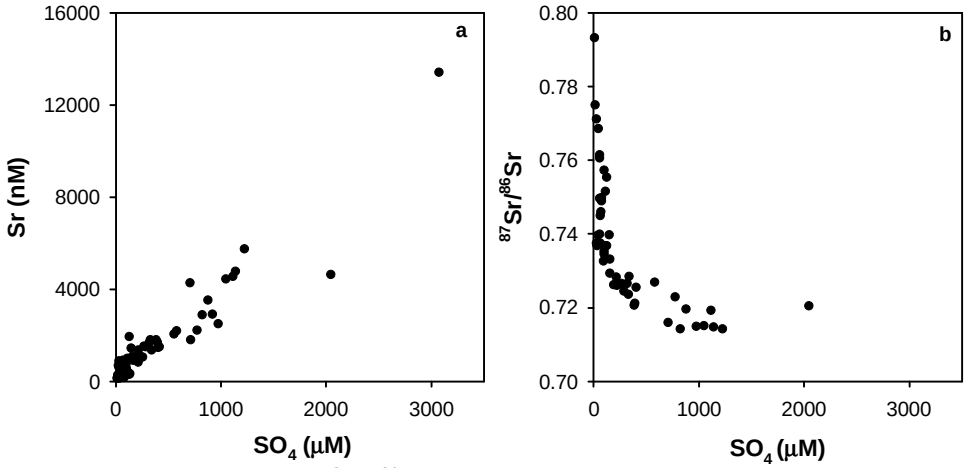

Fig. 4.19 Scatter plots of Sr (a) and $^{87}Sr/^{86}Sr$ (b) with SO_4 in the YRS waters. The trend in (a) can result from supply of Sr from evaporites. Weathering of sedimentaries by H_2SO_4 and evaporite dissolution play a significant role in influencing the Sr and its isotopic composition in the YRS (see text for detailed discussion).

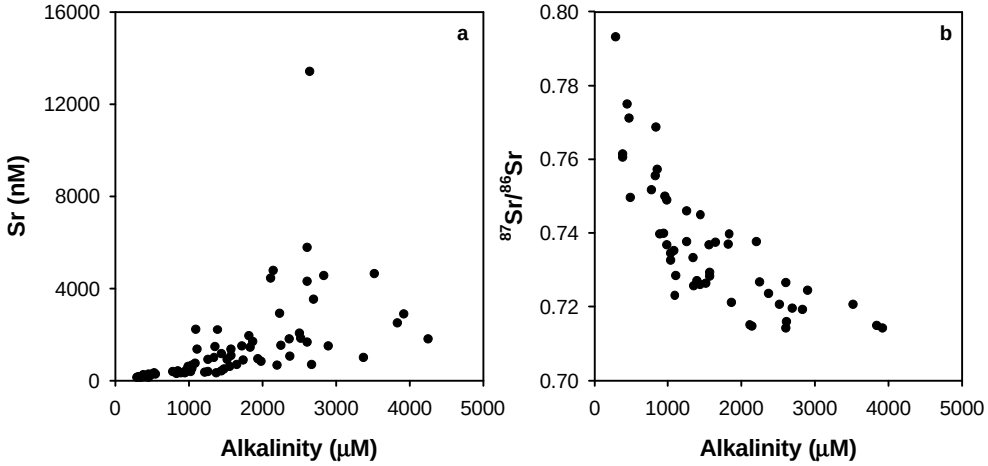

Fig. 4.20 Scatter plots of Sr (a) and $^{87}Sr/^{86}Sr$ (b) with alkalinity in the YRS waters. Limestone and dolomite weathering act as a diluent for the radiogenic Sr isotopic composition of the YRS rivers.

$^{87}Sr/^{86}Sr$ in the YRS covaries with SiO_2/TDS and $(Na^*+K)/TZ^+$ [Figs. 4.21a, b], both these ratios being measures of fraction of silicate contribution to the dissolved solids in rivers (Dalai et al., 2001b). Such covariations have implications to the source of Sr in rivers as discussed in the next section.

Sr abundances in the YRS and in the Ganga are generally lower during the monsoon than those during summer or post-monsoon (Table 4.1). In the Yamuna mainstream, $^{87}Sr/^{86}Sr$ during the monsoon season are in general higher (by 0.005 to 0.014) compared to post-monsoon (except at Rampur Mandi). The stream Godu Gad, draining predominantly silicates

has higher $^{87}Sr/^{86}Sr$ during post-monsoon (0.7750) compared to summer (0.7686). The tributaries in the lower reaches show no clear seasonal trend in their $^{87}Sr/^{86}Sr$.

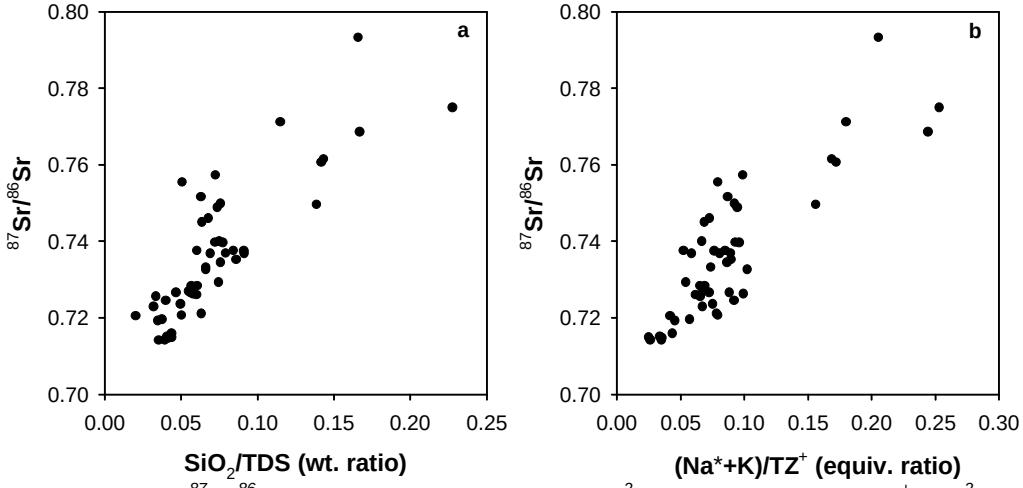

Fig. 4.21 Variation of $^{87}Sr/^{86}Sr$ in the YRS with SiO_2/TDS (a, r^2 = 0.70) and $(Na^*+K)/TZ^+$ (b, r^2 = 0.72). Positive trends of $^{87}Sr/^{86}Sr$ with these ratios (measure of silicate weathering) suggest that release of Na, K and Si to waters via silicate weathering is accompanied by an increase in $^{87}Sr/^{86}Sr$ of these rivers. The best fit lines yield intercept of 0.709 and 0.710, $^{87}Sr/^{86}Sr$ in the "non-silicate" components.

The Ganga at Rishikesh has higher $^{87}Sr/^{86}Sr$ during monsoon (0.7385) and post-monsoon (0.7386) than that during summer (0.7366). In the Yamuna at Saharanpur, $^{87}Sr/^{86}Sr$ remained the same during summer and post-monsoon (0.7266) while it decreased slightly during the monsoon (0.7262). These differences can be attributed to variability in weathering intensities of different minerals during various seasons and their mixing proportions in river. It is interesting to observe that in the Yamuna mainstream, an increase in $^{87}Sr/^{86}Sr$ in samples collected during monsoon is accompanied by a corresponding increase in silicate cation contributions $(\Sigma Cat)_s$ during this season. These trends further support the inference drawn earlier that during monsoon, exposure of fresh silicate mineral surfaces and their subsequent weathering occur in the YRS basin caused by rapid physical erosion.

4.2.4 Sources of Sr and their control on $^{87}Sr/^{86}Sr$

As already mentioned in the earlier sections, the YRS drains multilithological terrains comprising predominantly of crystallines, sedimentary silicates and carbonates, with minor amounts of evaporites, phosphates, black and gray shales. All these lithologies can contribute to the dissolved Sr of the YRS rivers/streams. One of the goals of this study is to constrain the relative contributions of Sr from these sources to the YRS and to assess their impact on

the riverine Sr isotopic composition. The co-variation of Sr with Ca, Mg, Na* and SO_4 (Figs. 4.17-4.20, 4.22), indicate that Sr in these waters can be derived from sources such as carbonates (Ca, Mg), silicates (Na*), evaporites (Ca, SO_4) and phosphorites (Ca) occurring in the catchment (Dalai et al., 2001c).

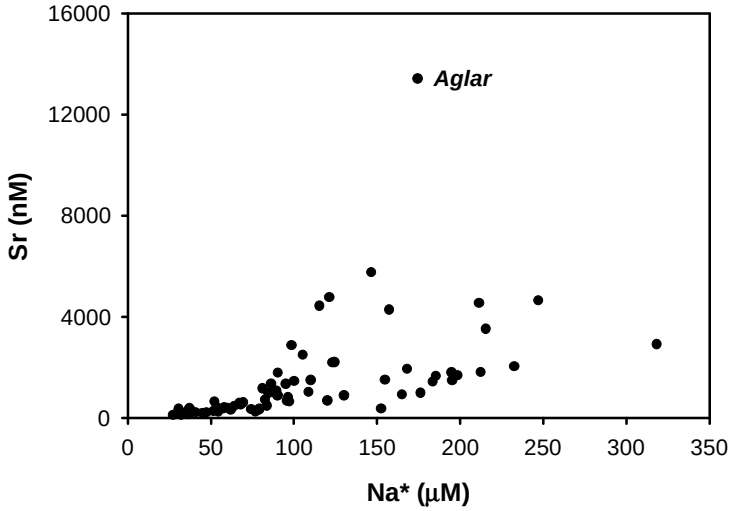

Fig. 4.22 Scatter plot of Sr vs. Na in the YRS waters. Sr shows an overall positive correlation with Na* though with significant scatter. The data fan out from a low Na*-Sr end member, indicative of multiple sources.*

In the YRS Na* and Sr though show an overall positive correlation (Fig. 4.22), the points fan out from low values suggesting Sr is derived from multiple sources. The river Aglar, as already mentioned, draining through the Krol carbonates might have a significant contribution of its Sr from evaporites which occur in these carbonates. Co-variation of $^{87}Sr/^{86}Sr$ with SiO_2/TDS and $(Na^*+K)/(TZ^+)^*$ (Figs. 4.21a, b) leads to infer that silicates dominate the high radiogenic Sr isotope end member of the YRS streams/rivers. This is further supported by the observation that the streams draining the crystallines in the Higher Himalaya have $^{87}Sr/^{86}Sr \geq 0.74$. The regression line plotted through the data (Figs 4.21a, b) have intercepts of 0.709 and 0.710, which is very similar to the average $^{87}Sr/^{86}Sr$ of Pc carbonates in the Yamuna basin (0.711), phosphates analyzed in this work (~0.711) and evaporites (based on the $^{87}Sr/^{86}Sr$ of Shahashradhara, 0.7097) supporting the idea that these lithologies are responsible for the low $^{87}Sr/^{86}Sr$ in the YRS rivers.

In a plot of 1/Sr vs. $^{87}Sr/^{86}Sr$, the data points fall by and large on a two end member mixing line with some scatter (r^2=0.84, Fig.4.23); indicating that as a first approximation, the

Sr abundance and $^{87}Sr/^{86}Sr$ in the YRS rivers may be considered as a mixture of two components, one with low Sr and high $^{87}Sr/^{86}Sr$ and the other with high Sr and low $^{87}Sr/^{86}Sr$. The intercept of the regression line, 0.719, is similar to observed intercepts in plots of $^{87}Sr/^{86}Sr$ vs. 1/Ca and $1/SO_4$ (Table 4.8) but marginally higher than the $^{87}Sr/^{86}Sr$ of Pc

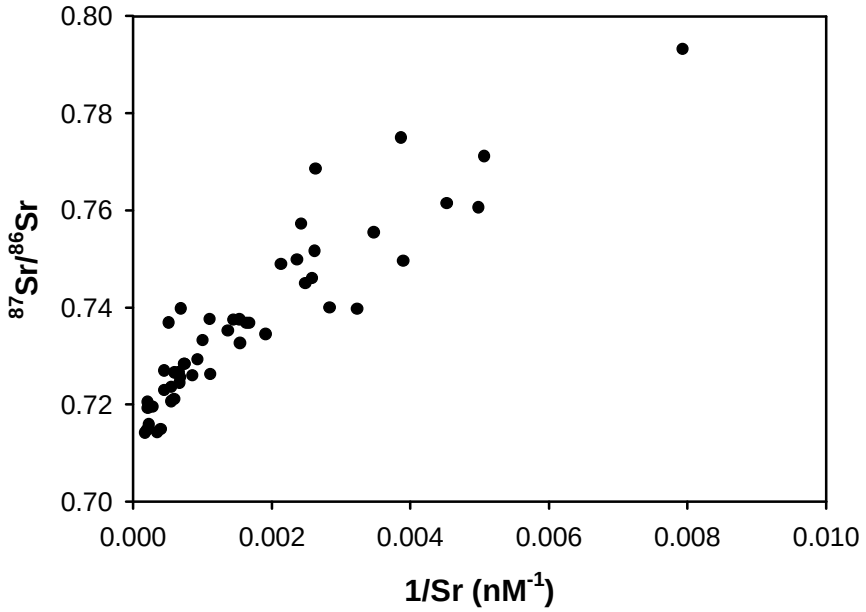

Fig. 4.23 Mixing plot of Sr and $^{87}Sr/^{86}Sr$ of the YRS waters. Samples by and large define a two component mixing trend (see text for discussion).

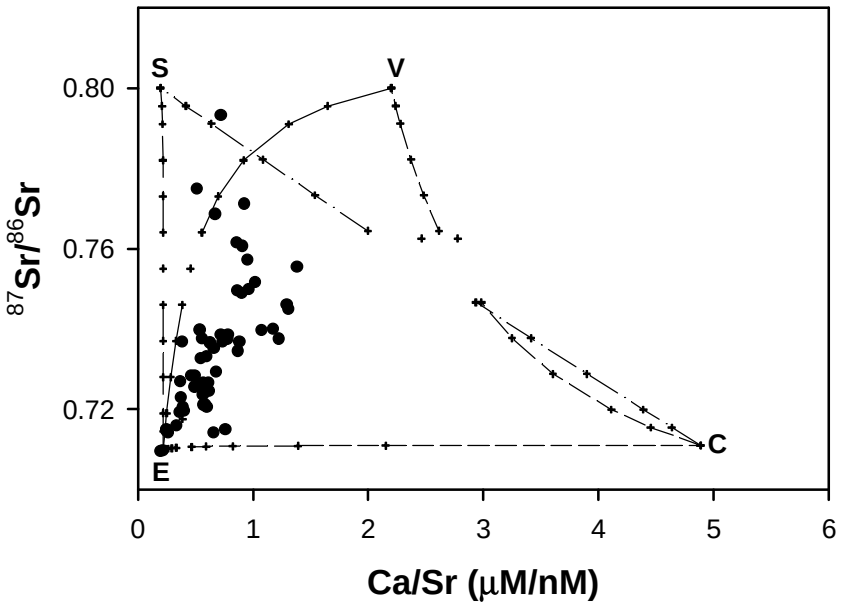

Fig. 4.24 Plot of $^{87}Sr/^{86}Sr$ vs. Ca/Sr in the YRS. Also plotted are end member compositions of silicates (S), Precambrian carbonates (C), evaporites (E) and vein-calcites (V). Sr and its isotopic composition in the YRS can be explained by mixing of carbonates, evaporites, silicates and/or vein-calcites (see text for discussion).

carbonates in the YRS basin (0.708-0.716), phosphorites (0.7095-0.7124) and evaporites (0.7097). A closer look at the data (Fig. 4.23) reveals the points fan out from (1/Sr) of ~10^{-4} nM^{-1} and $^{87}Sr/^{86}Sr$ of ~0.71, indicative of multiple end members. To resolve the various components contributing to Sr and its isotopes in the YRS better, Ca/Sr is plotted vs. $^{87}Sr/^{86}Sr$ (Fig. 4.24) as Ca/Sr vary significantly among the various lithologies (Table 4.7). In this diagram, vein-calcites are also plotted as an end member in addition to silicates, carbonates and evaporites. Recently, vein-calcites have been suggested as an important component in determining the $^{87}Sr/^{86}Sr$ of rivers draining the Himalaya (Blum et al., 1998; Jacobson and Blum, 2000). Silicates and vein-calcites may satisfy the high $^{87}Sr/^{86}Sr$ end member whereas carbonates, evaporites, phosphates all can be a part of low $^{87}Sr/^{86}Sr$ end member. Further, this plot shows the need for more than two components to account for the Sr and $^{87}Sr/^{86}Sr$ in the YRS.

Singh et al. (1998) based on a detailed analysis of Sr abundance and $^{87}Sr/^{86}Sr$ in Precambrian carbonates from the Lesser Himalaya, inferred that these carbonates are unlikely to be a major contributor to the high $^{87}Sr/^{86}Sr$ and Sr budget of the G-G-I source waters in the Himalaya on a basin wide scale. They arrived at this conclusion from the low $^{87}Sr/^{86}Sr$ and Sr/Ca ratios in carbonates relative to those in the river waters. The $^{87}Sr/^{86}Sr$ in Pc carbonates, sampled all across the Lesser Himalaya, average 0.725±0.043 and Sr/Ca 0.20±0.15 (Fig. 4.25, Singh et al., 1998). Bulk of these carbonates, however, have $^{87}Sr/^{86}Sr$ in the range of 0.706 to 0.732, with a few of them having values as high as ~0.89. This compares with the $^{87}Sr/^{86}Sr$ of 0.7142 to 0.7932 (mean: 0.736±0.018) and Sr/Ca of 0.5 to 5.7 (mean: 1.6±0.9) in the YRS (Fig. 4.25). In the Yamuna catchment, carbonates occurring in the inner belt (Chakrata-Tiuni-Deoban region) and outer belt (Dehradun-Mussoorie and Solan region) have a narrow range of $^{87}Sr/^{86}Sr$, 0.708-0.716, with a mean, 0.711±0.002. The spring waters of Kempti Fall have $^{87}Sr/^{86}Sr$ 0.7095, similar to that in carbonates collected near the fall (Singh et al., 1998). Out of 50 YRS river water samples analyzed, 44 have $^{87}Sr/^{86}Sr>0.716$ (Table 4.1), the maximum reported for Pc carbonates in the Yamuna catchment (Singh et al., 1998). Hence in most of these rivers/streams, sources in addition to Pc carbonates would have to be invoked to explain their high radiogenic $^{87}Sr/^{86}Sr$. For example, Shej Khad, the stream draining predominantly Pc carbonates of Deoban Formation (maximum reported $^{87}Sr/^{86}Sr$ 0.716), has $^{87}Sr/^{86}Sr$ 0.7293. The YRS rivers in the lower reaches; Aglar, Giri, *Tons* at

Dehradun and Asan, all have low $^{87}Sr/^{86}Sr$, 0.7142 to 0.7205. These rivers have a significant part of their drainage basins in carbonates of the inner and outer belts of the Lesser Himalaya (Fig. 2.3). It is tempting to infer from these observations that carbonate weathering could have a significant influence on their Sr isotopic composition.

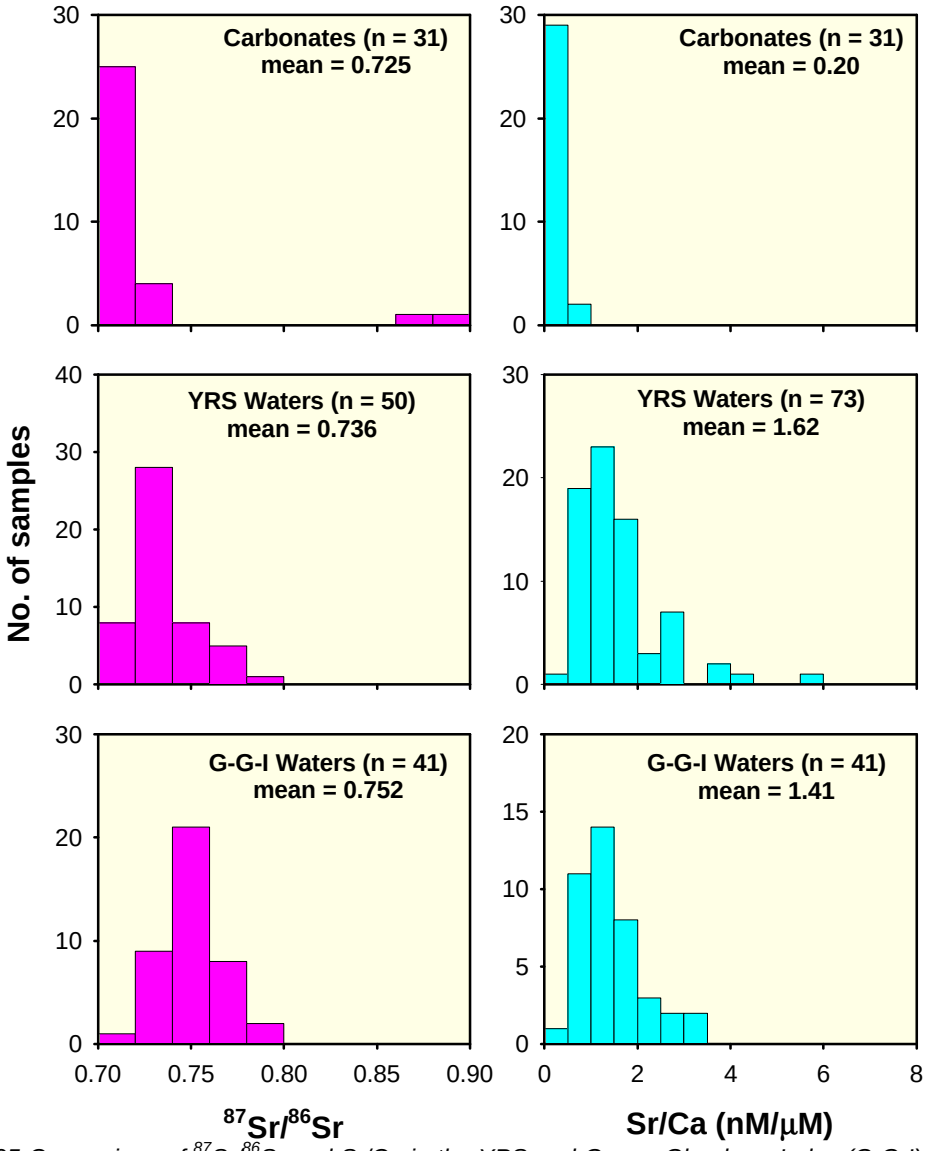

Fig. 4.25 Comparison of $^{87}Sr/^{86}Sr$ and Sr/Ca in the YRS and Ganga-Ghaghara-Indus (G-G-I) waters and Precambrian carbonates of the Lesser Himalaya. These carbonates have low $^{87}Sr/^{86}Sr$ and Sr/Ca compared to those in the river waters.

The role of carbonates as an important regulator of $^{87}Sr/^{86}Sr$ in these waters would also depend on their contributions to Sr budget. Estimates on this can be made from the Sr/Ca ratio of Pc carbonates and Ca concentrations of the rivers assuming that both Sr and Ca are released to waters in the same proportion as their abundances in the carbonates and that

they behave conservatively after their release to river (see latter section). There is a concern as to whether this requirement can be met, considering that many of the YRS river waters are supersaturated with calcite and the precipitation of calcite can enhance Sr/Ca in dissolved phase (English et al., 2000). As already discussed, it is unclear if precipitation of calcite occur in these waters. More work needs to be done to determine if calcite precipitation occurs from these waters and consequently elevates their Sr/Ca. Inspite of this uncertainty, it is evident that Precambrian carbonates is not a source for high $^{87}Sr/^{86}Sr$ of the YRS streams on a basin wide scale, as $^{87}Sr/^{86}Sr$ in most of the carbonates are ≤0.716. These carbonates, however, could become important on a local scale and for individual streams, if there are pockets of them with highly radiogenic Sr isotope composition such as those reported in Pithoragarh and Kanalichina (Singh et al., 1998). Such carbonates, however, have not been reported yet in the Yamuna basin. Further, as discussed in the next section, the contribution of Precambrian carbonates to the Sr budget of the YRS is estimates to be only ~15% on average.

Evaporites and phosphates are other lithologies, which can supply significant quantities of Sr to these waters with low $^{87}Sr/^{86}Sr$. Gypsum has been reported to occur as pockets in the Krol carbonates in the Lesser Himalaya (Valdiya, 1980). Phosphorites are known to be associated with black shales-carbonate sequences. However, the areal coverage and distribution of evaporites and phosphates in the YRS basin is not known. SO_4 is a major anion of YRS streams and account for ~2 to 35 % of anion abundance on a molar basis. SO_4 in rivers can be derived from both oxidation of pyrites and dissolution of evaporites. The strong correlation of Re and SO_4 in these waters has been attributed to ubiquitous pyrite oxidation in the drainage basin and suggests that it is an important source of SO_4 to the YRS waters (Chapter 5, Dalai et al., 2001a). This inference is drawn from the coexistence of pyrites with organic rich sediments, which are generally abundant in Re. Weathering of these sediments and pyrites release Re and SO_4 to rivers. The organic rich sediments are also often associated with carbonates and phosphorites e.g. black shales-carbonates-phosphates layers in Maldeota and Durmala phosphorite mines, near Dehradun. Weathering of these assemblage release Re, Ca, SO_4 and Sr to waters with low $^{87}Sr/^{86}Sr$. The strong correlation between Re and Sr and inverse correlation of Re and $^{87}Sr/^{86}Sr$ (Figs. 4.11, 4.26) very likely

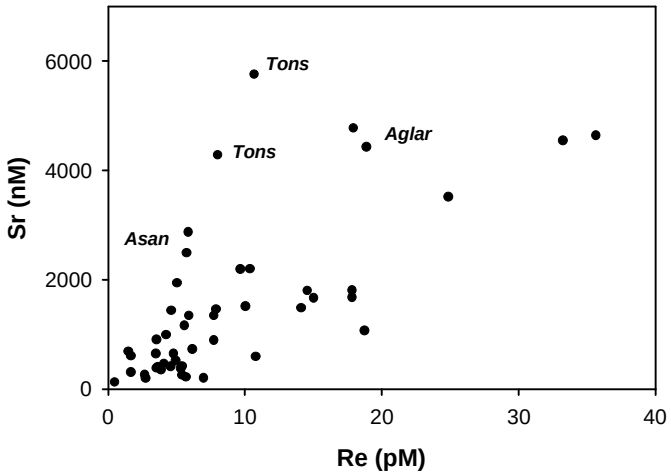

Fig. 4.26 Variation of Sr with dissolved Re in the YRS waters. Sr shows an over all increasing trend with Re though with considerable scatter. $^{87}Sr/^{86}Sr$ decreases with increasing Re (Fig. 4.11). These trends suggest that lithologies associated with Re rich sediments contribute Sr to the YRS waters with low $^{87}Sr/^{86}Sr$.

result from weathering of such multi-mineral assemblages. The scatter on Re-Sr plot supports the presence of multiple end members, fanning out from a low Sr, Re end member.

Sr mass balance in the YRS

As discussed earlier, the lithologies contributing to Sr of the YRS are silicates, carbonates, evaporites and phosphates.

Silicate contribution to the dissolved Sr load to the YRS can be estimated through the approaches outlined by Krishnaswami et al. (1999). In the first approach, it is assumed that Sr and Na in the silicates are released to solution in the same proportion as their abundance. Sr/Na (nM/μM) in the LH granites/gneisses average 1.68±0.72 (Krishnaswami et al. 1999). Granites occurring around the source region of the Yamuna, from Sayana Chatti (Biyani, 1998) and Hanuman Chatti (this study, Table 4.2) have an average Sr/Na 0.93±0.22, which is lower but overlaps within errors, with the LH average. Based on Sr/Na on soil profiles (Gardner and Walsh, 1996) developed on metamorphics in LH, Krishnaswami et al. (1999) estimated that Sr/Na released to the solution from silicate source rocks could range between 2.5-2.9. Another approach to assess the Sr/Na released to the waters from silicates is from the chemistry of streams flowing predominantly through silicate lithology. Among the rivers sampled, Godu Gad, with the lowest Ca/Na, SO_4/HCO_3 and high $^{87}Sr/^{86}Sr$ (0.77495) meets this requirement. It has Sr/Na* 2.48, which is the lowest among all the rivers analyzed in this study. These exercises, thus indicate that Sr/Na released to the rivers from silicate

weathering, $(Sr/Na)_{sol}$ can range between 1.0-2.9. For calculation of silicate contribution to the Sr load in the rivers, a value of 2.0±0.8 for $(Sr/Na)_{sol}$ is used, this is same as that used by Krishnaswami et al. (1999).

The silicate Sr contribution to the YRS (Sr_s) is calculates as:

$$Sr_s = (Sr/Na)_{sol} \times Na^*$$

where Na* is the sodium corrected for cyclic contributions, Na* = Na-Cl. The calculated values of Sr_s varies between ~55 to 640 nM, ~3 to 80% of the total dissolved Sr. It is seen that in the YRS streams/rivers, fraction of Sr derived from silicates decreases with increase in their Sr concentration (Fig. 4.27) resulting from contributions from components with high Sr such as evaporites and phosphates.

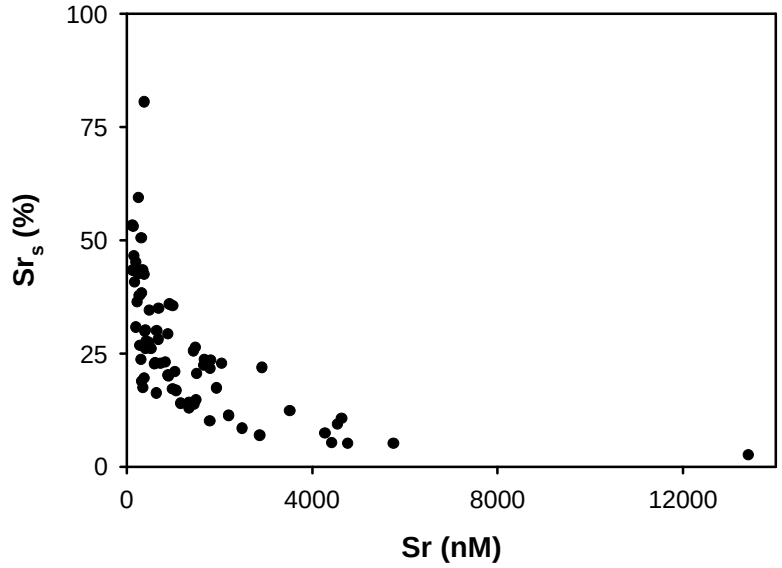

Fig. 4.27 Variation of Sr_s with Sr abundances in the YRS streams. Sr_s decreases with increase in Sr.

The average of Sr_s estimates for all the YRS streams analyzed in this study is 26±15%. Sr_s values for the Yamuna at Batamandi at the foothills of the Himalaya where the Yamuna integrates the Sr contributions from its entire catchment upstream varies from 22 to 26% for the three different sampling periods. The similarity in the average Sr_s value derived for all streams and that for the Yamuna at Batamandi lends further support to the estimate of 26% as the representative average silicate Sr contribution in the YRS. In the Yamuna at Hanuman Chatti, Sr_s constitute 20-27 percent of total Sr. In the streams Didar Gad and Godu

Gad, flowing mainly through silicates, Sr_s ranged from 43-53% and 53-81% respectively. Sr_s in the Ganga at Rishikesh is ~23%. The spring waters, as expected, have lower Sr_s in them, 0.1-0.3% for Kempti Fall and 0.9% for Shahashradhara. Using the lower and upper limits of $(Sr/Na)_{sol}$, 1.2 and 2.8, Sr_s in the YRS average at 16±9% (range 2-48%) and 36±20% (range 4-100%) respectively.

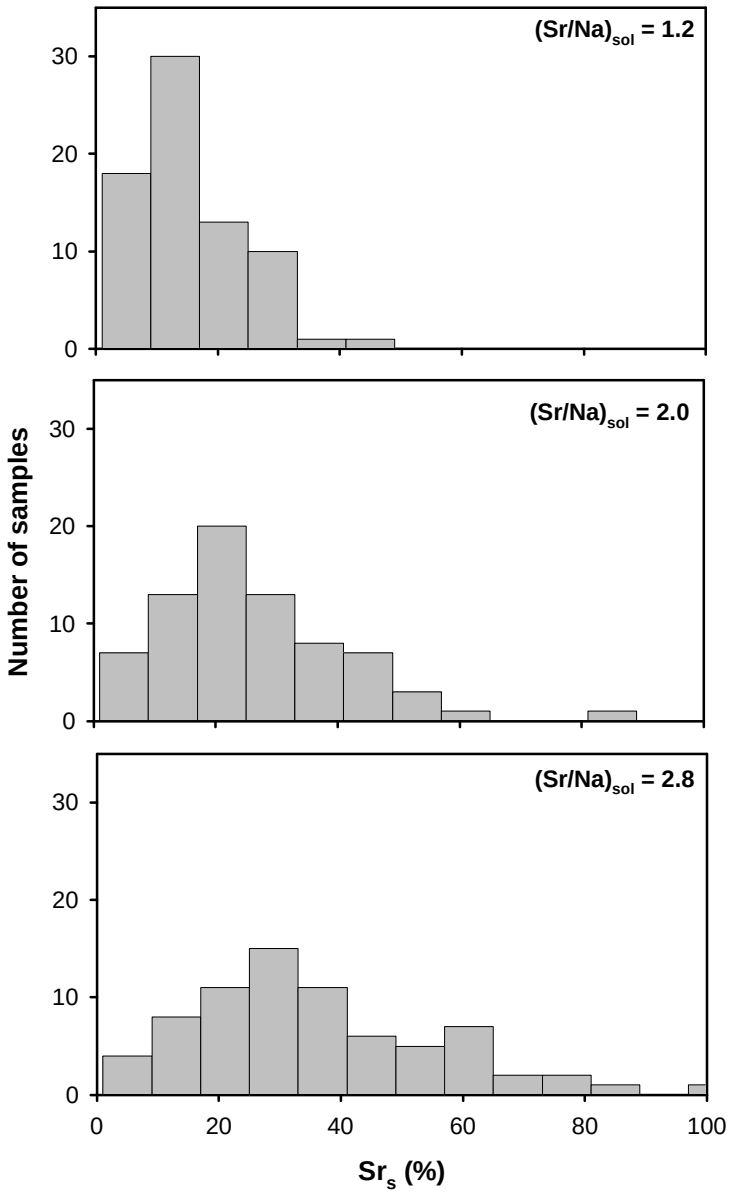

Fig. 4.28 Distribution of Sr_s estimated using three different values for $(Sr/Na)_{sol}$.

The distribution of Sr_s in the rivers calculated using three different values for $(Sr/Na)_{sol}$, 1.2, 2.0 and 2.8 are shown in Fig. 4.28.

Sr_s shows a significant positive correlation with $^{87}Sr/^{86}Sr$ (Fig 4.29) suggesting that silicate weathering in the catchment exerts a dominant control on the radiogenic composition of the rivers in YRS. The intercept of the regression line, 0.713, is very similar to the $^{87}Sr/^{86}Sr$ of non-silicate end members. A similar correlation is also there between silicate cations (ΣCat_s) and $^{87}Sr/^{86}Sr$ (Fig 4.30) further supporting this contention.

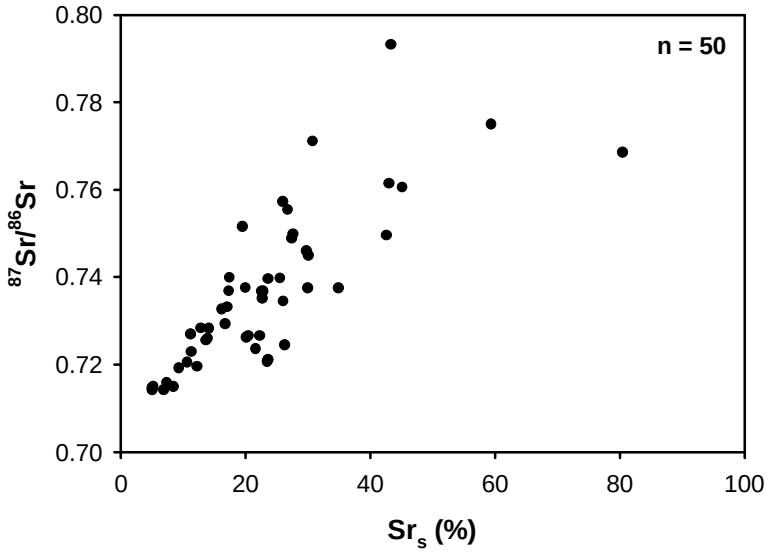

Fig. 4.29 Variation of $^{87}Sr/^{86}Sr$ with Sr_s in the YRS waters. A strong positive correlation (r^2 = 0.64) is suggestive of the dominance of silicate weathering in regulating the Sr isotopic composition of the YRS rivers.

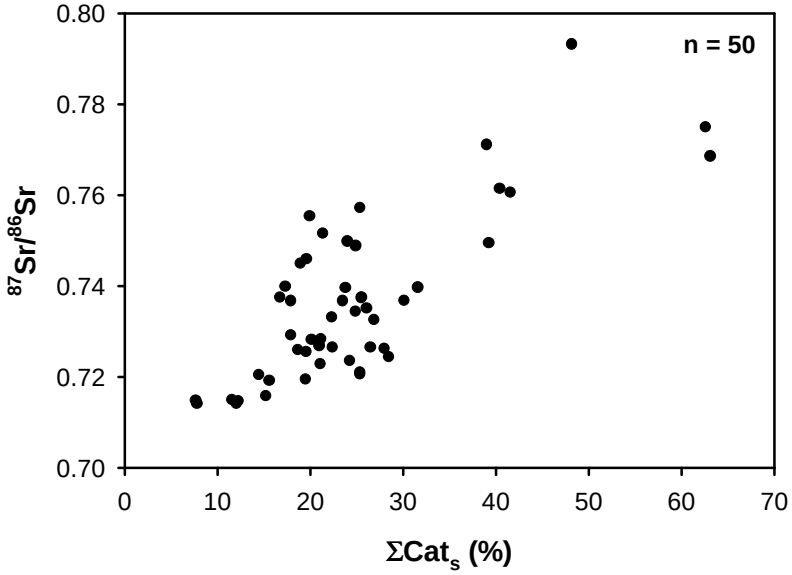

Fig. 4.30 Variation of $^{87}Sr/^{86}Sr$ with $SCat_s$ in the YRS waters. The strong positive correlation (r^2 = 0.61) suggests that silicate weathering exerts a dominant role on the radiogenic Sr isotopic composition of rivers.

The contribution of Sr from carbonate weathering can be calculated as:

$$Sr_c\ (nM) = (Ca_r - Ca_s) \times [Sr/Ca]_c$$

$(Sr/Ca)_c$ has been taken to be the abundance ratio in LH Precambrian carbonate outcrops, 0.20±0.15 nmol/μmol (Singh et al., 1998). This calculation assumes that all Ca in the rivers come from only two sources, silicates and carbonates, that Sr and Ca are released from carbonates in the same proportion as their abundances and behave conservatively after their release to rivers. Sr_c thus calculated has a range of 3 to 37% with an average of 14±7%. In the Yamuna sampled at Batamandi, Sr_c varies between 9 to 11% for the three different seasons and at Hanuman Chatti, Sr_c varies between 20-27%, quite similar to Sr_s. In the spring waters of Kempti Fall and Shahashradhara Sr_c is only 3-4%. Considering that easily weatherable rocks like evaporites and phosphates occurring in the Yamuna catchment also contribute to the Ca in the rivers, this estimate of Sr_c calculated as above would be a *maximum*. In most of the streams Sr_s and Sr_c do not add up to 100% though in a few of them the Sr balance can be achieved within the errors of estimation. This suggests that there are sources in addition to silicates and Precambrian carbonates for Sr in these rivers. From the knowledge on the lithology of the Yamuna basin, the additional sources contributing Sr to these rivers are evaporites, phosphates and/or carbonates other than the Precambrian carbonates studied by Singh et al. (1998). Assuming that *all* SO_4 in the YRS rivers are of evaporite origin (with equivalent amount of Ca), and using an average Sr/Ca ratio, 2.9 (nM μM^{-1}) for evaporites (Wedepohl, 1978), an *upper limit* of their contribution to the Sr budget can be estimated. The estimates show that, in a few of the streams, all Sr can be of evaporite origin.

An approach to resolve the contributions of various sources to the Sr budget in the waters is to plot $^{87}Sr/^{86}Sr$ vs. Ca/Sr (Blum et al., 1998; Fig. 4.24). The data points fall in the mixing space defined by evaporites, silicates and carbonates. The high $^{87}Sr/^{86}Sr$ in the YRS is a result of silicate Sr end member. It is seen that many of the data points fall close to the end member compositions of evaporites and phosphates (with Ca/Sr ~0.2-0.5 μM/nM, and $^{87}Sr/^{86}Sr$ ~0.71) underlining their importance in contributing to the Sr budgets of the YRS. The average composition of the Precambrian outcrops plot far off the river water data suggesting that their influence on the Sr load in the river waters is not quite significant consistent with the estimation of Sr_c (average ~15% for the YRS).

The results of Sr mass balance in a few selected YRS streams are given in Table 4.9. The calculations for $^{87}Sr/^{86}Sr$ were done using a value of 0.8 for silicate end member $^{87}Sr/^{86}Sr$ (Krishnaswami et al. 1999) and 0.71 for carbonates and evaporites. It is seen that for the streams which have comparable areal distribution of various lithologies (e.g. RW98-4, RW98-8, RW98-13, RW98-32, RW98-33), the calculated and the measured $^{87}Sr/^{86}Sr$ values agree reasonably. All these rivers have $^{87}Sr/^{86}Sr \leq 0.74$. In contrast, for rivers flowing mainly through crystallines (RW98-16, RW98-18, RW98-26, RW98-27) and which have $^{87}Sr/^{86}Sr > 0.75$, the calculated values are significantly lower than the measured ones. Even if a higher value of 0.83 (obtained for 100% $(\Sigma Cat)_s$ end member, Fig. 4.30) is used for silicate end member, the calculated $^{87}Sr/^{86}Sr$, though agrees better, still remains lower than the measured values. One likely explanation for this discrepancy is that ^{87}Sr may be preferentially released to these rivers from minerals such as biotite which generally have higher $^{87}Sr/^{86}Sr$ than the whole rock values used in the calculation. The recent experimental studies on biotite weathering show that ^{87}Sr, indeed, is preferentially released from them to the weathering solution (Taylor et al., 2000a).

Table 4.9 Sr mass balance in selected YRS streams.

Sample/River	Sr_s (%)	Sr_c (%)	Sr_{rest} (%)	$^{87}Sr/^{86}Sr_{cal}$	$^{87}Sr/^{86}Sr_{meas}$
RW98-16/Yamuna@Hanuman Chatti	20	19	61	0.7276	0.7516
RW98-18/Didar Gad	43	11	45	0.7490	0.7932
RW98-26/Godu Gad	59	6	34	0.7635	0.7749
RW98-27/Tons@Mori	45	15	40	0.7506	0.7606
RW98-4/Yamuna@Rampur Mandi	22	10	69	0.7295	0.7236
RW98-8/Aglar	5	5	90	0.7147	0.7150
RW98-13/Barni Gad	30	22	48	0.7370	0.7375
RW98-32/Tons@confluence	11	7	82	0.7201	0.7269
RW98-33/Yamuna@Saharanpur	21	11	69	0.7284	0.7266

Calculations were done using $^{87}Sr/^{86}Sr$ for silicate end member as 0.8 and 0.71 for carbonates and the rest (evaporites and phosphates) end members. It was assumed that $Sr_s+Sr_c+Sr_{rest} = 100\%$. Sr_s is estimated using value of $(Sr/Na)_{sol} = 2.0$. Sr_c is the lower limit, estimated assuming all SO_4 are of evaporite origin. Values of Sr_s, Sr_c and Sr_{rest} given have been rounded off, whereas $^{87}Sr/^{86}Sr$ were calculated using the actual values.

More recently, calcites occurring as veins in granites and granodiorites in the Himalaya have been proposed a source for the high radiogenic $^{87}Sr/^{86}Sr$ to the rivers draining these basins (Blum et al., 1998; Jacobson and Blum, 2000). The carbonate content of these

rocks from the Nanga Parbat massif in north Pakistan and Raikhot watershed coupled with their highly radiogenic Sr isotope composition (~0.9, quite similar to those in the host silicates) led to this proposition. The role of vein-calcites in the budget of Sr and its isotopes in the YRS is discussed below.

The carbonate contents in four granite samples from the Yamuna catchment collected around Hanuman Chatti range from ~0.2 to 0.9% with an average 0.6% (Table 4.2), similar to calcite contents in silicates of Nanga Parbat massif (Jacobson and Blum, 2000). The Sr/Ca in calcites from Nanga Parbat, determined by mild acid leach, is ~0.45 (nM/μM). Assuming that (i) the average carbonate content of the YRS crystallines is 0.6% with Sr/Ca of 0.45 nM/μM, (ii) the suspended matter concentration of the YRS is ~2 g $\ell^{-1}$and (iii) *all Ca and Sr* are released to waters from these calcites during weathering, it can be estimated that the contribution from the vein-calcites to the Sr budget of the YRS would be, on an average, about 10%. This estimate would go up by a factor of two, if bed load is also considered such that the total erosion is twice the suspended matter concentration (Galy and France-Lanord, 2001). Such an estimate, however, is not valid for rivers such as the Didar Gad, as the calculated Ca from vein-calcites exceeds the measured Ca concentration in them. Therefore, an *upper estimate* of Sr contribution from vein-calcites for such streams can be made assuming that *all Ca* in them is of vein-calcite origin. Such a calculation shows that in Didar Gad and Godu Gad, vein-calcites can contribute a maximum of ~33-40% and ~23-30% respectively of their total Sr, compared with their estimated silicate contributions of 43% and 59% respectively. These are *upper limits* of vein-calcite contributions, as part of Ca has to be from silicates and other sedimentaries. If all the non-silicate Ca is assumed to be of vein-calcite origin, then vein-calcite contribution to their Sr load would be ~26% and ~14% respectively. These calculations show that in the YRS streams flowing through crystallines, vein calcites can be an important contributor to their Sr budget, the magnitude of their contributions, however, awaits better determination of their abundance and their Sr content. Their role in influencing the high $^{87}Sr/^{86}Sr$ in the YRS needs to be evaluated by careful sampling and analysis of Sr, Ca and $^{87}Sr/^{86}Sr$ in them. In this study, co-variation of $^{87}Sr/^{86}Sr$ with SiO_2/TDS, $(Na^*+K)/TZ^+$, Sr_s and $(\Sigma Cat)_s$ favour the hypothesis that silicate weathering dominate the high radiogenic Sr isotopic composition of the YRS.

Laboratory experiments (Taylor et al., 2000a) on phlogopite and biotite containing trace calcites in them, show that at steady state, the rate of calcite dissolution is either similar to that of phlogopite or 50% slower than the biotite dissolution. In the initial phase of their experiments, release of Sr from trace calcites in phlogopites and biotites were about 3 and 2 times faster respectively than that at steady state. At steady state, the dissolution rate of trace calcites was limited by the rate of their exposure to the weathering solution, which in turn is controlled by the rate of silicate dissolution. In another laboratory experiment on rate of Sr release from labradorites and trace calcites in them (Taylor et al., 2000b), it was observed that in the first samples of output solutions in each experiment, even with faster Sr release from calcites, only ~1% of Sr was derived from their dissolution. The calcite contribution to Sr in these solutions decreased rapidly with time and at steady state, it became negligible. $^{87}Sr/^{86}Sr$ of the output solutions further indicated that calcite solution had minimal effect on Sr release rates, as none of the output solutions had $^{87}Sr/^{86}Sr$ significantly less than the plagioclase ($^{87}Sr/^{86}Sr$ of the calcite, based on acetic acid leach, was less than that of plagioclase). In the Himalaya, with high physical erosion, exposure of fresh calcites may not be a limiting factor for vein-calcite dissolution, however, considering that the abundance of vein calcites in the YRS basin is ~0.6% with Sr/Ca ~0.45, for them to be of comparable significance as silicates in Sr budgets of the rivers, they need to release Sr at a rate at least 10^3 times faster than silicates. Such a requirement is not likely to be met in the light of experimental studies (Taylor et al., 2001a, b) which show that at any stage of weathering, release of Sr from trace calcites can, at the most, be three times as fast as that from silicates. Hence though the upper estimates of Sr contributions of vein-calcites show that they can be significant in the YRS Sr budget, a proper assessment of their impact remains unresolved and needs better sampling and analysis of vein calcites for $^{87}Sr/^{86}Sr$, Sr and Ca. Available measurements are based on mild acid leaching (Jacobson and Blum, 2000), more careful analysis are needed to avoid silicate interference. Further, the origin of these vein calcites needs to be better understood. If these calcites formed as an intermediate step in the weathering of silicates then, at steady state, their contribution to Sr budget and $^{87}Sr/^{86}Sr$ can be considered as that arising from silicates themselves.

4.2.5 Dissolved Barium in the YRS

Ba abundances in the YRS range from ~17 to 870 nM (Table 4.1). Its abundance, in general, is lower (<100 nM) in the Yamuna and its tributaries in their upper reaches, a trend similar to that observed for major ions and Sr. The streams in the upper reaches draining predominantly crystallines have lower Ba, the Didar Gad has the lowest (17 nM, Table 4.1). In the lower reaches Ba concentrations are higher in the Yamuna mainstream as well as its tributaries and show large variation. The Asan river originating from the Mussoorie ridges and its tributary *Tons* at Dehradun have very high Ba (~760 and ~530 nM respectively in post-monsoon samples). Ba concentrations in the YRS rivers in the upper reaches are similar to those in the Trisuli draining the Higher Himalayan Crystallines in the Nepal Himalaya (Chabaux et al., 2001) whereas Ba in the lower reaches of the YRS are higher and similar to those observed in the Narayani and Kali rivers in the Nepal Himalaya (Chabaux et al., 2001). Ba abundances in the YRS water show significant positive correlation with Ca and Sr (Fig. 4.31), indicating that they may have a common source such as minerals rich in Ca; carbonates, evaporites and phosphates.

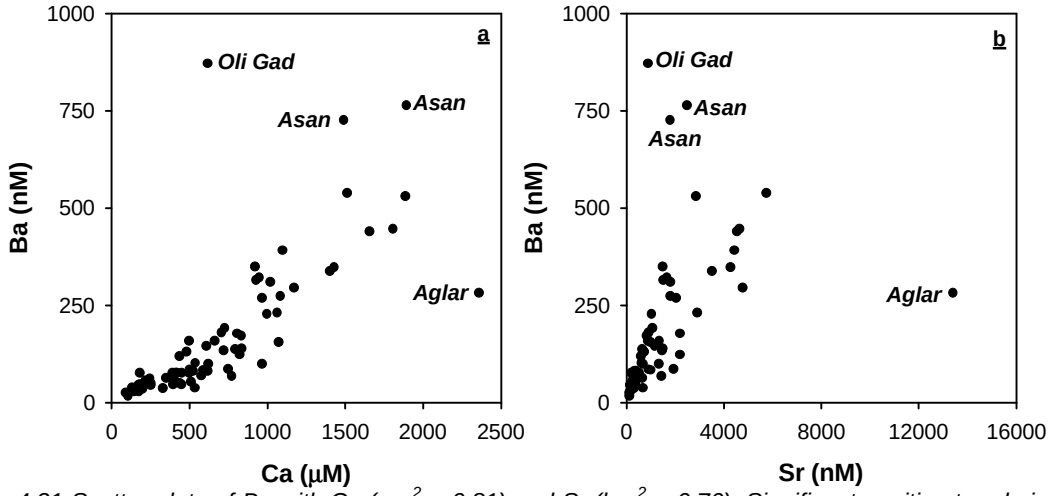

Fig. 4.31 Scatter plots of Ba with Ca (a, r^2 = 0.81) and Sr (b, r^2 = 0.76). Significant positive trends is an indication that these alkaline earth metals may have common sources. Regression analysis excludes four samples marked in the plots.

The relative importance of these lithologies in contributing to dissolved Ba in the YRS waters would be discussed in later sections. The stream Oli Gad with the highest Ba (870 nM) fall far away from the general trend (Fig. 4.31). The other two rivers that fall off the trend set by the other samples are the Asan and the Aglar. The river Asan originates from

around Mussoorie Ridge where phosphorites are known to occur containing high Ba concentrations (Mazumdar, 1996). A significant part of the Aglar drainage basin is in Krol carbonates, which are known to have pockets of gypsum in them. High Ca and Sr in the Aglar waters most likely are derived from gypsum dissolution.

Dissolved Ba shows co-variation with Ca, Mg, Na* and SO_4 (Figs. 4.31, 4.32), similar to Sr, suggesting that it is also derived from multiple sources such as silicates, carbonates, evaporites and phosphates. Ba/Ca (nM/μM) in the YRS waters range from 0.07

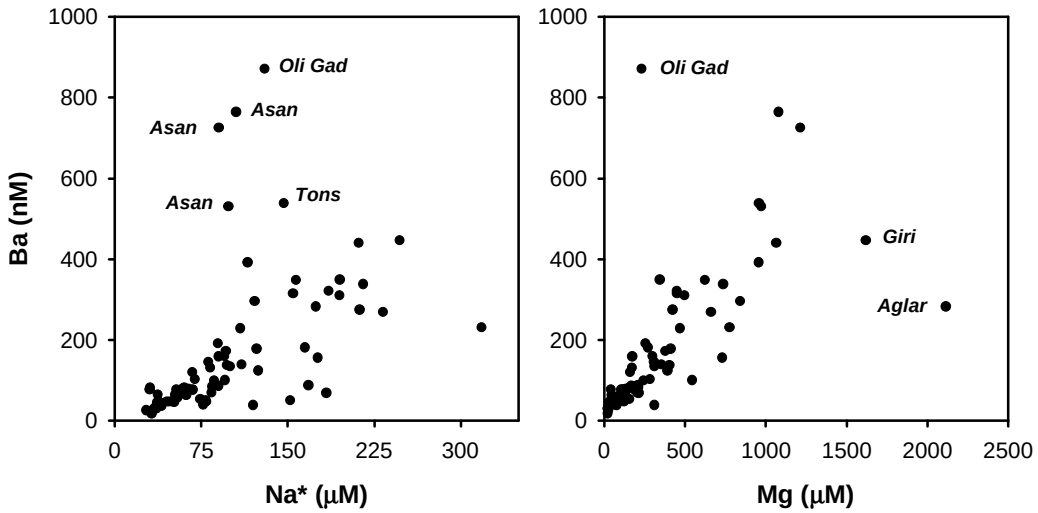

Fig. 4.32 Variation of Ba with Na and Mg in the YRS waters. Positive correlations suggest that weathering of silicates and dolomites (and associated assemblages) could be sources to dissolved Ba in these waters (see text).*

to 1.4 with a mean, 0.23. In order to assess if Ba/Ca in the YRS waters are changed via precipitation of barite, barite saturation index was calculated at 25 °C using Ba and SO_4 concentration data. It was found that all the water samples analyzed in this study are undersaturated with barite, which argues against any removal of Ba from the waters by $BaSO_4$ precipitation. It has already been discussed earlier that in the present study there is no evidence of calcite precipitation in the YRS waters. Ba abundance in the Krol carbonates are lower than those in the crystallines (Mazumdar, 1996), with Ba/Ca 0.03-0.11 nM μM^{-1} (mean: 0.06±0.03 nM μM^{-1}). Analogous to Sr, dissolved Ba/Ca in these waters are significantly higher than those in carbonates. This would indicate that these carbonates are not an important source of Ba to these waters on a basin wide scale. If average Ba/Ca in the Krol carbonates (0.06) is taken to be representative of all carbonates in the YRS basin, carbonate contributions to dissolved Ba in the YRS waters can be estimated under the

assumptions that (i) Ba and Ca are released to waters in the same proportion as their abundance in the carbonates, (ii) *all* Ca in the YRS waters are derived from carbonates and (iii) both Ba and Ca behave conservatively after their introduction to the rivers. The calculations show that carbonates can contribute ~4 to 85% of the dissolved Ba in the YRS waters (mean: 32±14%). Considering that Ca in these waters is also derived from silicates, evaporites and/or phosphates, these estimates are *upper limits*.

Crystallines and sedimentary silicates, which are dispersed throughout the drainage basin, can be another source for Ba. We can estimate silicate contributions to the dissolved Ba in the YRS waters using Na* as and index of silicate weathering. The difficulty in such estimation is proper assessment of the ratio Ba/Na, which is released from silicates to waters. The similar ionic radii of Ba and K allow Ba to replace K in crystal lattice of minerals in igneous rocks. This would make the release of Ba from crystallines difficult as K-bearing minerals are more resistant to chemical weathering. Further, during weathering of crystallines, Ba is likely to be retained in clay fractions and Fe-oxyhydroxides. Ba shows significant positive correlation with K and Al in the YRS bed sediments (Fig. 4.33). The outlier in these plots is the sample from the river Aglar, which drains a significant part of Krol carbonates and has as high as ~44% carbonate in its sediment. Co-variation of Ba with K and Al, together with the observation that Ba concentrations in the carbonate-free bed sediments, in general, are either similar or higher than those in the granites analyzed in this study (Table 4.2), is an indication that during silicate weathering Ba tends to remain in the clay fractions or Ba occurs in minerals more resistant to weathering, hence its release to waters may be minimal. Ba/Na in granitic bed rocks in the Yamuna basin is lower than those in the carbonate free bed sediments, suggesting that Na is preferentially released to waters from rocks relative to Ba which is either released slower or retained in the residual clay fractions. Hence Ba/Na in rivers would be lower than those in silicates. Godu Gad, a stream flowing predominantly through silicates, has the lowest Sr/Na* and Ba/Na* (~0.3 nM μM^{-1}), high $^{87}Sr/^{86}Sr$ (0.7750) and the highest proportion of silicate cations $(\Sigma Cat)_s$. Using this value (0.3) as the Ba/Na ratio released to waters from silicates, it can be estimated that silicates can contribute ~4 to 95% of the dissolved Ba in the YRS (mean: 27±18%). They can account for bulk of Ba in the streams with low Ba abundances, <70 nM. The observation that the streams Didar Gad and Godu Gad, draining predominantly silicates, have very low Ba, 17 and ~45

nM suggests that rivers with higher Ba concentrations have to derive their Ba from sources enriched in Ba. Ba abundances in the YRS show an inverse correlation with silicate cations $(\Sigma Cat)_s$ further supporting the idea that contribution from silicates can not account for the measured higher Ba concentrations in many of the rivers.

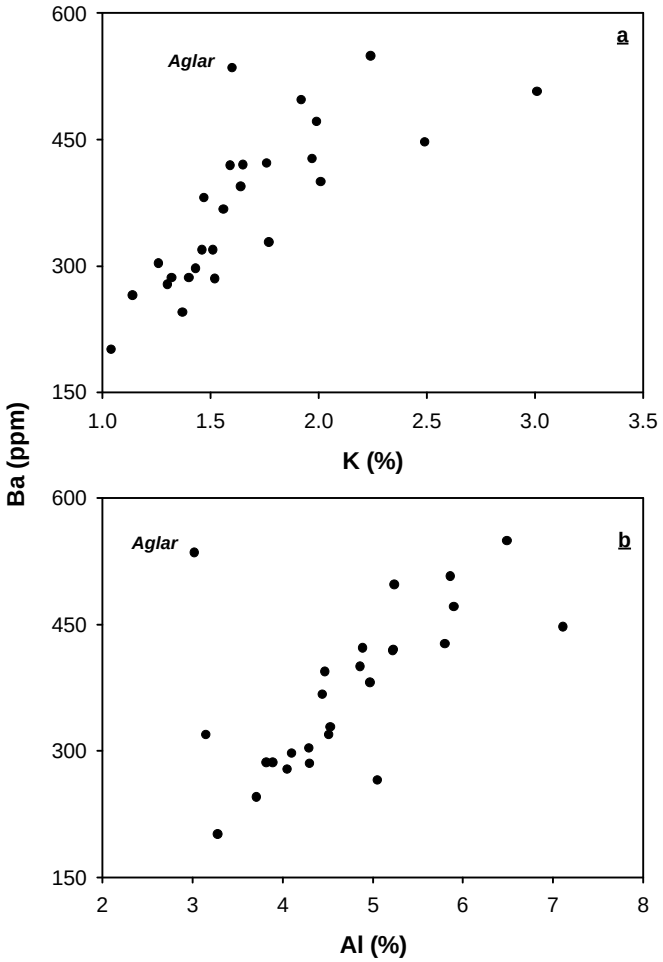

Fig. 4.33 Scatter plot of Ba vs. K (a) and Al (b) in the YRS bed sediments. Ba shows positive correlation with K (r^2=0.69) and Al (r^2=0.68), suggestive of more resistant host minerals of Ba and/or possible retention of Ba in the clay fractions during chemical weathering. Regression analysis excludes the sample from Aglar (RS98-8, see text)

A plot of $^{87}Sr/^{86}Sr$ vs. 1/Ba in the YRS waters shows that samples by and large fall on a two component mixing line (Fig. 4.34). The high $^{87}Sr/^{86}Sr$ and low Ba end member is defined by silicates, consistent with earlier estimates that for streams with low Ba abundances, silicates can be a major contributor. The intercept of the regression line in Fig. 4.34 is 0.716, similar to the $^{87}Sr/^{86}Sr$ of Pc carbonates of the YRS basin and phosphates analyzed in this study but marginally higher than that for evaporites, suggesting that for

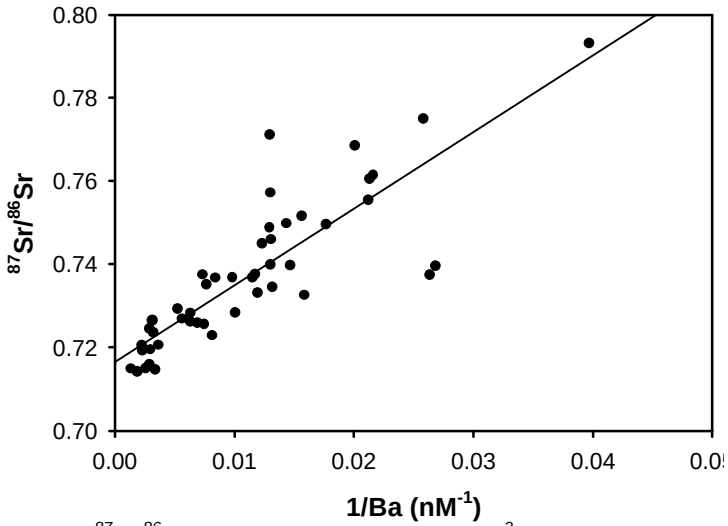

Fig. 4.34 $^{87}Sr/^{86}Sr$ vs. 1/Ba in the YRS waters (r^2=0.73). Samples by and large fall on a two component mixing line.

streams with higher Ba abundances, phosphates, carbonates and evaporites could be dominantly contributing to their Ba. The observation that spring waters of Shahashradhara has only ~80 nM Ba, suggests that evaporite contribution can not possibly account for high abundances of Ba in many of the YRS streams. Phosphorites from Maldeota and Deomala mines have been reported to have high Sr and Ba concentrations (Mazumdar, 1996). The river Asan and its tributary *Tons*, draining the area around Mussoorie, a region where phosphorites are known to occur in the Tal Formation, have very high Sr and the highest Ba concentrations among all the YRS streams analyzed. This spatial correlation is an indication that phosphorites may be a dominant source of Ba in rivers flowing thorough them.

Analogous to Sr, Ba correlates well with dissolved Re in the YRS, with more scatter at higher Ba concentrations (Fig. 4.35). As already discussed, Re is mainly derived from organic rich sediments, the sulphuric acid released via oxidation of pyrites associated with the organic sediments weather other lithologies which occur along with them, such as phosphorites and carbonates. This underlines the importance of H_2SO_4 weathering of phases such as phosphates in releasing these trace elements to the river waters. The outliers in the Re-Ba plot, the river Asan and its tributary *Tons*, draining phosphates and Krol carbonates (and possibly evaporites), may have derived high Ba from them with little contributions of Re. Barites are known to occur as pockets and veins in Krol limestones (Anantaraman and

Bahukhandi, 1984), however, considering that barites are relatively insoluble it is uncertain if they can dissolve and contribute significantly to dissolved Ba in these rivers.

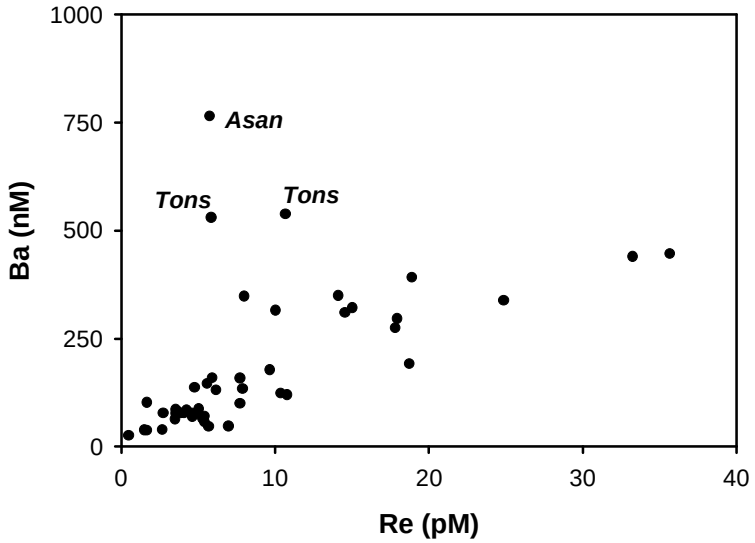

Fig. 4.35 Scatter plot of Ba vs. dissolved Re in the YRS waters. Both these dissolved properties co-vary, with more scatter at higher Ba concentrations. This trend suggests that release of Re to these waters is accompanied by proportionate release of Ba from lithologies associated with organic rich sediments such as phosphates and carbonates.

4.2.6 Weathering rates and CO_2 consumption

The data on silicate and carbonate components of cations in rivers, its silica concentration, coupled with information on the drainage area and discharge can be used to calculate the present day silicate and carbonate weathering rates in their basins. For the Yamuna, the discharge data is available at Tajewala, which is a few tens of kms downstream of Batamandi. For calculation of silicate weathering rate (SWR), the silicate cation contributions (K_s, Na_s, Ca_s and Mg_s) and silica abundances (all in mg ℓ^{-1}) are summed up and for carbonate weathering rate (CWR), Ca and Mg from carbonates and stoichiometric equivalent of carbonate were added up. Such calculations show that SWR in the YRS in the Himalaya is ~11 mm ky^{-1} which is ~4 times lower than the CWR, ~43 mm ky^{-1}. The SWR and CWR becomes ~10 and ~46 mm ky^{-1} respectively if $(Ca/Na)_{sol}$ is decreased from 0.7 to 0.35. The CWR has been estimated assuming all non-silicate Ca and Mg to be of carbonate origin. Considering that evaporites also contribute to Ca in the rivers, such an estimate of

CWR would be an *upper limit*. Assuming that all SO_4 in the river to be of evaporite origin, a *lower limit* of CWR is estimated to be ~31 mm ky^{-1}. Using a suspended load of 2 g ℓ^{-1} in the YRS (Subramanian and Dalavi, 1978; Hay, 1998), mechanical erosion in the basin is estimated to be ~2.3×10^3 tons km^{-2} y^{-1}, about 15 times higher than the total chemical erosion (silicate and carbonate weathering) rates in the basin. This underlines the importance of mechanical erosion in an active mountain chain such as the Himalaya.

The flux of CO_2 consumed during silicate weathering (ϕCO_2 in moles km^{-2} y^{-1}) in the Yamuna basin has been estimated from the calculated silicate cations, river discharge and the basin area: $(\phi CO_2) = \phi\ (TZ^+)_{sil}$. This estimation gives a value of (ϕCO_2) ~7×10^5 moles km^{-2} y^{-1} at Batamandi. This would become ~6×10^5 moles km^{-2} y^{-1} if a value of 0.35 is used for $(Ca/Na)_{sol}$ instead of 0.7. These estimates based on the major ion composition of the monsoon sample (RW99-55) would be upper limits considering that the sulphuric acid, as already discussed, also provide protons for chemical weathering in the YRS basin. If it is assumed that all SO_4 in the waters result from pyrite oxidation, the lower limit of CO_2 consumption would be is ~$(5\text{-}6)\times10^5$ moles km^{-2} y^{-1}. In making these calculations the protons provided by H_2SO_4 and H_2CO_3 are assumed to be in the same ratio (equivalence) as the SO_4/HCO_3 abundance in the water. Independent estimates of (ϕCO_2) can be made from the Si abundances in the waters: $(\phi CO_2) = 2\phi Si$, this relationship is derived for aluminosilicate weathering in general, based on the global fluvial dataset (Huh et al., 1998 and references therein). Such an approach gives an estimate of ~4×10^5 moles km^{-2} y^{-1}. Thus, CO_2 consumption flux via silicate weathering in the YRS estimated by various approaches is ~$(4\text{-}7)\times10^5$ moles km^{-2} y^{-1}.

4.2.7 Comparison of silicate weathering CO_2 consumption rates with other river basins

Comparison of results of weathering rates estimated in this study with those available for the headwaters of the Ganga, in the Alaknanda and Bhagirathi basins (Krishnaswami et al., 1999) suggest that SWR is ~2 times and CWR ~2-3 times higher in the YRS (Table 4.10). The CO_2 consumption flux for silicate weathering, in the Yamuna basin in the Himalaya calculated using various approaches vary between $(4\text{-}7)\times10^5$ moles km^{-2} y^{-1}. Krishnaswami et al. (1999) reported a value of ~4×10^5 moles km^{-2} y^{-1} for the Bhagirathi and Alaknanda basins in the Himalaya. This is about a factor of two lower than that in the YRS

basin, calculated following the same approach, assumptions and end member values. The CO_2 consumption flux calculated in this study for the Ganga at Rishikesh varies between 2-3×10^5 moles km^{-2} y^{-1} (Table 4.10), compared to ~4×10^5 moles km^{-2} y^{-1} reported by Krishnaswami et al. (1999). This difference arises from the variability in the major ion composition of river water samples used for calculations. In this study, calculations for the Ganga were done using the major ion concentrations of the monsoon sample (RW99-59) whereas Krishnaswami et al. (1999) used those for the sample of April collection. This underlines the importance of using discharge weighted concentrations for such calculations to have more reliable estimates of the CO_2 drawdown via silicate weathering. However, considering that about 80% of the water flow of the YRS occurs during monsoon season, estimates based on the cation concentrations during this period (an approach adopted in this work) is more representative of the whole year. The CO_2 consumption fluxes in these rivers basins in the Himalaya compare with values of ~0.5×10^5 moles km^{-2} y^{-1} in the Amazon, ~0.5×10^5 moles km^{-2} y^{-1} in the Congo-Zaire (Gaillardet et al., 1995; 1997;1999) and ~1.5×10^5 moles km^{-2} y^{-1} in the Orinoco (Edmond and Huh, 1997). The CO_2 consumption fluxes in the Ganga-Yamuna basins in the Himalaya are higher than those in the river basins of the Huanghe (~0.82×10^5 moles km^{-2} y^{-1}), the Xijiang (~0.55×10^5 moles km^{-2} y^{-1}), the Changjiang (~0.59×10^5 moles km^{-2} y^{-1}), in the northern slopes of the Himalaya (Gaillardet et al., 1999). In the Mekong basin it is ~2.4×10^5 moles km^{-2} y^{-1}, comparable to that in the Ganga basin but marginally lower than that in the Yamun basin.

Table 4.10 Weathering rates and CO_2 consumption in the river basins in the Himalaya[a)]

River basin	Location	Discharge 10^{12} ℓ y^{-1}	Area 10^3 km^2	SWR (i)	SWR (ii)	CWR (i)	CWR (ii)	CO_2 drawdown[b)]
Yamuna	Batamandi	10.8	9.6	25-28	~10	115-123	43-46	4-7
Bhagirathi[c)]	Devprayag	8.3	7.8	15.2	5.8	41.1	15.2	4.1
Alaknanda[c)]	Bhagwan	14.1	11.8	10.2	3.9	63.2	23.4	3.6
Ganga	Rishikesh	22.4	19.6	12-13	~5	54-56	20-21	2-3
Ganga[c)]	Rishikesh	22.4	19.6	12.9	4.9	51.7	19.1	3.8
Narayani[d)]	Narayangha	49.4	31.8		7.0		52.0	
G-B[c)]		1002	1555	13.6	5.3	31.7	11.7	3.3

Yamuna and Ganga estimates based on monsoon samples (RW99-55 and RW99-59). [a)]calculated using the mean density 2.6 and 2.7 g cm^{-3} for silicates and carbonates respectively; (i): tons km^{-2} y^{-1}; (ii): mm ky^{-1}. [b)]drawdown via silicate weathering in 10^5 moles km^{-2} y^{-1}. [c)]from Krishnaswami et al. (1999). [d)]from Galy and France-Lanord (1999).

From such comparisons, it is borne out that the present day CO_2 consumption rates in the river basins in the southern slopes of the Himalaya are significantly higher than those from other major global river basins in the world. These estimates indicate that the contemporary CO_2 drawdown by silicate weathering in the Yamuna and the Ganga basin in the Himalaya is disproportionately higher than other global rivers. Enhanced silicate weathering resulting from conducive climate, relief and environmental factors could be responsible for this (Raymo and Ruddiman, 1992). However, the impact of this on the global CO_2 consumption by silicate weathering is not that pronounced as the G-B basin account for only ~1.5% of the global drainage area and contribute only ~4% of the global CO_2 drawdown. The upper reaches of the Ganga and the Yamuna are dominated by physical erosion with less intense chemical weathering.

4.2.8 Chemical weathering: control of temperature and altitude

Earlier studies have shown that chemical weathering in river basins depends on several factors such as lithology, elevation, temperature and runoff (Drever and Zobrist, 1992; White and Blum, 1995). In many of the river systems the variation in solute fluxes with temperature, $r_{T,}$ has been described in terms of the Arrhenius relation:

$$r_T = Ae^{(-E_a / RT)}$$

where E_a is the activation energy (kJ mol^{-1}), T the temperature (K), R the gas constant and A the pre-exponential constant. A plot of ln r_T (or solute concentration) against 1/T would yield a straight line with a slope of ($-E_a/R$) from which the activation energy can be calculated. This relation, though is oversimplified to be applied to solute fluxes in natural watersheds in which chemical weathering reactions are dependent on multiple variables, has been used to empirically determine the activation energy for weathering of various lithologies (White and Blum, 1995; Dessert et al., 2001).

The use of such an approximation for studying granite weathering has been a topic of debate. Jenny (1941), based on study of large number of soils in the United States, had observed, in case of granite-gneiss weathering, an increase of clay content with temperature that is greater for higher precipitation. Berner and Berner (1997) observed that higher global temperature and greater rainfall should enhance silicate weathering. On the contrary,

Edmond and Huh (1997) and Huh and Edmond (1999), based on studies of Siberian rivers and other river basins in the tropical regions, concluded that lithology and their exposure to weathering plays the dominant role in regulating solute fluxes and weathering rates, the role of climate being secondary. In Fig. 4.36, the log concentrations of Na* and Si (proxies of silicate weathering) are plotted against (1/Temp.) in samples of selected rivers and streams of the YRS for the summer collection. (only data for tributaries are plotted to minimize averaging effects.

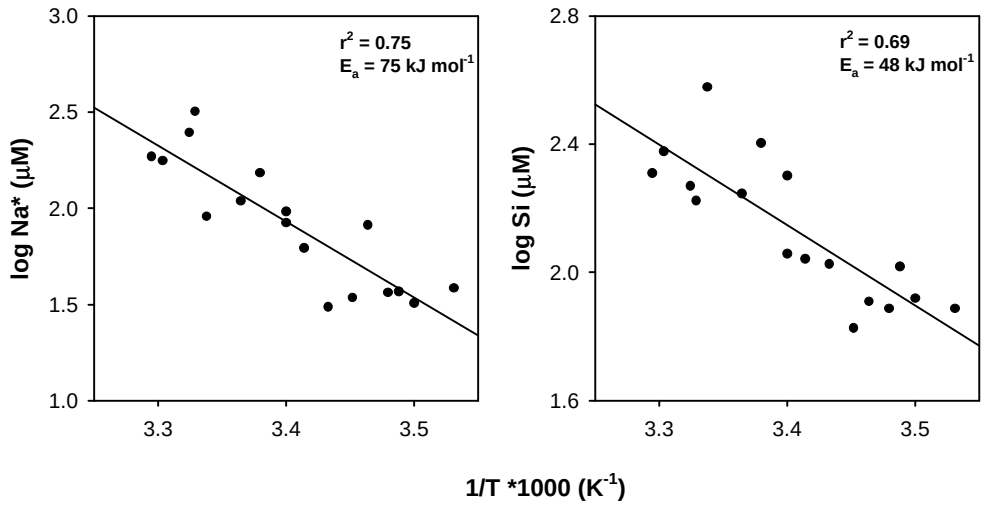

Fig. 4.36 Plots of logNa and Si vs. inverse of water temperature (1/T). The strong correlation is suggestive of dependence of silicate weathering on temperature. Apparent activation energy for overall silicate weathering in the basin has been calculated from the slopes of the regression lines to be 75 and 48 kJ mol^{-1}.*

The data of the Yamuna and Tons mainstreams are not included in the plot as they integrate the chemistry along their path). October samples could not be plotted, as temperature measurements were not made during this campaign. Similarly, the monsoon samples had marginal temperature spread, 15.7 to 27.4 °C, as sampling was restricted to lower reaches of the YRS. The plots show a significant anticorrelation of log concentration with inverse of temperature (r^2 = 0.75 for Na*, and 0.69 for Si). Such a trend is consistent with that expected based on Arrhenius relation. From the slope of the regression lines, the "apparent activation energy" for silicate weathering in the YRS basin is derived to be ~75 and ~48 kJ mol^{-1}.

In natural systems like the YRS basin, in addition to temperature, other factors such as altitude, rainfall and vegetation also influence the silicate weathering in the basin and hence the solute concentrations in the river waters. Indeed, the data show significant negative

correlation between logNa*(Si) and sampling altitude (Fig. 4.37). This may be a manifestation of temperature which decreases with altitude. In Chapter 3, the interdependence of $\delta^{18}O$ (a proxy for altitude) and ΣCat* has been used to assess the variation in weathering contribution (in terms of ΣCat*) in the Yamuna waters with altitude (Dalai et al., 2001d).

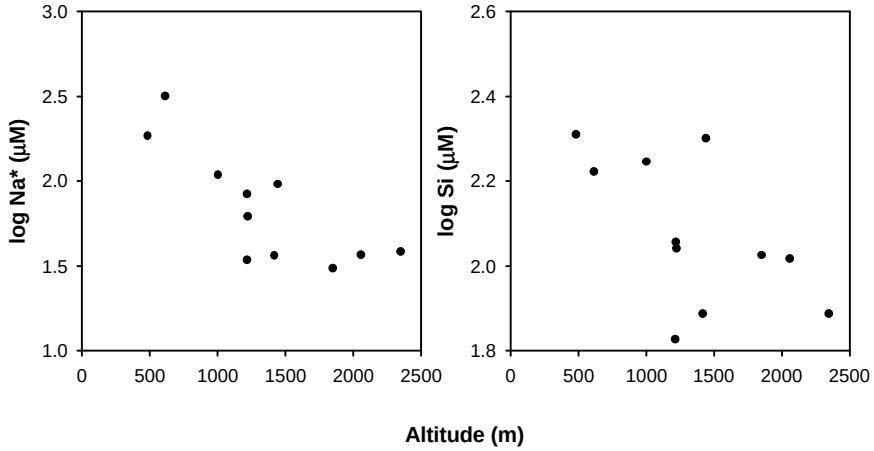

Fig. 4.37 Altitudinal variations of Na and Si in the YRS waters. Apparent dependence of Na* and Si concentrations on the altitude is caused by temperature variations with altitude (see text).*

The deduced values of activation energy are average for the silicates (crystallines and metasediments) as a whole in the YRS basin. These values are similar to those obtained for granitoid weathering in natural watersheds, 77 kJ mol^{-1} (Velbel, 1993), 69-78 kJ mol^{-1} (White and Blum, 1995) and 51 kJ mol^{-1} (White et al., 1999) and those determined from laboratory weathering studies, 56-61 kJ mol^{-1} for granitoid rocks (White et al., 1999), 60 kJ mol^{-1} for albite and 80 kJ mol^{-1} for oligoclase (White and Blum, 1995 and references therein). The strong negative correlation between logNa*(Si) and 1/T and the similarity between the activation energy estimated in natural watersheds and that measured in the laboratory experiments reinforces the idea that climatic parameters like temperature influences chemical weathering of silicates, though this dependence could manifest through other factors such as altitude, rainfall and vegetation.

4.3 CONCLUSIONS

The headwaters of the Yamuna and its tributaries in the Himalaya have been extensively sampled for three different seasons. The major ion, Sr and Ba abundances and $^{87}Sr/^{86}Sr$ in the river waters, sediments and bedrocks have brought out the following important observations and conclusions.

1. The YRS waters are mildly alkaline, with a wide range of TDS, ~32 to ~620 mg ℓ^{-1}. The streams in the lower reaches have higher TDS than those near the source region. This is caused by a number of factors, such as, the abundance of more easily weatherable rocks (carbonates and evaporites) in the lower reaches; higher temperature and vegetation. The Sr and its isotopic composition in the YRS is dictated by the lithology. $^{87}Sr/^{86}Sr$ in the Yamuna decreases downstream with a rise in Sr.
2. Ca and alkalinity are the most abundant among the major ions in the YRS waters, indicating the dominance of carbonate weathering in contributing to their dissolved loads. However, their contribution to the dissolved Sr and Ba in the YRS is comparatively lower (~15% and ~30% respectively). With lower Sr/Ca and $^{87}Sr/^{86}Sr$ than the river waters, carbonates are not a major contributor to the high $^{87}Sr/^{86}Sr$ of river waters. Bulk of the water samples is supersaturated with calcite. Furthermore, decrease of Ca/Mg in the waters with an increasing Ca suggest that either dolomite weathering or precipitation of calcites may result in such a trend. In the present study, however, no evidence of calcite precipitation was observed.
3. Silicates, on an average, contribute ~25% (on a molar basis) to the total cations in the YRS waters the rest coming from carbonates, evaporites and phosphates. Maximum contribution of cations from carbonates and evaporites in the YRS basin are ~74 and ~21%. The contributions of silicates to the YRS cation budget is similar to their contribution to the dissolved Sr (~25%) and Ba (~30%). Disseminated calcites though may contribute significantly to the dissolved Sr in the YRS, their role in regulating the $^{87}Sr/^{86}Sr$ of the rivers needs to be assessed by carrying out more detailed work. The present data set clearly show that silicate weathering dominates the high $^{87}Sr/^{86}Sr$ of the YRS, as evident from the correlation of $^{87}Sr/^{86}Sr$ with SiO_2/TDS, $(Na^*+K)/TZ^+$, Sr_s and $(\Sigma Cat)_s$. Minor lithologies such as evaporites and phosphates seem to be significant

contributors to the YRS Sr and Ba budgets and they play a diluting role in $^{87}Sr/^{86}Sr$ of these rivers.

4. The silicate weathering rate in the Yamuna basin is ~10 mm ky^{-1}, 3 to 4 times lower than the carbonate weathering rate, ~31-46 mm ky^{-1}. Chemical weathering of silicates in the Yamuna basin in the Himalaya, however, is not intense, as evident from the low values of Si/(Na*+K) in the waters (~1.2) and low values of CIA (~60) in the bed sediments. The CO_2 drawdown via silicate weathering in the YRS and the Ganga basins in the Himalaya are similar and a few times higher than those reported in the other major river basins of the world. The impact of such enhanced drawdown in the southern slopes of the Himalaya on the global CO_2 budget is not pronounced as the drainage area and discharge of the Yamuna and the Ganga in the Himalaya constitute only a low proportion of the global values.
5. The strong correlation of logNa*(Si) vs. 1/T implies the dependence of silicate weathering on temperature. Apparent activation energy calculated for overall silicate weathering in the basin, ~50-75 kJ mol^{-1}, is similar to those reported for granitoid weathering in other watersheds and laboratory experiments.

Chapter 5

Dissolved Rhenium in the Yamuna River System: Black shale weathering and its role on riverine trace metal budgets

5.1 INTRODUCTION

The surficial geochemistry of Re plays a significant role in determining the utility of the Re-Os system for dating. The application of ^{187}Re-^{187}Os pair as a chronometer to date sedimentary formations and igneous rocks is getting increasingly recognized (Ravizza and Turekian, 1989; Allegre et al., 1999; Singh et al., 1999). Despite its low crustal abundance, Re has relatively high concentration in seawater (Anbar et al., 1992) due to the solubility of perrhenate (ReO_4^-) anion in oxidizing environments. From seawater, Re is removed via scavenging under suboxic-anoxic conditions leading to its strong enrichment in organic rich marine sediments. Since ^{187}Re, more abundant of the two isotopes of Re, decays to ^{187}Os, organic rich sediments such as black shales serve as an important crustal reservoir for radiogenic ^{187}Os. These sediments, being reduced in nature, are prone to oxidative weathering in aqueous oxic environments. Hence weathering of these sediments would release both Re and ^{187}Os to solution. Therefore, drainage basins abundant in organic rich sediments are potential sources of Re and radiogenic Os to the oceans. The $^{187}Os/^{188}Os$ of seawater shows a steady rise since last ~40 my to present (Pegram et al, 1992; Ravizza, 1993; Peucker-Ehrenbrink et al., 1995; Turekian and Pegram, 1997). The timing of the increase coupled with the knowledge of presence of black shales in the Himalaya (Valdiya, 1980) led to the suggestion that their weathering is an important driver in determining the steady increase of seawater $^{187}Os/^{188}Os$ through Cenozoic (Pegram et al., 1992). The validity of this suggestion though being debated, it has been found that rivers draining the Himalaya have Os isotopic composition generally more radiogenic compared to other major world rivers (Levasseur et al., 1999; Sharma et al., 1999). The $^{187}Os/^{188}Os$ of rivers is determined by the Re/Os ratios and age of the basins drained by them. Relatively higher $^{187}Os/^{188}Os$ in rivers can result if they drain basins with high Re/Os such as those containing organic rich sediments. Considering that weathering of these sediments by oxic river waters would also release Re to solution as perrhenate oxyanion (Brookins, 1986; Koide et al., 1986), the concentration of Re in such rivers are expected to be relatively high. Hence data on the abundance of Re in river waters in the Himalaya can aid not only in constraining their sources but also provide better understanding of the comparative geochemistry of Re and Os during weathering.

Knowledge of the sources of Re in river waters and understanding its geochemical behaviour in surficial weathering environment also has implications to the use of ^{187}Re-^{187}Os isotope pair for geochronology. The application of this pair for age determination requires, among other conditions, closed system behavior of both Re and Os in the rock/sediment system to be dated (Ravizza and Turekian, 1989; Raviza et al., 1991; Allegre et al., 1999; Cohen et al., 1999; Singh et al., 1999; Peucker-Ehrenbrink and Hannigan, 2000). Studies of Re in rivers is one approach to learn about the extent of its mobility from various rock types during surficial weathering and its possible consequences to Re-Os chronometry.

Some of these considerations, coupled with the availability of high sensitive measuring techniques such as the ID-NTIMS and ICP-MS which have considerably improved the precision and accuracy of Re determinations (Anbar et al., 1992; Colodner et al., 1993a,b) have contributed to recent studies of Re in natural waters. Colodner et al. (1993b) in their reconnaissance study of the geochemical cycle of Re observed that rivers draining black shales, such as those in the Venezuelan Andes, have higher dissolved Re concentrations. Hodge et al. (1996), on the other hand, proposed carbonates to be an important source of Re to groundwaters based on their observation that Re/Mo/U ratios in groundwaters from Palaeozoic carbonate aquifers in the southern Great Basin, USA and seawater are quite similar. This finding led them to suggest quantitative uptake of these trace elements from seawater by carbonates during their precipitation and their subsequent release to groundwater during dissolution.

This chapter presents and discusses Re abundances in the Yamuna and many of its major as well as a number of minor tributaries in the Himalaya. For comparison, a few samples from the Ganga collected at Rishikesh at the base of the Himalaya were also analyzed for Re. In addition, Re has been measured in various source rocks from the catchment, such as carbonates and granites, and a few groundwaters percolating through a phosphorite-black shale-carbonate sequence in a phosphorite mine in the Lesser Himalaya. This work, which forms the first comprehensive study on the geochemistry of Re in a river system in the Himalaya, aims at (i) determining dissolved Re flux from the Yamuna and the Ganga at their outflow at the foothills of the Himalaya, an important data set to assess the role of weathering in the Himalaya in contributing to Re budget of the oceans, (ii) delineating the source(s) of dissolved Re to these rivers based on Re in granites, carbonates and those

available in literature for black shales in the Lesser Himalaya (Singh et al., 1999) (iii) understanding the implications and influence of weathering of organic rich sediments such as black shales on the riverine trace metal (Re, Os and U) budgets and global carbon cycle, using dissolved Re in rivers as a proxy.

5.2 RESULTS AND DISCUSSION

The concentration of dissolved Re in the Yamuna and its tributaries are given in Table 5.1 and Re abundances in granites collected from the YRS catchment and the Precambrian carbonates from the Lesser Himalaya in Table 5.2.

Table 5.1 Dissolved Re in the Yamuna River System, the Ganga and mine waters.

Code[a)]	River	Location	Season[b)]	SO_4 (μM)	Re[c)] (pM)	ΣCat* (mg ℓ^{-1})	TDS* (mg ℓ^{-1})
Yamuna mainstream							
RW98-16	Yamuna	Hanuman Chatti	PM	113	5.3±0.2	20.7	88
RW98-20	Yamuna	D. of Paligad Bridge	PM	100	4.6±0.1	21.2	93
RW98-25	Yamuna	Barkot	PM	76	5.4±0.4	22.2	100
RW98-22	Yamuna	U. of Naugaon	PM	76	4.1±0.2	23.0	103
RW98-15	Yamuna	U. of Barni Gad's confluence	PM	72	3.5±0.1	27.2	124
RW98-14	Yamuna	D. of Barni Gad's confluence	PM	63	3.7±0.2	28.8	136
RW98-12	Yamuna	D. of Nainbag	PM	66	3.6±0.1	27.1	125
RW98-9	Yamuna	D. of Aglar's confluence	PM	220	5.6±0.4	34.9	157
RW99-51	Yamuna	D. of Aglar's confluence	M	40	1.7±0.1	17.7	85
RW98-6	Yamuna	U. of Ton's confluence	PM	216	5.9±0.2	37.1	168
RW99-64	Yamuna	U. of Ton's confluence	M	154	4.2±0.2	31.2	140
RW99-31	Yamuna	D. of Ton's confluence	S	405	7.9±0.1	39.5	172
RW99-53	Yamuna	D. of Ton's confluence	M	93	3.5±0.1	19.4	102
RW98-1	Yamuna	Rampur Mandi, Paonta sahib	PM	101	6.2±0.2	26.8	117
RW99-58	Yamuna	Rampur Mandi, Paonta sahib	M	100	4.9±0.1	24.2	109
RW98-4	Yamuna	D. of Bata's confluence	PM	333	14.6±0.3	58.7	254
RW99-55	Yamuna	D. of Bata's confluence	M	288	14.1±0.4	51.3	274
RW98-33	Yamuna	Yamuna Nagar, Saharanpur	PM	268	10.0±0.2	53.4	236
RW99-7	Yamuna	Yamuna Nagar, Saharanpur	S	321	15.0±0.2	55.8	262
RW99-54	Yamuna	Yamuna Nagar, Saharanpur	M	192	7.7±0.2	28.2	151
Tributaries							
RW98-17	Jharjhar Gad	Hanuman Chatti-Barkot Road	PM	27	2.7±0.1	11.5	51
RW98-18	Didar Gad	Hanuman Chatti-Barkot Road	PM	11	0.50±0.02	6.1	32
RW98-19	Pali Gad	Pali Gad Bridge	PM	61	3.9±0.2	21.6	94
RW98-13	Barni Gad	Kuwa	PM	27	4.8±0.1	44.8	200
RW98-21	Kamola	Between Naugaon and Pirola	PM	32	1.7±0.2	30.9	142

RW98-24	Gamra Gad	Near the bridge over it	PM	26	1.5±0.1	32.1	153
RW98-26	Godu Gad	Purola-Mori Road	PM	19	2.7±0.2	10.2	53
RW98-27	Tons	Mori	PM	62	7.0±0.4	10.7	49
RW98-28	Tons	D. of Mori	PM	58	5.7±0.5	11.1	50
RW98-29	Tons	Tiuni	PM	62	5.4±0.7	12.8	60
RW98-31	Shej Khad	Minas	PM	159	18.7±0.8	37.8	166
RW98-30	Tons	Minas	PM	100	10.8±0.6	24.0	107
RW98-5	Amlawa	Kalsi-Chakrata Road	PM	127	5.1±0.2	39.4	181
RW99-62	Amlawa	Kalsi-Chakrata Road	M	150	4.6±0.2	40.7	184
RW98-32	Tons	Kalsi, U. of confluence	PM	581	9.7±0.2	46.9	202
RW99-29	Tons	Kalsi, U. of confluence	S	777	10.4±0.4	46.9	197
RW99-63	Tons	Kalsi, U. of confluence	M	340	7.7±0.2	34.1	146
RW98-7	Kemti Fall	Dehradun-Mussourie Road	PM	2913	23.8±0.4	151	587
RW98-8	Aglar	Upstream of Yamuna Bridge	PM	1052	18.9±0.9	70.6	318
RW99-52	Aglar	Upstream of Yamuna Bridge	M	1139	17.9±0.6	70.8	328
RW98-2	Giri	Rampur Mandi	PM	1115	33.3±0.5	98.6	399
RW99-3	Giri	Rampur Mandi	S	2046	35.7±1.2	119	547
RW99-57	Giri	Rampur Mandi	M	881	24.9±0.6	80.3	348
RW98-3	Bata	Bata Mandi	PM	395	17.8±0.2	54.7	229
RW99-56	Bata	Bata Mandi	M	386	17.8±0.3	59.3	274
RW98-10	*Tons*	*Tons Pol*, Dehradun	PM	1226	10.7±0.4	87.9	384
RW99-65	*Tons*	*Tons Pol*, Dehradun	M	707	8.0±0.1	76.8	320
RW98-11	Asan	Simla Road Bridge	PM	975	5.7±0.3	104	479
RW99-61	Asan	Simla Road Bridge	M	822	5.9±0.1	101	461
RW99-60	Spring	Shahashradhara	M	15400	16.1±0.2	640	2412
Ganga							
RW98-34	Ganga	Rishikesh	PM	165	6.7±0.2	26.0	117
RW99-6	Ganga	Rishikesh	S	204	7.9±0.1	25.5	115
RW99-59	Ganga	Rishikesh	M	145	5.3±0.2	22.0	99
Mine Waters and Misc. samples							
RW99-8	Bandal	Near Maldeota	S	909	32.2±2.3	82.9	366
MW-1		Maldeota mines	S	4123	61.9±0.9	n.m.	n.m.
MW-2		Maldeota mines	S	4750	7.5±0.3	n.m.	n.m.
MW-3		Maldeota mines	S	2571	111±1	n.m.	n.m.
MW-4		Maldeota mines	S	6854	86.9±1.2	n.m.	n.m.

[a)]RW - river water, MW - mine water. [b)]S = summer, M = monsoon, PM = post-monsoon. U: upstream, D: downstream. [c)]Re values are blank corrected, errors are ±2σ. ΣCat* = (Na*+K+Mg+Ca), Na* is Na corrected for chloride, major ion data from Table 4.1. n.m.: not measured.

In rivers, dissolved Re varies by about two orders of magnitude, during the three periods, from 0.5 to 35.7 pM (Table 5.1; Fig. 5.1), with an average of 9.4 pM (~1.8 ng ℓ^{-1}). This compares well with the discharge weighted Re concentration, 8.9 pM, in the Yamuna at Saharanpur suggesting that the Yamuna mainstream receives Re and water roughly in the

same proportion till it flows at at the fothills. The average Re in the Yamuna system and in the Yamuna and the Ganga samples at Batamandi and Rishikesh respectively, near the

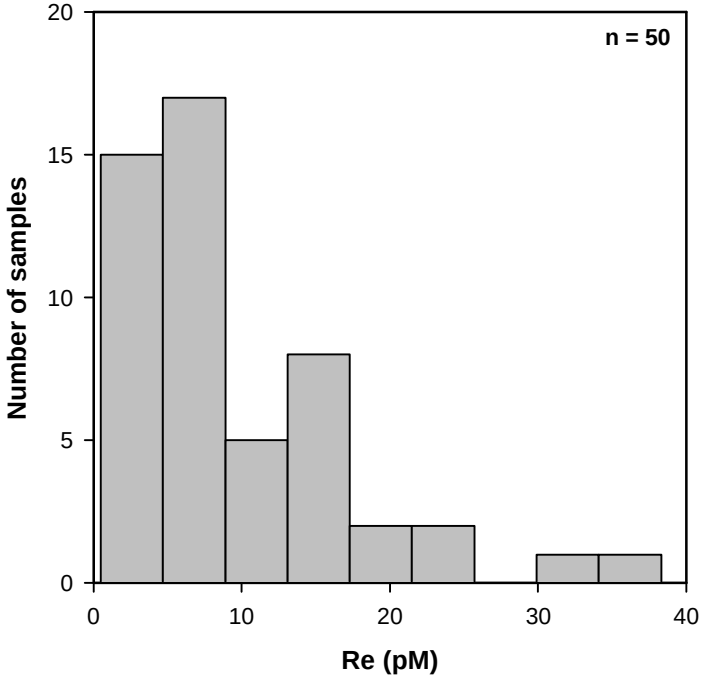

Fig. 5.1 Frequency distribution of dissolved Re in the Yamuna and its tributaries. The concentrations range from 0.5 to 35.7 pM with an average of 9.4 pM.

foothills of the Himalaya, is significantly higher than the global average value of 2.1 pM, reported by Colodner et al. (1993b; their average value of 2.3 pM is reduced by 10% to correct for spike calibration, Colodner et al., 1995). Re concentrations of the Ganga water at Rishikesh varied between 5.3 to 7.9 pM during the three seasons, compared to ~14 pM for the Yamuna at Batamandi (downstream of Bata's confluence), both at the foothills of the Himalaya. Re concentration of the Ganga at Rishikesh is marginally lower than the value of 8.2 pM reported near its out flow at Aricha Ghat, Bangladesh (before the confluence of the Ganga and the Brahmaputra, data corrected for spike calibration Colodner et al., 1993b, 1995).

Dissolved Re concentrations show a significant positive correlation with ΣCations* (Fig. 5.2) and total dissolved solids (TDS) in these rivers albeit with some scatter (ΣCations* = Na*+K+Ca+Mg, where Na* is Na corrected for cyclic component). This is also reflected in the seasonal variations in the Re abundances. The waters collected during June (summer) often have both higher TDS and Re concentrations than those collected during October (post-

monsoon) and September (monsoon) periods. Considering that the Yamuna and its tributaries drain different sub-basins with their own characteristic lithology and hence (Re/major ion) ratios, such a scatter is not unexpected. For example, the tributaries sampled in and around the foothills of the Himalaya have, in general, higher Re than the streams flowing in the

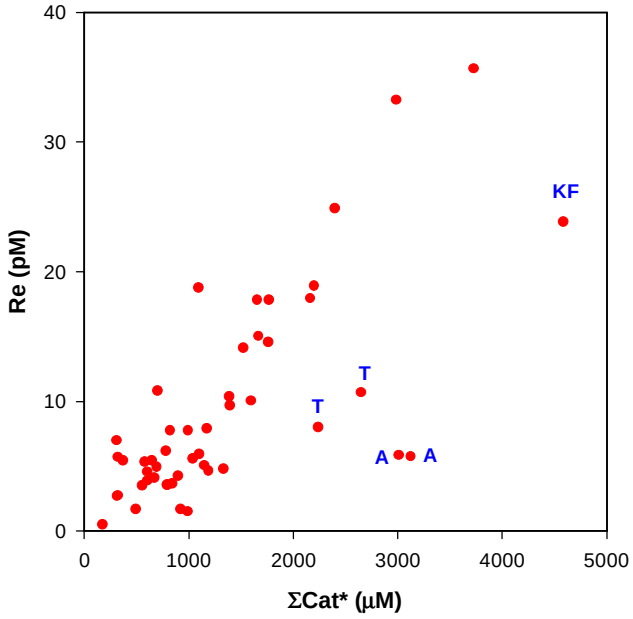

Fig. 5.2 Scatter diagram of Re vs. SCations in the water samples analyzed (excluding Shahashradhara sample). SCations* = Na*+K+Ca+Mg. The data show a strong positive correlation (r = 0.90, p<0.005) suggesting that Re and (Na*+K+Mg+Ca) are released to the rivers in roughly the same proportion along its entire stretch. Regression analysis excludes Kempti Fall (KF), Tons at Dehradun (T), and Asan (A) rivers which fall far outside the trend set by other rivers.*

upper reaches probably because of more widespread occurrences of organic rich sedimentary rocks in their drainage basins. Another contributing factor for the scatter in Fig. 5.2 could be seasonal variations in Re/ΣCations*. The intensity of weathering of different lithologies in the drainage basin and hence Re/ΣCations* of the rivers could be season dependent. It is also observed that Re/ΣCations* in the Tons and its tributaries are generally higher than those in the Yamuna and its tributaries.

The strong positive correlation between Re and ΣCations* (Fig. 5.2) is an indication that both of them are released to the rivers in roughly the same proportion throughout the drainage basin. Samples from the Kempti Fall, the Asan river, and the *Tons* at Dehradun (Table 5.1) plot significantly away from the trend set by the bulk of the samples (Fig. 5.2). The ΣCations* of these streams seem to have a significant evaporite component (Chapter 4)

which may be contributing to their low (Re/ΣCations*) ratios. The observation, that the Shahashradhara sample (RW99-60, Table 5.1) having the highest SO_4 concentration, 15.4 mM has only ~16 pM Re, attests to the idea that evaporites are not a significant source of Re (Colodner et al., 1993b). The regression line (Fig. 5.2, r = 0.90) plotted through the data (excluding Kempti Fall, Asan, and *Tons* at Dehradun,) yields a (Re/ΣCations*) slope of ~9.9 pM mM^{-1} (~60 pg Re mg^{-1} ΣCations*). The implications of this, in determining the source of Re to these river waters, are discussed in the following sections.

5.2.1 Sources of dissolved Re in the YRS

(i) Re contribution from Crystallines

Granites and granodiorites, as already mentioned in Chapter 2 (Chapter 2, section 2.1.1), constitute a significant proportion of the Yamuna catchment particularly in its higher reaches. Previous studies (Pierson-Wickmann et al., 2000) have reported Re concentrations ranging from 26 to ~1430 pg g^{-1} (geometric mean ~270 pg g^{-1}) in granites and gneisses from the Central Nepal Himalaya. Peucker-Ehrenbrink and Blum (1998) reported Re concentrations for two samples of Precambrian granitoid rocks (gneiss) from Wyoming, 109 and 55 pg g^{-1}. In the present study, analysis of four granites from the Yamuna catchment yielded 14 to 46 pg g^{-1} of Re (Table 5.2).

The average Re in these four samples is about an order of magnitude lower than the mean Re in granites and gneisses from Nepal Himalaya, however, a critical comparison may not be appropriate considering that the samples analyzed are few and from different locations. If, however, this difference is indeed valid, then their conditions of formation and their mineralogical composition may be contributing to it. Taking a value of 50 pg g^{-1} Re for granites, (close to the maximum concentration measured in samples from the Yamuna catchment, Table 5.2), it can be estimated that about ~35 grams of them would have to be dissolved /leached per liter of Yamuna water to yield the average dissolved Re of 1.8 ng ℓ^{-1}. This requirement, as discussed below, is very difficult to be met either through congruent dissolution of crystallines or preferential release of Re from them.

Table 5.2 Re abundances in granites and Precambrian carbonates from the Himalaya

Granites[a)]	**Re** pg g^{-1}	**Re/Na** pg mg^{-1}	pM mM^{-1}	**Re/ΣCat** pg mg^{-1}	pM mM^{-1}
GR98-1(A)	45.8±1.9	1.25	0.154	0.69	0.103
GR98-1(B)	41.6±2.7	—	—	—	—
GR98-2	26.9±2.8	0.65	0.080	0.29	0.045
GR99-1	17.4±1.7	0.50	0.062	0.20	0.032
GR99-2	13.7±1.7	0.38	0.047	0.16	0.025
Mean	***26±14***	***0.7±0.4***	***0.09±0.05***	***0.3±0.2***	***0.05±0.04***
Carbonates[b)]	**Re** pg g^{-1}	**Re/Ca** pg mg^{-1}	pM mM^{-1}	**Re/Ca+Mg** pg mg^{-1}	pM mM^{-1}
KU92-9 (D)	54.0±5.1	0.32	0.069	0.21	0.037
KU92-43 (D)	30.4±0.9	0.24	0.052	0.16	0.027
KU92-48 (D)	35.6±1.0	0.17	0.037	0.11	0.018
HP94-42 (C)	~0	~0	~0	~0	~0
UK94-77 (D)	225±3	1.07	0.230	0.68	0.118
UK94-45 (C)	5.0±3.5	0.01	0.002	0.01	0.003
UK94-50 (C,D)	35.9±2.1	0.10	0.022	0.09	0.019
UK95-23 (D)	29.7±0.2	0.13	0.028	0.09	0.015
Mean	***52±72***	***0.26±0.34***	***0.06±0.07***	***0.17±0.21***	***0.03±0.04***

[a)]Collected in and around Hanuman Chatti. [b)] Samples and their Ca, Mg data from Singh et al. (1998), C: calcite, D: dolomite. (A) and (B) are duplicates.

Another approach to gauge the role of crystallines in contributing to dissolved Re is from the Re-ΣCations* scatter plot (Fig. 5.2). The slope of the Re-ΣCations* regression line, as mentioned earlier, is ~9.9 pM/mM. This is more than two orders of magnitude higher than the [Re/(Na+K+Mg+Ca)] ratio in crystallines ~0.05 pM mM^{-1} (0.3 pg mg^{-1}, Table 5.2). Comparison of these two ratios and the calculations to follow, suggest that crystallines can account only for a small fraction of dissolved Re in the YRS, if Re and (Na+K+Mg+Ca) from them are released to the rivers in the same proportion as their abundance. Using the mean Re/(Na+K+Mg+Ca) in granites 0.3 pg mg^{-1} (Table 5.2) and ΣCat* in the YRS rivers, it is estimated that silicates can contribute ~2 to 45 pg ℓ^{-1} Re (mean: ~13 pg ℓ^{-1}) to these rivers. This estimate, based on the assumption that *all* dissolved major cations are derived from crystallines, would be an *upper limit* as a significant fraction of Ca and Mg in these waters is from carbonates and/or evaporites (Chapter 4). Therefore, to obtain a more realistic estimate of Re contribution from the crystallines, calculation was done using Na as an index of silicate

weathering. Comparison of Re/Na ratio in crystallines with Re/Na* in rivers reinforces our earlier inference that weathering of crystallines is not an important source of Re to the

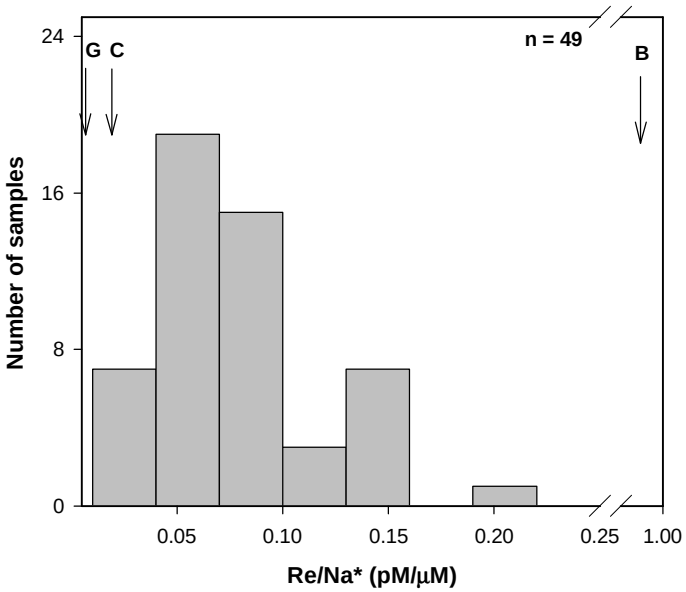

Fig. 5.3 Frequency distribution of Re/Na in the water samples. The ratio varies between 0.01 to 0.21 pM/mM with a mean of 0.08. Typical ratios for granites from the Yamuna catchment (G), Precambrian carbonates (C) and Black shales from the Lesser Himalaya (B) are also shown. Data for Kempti Fall is not plotted.*

Yamuna waters (Fig. 5.3). The Re contribution to the YRS waters, based on their Na* content and the mean Re/Na ratio in crystallines, ~0.09 pM mM^{-1} (~0.7 pg mg^{-1}, Table 5.2) is in the range of ~0.1 to 4 pg ℓ^{-1} (mean: ~2 pg ℓ^{-1}). This estimate is based on the assumption that Re and Na are supplied from silicates to the rivers in the same proportion as their abundances. The estimated contribution accounts for less than one percent of the mean dissolved Re in the Yamuna system. This conclusion would be valid even if a much higher average Re concentration is used for the crystallines, ~270 pg g^{-1} (geometric mean of the values reported by Pierson-Wickmann et al., 2000).

The role of preferential release of Re to solution from crystallines is more difficult to assess. One approach is to assume that all the suspended matter in the Yamuna system is derived from crystallines and that all Re in them is released to solution during weathering. Both these assumptions may be quite exaggerated (cf. Peucker-Ehrenbrink and Blum, 1998), however, the estimates based on them can place useful constraints. Using a suspended matter concentration of ~2 g ℓ^{-1} (Subramanian and Dalavi, 1978; Hay, 1998) and assuming them to be derived entirely from crystallines with 50 pg g^{-1} Re in them, the maximum Re supply

would be ~100 pg $\ell^{-1}$of Re, only a few percent of the average Re abundance in these rivers. This contribution may increase by a factor of ~2 if the recent estimate of Galy and France-Lanord (2001) on the total erosion in the Himalaya is considered. Their results suggest that the contribution of bed load and flood plain deposition is comparable to the sum of suspended and dissolved loads. A similar conclusion is also borne out for the Ganga at Rishikesh if the granites analyzed in this work (Table 5.2) are taken to be representative of its catchment. Calculation of the impact of preferential release of Re from suspended matter for individual rivers and streams has not been attempted due to non availability of suspended/bed load data.

Thus, if granites analyzed in this study (Table 5.2) are typical of the crystallines of the Yamuna and the Ganga catchments in the Himalaya, then the present results show that on an average these lithologies can make only a minor contribution to the dissolved Re budgets of the Yamuna and the Ganga rivers on a basin wide scale. However, for rivers with low Re (e.g. Didar Gad, 0.1 ng ℓ^{-1}, Table 5.1) the contribution by preferential leaching can become significant if they have suspended matter concentrations comparable to those of the Yamuna and if a large fraction of their Re can be mobilized. The later requirement, as already discussed, may be difficult to comply.

The strong positive correlation between Re and ΣCations* in the Yamuna system (Fig. 5.2) is intriguing in light of the above calculations and conclusions and suggests the need for a source with significantly higher Re/(Na + K + Mg + Ca) or Re/Na compared to those in the granites of the Yamuna catchment (Table 5.2). Pierson-Wickmann et al. (2000) reported one gneiss sample with ~1430 pg g^{-1} Re from Nepal Himalaya. Such Re rich crystallines or organic rich sediments, which are known to be abundant in Re, could fit in the requirement (see later section on black shales). More analysis of Re in crystallines is necessary to assess the distribution of Re rich granites and gneisses in the Yamuna and the Ganga catchments and to determine if they are abundant and typical. From the data available at present, however, the crystallines seem to be only a minor source of dissolved Re to the Yamuna and Ganga waters in the Himalaya.

(ii) Re contribution from Precambrian Carbonates

Precambrian carbonates (calcites and dolomites), occurring in the drainage basins of the headwaters of the Yamuna and the Ganga in the Lesser Himalaya, significantly influence

their water chemistry, contributing bulk of the total cations in them (Sarin et al., 1989; Chapter 4). Dissolved Re shows positive correlation with Ca and alkalinity, which dominate the cation and anion budgets in the YRS respectively. The regression line through the data points (excluding the *Tons* at Dehradun and the Asan, which fall far away from the line) has a slope ~0.019 pM Re/μM Ca with r^2 = 0.79 (Fig. 5.4). It is tempting to infer, from this observation, that major source of Ca (carbonates) might also be contributing significantly to the dissolved Re of these waters. To test this, Re was measured in the Precambrian carbonates of the Lesser Himalaya.

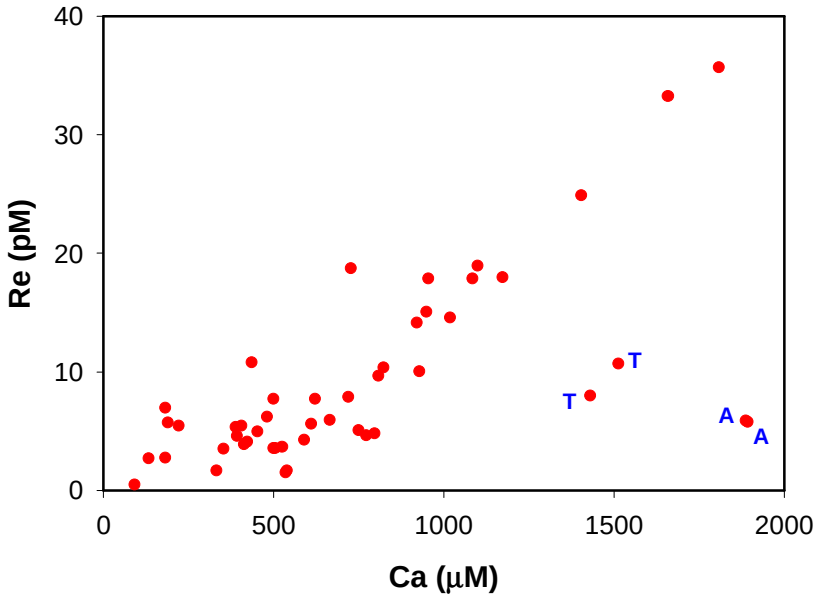

Fig. 5.4 Scatter diagram of Re vs. Ca in the YRS waters. The data show a strong positive correlation (r^2 = 0.79). Regression analysis excludes Tons at Dehradun (T), and Asan (A) rivers which fall outside the trend set by other rivers.

The Re abundances in the Precambrian carbonate outcrops from the Lesser Himalaya (both calcites and dolomites), based on the analysis of nitric acid *leach* of eight samples vary from ~0 to 225 pg g^{-1} with an average of 52 pg g^{-1} (Table 5.2). Pierson-Wickman et al. (2000) reported values of 187, 273 and 1160 pg g^{-1} Re for three *whole rock* limestone/marble samples from the Nepal Himalaya. These values are higher than those measured in this study. This can be because of a variety of reasons, such as difference in leach vs. whole rock concentrations, the extent and nature of metamorphism of carbonates and abundance of Re rich phases in them. Among the samples analyzed (Table 5.2), the two calcites have the lowest Re, 5 pg g^{-1}. If data in Table 5.2 can be considered typical of calcites and dolomites,

then it would suggest that dolomites incorporate in them measurable quantities of Re during their formation or that they contain minor amounts of Re rich phases such as organic matter. The Re concentrations of these samples do not seem to show any discernible trend with their $^{87}Sr/^{86}Sr$, the Re content of the sample KU92-43 with a high $^{87}Sr/^{86}Sr$, 0.8786 (Singh et al., 1998) is very similar to other samples with lower $^{87}Sr/^{86}Sr$. This is an indication that metamorphic alteration of these carbonates may not have caused substantial modification of their Re abundances. Using the highest measured concentration, 225 pg g^{-1} as typical of Re in these carbonates, it can be estimated that on an average, Re from ~8 grams of them needs to be supplied per liter of Yamuna waters to give rise to the average 1.8 ng $\ell^{-1}$of dissolved Re. As in the case of crystallines discussed above, this requirement is also almost impossible to comply with. Using Ca+Mg in the YRS waters (Table 4.1, Chapter 4) and Re/(Ca+Mg) in the Pc carbonates (Table 5.2), their contribution to the dissolved Re can be estimated. This estimate assumes (i) all Ca and Mg in the waters are derived from carbonates, (ii) Re, Ca and Mg are released to the waters in the same ratio as their abundances and (iii) once supplied to the rivers, Re, Ca and Mg behave conservatively. Using the maximum value of Re/(Ca+Mg), 0.12 pM mM^{-1} (0.7 pg mg^{-1}, Table 5.2), it is estimated that carbonates can contribute ~3 to 105 pg ℓ^{-1} (with a mean ~30 pg ℓ^{-1}) to the YRS waters, less than 2% of their average Re concentration. A similar conclusion also results for Re in the Ganga at Rishikesh. As the carbonate content of suspended matter is quite low (between 0.1 to 7 % in the bed load of Yamuna, Table 4.2) its selective leaching is also unlikely to be a significant source of dissolved Re to the waters. Assuming that the suspended and bed load in the YRS waters (~4 g ℓ^{-1}) have 5% carbonates with 225 pg g^{-1} Re in them (the maximum Re in the carbonates analyzed, Table 5.2) and all Re is leached from them, it is estimated that carbonates account for ~45 pg ℓ^{-1}, <3 % of the average dissolved Re. The slope of the regression line in the Ca-Re plot (Fig. 5.4), ~0.019 pM Re/μM Ca, is more than two orders of magnitude higher than the average Re/Ca in the Precambrian carbonates, $\sim 5\times10^{-5}$ pM/μM, attesting to the earlier estimates that these carbonates play only a minor role in contributing to dissolved Re in the YRS streams/rivers. Thus, it is evident from the present study that Precambrian carbonates of the Lesser Himalaya are not a major contributor to the Re budget of the Yamuna River System. If, however, there are wide spread occurrences of carbonates with high Re

abundance (such as the limestone with 1160 pg g^{-1}, Pierson-Wickmann et al., 2000) in the Yamuna and the Ganga catchments, their leaching can contribute significantly to the dissolved Re in these rivers.

Hodge et al. (1996), based on the similarity in Re/Mo/U ratios in groundwater draining carbonate aquifers from Southern Great Basin, USA and that in seawater, suggested that these elements are sequestered quantitatively by carbonates during their precipitation from seawater and are subsequently released to groundwater during their weathering. The results obtained in this study, on the Re abundances in Precambrian calcites and dolomites of the Lesser Himalaya and in rivers draining them, lead to the conclusion that at least for these rivers such carbonates are not a significant source of Re. The average Re/Ca in the Precambrian carbonates analyzed in this study (~0.05 pM/mM, this is obtained by taking the ratio of average Re in the carbonates analyzed in this study given in Table 5.2, 52 pg g^{-1} and average Ca in the Pc carbonates, 24.3%, Singh et al., 1998) and that in calcareous oozes (Colodner et al., 1993b) from the major ocean basins (~0.025 pM/mM) is nearly two orders of magnitude lower than that in seawater ~4 pM/mM. This coupled with the observation that burial of Re in suboxic and reducing marine sediments is its primary sink in the ocean (Colodner et al., 1993b; Morford and Emerson, 1999; Crusius and Thomson, 2000), points out the need to re-evaluate the suggestion that Re is quantitatively scavenged by carbonates during their precipitation from seawater and that they form an important source of Re to groundwaters (Hodge et al., 1996).

(iii) Re contribution from organic rich sediments

The hypothesis that weathering of black shales can be an important source of dissolved Re to rivers comes from the work of Colodner et al. (1993b). Their hypothesis is based on the observations of high Re concentrations in some of the tributaries of the Orinoco draining black shales and bituminous limestones and the strong correlation between Re and SO_4 in the waters. The knowledge that Re is highly enriched in black shales relative to its crustal abundance (Ravizza and Turekian, 1989) and that these organic rich sediments are more easily weatherable further supports their suggestion.

In the present study, there is evidence of the dominant role of weathering of black shales and other organic rich sediments in contributing dissolved Re to the headwaters of the Yamuna and the Ganga in the Himalaya. Firstly, there are reports of exposures of greyish

black and black shales in the Lesser Himalaya (Valdiya, 1980) and association of carbonaceous matter with the crystallines and carbonates (Gansser, 1964; Valdiya, 1980) many of which form part of the drainage basins of the Giri, the Aglar and the Bata, tributaries of the Yamuna. These rivers have dissolved Re concentrations about a factor of 2-4 higher (Table 5.1) than the average for the YRS. The river Bandal draining black shale deposits near Maldeota mines has Re as high as 32.2 pM (Table 5.1).

The black shales in the Lesser Himalaya have Re concentrations spanning a wide range, 0.2 to 264 ng g^{-1} (Table 5.3, Singh et al., 1999 had designated all shale samples they analyzed as black shales, though some of them had C_{org} <1% wt. The same convention is also followed here). Among these samples, those from the underground mines, which are better preserved, have higher Re (3.1 to 264 ng g^{-1}) and C_{org} (1 to 7.3% wt.), compared to surface outcrops (Re: 0.2 to 16.9 ng g^{-1} and C_{org}: 0.2 to 5.9% wt.) indicating that Re and C_{org} are lost during weathering. This inference is also supported by more recent results of Peucker-Ehrenbrink and Hannigan (2000) on Re abundances in black shale weathering profiles from Utica Shale, Quebec.

Table 5.3. C_{org}, Re, Os and U in black shales from the Lesser Himalaya[a)]

Element	Outcrop		Mine		All samples	
	n	range	n	range	n	(X/Re)[b)]
C_{org} (wt %)	19	0.21 - 5.85	14	1.01 - 7.28	26	$\sim 2\times10^{7}$
Re (ng g^{-1})	14	0.22 -16.9	14	3.05 - 264	28	—
Os (ng g^{-1})	16	0.02 - 4.13	14	0.17 - 13.5	25	0.05
U (μg g^{-1})	—	—	8	16.6 - 94.8	8	1900

[a)] C_{org}, Re and Os, from Singh (1999), U this study, n = number of samples. [b)] working ratio used in calculations, C_{org}/Re is molar ratio, Os/Re and U/Re in ng ng^{-1}.

The mobility of Re during weathering is also borne out from the analysis of water percolating through the phosphorite-blackshale-carbonate layers of Maldeota mines, near Dehradun, (MW-1—MW-4, Table 5.1). Three of the four mine waters have dissolved Re factors of 2-3 higher than the maximum river water Re concentrations measured in this study (Table 5.1) with the highest value ~21 ng ℓ^{-1} (111 pM). All these data provide evidence that black shales can release high concentrations of Re to waters draining them. Since black shales (and other organic rich sediments) are generally associated with pyrites, their

oxidative weathering produces sulfuric acid that attacks these shales as well as other rocks associated with them releasing SO_4 and a host of cations to waters. Hence Re, SO_4 and the cations released to waters from weathering of such sediments is very likely to show a

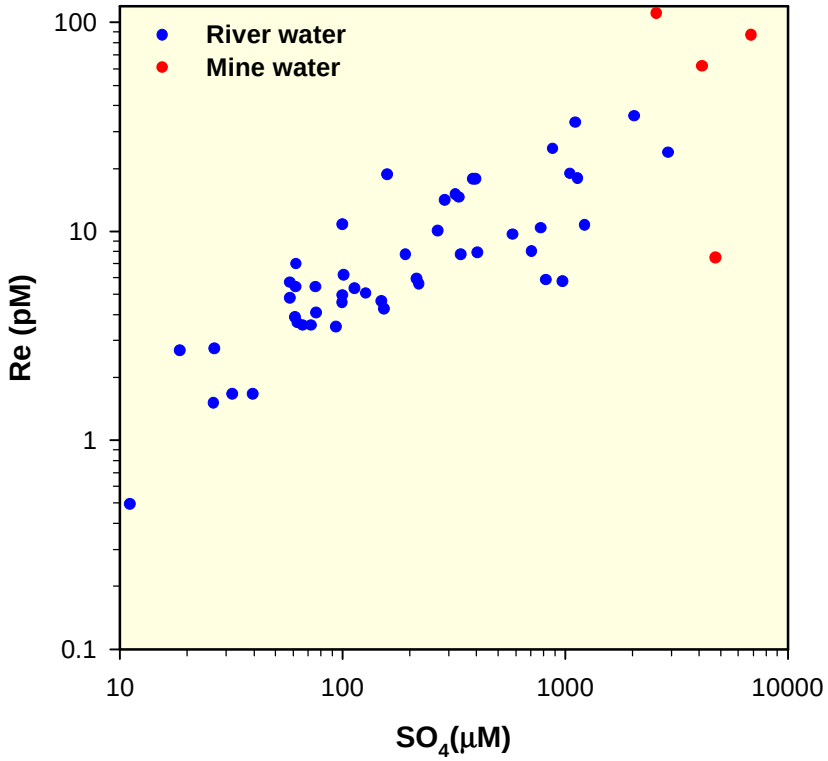

Fig. 5.5 Re-SO_4 scatter plot on log-log scale. Data for the YRS (excluding Shahashradhara sample) and mine waters are presented. Three of the four mine waters analyzed also fall in the trend set by the YRS data. The significant correlation (r = 0.84, p <0.005) between Re and SO_4 supports the hypothesis that black shale weathering is a major source for dissolved Re to these waters.

positive correlation with each other (Colodner et al., 1993b). Indeed, a significant correlation between Re and SO_4 in these waters has been observed (Fig. 5.5) supporting the idea that black shales are an important source of dissolved Re to these rivers (Fig. 5.5 is a log-log plot of Re as SO_4 concentrations range over two to three orders of magnitude). It is seen from Fig. 5.5 that the data of three of the four mine water samples are also consistent with the trend of Yamuna waters. Statistical analysis of the data in Fig. 5.5 yields a correlation coefficient of 0.84 (n = 53) which becomes 0.83 if the four mine waters are excluded. The scatter in Fig. 5.5 probably results from supply of SO_4 to the waters from evaporite dissolution (Chapter 4) and/or the presence of multiple end members with different Re/SO_4 ratios. The wide range in Re/SO_4 of mine waters (Table 5.1) is an indication for the

occurrence of various end members and/or dilution effect caused by mixing with SO_4 from evaporites. As mentioned earlier, Re also shows positive correlation with Ca and alkalinity. This suggests that sulphuric acid released via pyrite oxidation weathers, in addition to black shales, carbonates associated with them with a consequent release of Re, Ca, SO_4 and alkalinity to waters. But Ca and alkalinity when normalized with SO_4 show a negative correlation with Re suggesting that very little dissolved Re is associated with Ca and alkalinity released via dissolution of carbonates by carbonic acid (hence not associated with SO_4).

An important consideration in assessing the role of black shales and other carbonaceous sediments as a major source of Re to the Yamuna waters is their volumetric abundance and distribution in their drainage basins. The occurrence of black shales and carbonaceous sediments, though, are reported in the Lesser Himalaya (Gansser, 1964; Valdiya, 1980), there is no quantitative data on their areal coverage, abundances and distribution in the river basins. The paucity of such data makes it difficult to attest the inference drawn earlier, based on geochemical evidences, that these sediments are a major supplier of Re to the Yamuna waters. The geochemical data, however, allow us to make rough estimates on the quantity of organic rich sediments that needs to be weathered to account for the measured dissolved Re in the Yamuna waters. The average Re concentration in black shales in the Lesser Himalaya, based on both the outcrop and underground mine samples, is ~30 ng g^{-1} (Singh et al., 1999). Taking this as the typical Re concentration in black shales of the Yamuna basin, it can be estimated that on an average all Re from ~60 mg black shales will have to be released per liter of river water to yield 1.8 ng ℓ^{-1} Re. If Re is mobilized preferentially and the weathered black shales are added to the particulate load of the rivers, it would make up 1-2 % of the total abundance of their suspended and bed loads. These calculations are based on the assumption that *all* Re from the black shales be released to rivers and hence the estimates of black shales required to account for the dissolved Re in the YRS are *lower limits*. These estimates require that black shales occur at least at levels of a few percent in the drainage basin. The available data, as mentioned earlier, is not sufficient to determine if they occur in such abundance. Pierson-Wickmann et al. (2000) in attempting to balance Os isotope composition in river bedloads from the Nepal Himalaya also came to the conclusion that the abundance of black shales in the catchment has to be at a few percent

level, a requirement which they indicate may be difficult to comply with. Further, to explain the strong positive correlation between Re and ΣCations* (Fig. 5.2) it would require that black shales and other reducing sediments be dispersed throughout the drainage basin such that both Re and ΣCations* are released to rivers in roughly the same proportion along their entire stretch in the Himalaya.

In addition to black shales, other reducing sediments and Re rich phases (e.g. sulfides) could also serve as source(s) to dissolved Re. In this context, recent studies of Re in mildly reducing suboxic sediments show that they are a dominant sink for Re in the oceans (Morford and Emerson, 1999; Crusius and Thomson, 2000). The role of such sediments in contributing to the Re budgets of rivers in the Himalaya needs to be assessed. It is also interesting to note that even at Hanuman Chatti, near the origin of the Yamuna, where the predominant lithology is of granitic-granodioritic composition, the Yamuna water has Re concentration as high as 1 ng ℓ^{-1} (Table 5.1). Calculations based on Re in granites (Table 5.2) do not allow such high Re concentrations to be achieved from their weathering and suggest the need of Re rich phases. There are reports of organic matter associated with these rocks (Valdiya, 1980) and sulphide mineralization at places upstream of Hanuman Chatti (Jaireth et al., 1982), either or both of which may be contributing Re to these waters, however, their analysis is required to verify such a speculation. Silicates of sedimentary origin and with widespread occurrence in the YRS basin, could be another possible source of dissolved Re to the rivers. This speculation results from higher abundance of organic matter in such sediments. There is no data available on Re abundances in them.

The role of crystallines, Precambrian carbonates and black shales in determining the composition and Re abundances of the Yamuna System is summarized in the Ca/Na* vs. Re/Na* plot (Fig. 5.7). The plot also presents the average Ca/Na and Re/Na ratios of these lithologies from the Lesser Himalaya (Table 5.4).

Considering that bulk of the drainage of the YRS lies in the Lesser Himalaya, for mixing calculations the average abundances of Ca and Na in the Lesser Himalaya crystallines have been used. Ca/Na ratio in the LH crystallines (R_1) is calculated to be 0.34 μM μM^{-1} (Table 5.4).

Table 5.4 Ca, Na and Re abundances in various lithologies from the Lesser Himalaya

End member	Ca (% wt)	Na (% wt)	Re (pg g^{-1})	Ca/Na (μM/μM)	Re/Na (pM/μM)
LH Crystallines	1.04	1.76	26	0.34	0.0002
Pc Carbonates	24	0.03	52	460	0.02
LH Black shales	0.67	0.58	30000	0.68	0.66

[$R_1 = \frac{\overline{C}_{Ca}}{\overline{C}_{Na}}$ where $\overline{C}_{Ca}$ and $\overline{C}_{Na}$ are average Ca and Na concentrations in the LH crystallines (1.04% wt. and 1.76% wt. respectively). This value is different from the average Ca/Na ratio for LH crystallines reported by Krishnaswami et al. (1999), 0.46±0.28 as they had calculated the ratio (R_2) as: $R_2 = \Sigma R/N$ where R is the (Ca/Na) ratios in the individual samples and N is the number of samples for which the data was compiled. Similarly, the difference in the Re/Na in the LH crystallines, listed in Table 5.4 and in Table 5.2, is due to the difference in approach and database used for calculations. The Re/Na in Table 5.4, 0.0002 pM μM^{-1}, is the ratio of average Re in granites analyzed in this study and average Na for the LH crystallines whereas that in Table 5.2, ~0.0001 pM μM^{-1}, is the average of the Re/Na in the individual four granite samples]. In the calculations made for the plots in Fig. 5.7, Re in LH crystallines and Pc carbonates are from present study, Na and Ca in the Precambrian carbonates are from Mazumdar (1996) and Singh et al. (1998) and all the black shale data from Singh (1999).

The ratios of concentrations of elements C_1 and C_2 in a mixture of two components (1 & 2) were calculated as:

$$\left(\frac{C_1}{C_2}\right)_{mix} = \frac{X_{comp1}C_{1,comp1} + X_{comp2}C_{1,comp2}}{X_{comp1}C_{2,comp1} + X_{comp2}C_{2,comp2}}$$

where $C_{1,comp1}$ and $C_{1,\ comp2}$ are the concentrations of element C_1 in component 1 and component 2 respectively, $C_{2,comp1}$ and $C_{2,\ comp2}$ are the concentrations of element C_2 in component 1 and component 2 respectively, X is the mixing proportion so that X_{comp1} and X_{comp2} add to 100%. In the first step, such mixing calculations were performed for elements (Re, Ca and Na) in the mixtures with various proportions of two components, crystallines and Pc carbonates. From these calculations, it is seen that Ca/Na* in the waters is by and large a

mixture of ~40-70% Precambrian carbonate end member with the balance from an end member having LH crystalline composition. (Fig. 5.6).Hence in the next step, these two different mixtures, were fixed as components to which various proportions of black shales were added using the above equation.

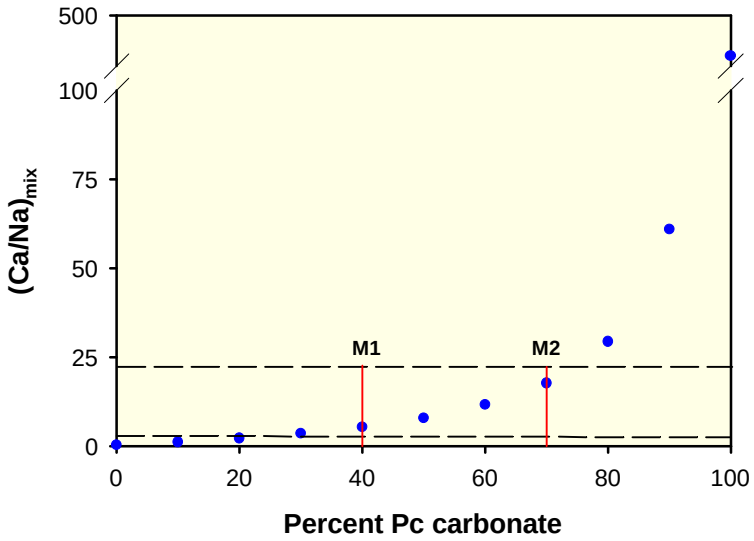

Fig. 5.6 Variation of Ca/Na in the granite-carbonate mixtures. The blue filled circles represent the mixture proportions with their Ca/Na, the horizontal dashed lines mark the limits for Ca/Na in the YRS waters. It is seen that Ca/Na in bulk of the water samples can be explained by a mixture of 40% carbonate+60% crystalline (M1) and 70% carbonate+30% crystalline (M2).

The Re/Na* in these carbonate-crystalline mixtures is only ~5×10^{-4} about two orders of magnitude lower than those measured in river waters, ~5×10^{-2}. Addition of 10-30% of an end member having Re/Na as in LH black shales, to this carbonate-crystalline mixture would yield Re/Na* values similar to the measured ratios in waters (Fig. 5.7). Thus it is seen that several percent contribution from black shale end member is required to reproduce the Re/Na* measured in the Yamuna and the Ganga waters. These estimates rely on the assumption that Ca/Na and Re/Na are released to waters from the crystallines, carbonates and black shales in the same ratio as their abundances. Considering that Re is a redox sensitive element and that in reducing sediments it may be associated with organic matter (Peucker-Ehrenbrink and Hannigan 2000; Crusius and Thomson, 2000) it is possible that during weathering Re is more rapidly and readily lost compared to Na. If, for example, the Re/Na released to the waters from black shale weathering is five times their abundance ratio, then the proportion of black shales required to match the measured ranges of Re/Na in the YRS reduces to ~1-5% (Fig. 5.8). Thus it is seen that to account for measured Re abundances and

Re/Na ratios in the YRS, several percent contributions from black shales/organic rich sediments are required. Currently available data on these lithologies are insufficient to determine if such a requirement can be met.

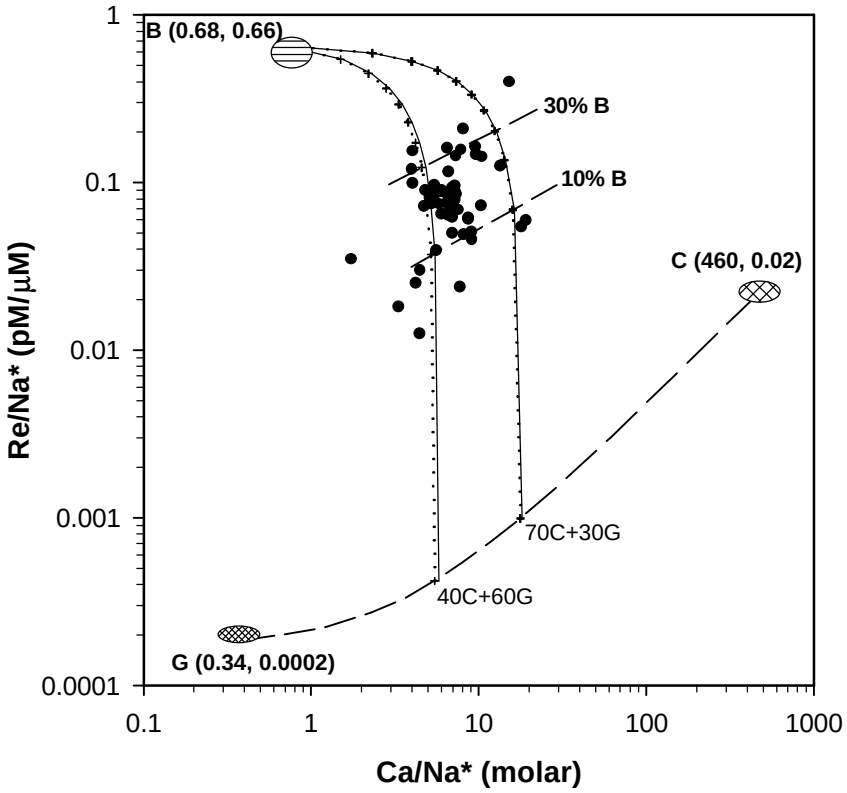

Fig.5.7 Re/Na vs Ca/Na* plot for the waters analyzed. The points plot within the mixing space bound by the three end members; crystallines (G), Precambrian carbonates (C) and LH black shales (B). The dotted evolution line calculated on the basis that Ca/Na and Re/Na are released to waters in the same ratio as their abundances in the three end members. The Ca/Na* in the waters is governed by and large by mixing between crystallines and carbonates, whereas Re/Na* is predominantly controlled by contribution from black shales. The solid line represents the evolution in which the Ca/Na ratio released to the waters from the granites is twice their abundance ratio. The proximity of the solid and dotted lines is an indication that the Ca/Na in the granite-carbonate mixture is not significantly affected by the preferential release of Ca (over Na) from granites.*

Data on Re/Na and Ca/Na in streams draining monolithologic units and/or laboratory leaching experiments with various rock types would help in better constraining the sources of dissolved Re of rivers.

This study reveals that organic rich sediments such as black shales could be a major source of dissolved Re to the river waters and hence "closed system" assumption required for their chronology by Re-Os systematics may not be satisfied in all cases. Therefore, to achieve a valid Re-Os isochron, it is necessary to ensure the "pristine" character of the rock samples

to be dated. Open system behavior of Re and Os involving their differential mobility, owing to their different geochemistry in the natural oxic environment, may yield isochron ages different than the true depositional ages of the sediments. That differential mobility of Re and Os from black shales during weathering can disturb the Re-Os isochron was borne out from the studies of Peucker-Ehrenbrink and Hannigan (2000) and Jaffe et al. (2000).

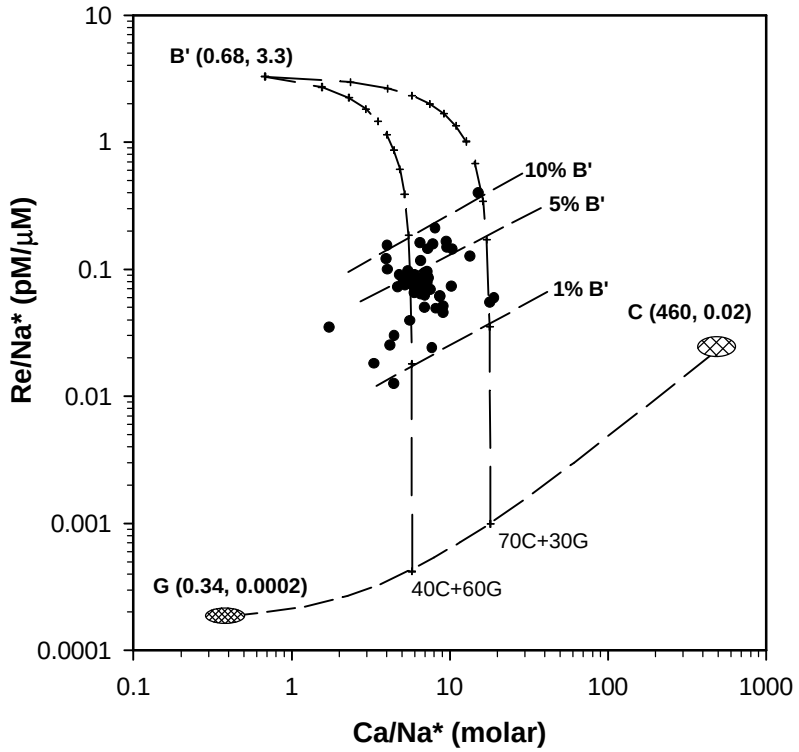

Fig. 5.8 Three end member mixing diagram as in Fig. 5.7. Mixing calculations done by assuming preferential release of Re over Na from the black shales, the Re/Na in solution being five times their abundance ratio. It is seen that the proportion of black shales needed to explain the Re/Na in the river waters reduces to 1 to 5% from 10 to 30% (Fig. 5.7).*

5.2.2 Re Flux from the Yamuna and the Ganga basins

The dissolved Re fluxes from the Yamuna and the Ganga at the foothills of the Himalaya have been determined from the data in Table 5.1. These calculations, based on Re concentrations in September (peak flow), yield ~150 and ~100 moles y^{-1} Re from the Yamuna at Batamandi and Saharanpur respectively and 120 moles y^{-1} from the Ganga at Rishikesh. [These values differ from the earlier reported values of Dalai et al. (2000) for two reasons. Firstly, the fluxes of the Yamuna and the Ganga in Dalai et al. (2000) are presented in reverse order; they should have been reported as 200 and 120 moles y^{-1} instead of 120 and

200 moles y^{-1} as given. The value of ~200 moles y^{-1} from the Yamuna basin is based on its Re concentration at Batamandi and water discharge at Okhla-Delhi (13.7×10^{12} ℓ y^{-1})]. The Yamuna (at Batamandi) and the Ganga (at Rishikesh) together contribute 270 moles Re per year at their outflow at the foothills of the Himalaya (Table 5.5). This constitutes ~0.4% of global Re flux (Colodner et al., 1993b), about thrice their contribution to the global water discharge (~0.1%). The flux calculation also shows that Re is released from the catchment of these rivers in the Himalaya at a rate of ~6-16 mmoles km^{-2} y^{-1}, an order of magnitude higher than the global average (Table 5.5).

Table 5.5 Re fluxes from the Yamuna and the Ganga at the base of the Himalaya

River	Location	Discharge (10^{12} ℓ)	Area (10^3 km^2)	Re (pM)	Flux (moles y^{-1})	Flux (mmoles km^{-2} y^{-1})
Yamuna[a)]	Batamandi	10.8	9.6	14.1	150	16
Ganga	Rishikesh	22.4	19.6	5.3	120	6
Ganga[b)]	Aricha Ghat	450	975	8.2	3700	4
Global[b)]		36000	101000	2.1	75000	0.7

[a)]based on Re of sample RW99-55 (Table 5.1) and discharge at Tajewala, few tens of kilometers downstream of Batamandi. [b)]Re concentrations for Ganga at Aricha Ghat and Global average from Colodner et al. (1993b)

It is important to note that the dissolved Re concentration in the Ganga at Rishikesh, 5.3-7.9 pM, is similar to that in the Ganga at Aricha Ghat before its confluence, 8.2 pM (Colodner et al., 1993b). This would suggest that other tributaries joining the Ganga after it drains past the Himalaya at Rishikesh add Re and water in the same proportion as they are at Rishikesh.

These estimates of Re flux from the Yamuna and the Ganga at the foothills of the Himalaya is disproportionately high compared to their contribution to water discharge. The available data for the Ganga at Aricha Ghat also shows a similar trend. The impact of this impact on a global scale is not pronounced as the drainage area and water discharge of these rivers are only a small fraction of the global value. However, if all Himalayan rivers exhibit a trend similar to that of the Ganga, then supply from these rivers could be a major component of the Re budget of the global rivers. Sarin et al. (1990) reported that the weathering rate of uranium in the Himalaya is about a factor of ten higher than the global average. Similarly, based on Os abundances in the Ganga waters (Levasseur et al., 1999) it can be estimated that Os is released by weathering from the Himalaya at a rate of about three times the global

average. These estimates show that chemical weathering in the Yamuna and the Ganga basins liberates Re, Os and U in amounts disproportionately higher than their contribution to global water discharge and drainage area.

In the previous sections it was discussed that black shales exert dominant control on the Re budgets of the Yamuna and the Ganga rivers. This makes it possible to use Re a proxy to estimate the quantity of black shales being weathered in the Yamuna and Ganga basins. Based on the Re flux (Table 5.5) and using 30 ng g^{-1} Re as an average, it is estimated that ~(6-9)×10^8 kg of black shales are being weathered annually in the Yamuna and the Ganga basins in the Himalaya. This estimate assumes that all Re in rivers is from the black shales. If a part of Re is from other sources, then the quantity of black shales weathered would be lower than that calculated above.

5.2.3 Black shale weathering: Implications to riverine trace metal budgets and carbon cycle

Black shales, in addition to Re, are abundant in carbon, PGE and redox sensitive metals such as V, U and Mo (Horan et al., 1994; Peucker-Ehrenbrink and Hannigan 2000). Their oxidative weathering can also release these elements and CO_2 in addition to Re to the river waters draining them (Petsch et al., 2000; Peucker-Ehrenbrink and Hannigan 2000). We have evaluated the influence of black shale weathering on the budgets of some of these elements in the Yamuna and the Ganga rivers based on available data on Re, Os and U in rivers and Re, Os, U and organic carbon in black shales (Table 5.3, Singh et al., 1999). These calculations assume that all Re in the YRS are of black shale origin.

The Os/Re weight ratios in black shale samples from the outcrops and under ground mines overlap with each other and center around a value of 0.05±0.03 (Singh et al., 1999). If Re and Os are supplied to rivers in the same ratio as their abundance in black shales, then it can be estimated from Os/Re in them and Re content of the Ganga at Rishikesh (1.0 ng ℓ^{-1}, Table 5.1) that black shales would contribute about 20-80 pg of Os per liter of water. This estimate is significantly higher than the Os measured in the Ganga water at Rishikesh (6.2 pg ℓ^{-1}, Levasseur et al., 1999) indicating that black shale weathering can account for the dissolved Os levels in the Ganga. It is also interesting to note that the estimated Os value is similar to the desorbable Os concentration, as determined by leaching the Ganga bed sediments at Patna (30 pg ℓ^{-1}, Pegram et al., 1994). The Os/Re in the Ganga at Rishikesh and

at Rajashahi (based on Os data of Levasseur et al., 1999 and Re from present study and Colodner et al., 1993b) is ~0.006, an order of magnitude lower than those in the Lesser Himalayan black shales. This would suggest that Os is less mobile than Re during weathering of black shales and/or that the Os released is removed by scavenging on to the sediment surfaces by Fe-Mn oxyhydroxides. The geochemical behaviour of Re, i.e. inertness and stability of ReO_4^- in oxygenated aqueous environment (Koide et al., 1986; Colodner et al., 1993b) and the particle reactivity of Os (Williams et al., 1997; Levasseur et al., 2000) would favour the latter hypothesis, that it is removed from dissolved phase to particulates to explain the low Os/Re in rivers. The presence of significant desorbable component of Os in river sediments further attests to this hypothesis (Pegram et al., 1994; Pierson-Wickmann et al., 2000). The available data on Os and Re abundances in black shale weathering profiles show evidence for differential mobility of Re and Os (Peucker-Ehrenbrink and Hannigan, 2000; Jaffe et al., 2000). It is, however, difficult to assess from these results whether Re is more mobile than Os or vice versa. The results of Peucker-Ehrenbrink and Hannigan (2000) show that in three of the four profiles Os is lost from black shales more than Re during weathering whereas the data of Jaffe et al. (2000) indicate that Re is more mobile than Os. More importantly, it is borne out from the above calculations that even if the Os mobility from black shales during weathering is lower than that for Re it may still account for the reported dissolved Os concentration in the Ganga. Ganga water at Rishikesh has higher radiogenic Os isotopic composition of ($^{187}Os/^{188}Os = 2.65$, Levasseur et al., 1999) compared to other major rivers. Black shales from outcrops and the mines in the Lesser Himalaya have $^{187}Os/^{188}Os$, 1.02-11.5 (Singh et al., 1999), with many of the samples having values much higher than 2.65. Crystallines (granites and gneisses) from the Central Nepal Himalaya have been reported to have $^{187}Os/^{188}Os \leq 1.63$ (Pierson-Wickmann et al., 2000). These observations support the hypothesis that black shales, with much higher Os concentrations and $^{187}Os/^{188}Os$ than other lithologies, can be a major contributor to the Os budget and its high radiogenic isotopic composition in rivers draining the Himalaya.

Using the available data, it is possible to place an upper limit of Os contribution from silicates. The average Os in seven granite/gneiss samples reported by Pierson-Wickmann et al. (2000) is ~8 pg g^{-1}. Assuming this as representative for the granites in the Yamuna catchment and using the average ΣCations* in the YRS waters, ~40 mg ℓ^{-1}, it can be

estimated that silicates (with Σcations ~80 mg g^{-1}) contribute ~4 pg of Os per liter of these waters. This estimate is based on the assumptions that all the cations in the river waters are of silicate origin and that Os and the cations are released to water in the same proportion as their abundances in silicates. Considering that bulk of the cations in these waters is derived from carbonates and/or evaporites, this estimate is an *upper limit*.

Following the approach similar to that adopted for Os, it can be estimated from the average U/Re of ~1900 in black shales (Table 5.3) and dissolved Re of ~1.8 ng ℓ^{-1}, that their weathering can contribute on an average ~3 μg $\ell^{-1}$of U to the rivers. The estimated uranium concentration is very similar to the values reported for some of these rivers and the Ganga headwaters (Sarin et al., 1990, 1992b) indicating that black shales can be a significant source of dissolved uranium to them. The significant correlation between U and ΣCations* in the Ganga waters prompted Sarin et al. (1990, 1992b) to suggest that weathering of silicates and uraniferous minerals could be important source(s) of U to these waters. Colodner et al. (1993b), though proposed carbonaceous shales as a possible source for U and Re in these waters, they also suggested that there could be additional sources for U as the U/Re in the Ganga-Brahmaputra were much higher than those in typical organic rich sediments. Analysis of a few black shales from the Lesser Himalaya shows that U/Re (wt. ratio) are ~200 to 30000 with an average of ~1900 (Table 5.3) which is very similar to those found in the river waters. Using the lowest U/Re ratio ~200, a *lower limit* of U contribution from black shales to river waters, can be estimated to be ~0.4 μg ℓ^{-1}. This is ~20% of the average river water U in the Ganga and the Indus headwaters, ~1.7 μg ℓ^{-1} (Sarin et al., 1992b; Pande et al., 1994). The average U/Re in the black shales, ~1900 (U data from Sarin et al., 1990) is much higher than that in the Yamuna waters in Saharanpur, ~1350 suggesting that all U in the water can be contributed from black shales if U and Re are released in the same proportion as their abundances. These calculations show that organic rich sediments in the catchment can be a candidate for contributing to high uranium to the rivers draining the Himalaya.

In addition to the discussion on the trace elements presented above, another important aspect of black shale weathering is the fate of organic carbon in them. Petsch et al. (2000), based on a study of black shale weathering profiles, proposed that the rate of black shale weathering is controlled by the rate of physical erosion and their subsequent exposure to

oxygenated surface waters. In the Himalaya, black shale weathering rate is expected to be high since the basin is dominated by physical erosion resulting from steep gradients and intense precipitation (rain and snow melt) throughout the year. The C_{org}/Re molar ratio in the black shales in the Lesser Himalaya range between (0.23-24) $\times 10^7$ (Singh et al., 1999). Using a typical value of 2×10^7 for C_{org}/Re (Table 5.3) it can be estimated that ~$(1\text{-}3)\times10^5$ moles km^{-2} y^{-1} of CO_2 would be released from them in the Ganga and the Yamuna basins in the Himalaya (Table 5.6).

Table 5.6 Uptake and release of CO_2 in the Yamuna and the Ganga basins in the Himalaya.

River	Area (10^3 km^2)	Discharge (10^{12} ℓ)	Re Flux[a)]	CO_2 flux (moles km^{-2} y^{-1})[b)]	
				Uptake	Release
Ganga	19.6	22.4	6	$(2\text{-}4)\times10^5$	1.2×10^5
Yamuna	9.6	10.8	16	$(4\text{-}7)\times10^5$	3.1×10^5

[a)] Re flux in units of mmoles km^{-2} y^{-1}. [b)] uptake is the CO_2 consumption due to silicate weathering and release is the flux of CO_2 from black shale weathering.

This calculation assumes (i) dissolved Re in rivers can be used as an index to derive the quantity of the black shales being weathered and (ii) all organic carbon in the black shales is oxidized to CO_2 during weathering. Study on chemical weathering of black shales (Petsch et al., 2000) shows that they lose between 60 to 100% of their original organic matter during weathering. The fate of weathered organic matter is not yet well known though it is assumed to be oxidized to CO_2. Experimental study on coal weathering (Chang and Berner, 1999) shows that not all the coal is oxidized to CO_2, rather the organic carbon is transformed into basically three forms, (i) oxidation of C_{org} to CO_2, (ii) production of solid oxidation products such as humic substances and (iii) dissolved organic carbon (DOC) in rivers. Petsch et al. (2000) observed that organic matter in the black shales is extremely labile when exposed to O_2-rich surface waters and they are rapidly removed from the outcrops by an as yet undetermined mechanism likely associated with slow oxidation followed by rapid cleavage, dissolution and advection (as either $CO_{2(aq)}$ or dissolved organic matter). Quantification of the relative amounts these various forms of organic matter, during their weathering in the surficial aqueous environments, remains uncertain. Our estimate of CO_2 release via oxidation

of organic matter, however, is an upper limit as it assumes that *all* C_{org} is oxidized to CO_2. Such estimations (Table 5.6) show that the amount of CO_2 release from the Yamuna basin is about a factor of 2-3 more than that from the Ganga (Table 5.6). [This value is higher than the preliminary estimate reported in Dalai et al. (2000) the cause for the increase being higher C_{org}/Re used in the present calculation]. In the chapter 4, based on various approaches, CO_2 consumption rates via silicate weathering in the YRS and Ganga basins have been estimated to be (4-7)$\times 10^5$ moles km^{-2} y^{-1} and (2-4)$\times 10^5$ moles km^{-2} y^{-1} respectively (Table 5.6). Comparison of the estimates of CO_2 release and consumption rates suggests that CO_2 release rate via black shale oxidation can roughly balance the CO_2 consumption via silicate weathering in the river basins in the southern slopes of the Himalaya (Table 5.6).

5.3 CONCLUSIONS

The focus of this work has been to assess the importance of black shale (organic rich sediments) weathering in contributing to dissolved Re in the YRS and the Ganga and its impact on the budgets of a few other elements; Os, U and C. This has been done through (a) systematic study of dissolved Re in the YRS and the Ganga, (b) measurements of Re abundances in granites and Precambrian carbonates, some of the major lithologies of their drainage basins and (c) the use of available data on Re and other elements in black shales from the Lesser Himalaya and information on its behaviour during weathering. The following observations and conclusions result from this study:

(i) The average dissolved Re in the YRS is 9.4 pM (~1.8 ng ℓ^{-1}), significantly higher than the reported global average river water concentration of 2.1 pM (Colodner et al., 1993b). Re in the Yamuna and the Ganga collected at Batamandi and Rishikesh, locations near the foothills of the Himalaya are also factor about 6 and 3 higher than the global average. The fluxes of dissolved Re from the Yamuna (at Batamandi) and the Ganga (at Rishikesh) are 150 and 120 moles y^{-1} respectively. These fluxes translate to Re weathering rate of ~1 to ~3 g km^{-2} y^{-1}, an order of magnitude higher than the global average of ~0.1 g km^{-2} y^{-1} (Colodner et al., 1993b). These results suggest that dissolved Re flux from the Yamuna and the Ganga are disproportionately high compared to their water discharge and drainage area. The impact of such high Re mobilization in the basins of these rivers, however, is not pronounced on the global riverine Re fluxes as the water discharge of the Yamuna and the Ganga at the foothills of the Himalaya is only ~0.1% of the global discharge.

(ii) The Re abundances in the granites of the Yamuna basin and Precambrian carbonates average ~26 and ~52 pg g^{-1} respectively. Calculations using Re/element ratios, ΣCations* and (Ca+Mg) abundances in river waters to estimate the contribution of Re from these lithologies show that the Re concentrations in them are too low to make a significant impact on the dissolved Re budget of these rivers on a basin wide scale.

(iii) The significant correlation between Re and SO_4 in waters and higher Re in rivers flowing through known black shale occurrences and ground waters dripping through black shale - phosphorite - carbonate layers all favour the idea that black shales could be a major source of Re to these waters. Further, the strong correlation between ΣCations* and Re in these waters require that both these are supplied to the YRS along its entire stretch in roughly the same proportion. An important consideration to decide if black shales can be a dominant source for dissolved Re in the YRS and the Ganga is their abundance and distribution in the drainage basins. The concentration of 1.8 ng ℓ^{-1} in the YRS requires that on average Re from at least ~60 mg black shales be released per liter of water. This is a few percent of the suspended and bed loads in these rivers. The available data is too sparse to determine if this requirement can be met.

(iv) Using dissolved Re as an index, it is shown that the reported concentrations of Os and U in these rivers can be supplied via black shale weathering if all these metals are released to water in the same proportion as their abundance. Extension of these calculations to C_{org} in black shales shows that if it is oxidized entirely to CO_2, its flux released to waters/atmosphere in the Yamuna and the Ganga basins in the Himalaya is similar to its consumption via silicate weathering.

Chapter 6

Synthesis and Scope of future research

This work described in this thesis is an attempt to understand and quantify chemical weathering of various lithologies in the southern slopes of the Himalaya in contributing to the riverine budgets of major cations, trace elements (Sr, Ba, Re, U and Os) and isotopes ($^{87}Sr/^{86}Sr$). A part of this also deals with characterization of processes in regulating the stable isotope composition of the YRS waters. These objectives have been achieved by extensive measurements of major ions, Sr, Ba, Re, stable isotopes ($\delta^{18}O$ and δD) and $^{87}Sr/^{86}Sr$ in the YRS waters and sediments collected during three different seasons. The results and findings of this study have been integrated with those available for other rivers, the Ganga, the Indus and rivers draining the Nepal Himalaya, to achieve a synoptic scenario on the contemporary chemical weathering and erosion rates and associated CO_2 consumption in the southern slopes of the Himalaya. In the following, the results obtained in this study are summarized and important conclusions drawn from them are presented.

6.1 Stable isotopes in the Yamuna River System

The Yamuna and its tributaries in the Himalaya have been extensively sampled and analyzed for their oxygen and hydrogen stable isotopes. These data, in conjunction with those available on rainwater at New Delhi, has been used to infer about various meteorological and hydrological processes regulating their isotopic composition. Further, these results have been integrated with those from the Ganga, the Indus and Gaula catchment in the Himalaya to understand the processes controlling the river water stable isotopic composition in this region

The river waters show seasonal and altitudinal variations in $\delta^{18}O$ and δD, with more depleted values during the monsoon and at higher altitudes. Such variations can be explained by "amount effect", more pronounced during monsoon season and possible evaporation of rainwater during their fall during summer. The river waters during monsoon season have a slope of 7.71 in $\delta^{18}O$-δD space, quite similar to that for rainwater of New Delhi during the same period, suggesting that the rainwater signature is well preserved in the rivers and not altered by processes such as evaporation. A reduced slope of ~6 for the YRS waters during summer and post-monsoon is also similar to that for New Delhi rainwater during June, suggesting that rivers receive waters from precipitation which have already undergone evaporation during their fall. This inference is further attested by the lower deuterium excess in rivers and rainwater during June. The higher d values in the YRS during October can be

due to an inherent signature of a source with a significant component of recycled moisture. The "altitude effect" in $\delta^{18}O$ in the YRS samples is derived to be 0.11‰ per 100 m, about a factor of two less than that reported for the Ganga headwaters. Large variability in the altitude effect among adjacent river catchments in the Himalaya is intriguing and is attributable to amount effect on isotope fractionation. This needs to be understood in greater detail, as it has implications to reconstruction of paleoelevation in the Himalaya. The relation between $\delta^{18}O$ and cations of the YRS has been used to assess the altitudinal variation of dissolved cation load in the Yamuna mainstream and shows that major cation abundance doubles as the Yamuna flows about 1.4 km. downstream. The altitudinal dependence of cation concentrations mainly results from variation in lithology and temperature with altitude.

6.2 Major ions, Sr, Ba and $^{87}Sr/^{86}Sr$ in the Yamuna River System

Knowledge on contemporary rates of silicate and carbonate weathering and CO_2 consumption via silicate weathering in the Himalaya is important to assess the role of Himalayan uplift and its influence on global climate change. This requires determination of various sources and quantification of their relative contributions to the cation budgets of the rivers in the Himalaya. Mass balance of Sr and its isotope (^{87}Sr) in rivers in the Himalaya has implications to use of $^{87}Sr/^{86}Sr$ in rivers as a potential tracer for silicate weathering and hence interpretation of marine strontium isotope record. This study, based on extensive measurements of major ions, Sr, Ba and $^{87}Sr/^{86}Sr$ in the YRS waters and sediments, aims at identifying sources of major cations, Sr and its isotope (^{87}Sr) and Ba to these waters. Further, these data have been used to estimate rates of silicate and carbonate weathering and CO_2 consumption in the basin.

Silicate contributions to cation budget, $(\Sigma Cat)_s$, have been estimated using Na* (Na corrected for atmospheric and cyclic contributions) as an index of silicate weathering. For carbonate weathering, *upper limit* of carbonate cations $(\Sigma Cat)_{carb}$ have been estimated assuming *all* non-silicate Ca is derived from carbonates. *Lower limits* of $(\Sigma Cat)_{carb}$ have been estimated assuming *all* SO_4 to be of evaporite origin. This provides *upper limits* of evaporite contributions to YRS cation budget. Using estimates of $(\Sigma Cat)_s$ and $(\Sigma Cat)_{carb}$, river discharge and drainage area, contemporary rates of silicate and carbonate weathering and CO_2 consumption by silicate weathering have been determined.

Similar approaches have been adopted to quantify contributions of Sr and Ba from silicates, carbonates and evaporites. Water chemistry and available information on catchment lithology have been used to evaluate the relative importance of various lithologies in regulating high radiogenic Sr isotopic composition of river waters. The study also addresses to an issue of recent debate, i.e. the role of vein-calcites, occurring in granites, in contributing to the Sr budget and $^{87}Sr/^{86}Sr$ of YRS waters. The main conclusions are:

1. The YRS waters demonstrate the control of lithology on their chemistry. The rivers draining predominantly silicates in the upper reaches, have low TDS, Sr, Ba and high $^{87}Sr/^{86}Sr$. In the lower reaches, the tributaries draining more easily weatherable lithologies such as carbonates, evaporites and phosphates have high TDS, Sr, Ba and low $^{87}Sr/^{86}Sr$.
2. Major ion chemistry of YRS waters is dominated by carbonate weathering, Ca and alkalinity being the most abundant. Evidence of dolomite weathering, which has significant volumetric abundance in the Lesser Himalaya, is also seen. Many of the samples are supersaturated with calcite, however, no evidence of calcite precipitation has been observed in this study. The estimated lower and upper limit of carbonate contributions to the YRS cations average ~50% and ~70%. The impact of carbonate weathering on the YRS dissolved Sr load, average ~15%. The carbonates with low Sr/Ca and $^{87}Sr/^{86}Sr$ than the YRS waters, are not an important source for the high radiogenic Sr isotopic composition in many of the rivers. The upper limit of carbonate contributions to the YRS dissolved Ba average ~30%.
3. Silicate weathering is an ongoing process in the Himalaya, as evident from abundances of Si, K and Na* in the YRS waters. Their contributions to the YRS cations is lower than the carbonates and average ~25%. Their average contribution to the YRS Sr is roughly the same ~25%. Silicate weathering is the dominant contributor to the ^{87}Sr load in the waters, an inference drawn from the observation that streams draining predominantly silicates have high $^{87}Sr/^{86}Sr$ and that $^{87}Sr/^{86}Sr$ shows strong linear correlation with silicate cations $(\Sigma Cat)_s$, (Na^*+K/TZ^+) and (SiO_2/TDS). Our estimates of upper limit of vein-calcite contributions to the dissolved Sr in rivers show that they can be significant, however, proper evaluation of their role in regulating the river water Sr and $^{87}Sr/^{86}Sr$ needs more detailed work.

4. Minor lithologies such as evaporites and phosphorites, more abundant in the lower reaches, seem to be contributing significantly to the dissolved Sr and Ba of the YRS waters as evident from the observation that the streams draining them have high Sr and Ba. They however, dilute the high radiogenic Sr isotopic composition of the river waters.
5. Silicate weathering in the YRS basin is not so intense, as evident from the low values of chemical index of alteration ~60 and Si/(Na*+K) in the rivers (~1.2). This is likely to be caused by high physical erosion rates, at least an order of magnitude higher than the chemical weathering rates. The carbonate weathering rates, ~31-46 mm ky^{-1} is three to four times higher than the silicate weathering rate in the catchment, ~10 mm ky^{-1}. The CO_2 drawdown via silicate weathering in the Yamuna and the Ganga basins are roughly similar but significantly higher than those reported in other major river basins in the world. This enhanced drawdown is unlikely to have pronounced impact on the global CO_2 consumption, as the Ganga and the Yamuna in the Himalaya constitute only low proportion of the global drainage area and water discharge. If such high drawdown is also characteristic of other rivers draining the Himalaya, then weathering in the Himalaya can be important in regulating the atmospheric CO_2 in a million-year time scale.
6. This study brings out the influence of climatic parameters such as temperature on silicate weathering. From relations of Si and Na* (silicate Na) with water temperature, the activation energy for overall silicate weathering in the catchment is estimated to be ~50-75 kJ mol^{-1}, similar to those reported for granitoid weathering.

6.3 Dissolved Re in the Yamuna River System

In this study, extensive measurements of Re has been carried out in YRS waters and some of the source rocks (granites and Precambrian carbonates). These data, along with those available on black shales from the Lesser Himalaya, have been used to calculate contributions of Re to the YRS from various sources. In addition to these data, these estimates also rely on certain assumptions on the release of Re to the rivers.

Further, dissolved Re in rivers has been used as an index to quantify the role of black shale weathering in contributing to trace metal budgets of rivers such as Os and U. For the first time, an attempt has been made to estimate the rate of CO_2 release via oxidation of organic rich sediments, using dissolved Re as a proxy for weathering of these sediments. The salient features of this study are as the following:

1. The average dissolved Re in the YRS, 9.4 pM is much higher than the global average river water value, 2.1 pM. The dissolved Re flux from the Ganga and the Yamuna in the Himalaya, ~270 moles y^{-1} is disproportionately higher compared to their drainage area and water discharge.
2. Based on Re measurements in granites in the Yamuna basin and Precambrian carbonates in the Lesser Himalaya, it is estimated that their contributions to the dissolved Re budget of the YRS waters is only minor on a basin wide scale.
3. Higher Re concentrations in rivers flowing through black shale occurrences and mine waters dripping through black shale-phosphorite-carbonate layers and significant Re-SO_4 correlation in the YRS waters, all suggest that organic rich sediments can be a major contributor to dissolved Re in the YRS. Using average Re concentration in the LH black shales, it is estimated that all Re from ~60 mg black shales have to be released per liter of water to account for the measured average Re in the YRS waters. Data on the distribution of organic rich sediments in the drainage basin and Re abundance in them are needed to determine if such a requirement can be met.
4. Weathering of black shales can also account for the reported dissolved Os and U concentrations in the rivers in the Himalaya, as shown by estimates using dissolved Re in rivers and Re, U and Os in black shales.
5. Using Re in river as an index of weathering of organic rich sediments, it has been estimated that $(6\text{-}9)\times10^8$ kg of such sediments are weathered in the YRS and the Ganga basins annually. If their weathering results in oxidation of all organic carbon to CO_2, then it would release a maximum of $(1\text{-}3)\times10^5$ moles km^{-2} y^{-1} of CO_2. This flux is roughly similar to the CO_2 consumption via silicate weathering in the basin.

6.4 Scope of future research

This study has used mass balance calculations to assess the importance of various components in contributing to the budgets of major cations, Sr, Ba and Re to river waters. These calculations critically depend on the end member compositions and the validity of the assumptions involved. A case to be emphasized is the role of vein-calcites in contributing to Sr and $^{87}Sr/^{86}Sr$ of rivers. Evaluation of the impact of this lithology on river water Sr isotope budgets needs proper sampling and analysis of them from granites in the Himalaya. Available data on major ions and Sr in the vein calcites are based on leaching of granite

samples. It is essential that "pure" vein-calcites be separated from granites to avoid interference from silicates to the contribution of Ca and Sr during leaching.

Another issue addressed in this study is uncertainties in the assessment of sources of Ca and Sr from evaporite dissolution and pyrite oxidation. Considering the very large range in the sulphur isotopic values ($\delta^{34}S$) in the pyrites associated with the black shales and phosphorites in the Lesser Himalaya, analysis of pyrites for sulphur isotopes to determine the source of SO_4 to rivers may not be very rewarding. The oxygen in dissolved SO_4 would carry in them signatures of evaporite oxygen (marine value at time of their formation) and of weathering solution (a mixture of surface water and atmospheric O_2). These components of oxygen involved have very different isotopic compositions. Hence analysis of oxygen isotopes in dissolved SO_4 may provide better handle to discriminate the contribution of evaporite and pyrites to dissolved SO_4. This in turn can help in better assessing the riverine Ca and Sr budgets. Data on areal distribution of minor lithologies such as evaporites and phosphates are needed to support the inferences drawn from the geochemical evidence that they may be dominant contributors to the dissolved Sr and Ba in the YRS.

It has been shown that preferential release of Re over Na (and other cations) to solution from black shales can significantly change their contribution to the dissolved Re budget in the rivers. This has implications to the quantity of black shales being weathered and hence to the CO_2 budget of the atmosphere. Hence experiments of stepwise leaching of black shales should be carried out to determine the relative ease with which the elements are released from them. In this context, sampling and analysis of streams exclusively passing through black shales should also be carried out to couple the laboratory experiments with field observation. Further, volumetric abundance of organic rich sediments in the drainage basin should be assessed in more detail to determine if they can be dominant contributor to dissolved Re in many of the streams throughout the catchment.

Proper assessment of mechanism regulating "altitude effect" in the Himalaya requires sampling and analysis of rain and fresh snow at a number of places spanning over different seasons in a year and also during different years. These should be coupled with river water data to determine the extent of "averaging effect" in rivers and the utility to derive "altitude effects".

References

Agarwal A. and Chak A. (1991) Havoc in the Himalaya. In: *Floods, flood plains and environmental myths*. Centre for Science and Environment, New Delhi, 23-39.

Ahmad T., Khanna P. P., Chakrapani G. J. and Balakrishnan S. (1998) Geochemical characteristics of water and sediment of the Indus river, Trans-Himalaya, India: constraints on weathering and erosion. *Jour. Asian Earth Sci* **16**, 333-346.

Allegre C. J., Birck J. L., Capmas F. and Cortillot V. (1999) Age of the Deccan Traps using ^{187}Re-^{187}Os systematics. *Earth Planet. Sci. Lett*. **170**, 197-204.

Allison C.E., Francey R.J. and Meijer H.A.J. (1995). Recommendations for the reporting of stable isotope measurements of carbon and oxygen in CO_2 gas. In: *Reference and intercomparison materials for stable isotopes of light elements*, IAEA, Vienna, 155-162.

Anantharaman M. S. and Bahukhandi P. C. (1984) A Study of the mineral resources of Mussoorie Syncline, Garhwal Lesser Himalaya. In: *Current Trends in Geology, Sedimentary Geology of the Himalaya* **5**, 191-196.

Anbar A. D., Creaser R. A., Papanastassiou D. A. and Wasserburg G. J. (1992) Rhenium in seawater: Confirmation of generally conservative behavior. *Geochim. Cosmochim. Acta* **56**, 4099-4103.

Araguas-Araguas L., Froehlich K. and Rozanski K. (1998). Stable isotope composition of precipitation over southeast Asia. *Jour. Geophy. Res*. **103**, 28721-28742.

Bartarya S. K., Bhattacharya S. K., Ramesh R. and Somayajulu B. L. K. (1995) δ^{18}O and δD systematics in the surficial waters of the Gaula catchment area, Kumaun Himalaya, India. *Jour. Hydrol*. **167**, 369-379.

Berner E. K. and Berner R. A. (1996) *Global Environment: Water, Air and Geochemical Cycles.* Prentice Hall, New Jersey, pp. 376.

Berner R. A and Berner E. K. (1997) Silicate weathering and Climate. In: *Tectonic Uplift and Climate Change*, (Editor: W. F. Ruddiman), Plenum Press, New York, 354-365.

Bhattacharya A. K., Bhatnagar G. S., Das G. R. N., Gupta J. N., Chhabria T. and Bhalla N. S. (1984) Rb/Sr dating and geological interpretation of sheared granite-gneisses of Brijranigad-Ingedinala, Bhilangana Valley, Their District, U.P. *Him. Geol.* **12**, 212-224.

Bhattacharya S.K., Gupta, S.K. and Krishnamurthy, R.V. (1985) Oxygen and hydrogen isotopic ratios in groundwaters and river waters from India. *Proc. Ind. Acad. Sci*. **94**, 283-295.

Bickle M. J., Harris N. B. W., Bunbury J. M., Chapman H. J., Fairchild I. J. and Ahmad T. (2001) Controls on the ^{87}Sr/^{86}Sr ratio of the carbonates in the Garhwal Himalaya, Headwaters of the Ganges. *The Jour Geol*. **109**, 737-753.

Biyani A.K. (1998) Geochemistry and Petrogenesis of Sayan a Chatti Mylonitic granite of Higher Himalayan Yamuna Valley, District Uttarkashi - U.P. *Indian. Jour. Earth Sci.* **25,** 29-41.

Blum J. D., Gazis C. A., Jacobson A. D. and Chamberlain C. P. (1998) Carbonate versus silicate weathering in Raikhot watershed within the High Himalayan crystalline series. *Geology* **26,** 411-414.

Boeglin J.-L. and Probst J.-L. (1998) Physical and chemical weathering rates and CO_2 consumption in a tropical lateritic environment: the upper Niger basin. *Chem. Geol*. **148**, 137-156.

Brand, W.A. Avak H., Seedorf R., Hofmann D. and Conradi Th. (1996). New methods for fully automated isotope ratio determination from hydrogen at the natural abundance level. *Isotopes Environ. Health Stud*. **32**, 263-273.

Brenner I., Bremier P. and Lemarchand A. (1992) Performance characteristics of an ultrasonic nebulizer coupled to a 40.68 MHz Inductively Coupled Plasma Atomic Spectrometer. *Jour. Anal. Atomic Spectrometry* **7**, 819-824.

Brookins D. G. (1986) Rhenium as an analog for fissiogenic technicium:Eh-pH diagrams (25^{o}C, 1 bar) constraints. *Appl. Geochem*. **1**, 513-517.

Cerling T. E. (1997) Late Cenozoic vegetation change, atmospheric CO_2, and tectonics. In: *Tectonic Uplift and Climate change* (Editor: W. F. Ruddiman), Plenum Press, New York, 383-397.

Chabaux F., Riotte J., Clauer, N. and France-Lanord C. (2001). Isotopic tracing of the dissolved U fluxes of Himalaya rivers: Implications for present and past U budgets of the Ganges-Brahmaputra system. *Geochim. Cosmochim. Acta* **65**, 3201-3217.

Chamberlain C.P. and Poage M. A. (2000) Reconstructing the paleotopography of mountain belts from the isotopic composition of authigenic minerals. *Geology* **28,** 115-118.

Chang S. and Berner R. A. (1999) Coal weathering and the geochemical carbon cycle. *Geochim. Cosmochim. Acta* **63**, 3301-3310.

Clark I. and Fritz P. (1997) *Environmental Isotopes in Hydrogeology*, Lewis Publishers, New York, pp. 328.

Cohen A. S., Coe A. L., Bartlett J. M. and Hawkesworth C. J. (1999) Precise Re-Os ages of organic-rich mudrocks and the Os-isotope composition of Jurassic seawater. *Earth Planet. Sci. Lett*. **167**, 159-173.

Collins R. and Jenkins A. (1996) The impact of agricultural land use on stream chemistry in the Middle Hills of the Himalaya, Nepal. *Jour. Hydrol*. **185**, 71-86.

Colodner D.C., Boyle E. A. and Edmond J. M. (1993a) Determination of rhenium and platinum in natural waters and sediments and iridium in sediments by flow injection isotope dilution inductively coupled plasma mass spectrometry *Anal. Chem*. **65**, 1419-1425.

Colodner D., Sachs J., Ravizza G., Turekian K. K., Edmond J. M. and Boyle E. (1993b) The geochemical cycle of rhenium: a reconnaissance. *Earth Planet. Sci. Lett*. **117**, 205-221.

Colodner D., Edmond J. and Boyle E. (1995) Rhenium in the Black Sea: Comparison with molybdenum and uranium. *Earth Planet. Sci. Lett*. **131**, 1-15.

Cooper L. W. (1998) Isotopic fractionation in snow cover. In *Isotope Tracers in Catchment Hydrology*, (Editors: Kendall C and McDonnel JJ), Elsevier Science B.V.: Amsterdam; 119-136.

Craig H. (1961) Isotopic variations in meteoric waters. *Science* **133**, 1702-1703.

Creaser R. A., Papanastassiou D. A. and Wasserburg G. J. (1991) Negative thermal ion mass spectrometry of osmium, rhenium and iridium. *Geochim. Cosmochim. Acta* **55,** 397-401.

Crusius J., Calvert S. E., Pederson T. F. and Sage D. (1996) Rhenium and molybdenum enrichments in sediments as indicators of oxic, suboxic and anoxic conditions of deposition. *Earth Planet. Sci. Lett.* **145**, 65-79.

Crusius J. and Thomson J. (2000) Comparative behavior of authigenic Re, U, and Mo during reoxidation and subsequent long-term burial in marine sediments. *Geochim. Cosmochim. Acta* **64**, 2233-2242.

Dalai T. K., Trivedi J. R. and Krishnaswami S. (2000) Re geochemistry in the Yamuna River in the Himalaya, Goldschimdt 2000, An International Conference for Geochemistry, Oxford, U.K., *Journal of Conference Abstracts* **5**, Cambridge publications, 329.

Dalai T. K., Singh Sunil K., Trivedi J. R. and Krishnaswami S. (2001a): Dissolved Rhenium in the Yamuna River System and the Ganga in the Himalaya: Role of black shale weathering on the budgets of Re, Os, and U in rivers and CO_2 in the atmosphere. *Geochimica Cosmochimica Acta* (in press).

Dalai T. K., Krishnaswami S. and Sarin M. M. (2001b) Major ion chemistry in the headwaters of the Yamuna River System: Chemical weathering and CO_2 consumption in the Himalaya (communicated to *Geochimica Cosmochimica Acta*).

Dalai T. K., Krishnaswami S. Kumar A. and Trivedi J. R. (2001c): Sr Isotopes in the Yamuna River System in the Himalaya, *Addenda Abstracts: 16th Himalaya-Karakorum-Tibet Workshop (HKTW-16)*, Schloss Seggau, Austria, 4-5.

Dalai T. K., Bhattacharya S. K. and Krishnaswami S. (2001d): Stable isotopes and in the source waters of the Yamuna and its tributaries: Seasonal and altitudinal variations and relation to major cations (communicated to *Hydrological Processes*).

Dansgaard W. (1964) Stable isotopes in precipitation, *Tellus* **16**, 436-468.

Datta P. S., Tyagi S. and Chandrasekharan H. (1991) Factors controlling stable isotope composition of rainfall in New Delhi, India. *Jour. Hydrol*. **128**, 223-236.

Derry L. A. and France-Lanord C. (1996) Neogene Himalayan weathering history and river $^{87}Sr/^{86}Sr$: impact on marine Sr record. *Earth Planet. Sci. Lett.* **142**, 59-74.

Derry L. A. and France-Lanord C. (1997) Himalayan weathering and erosion fluxes: Climate and tectonic controls. In: *Tectonic Uplift and Climate Change*, (Editor: W. F. Ruddiman), Plenum Press, New York, 289-312.

Dessert C., Dupre B., Francois, L. M., Schott J., Gaillardet J., Chakrapani G. and Bajpai S. (2001). Erosion of Deccan Traps determined by river geochemistry: impact on the global climate and the $^{87}Sr/^{86}Sr$ ratio of seawater. *Earth Planet Sci. Lett.* **188**, 459-474.

Devi L. (1992) *Climatic characteristics and water balance* (A study of Uttar Pradesh) Concept Publishing Company, New Delhi, pp. 207.

Drever J. I. (1997) *The geochemistry of natural waters: Surface and groundwater environments*. Prentice Hall, New Jersey, pp. 436.

Drever J. L. and Zobrist J. (1992) Chemical weathering of silicate rocks as a function of elevation in the southern Swiss Alps. *Geochim. Cosmochim. Acta* **56**, 3209-3216.

Edmond J. M. (1992) Himalayan tectonics, weathering processes, and the strontium isotope record in marine limestone. *Science* **258**, 1594-1597.

Edmond J. M., Palmer M. R., Measures C. I., Grant B. and Stallard R. F. (1995) The fluvial geochemistry and denudation rate of the Guayana shield in Venezuela, Colombia, and Brazil. *Geochim. Cosmochim. Acta* **59**, 3301-3325.

Edmond J. M. and Huh Y. (1997) Chemical weathering yields from basement and orogenic terrains in hot and cold climates. In: *Tectonic Uplift and Climate Change*, (Editor: W. F. Ruddiman), Plenum Press, New York, pp. 330-351.

English N. B., Quade J., DeCelles P. G. and Garzione C. N. (2000) Geologic control of Sr and major element chemistry in Himalayan Rivers, Nepal. *Geochim. Cosmochim. Acta* **64**, 2549-2566.

Epstein S. and Mayeda T. (1953). Variation of $\delta^{18}O$ content in waters from natural sources. *Geochim. Cosmochim. Acta* **4**, 213-214.

Esser B. K. and Turekian K. K. (1993) The osmium isotopic composition of the continental crust. *Geochim. Cosmochim. Acta* **57**, 3093-3104.

Gaillardet J., Dupre B. and Allegre C.J. (1995) A global geochemical mass budget applied to the Congo basin rivers: Erosion rates and continental crust compositions. *Geochim. Cosmochim. Acta* **59**, 3469-3485.

Gaillardet J., Dupre B., Allegre C. J. and Negrel P. (1997) Chemical and physical denudations in the Amazon river basin. *Chem. Geol.* **142**, 141-173.

Gaillardet J., Dupre B. and Allegre C. J. (1999) Global silicate weathering and CO_2 consumption rates deduced from the chemistry of large rivers. *Chem. Geol.* **159**, 3-30.

Galli P. and Oddo N. (1992) Ultrasonic nebulisation in Inductively coupled plasma atomic spectrometry. *Microchemical Journal* **46**, 327-334.

Galy A. and France-Lanord C. (1999) Weathering processes in the Ganges-Brhmaputra basin and the riverine alkalinity budget. *Chem. Geol.* **159**, 31-60.

Galy A., France-Lanord C. and Derry L. (1999) The strontium isotopic budget of Himalayan Rivers in Nepal and Bangladesh. *Geochim. Cosmochim. Acta* **63**, 1905-1925.

Galy A. and France-Lanord C. (2001) Higher erosion rates in the Himalaya: Geochemical constraints on riverine fluxes. *Geology* **29**, 23-26.

Gansser A. (1964) *Geology of the Himalayas*. Interscience Publishers, London, pp. 289.

Gardner R. and Walsh N. (1996) Chemical weathering of metamorphic rocks from low elevations in the Himalaya. *Chem.* Geol. **127,** 161-176.

Garzione C. N., Dettman D.L., Quade J., DeCelles P.G. and Butler R. F. (2000a) High times on the Tibetan Plateau: Plaeoelevation of the Thakkhola graben, Nepal. *Geology* **28,** 339-342.

Garzione C. N., Quade J., DeCelles P. G., English N. B. (2000b) Predicting paleoelevation of Tibet and the Himalaya from $\delta^{18}O$ vs. altitude gradients in meteoric waters across the Nepal Himalya. *Earth Planet Sci. Lett.* **183,** 215-229.

Gat J. R. and Matsui E. (1991) Atmospheric water balance in the Amazon Basin: An isotopic evapotranspiration model. *J. Geophy. Res.* **96 (D7),** 13179-13188.

Gazis C. A., Blum J. D., Chamberlain C.P. and Poage M. (1998) Isotope systematics of granites and gneisses of the Nanga Parbat Massif, Pakistan Himalaya. *Am. Jour. of Sci.* **298**, 673-698.

Ghildiyal B. P. (1990) Soils of the Himalaya. In: *Himalaya: Environment, resources and development* (Editors: N. K. Sah, S. K. Bhatt and R. K. Pande), Shree Almora Book Depot, Almora, 185-193.

Handa B. K. (1972) Geochemistry of the Ganga River water. *Ind. Geohydrol* **2**, 71-78.

Harris N. (1995) Significance of weathering of Himalayan metasedimentary rocks and leucogranites for the Sr isotope evolution of seawater during early Miocene. *Geology* **23**, 795-798.

Harris N., Bickle M., Chapman H., Fairchild I. and Bunbury J. (1998) The significance of Himalayan rivers for silicate weathering rates: evidence from Bhote Kosi tributary. *Chem Geol* **144**, 205-220.

Hasnain S. I., Subramanian V. and Dhanpal K. (1989) Chemical characteristics and suspended sediment load of meltwaters from a Himalayan glacier in India. *Jour. Hydrol.* **106**, 99-108.

Hasnain S. I. and Thayyen R. (1999) Controls on the major-ion chemistry of the Dokriani glacier meltwaters, Ganga basin, Garhwal Himalaya, India. *Jour. Glaciol.* **45**, 87-92.

Hay W. W. (1998) Detrital sediment fluxes from continents to oceans. *Chem Geol*. **145**, 287-323.

Hodge V. F., Johannesson K. and Stetzenbach K. J. (1996) Rhenium, molybdenum and uranium in groundwater from the southern Great Basin, USA: Evidence for conservative behavior. *Geochim. Cosmochim. Acta* **60**, 3197-3214.

Hoffmann G. and Heimann M. (1997). Water isotope modeling in the Asian monsoon region. *Quaternary International* **37,** 115-128.

Horan M F., Morgan J. W., Grauch R. I., Conveney Jr. R. M., Murowchick J B. and Hulbert L. J. (1994) Rhenium and osmium isotopes in black shales and Ni-Mo-PGE-rich sulfide layers, Yukon Territory, Canada, and Hunan and Guizhou provinces, China. *Geochim. Cosmochim. Acta* **58**, 257-265.

Huh Y., Tsoi M.-Y., Zaitsev A. and Edmond J. (1998) The fluvial geochemistry of the rivers of Eastern Siberia: I. Tributaries of the Lena River draining the sedimentary platform of the Siberian Craton. *Geochim. Cosmochim. Acta* **62**, 1657-1676.

Huh Y. and Edmond J. (1999) The fluvial geochemistry of the rivers of Eastern Siberia: III. Tributaries of the Lena and Anbar draining the basement terrain of the Siberian Craton and the Trans-Baikal HIghlands. *Geochim. Cosmochim. Acta* **63**, 967-987.

IAEA/WMO (1998) *Global Network for Isotopes in Precipitation. The GNIP Database*. Release: March,1998. URL http://www.iaea.org/programs.ri/gnip/gnipmain.htm.

Ingraham N. L. (1998) Isotopic variations in precipitation. In *Isotope tracers in catchment hydrology*, (Editors: C. Kendall and J. J. McDonnel), Elsevier Science B.V.: Amsterdam; 87-136.

Jacobson A. D. and Blum J. D. (2000) Ca/Sr and $^{87}Sr/^{86}Sr$ geochemistry of disseminated calcite in Himalayan silicate rocks from Nanga Parbat: Influence on river-water chemistry. *Geology* **28,** 463-466.

Jaffe L. A., Peucker-Ehrenbrink B. and Petsch S. (2000) Re-Os Mobility upon Weathering of Organic-Rich Sediments. *EOS* **81** (48), 1263-1264.

Jaireth S. K., Gupta S. K. and Dave V. K. S. (1982) Mineralogy, geochemistry and geothermometry of sulphide mineralization of the Central Himalayan region of Uttarkashi, U. P. *Him. Geol.* **12**, 280-294.

Jenny H. (1941) *Factors of soil formation*, McGraw-Hill, New York.

Jha P. K., Subramanian V. and Sitasawad R. (1988) Chemical and sediment mass transfer in the Yamuna River- A tributary of the Ganges System. *Jour. Hydrol*. **104**, 237-246.

Karim A. and Veizer J. (2000) Weathering processes in the Indus River Basin: implications from riverine carbon, sulfur, oxygen, and strontium isotopes. *Chem. Geol*. **170**, 153-177.

Koide M., Hodge V.F., Yang J., Stallard M., Goldberg E., Calhoun J. and Bertine K. (1986) Some comparative marine chemistries of rhenium, gold, silver and molybdenum. *Appl. Geochem.* **1**, 705-714.

Krishnamurthy, R.V. and Bhattacharya, S.K. (1991). Stable oxygen and hydrogen isotope ratios in shallow ground waters from India and a study of the role of evapotranspiration in the Indian monsoon. In *Isotope Geochemistry: A tribute to Samuel Epstein*, (Editors: Taylor H., O'Neil J. and Kaplan I.) Sp. Pub. Geochemical Society, 1-7.

Krishnaswami S., Trivedi J. R., Sarin M. M., Ramesh R. and Sharma K.K. (1992) Strontium isotopes and rubidium in the Ganga-Brahmaputra river system: Weathering in the Himalaya, fluxes to the Bay of Bengal and contributions to the evolution of the oceanic $^{87}Sr/^{86}Sr$. *Earth Planet. Sci. Lett*. **109**, 243-253.

Krishnaswami S. and Singh S. K. (1998) Silicate and carbonate weathering in the drainage basins of the Ganga-Ghaghara-Indus headwaters: Contributions to major ion and Sr isotope geochemistry. *Proc. Indian Acad. Sci. (Earth Planet. Sci.)* **107** (4), 283-291.

Krishnaswami S., Singh S. K. and Dalai T. K. (1999) Silicate weathering in the Himalaya: Role in contributing to major ions and radiogenic Sr to the Bay of Bengal. In: *Ocean Science, Trends and Future Directions* (Editor: B. L. K. Somayajulu), Indian National Science Academy and Akademia International, New Delhi, 23-51.

Lambs L. (2000) Correlation of conductivity and stable isotope ^{18}O for the assessment of water origin in river system. *Chem. Geol*. **164**, 161-170.

Levasseur S., Birck J.-L. and Allegre C. (1998) Direct measurement of femtomoles of osmium and the $^{187}Os/^{186}Os$ ratio in seawater. *Science* **282**, 272-274.

Levasseur S., Birck J.-L. and Allegre C. (1999) The osmium riverine flux and the oceanic mass balance of osmium. *Earth Planet. Sci. Lett*. **174**, 227-235.

Levasseur S., Rachold V., Birck J.-L. and Allegre C. (2000) Osmium behavior in estuaries: the Lena River example. *Earth Planet. Sci. Lett.* **177**, 7-23.

Louvat P. and Allegre C. (1997). Present denudation rates on the island of Reunion determined by river geochemistry: Basalt weathering and mass budget between chemical and mechanical erosions. *Geochim. Cosmochim. Acta* **61**, 3645-3669.

Luck J. M. and Allegre C. J. (1983) ^{187}Re-^{187}Os systematics in meteorites and cosmochemical consequences. *Nature* **302,** 130-132.

Luck J. M. and Allegre C. J. (1991) Osmium isotopes in ophiolites. *Earth Planet. Sci. Lett*. **107**, 406-415.

Mazumdar A.. (1996) *Petrographic and geochemical charaterisation of the Neoproterozoic-Lower Cambrian succession in a part of the Krol belt, Lesser Himalaya*. Ph. D. Dissertation, University of Delhi, pp. 246.

McCauley S. E. and DePaolo D. J. (1997) The marine $^{87}Sr/^{86}Sr$ and $\delta^{18}O$ records, Himalayan Alkalinity Fluxes and Cenozoic climate models. In: *Tectonic Uplift and Climate change* (Editor: W. F. Ruddiman), Plenum Press, New York, 428-467.

Milliman J. D. and Meade R. H. (1983) World-wide delivery of river sediment to the oceans. *Jour. Geol.* **21**, 1-21.

Morford J. L. and Emerson S. (1999) The geochemistry of redox sensitive metals in sediments. *Geochim. Cosmochim. Acta* **63**, 1735-1750.

Negi, S.S. (1991). *Himalayan Rivers, Lakes and Glaciers*. Indus Publishing Company, New Delhi, pp. 182.

Negrel P., Allegre C. J., Dupre B. and Lawin E. (1993) Erosion sources determined by inversion of major and trace element ratio in river water: The Congo basin case. *Earth Planet. Sci. Lett.* **120**, 59-76.

Nesbitt H. W. and Young G. M. (1982) Early Proterozoic climates and plate motions inferred from major element chemistry of lutites. *Nature* **299**, 715-717.

Nham T. T. (1992) Water analysis using ICP-AES with an ultrasonic nebulizer. *Varian Technical Report, ICP-8*, Dec. 1992, 1-9.

Nijampurkar V. N., Sarin M. M. and Rao D. K. (1993) Chemical compostition of snow and ice from Chhota Shigri glacier, Central Himalaya. *Jour. Hydrol*. **151**, 19-34.

Njitchoua R., Sigha-Nkamdjou L., Dever L., Marlin C., Sighomnou D. and Nia P. (1999) Variations of the stable isotopic compositions of rainfall events from the Cameron rain forest, Central africa. *Jour. Hydrol*., **223**, 17-26.

Palmer M. R. and Edmond J. M. (1989) The strontium isotopic budget of the modern ocean. *Earth Planet. Sci. Lett*. **92**, 11-26.

Palmer M. R. and Edmond J. M. (1992) Controls over the strontium isotope composition of river water. *Geochim. Cosmochim. Acta* **56**, 2099-2111.

Pande, K., Sarin, M.M., Trivedi, J.R., Krishnaswami, S. and Sharma, K.K. (1994). The Indus river system (India-Pakistan): Major-ion chemistry, uranium and strontium isotopes. *Chem. Geol*. **116**, 245-259.

Pande K., Padia J. T., Ramesh R. and Sharma, K. K. (2000) Stable isotope systematics of surface water bodies in the Himalayan and Trans-Himalayan (Kashmir) region. *Proc. Ind. Acad. Sci. (Earth Planet. Sci.)* **109**, 109-115.

Pandey S. K., Singh A. K. and Hasnain S. I. (2001) Hydrochemical characteristics of meltwater draining from Pindari glacier, Kumaon Himalaya. *Jour. Geol. Soc. India* **57**, 519-527.

Pant, G.B. and Rupa Kumar, K. (1997). *Climates of South Asia*. John Wiley and Sons, pp. 320.

Payne B. R. (1983) Interaction of surface water with groundwater. *Guidebook on nuclear techniques in Hydrology, IAEA Technical Report Series* **91,** 319-326.

Pegram W. J., Krishnaswami S., Ravizza G. E. and Turekian K. K. (1992) Record of seawater $^{187}Os/^{186}Os$ variation through the Cenozoic. *Earth Planet. Sci. Lett.* **113**, 569-576.

Pegram W. J., Esser B. K., Krishnaswami S. and Turekian K. K. (1994) The isotopic composition of the leachable osmium from river sediments. *Earth Planet. Sci. Lett.* **128**, 591-599.

Peucker-Ehrenbrink B., Ravizza G. E. and Hofmann A. W. (1995) The marine $^{187}Os/^{186}Os$ record of the past 80 million years. *Earth Planet. Sci. Lett.* **130,** 155-167.

Peucker-Ehrenbrink B. and Blum J. (1998) Re-Os isotope systematics and weathering of Precambrian crustal rocks: Implications for the marine osmium isotope record. *Geochim. Cosmochim. Acta* **62**, 3193-3203.

Peucker-Ehrenbrink B. and Hannigan R. E. (2000) Effects of black shale weathering on the mobility of rhenium and platinum group elements. *Geology* **28**, 475-478.

Petsch S. T., Berner R. A. and Eglinton T. I. (2000) A field study of the chemical weathering of ancient sedimentary organic matter. *Org. Geochem.* **31**, 475-487.

Pierson-Wickmann A-C., Reisberg L. and France-Lanord C. (2000) The Os isotopic composition of Himalayan river bedloads and bedrocks: importance of black shales. *Earth Planet. Sci. Lett.* **176**, 203-218.

Potts P. J., Tindle A. G. and Webb P. C. (1992) *Geochemical reference material compositions*, Whittles Publishing, U.K.

Prell W. L. and Kutzbach J. E. (1997) The impact of Tibetan-Himalayan elevation on the sensitivity of the monsoon climate system changes in solar radiation. In: *Tectonic Uplift and Climate change* (Editor: W. F. Ruddiman), Plenum Press, New York, 171-201.

Quade J., Roe L., DeCelles P. G. and Ojha T. P. (1997) The Late Neogene $^{87}Sr/^{86}Sr$ record of lowland Himalayan Rivers. *Science* **276**, 1828-1831.

Ramesh R. and Sarin M. M. (1992) Stable isotope study of the Ganga (Ganges) river system. *Jour. Hydrol*. **139**, 49-62.

Rao. K.L. (1975). *India's Water Wealth. Orient Long man Ltd.*, New Delhi, pp.255.

Ravizza G. E. and Turekian K. K. (1989) Applications of ^{187}Re-^{187}Os system to black shale geochronometry. *Geochim. Cosmochim. Acta* **53**, 3257-3262.

Ravizza G. E. Turekian K. K. and Hay B. J. (1991) The geochemistry of Rhenium and Osmium in recent sediments of the Black Sea. *Geochim. Cosmochim. Acta* **55**, 3741-3752.

Ravizza G. E. (1993) Variations of $^{187}Os/^{186}Os$ ratio of seawater over the past 28 million years as inferred from metalliferous carbonates. *Earth Planet. Sci. Lett.* **118,** 335-348.

Ravizza G. E. and Esser B .K. (1993) A possible link between the seawater osmium isotope record and weathering of ancient sedimentary organic matter. *Chem. Geol.* **107**, 255-258.

Ravizza G. E. and Turekian K. K. (1992) The osmium isotopic composition of organic-rich marine sediments. *Earth Planet. Sci. Lett.* **110**, 1-6.

Raymo M. E. and Ruddiman W. F. (1992) Tectonic forcing of late Cenozoic climate. *Nature* **359**, 117-122.

Raymo M. E., Ruddiman W. F. and Froelich, P. N. (1988) Influence of late Cenozoic mountain building on ocean geochemical cycles, *Geology* **16**, 649-653.

Richter F. M., Rowley D. B. and Depaolo D. J. (1992) Sr isotope evolution of seawater: The role of tectonics. *Earth Planet. Sci. Lett*. **109**, 11-23.

Rodhe A. (1998) Snowmelt-dominated systems. In: *Isotope Tracers in Catchment Hydrology*, (Editors: C. Kendall and J.F. McDonnell), Elsevier Science B.V., Amsterdam, pp.839.

Rozanski K., Araguas-Araguas L. and Gonfiantini R. (1993) Isotopic Patterns in Modern Global Precipitation. In: *Climate Change in Continental Isotopic Records*, Geophysical Monograph, **78**, AGU, 1-36.

Ruddiman W. F. (1997) *Tectonic Uplift and Climate Change* (ed. W.F. Ruddiman), Plenum Press, New York, pp. 535.

Ruddiman W. F. and Prell W. L. (1997) Introduction to the Uplift-Climate Connection. In *Tectonic Uplift and Climate Change* (Editor: W.F. Ruddiman), Plenum Press, New York, 3-15.

Sachan H. K. and Sharma R. (1993) Genesis of Barite mineralisation in the Nagthat Formation, Lesser Himalaya, near Dehradun. *Jour. Him. Geol*., **4**, 165-170.

Sarin, M.M. and Krishnaswami, S. (1984). Major ion chemistry of the Ganga-Brahmaputra river systems, India. *Nature* **312**, 538-541.

Sarin M. M., Krishnaswami S., Dilli K., Somayajulu B. L. K. and Moore W. S. (1989) Major ion chemistry of the Ganga-Brahmaputra river system: Weathering processes and fluxes to the Bay of the Bengal. *Geochim. Cosmochim. Acta* **53**, 997-1009.

Sarin M. M., Krishnaswami S., Somayajulu B. L. K. and Moore W. S. (1990) Chemistry of uranium, thorium, and radium isotopes in the Ganga-Brahmaputra river system: Weathering processes and fluxes to the Bay of the Bengal. *Geochim. Cosmochim. Acta* **54**, 1387-1396.

Sarin, M.M., Krishnaswami, S., Trivedi, J.R. and Sharma, K.K. (1992a) Major ion chemistry of the Ganga sources waters: Weathering in the high altitude Himalya. *Proc. Ind. Acad. Sci. (Earth Planet. Sci.)* **101**, 89-98.

Sarin M. M., Krishnaswami S., Sharma K. K. and Trivedi J. R. (1992b) Uranium isotopes and radium in the Bhagirathi-Alaknanda river system: Evidence for high uranium mobilization in the Himalaya. *Curr. Sci*. **62**, 801-805.

Sarin M. M. and Rao D. K. (2001) Atmospheric deposition of chemical constituents on a Central Himalayan Glacier: Inferences from snow chemistry. Proc. "National Workshop on Atmospheric Chemistry", NWAC 99, IITM, Pune, October 1999 (in press).

Schotterer U, Oldfield F, Frohlich K. (1996) In *Global Network for Isotopes in Precipitation*. IAEA/PAGES/WMO/IAHS/AISH, Switzerland.

Sharma M., Papanastassiou D. A. and Wasserburg G. J. (1997) The concentration and isotopic composition of osmium in the oceans. *Geochim. Cosmochim. Acta* **61**, 3287-3299.

Sharma M. and Wasserburg G. J. (1997) Osmium in rivers. *Geochim. Cosmochim. Acta* **61**, 5411-5416.

Sharma M., Wasserburg G. J., Hoffmann A. W. and Chakrapani G. J. (1999) Himalayan uplift and osmium isotopes in oceans and rivers. *Geochim. Cosmochim. Acta* **63**, 4005-4012.

Shiller A. M. and Boyle E. A. (1987) Dissolved vanadium in rivers and estuaries. *Earth Planet. Sci. Lett*. **86**, 214-224.

Shiller A. M. and Mao L (2000) Dissolved vanadium in rivers: effects of silicate weathering. *Chem. Geol*. **165**, 13-32.

Singh S. K., Trivedi J. R., Pande K., Ramesh R. and Krishnaswami S. (1998) Chemical and Sr, O, C isotopic compositions of carbonates from the Lesser Himalaya: Implications to the Sr isotope composition of the source waters of the Ganga, Ghaghara and the Indus Rivers. *Geochim. Cosmochim. Acta* **62**, 743-755.

Singh S. K. (1999) *Isotopic and Geochemical Studies of the Lesser Himalayan Sedimentaries*. Ph. D. Dissertation, M. S. University, Baroda, pp. 160.

Singh S. K., Trivedi J. R. and Krishnaswami S. (1999) Re-Os isotope systematics in black shales from the Lesser Himalaya: Their chronology and role in the $^{187}Os/^{188}Os$ evolution of seawater. *Geochim. Cosmochim. Acta* **63**, 2381-2392.

Srikantia S. V. and Bhargava O. N. (1998) *Geology of Himachal Pradesh*. Geological Society of India, Bangalore. pp. 406.

Subramanian V. and Dalavi R. A. (1978) Some aspects of stream erosion in the Himalaya. *Him. Geol*. **8**, 822-834.

Taylor A. S., Blum J. D., Lasaga A. C. and MacInnis I. N. (2000a) Kinetics of dissolution and Sr release during phlogopite weathering. *Geochim. Cosmochim. Acta* **64**, 1191-1208.

Taylor A. S., Blum J. D. and Lasaga A. C. (2000b) The dependence of labradorite dissolution and Sr isotope release rates on soultion saturation rate. *Geochim. Cosmochim. Acta* **64**, 2389-2400.

Trivedi J. R. (1990) *Geochronological studies of Himalayan granitoids. Ph. D. dissertation*, Gujarat University, Ahmedabad.

Trivedi, J.R., Pande K., Krishnaswami, S. and Sarin, M.M. (1995). Sr isotopes in rivers of India and Pakistan: A reconnaissance study. *Curr. Sci*., **69**, 171-178.

Trivedi J R., Singh S. K. and Krishnaswami S. (1999) ^{187}Re-^{187}Os in Lesser Himalayan sediments: Measurement techniques and preliminary results. *Proc. Indian Acad. Sci. (Earth Planet. Sci.)* **108**, 179-187.

Turekian K. K. and Pegram W. J. (1997) Osmium isotope record in a Cenozoic deep-sea core: Its relation to global tectonics and climate. In: *Tectonic Uplift and Climate Change*, (Editor: W.F. Ruddiman), Plenum Press, New York, 383-397.

Valdiya K. S. (1980) *Geology of the Kumaun Lesser Himalaya*. Wadia Institute of Himalayan Geology, Dehradun, pp. 291.

Valdiya K. S. (1998) *Dynamic Himalaya*. Sangam Books Limited, London, pp.178.

Velbel M. A. (1993) Temperature dependence of silicate weathering in nature: How strong of a negative feedback on long term accumulation of atmospheric CO_2 and global greenhouse warming? *Geology* **21**, 1059-1062.

Viers J., Dupre B., Braun J.-J., Deberdt S., Angeletti B., Ngoupayou J. N. and Michard A. (2000). Major and trace element abundances, and stontium isotopes in the Nyong basin rivers

(Cameroon): constraints on chemical weathering processes and elements transport mechanisms in humid tropical environments. *Chem Geol*., **169**, 211-241.

Volkening J., Walczyk T. and Heumann K.G. (1991) Osmium isotope ratio determinations by negative thermal ionization mass spectrometry. *Int. J. Mass. Spec. Ion Proc.* **105,** 147-159.

Wedepohl K. H. (1978) *Handbook of Geochemistry*, Vol II-5. Springer-Verlag, Berlin.

White A. F. and Blum A. E. (1995) Effects of climate on chemical weathering in watersheds. *Geochim. Cosmochim. Acta* **59**, 1729-1747.

White A. F., Blum A. E., Bullen T. D., Vivit D. V., Schultz M. and Fitzpatrick J. (1999) The effect of temperature on experimental and natural chemical weathering rates of granitoid rocks. *Geochim. Cosmochim. Acta* **63**, 3277-3291.

Williams G., Marcantonio F. and Turekian K. K. (1997) The behavior of natural and anthropogenic osmium in Long Island Sound, an urban estuary in the eastern U.S. *Earth Planet. Sci. Lett*. **148**, 341-347.

Williamson J. H. (1968) Least square fitting of a straight line. *Can. J. Phys.* **46**, 1845-1847.

Yurtsever Y. and Gat J. R. (1981) Atmospheric waters. In: *Stable Isotope Hydrology, IAEA Tech. Rep.* (Editors: J.R. Gat and Gonfiantini), Ser., **210**, 103-142.

List of Publications

1. S. Krishnaswami, Sunil K. Singh and Tarun K. Dalai (1999): Silicate Weathering in the Himalaya: Role in Contributing to Major Ions and Radiogenic Sr to the Bay of Bengal. ***Ocean Science: Trends and Future Directions*** (Ed: B.L.K. Somayajulu), Indian National Science Academy and Akademia Books International, New Delhi, pp. 23-51.
2. M.M. Sarin, S. Krishnaswami, Tarun K. Dalai, V. Ramaswamy and V. Ittekkot (2000): Settling fluxes of U- and Th- series nuclides in the Bay of Bengal: Results from time-series sediment trap studies. ***Deep Sea Research I***, 47, 1961-1985.
3. Tarun K. Dalai, Sunil K. Singh, J. R. Trivedi and S. Krishnaswami (2002): Dissolved Rhenium in the Yamuna River System and the Ganga in the Himalaya: Role of black shale weathering on the budgets of Re, Os, and U in rivers and CO_2 in the atmosphere. ***Geochimica Cosmochimica Acta***, 66, 29-43.
4. Tarun K. Dalai, S. K. Bhattacharya and S. Krishnaswami (2001) Stable isotopes and in the source waters of theYamuna and its tributaries: Seasonal and altitudinal variations and relation to major cations. ***Hydrological Processes*** 16, 3345-3364.
5. T. K. Dalai, S. Krishnaswami and M. M. Sarin (2002) Major ion chemistry in the headwaters of the Yamuna River System: Chemical weathering, its temperature dependence and CO_2 consumption in the Himalaya. ***Geochimica Cosmochimica Acta,*** 66, 3397-3416.
6. Tarun K. Dalai, S. Krishnaswami and M. M. Sarin (2002) Barium in the Yamuna River System in the Himalaya: Sources, fluxes and its behavior during weathering and transport ***Geochemistry, Geophysics, Geosystems***, 3, 10.1029/2002GC000381.
7. Tarun K. Dalai and Manmahon Sarin (2002) Trace determination of strontium and barium in river waters by inductively coupled plasma-atomic emission spectrometry, using an ultrasonic nebulizer. ***Geostandards Newsletter, The Journal of Geostandards and Geoanalysis***, **26**, 301-306.
8. Sunil K. Singh, Tarun K. Dalai and S. Krishnaswami (2003) U-Th series isotopes in carbonates and black shales from the Lesser Himalaya: Implications to dissolved uranium abundances in Ganga-Indus source waters. ***The Journal of Environmental Radioactivity***, 67, 69-90.
9. Tarun K. Dalai, S. Krishnaswami and A. Kumar (2003) Sr and $^{87}Sr/^{86}Sr$ in the Yamuna River System in the Himalaya: Sources, fluxes and controls on the radiogenic Sr isotopic composition. ***Geochimica Cosmochimica Acta,*** 67, 2931-2948.

10. Tarun K. Dalai, R. Rengarajan and P. P. Patel (2004) Sediment geochemistry of the Yamuna River System in the Himalaya: Implications to weathering and transport (***Geochemical Journal***, in press)